

be placed on automatic control by the station operator, in accordance with the orders of the dispatcher.

15. Carrier Supervisory Control⁷

Supervisory control is a system of controlling and supervising from a central point to operation of equipment at one or more remote locations. Control and supervision of several separate pieces of equipment are accomplished with relatively few conductors or channels. In the Visicode supervisory-control system, which is the system considered in the subsequent discussion, only a single pair of wires or

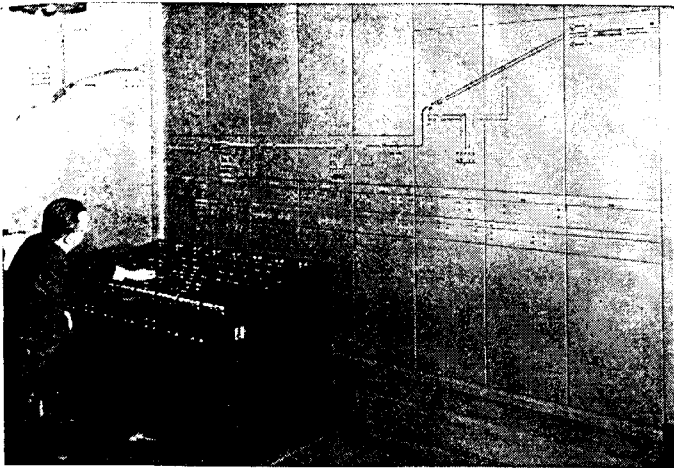


Fig. 9—Typical Visicode supervisory control desk.

a single carrier channel is required. A typical Visicode control desk is shown in Fig. 9.

In the Visicode supervisory-control system, supervision and control of many individual units of equipment are obtained by selective relay systems. These automatically generate and receive impulses in coded groups to perform the functions of selecting the apparatus to be controlled, performing the desired operation, and indicating that an operation has taken place. The latter function is performed whether the operation is initiated through the supervisory system or not.

16. Channel Requirements of Supervisory-Control Systems

The rate of impulsing of supervisory equipment is from 9 to 14 impulses per second, comparable to the speed of impulsing of a telephone dial. This rate of impulsing is considerably higher than the highest rate of any standard impulse telemetering system. The fastest such system in use has a maximum impulse rate of approximately 3.5 per second. In an impulse-rate telemetering system, it is necessary only that the channel preserve the rate of impulsing. The relative duration of the "on" and "off" periods is not important.

In the supervisory-control system the duration of the "on" period is approximately twice that of the "off" period. This relation must be preserved in order to allow proper sequential relay operations, some of which occur during the "on" period and some of which occur during the "off" period of the impulse cycle.

The high impulsing speed of the supervisory system and the requirement that the relative duration of the "on" and "off" periods be preserved make it undesirable to use more than one relaying point to retransmit mechanically supervisory impulses received from a distant point.

There are two types of Visicode supervisory control, one in which all the equipment to be controlled is located at a single point, and one in which the equipment is in several groups at different locations. These two types are referred to as the single-station and multistation systems, respectively.

A fundamental requirement of the multistation system is that a control or supervision function in progress between the dispatching office and a controlled station not be interfered with by supervisory signals from other controlled stations. This requirement is met by assigning different group codes to each station and arranging each station so that reception of a group code not associated with it locks out the supervisory equipment at that station. Each station must be able to receive all signals transmitted from any other station. In this way synchronism of impulses and successful lockout are assured, because the impulsing of any station is governed by impulses sent simultaneously from other stations.

When supervisory control is operated over a carrier channel provided for its exclusive use, impulsing of an otherwise unmodulated carrier signal normally is used. For this type of operation the transmitters and receivers at all locations operate on the same frequency, and all stations receive each other. Modifications of this arrangement are made in some cases to combine the supervisory system with other functions. In these cases supervisory control is usually operated over an audio-tone channel, a single tone receiver and transmitter being provided for supervisory in the carrier assembly at each location involved.

17. Combined Functions on a Carrier Channel^{3,4,7}

Many of the functions of power-line carrier that have been described can be performed simultaneously over a single carrier channel, and usually several carrier channels on the same line can make joint use of coupling and tuning equipment. Such efficient use of carrier equipment often justifies an investment in the apparatus that might not be justifiable for a single function alone.

Many functions that require the transmission of intelligence in the form of impulses, such as telemetering and load control, can be performed simultaneously over a single carrier frequency by modulating the carrier with audio-frequency tones. Each tone frequency is in effect a separate carrier channel itself, using the radio-frequency carrier channel as its "conductor". At the receiving end of such a channel, separate tone receivers are operated from the output of the radio-frequency receiver, each individual tone receiver being tuned to receive one particular audio tone and reject the others.

If continuous telemetering and simultaneous emergency communication are desired on a relaying channel, audio tones below 500 cycles can be used for several simultaneous telemetering functions, the audio frequencies above 500 cycles being used for speech. A filter is used to eliminate the tone frequencies from the speech at the sending and

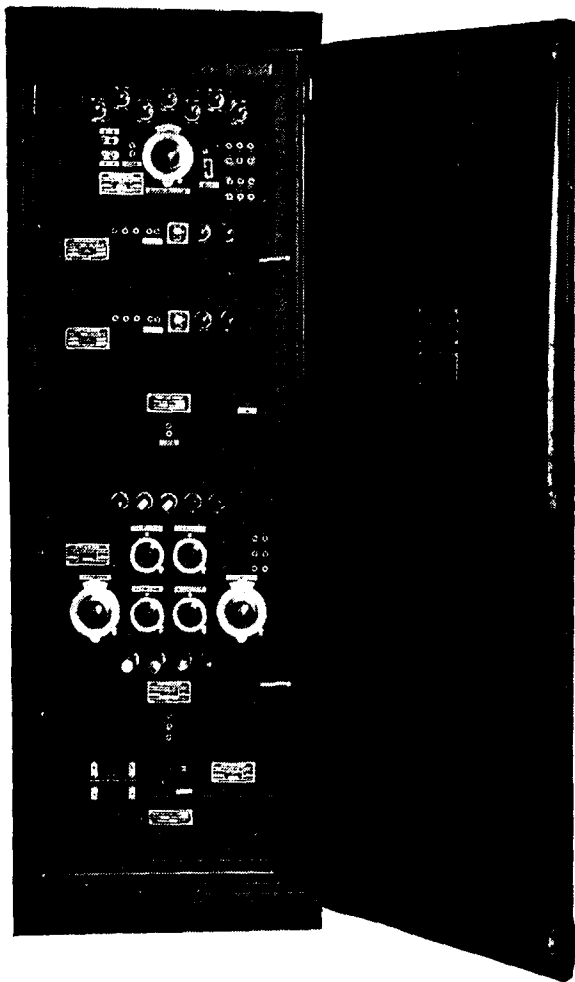


Fig. 10—A carrier assembly for simultaneous voice communication (emergency type), reception of two telemetered indications, and phase-comparison relaying. Top to bottom, carrier transmitter, two tone receivers, modulator, double-carrier receiver, phase-comparison relay control unit, switch and fuse panel, and high-pass filter for removing telemetering tones from speech.

receiving ends. Speech intelligibility is not perceptibly affected by the elimination of the speech frequencies below 500 cycles, because practically all the intelligibility is furnished by the frequencies above this figure. The carrier assembly shown in Fig. 10 is intended for relaying, emergency communication, and simultaneous reception of two telemetering tones.

With supervisory-control equipment, any number of quantities can be telemetered one at a time. Each telemetering function is made a point on the supervisory system, and the dispatcher selects the quantity he desires to read. Communication can be made a point on the supervisory system of single-station supervisory systems, and such supervisory systems can operate over relaying carrier channels.

Single-station supervisory-control systems on point-to-point carrier channels can be used in almost any desired combination with relaying, telemetering, load control, or communication. Two-frequency carrier channels are required for the combination of supervisory control with

continuous functions, such as telemetering or load control.

In multistation supervisory-control systems, all stations must receive all signals. Continuous carrier functions cannot be combined with multistation supervisory control on single-frequency carrier channels, and certain combinations of multistation supervisory control with relaying and communication equipment are not practical. Among these is the combination of supervisory control with multistation automatic simplex communication, and any combination of supervisory control with relaying that involves the use of carrier transmitters outside a protected line section, operating on the same frequency as those within the line section.

18. Modulation Systems

Three different modulation systems are available for use in power-line carrier applications. These are the amplitude modulation, the frequency modulation, and the single-sideband systems^{10,11}. Of these, amplitude modulation is by far the most widely used. In amplitude modulation (a-m) the amplitude or intensity of the transmitted wave is varied in accordance with the waveform of the intelligence to be transmitted. A mathematical analysis of the frequency components of the resulting signal shows that they include the carrier wave itself, unchanged in magnitude, frequency, or phase, plus so-called sideband components, two for each frequency contained in the modulating wave. These sideband components appear at frequencies equal to the carrier frequency plus each modulating frequency (upper sideband components) and carrier frequency minus each modulating frequency (lower sideband components). It is the beating of these sideband components with the carrier in the detector of an a-m receiver that results in the reproduction of the original intelligence at the receiving point.

The bandwidth occupied by an a-m signal is twice the frequency of the highest-frequency modulating signal, and the tuned circuits of an a-m receiver must be sufficiently broad to accept this bandwidth without appreciable attenuation at the extreme frequencies.

Since sideband components occur in pairs, one group above the carrier frequency and one below, it is evident that each sideband group contains all of the intelligence of the original signal. This indicates the possibility of halving the bandwidth required for transmission by suppressing one complete set of sideband components before transmitting the signal. Furthermore, since the carrier wave itself carries no intelligence and requires a large portion of the transmitted power, it is evident that an appreciable saving in power can be made by partially or completely eliminating the carrier wave at the transmitter, emphasizing or regenerating it at a low power level in the receiver.

This is done in the single-sideband system, in which one set of sideband components is suppressed and the carrier is partially or completely suppressed at a low level in the transmitter. If the original peak power used in the transmitter (as an a-m transmitter) is concentrated in the intelligence-bearing components of a single sideband, and if the receiver used has only the necessary bandwidth (half the bandwidth required for a-m service), there is a gain in

signal-to-noise ratio of nine db in favor of single-sideband transmission. Thus, single-sideband transmission offers the equivalent of increasing the original carrier power eight times, and requires only half the bandwidth required by the a-m system.

The frequency-modulation (f-m) system is also used in power-line carrier work. In this system the amplitude or intensity of the transmitted signal is constant and the frequency varies above and below a reference frequency in accordance with the intelligence being transmitted.

The deviation ratio, defined as the ratio of the maximum departure of the frequency from the reference value to the maximum frequency contained in the modulating signal, is a measure of the gain in signal-to-noise ratio of an f-m system over an a-m system of the same power. The f-m system provides marked increases in signal-to-noise ratio as the deviation ratio is increased. However, the minimum bandwidth required by frequency modulation is the same as that for a-m transmission of the same intelligence, and if a deviation ratio large enough to give a worthwhile increase in signal-to-noise ratio is used, the a-m bandwidth must be exceeded.

The frequency-shift system is a special form of frequency modulation that is used for telegraphic functions such as telemetering. In this system two closely-spaced frequencies are used. A continuous carrier wave of constant amplitude is shifted back and forth between the two frequencies, one frequency denoting a "mark" and one a "space" in the transmission of the impulses. By using highly stable crystal oscillators for the transmitted frequencies, and correspondingly stable and highly selective circuits in the receivers, it is possible to place the mark and space frequencies within 0.06 per cent of each other in the carrier spectrum. Even with this spacing, the equivalent f-m deviation ratio with the slow-speed keying required by practical impulse-telemetering systems is extremely high, with the result that a properly-designed frequency-shift system can provide substantial gains in signal-to-noise ratio with a small transmitted bandwidth.

III. PROPAGATION OF CARRIER ON TRANSMISSION LINES

19. Propagation Between Two Phase Conductors

Practically all textbooks on transmission give the classical solution for steady-state voltage and current at any point along a two-wire line^{12,13}. This solution is approximately valid for carrier propagation between two phase conductors of a transposed three-phase power line, because transpositions tend to nullify the effect of the presence of the third conductor. The solution is based on the assumption that the line is composed of an infinite number of resistors and inductors in series, with an infinite number of capacitors and resistors shunting the line at equally-spaced points. This solution can be written as follows:

$$E_s = \left(\frac{E_r + I_r Z_c}{2} \right) e^{(\alpha+j\beta)l} + \left(\frac{E_r - I_r Z_c}{2} \right) e^{-(\alpha+j\beta)l} \quad (1a)$$

$$I_s = \left(\frac{I_r + \frac{E_r}{Z_c}}{2} \right) e^{(\alpha+j\beta)l} + \left(\frac{I_r - \frac{E_r}{Z_c}}{2} \right) e^{-(\alpha+j\beta)l}, \quad (1b)$$

in which E_s and I_s are the sending end voltage and current, respectively.

E_r and I_r are the receiving end voltage and current, respectively.

Z_c is the characteristic impedance as defined in the next paragraph.

$\alpha+j\beta$ is the propagation constant, to be defined later.

l is the distance from the receiving end, in the units of length used to define $\alpha+j\beta$.

20. Characteristic Impedance

Equations (1a) and (1b) show that when a voltage is applied to the sending end of the line, the voltage at any point on the line actually consists of two voltages, one a voltage traveling from the sending end of the line toward the receiving end, the other traveling from the receiving end back to the sending end. The former will be designated as E^+ , the latter as E^- . Each of these voltages is accompanied by a corresponding current, I^+ and I^- , respectively. The ratio of either voltage to its corresponding current at any point in the line is a constant Z_c which is independent of the line length but is a function of the series resistance, the series inductance, the shunt conductance, and the shunt capacitance of the line per unit of length. This constant is the characteristic impedance of the line and can be expressed as

$$\frac{E^+}{I^+} = -\frac{E^-}{I^-} = Z_c = \sqrt{\frac{R+j\omega L}{G+j\omega C}} \quad (2)$$

where R = resistance in ohms per unit length.

L = inductance in henrys per unit length.

G = shunt conductance in mhos per unit length.

C = shunt capacitance in farads per unit length.

and $\omega = 2\pi f$ where f is the frequency in cycles per second.

In actual practice at high frequencies, such as those used in carrier transmission, the quantities $j\omega L$ and $j\omega C$ are so large by comparison with R and G that the latter can be neglected and the characteristic impedance expressed simply as

$$Z_c = \sqrt{\frac{L}{C}} \quad (3)$$

or by applying conventional formulas for L and C as

$$Z_c = 276 \log_{10} \frac{2D}{d} \quad (4)$$

where D is the distance between conductors and d is their diameter in the same units. Ordinary high-voltage transmission lines show characteristic impedances of 600 to 900 ohms between any pair of phase wires. Table 3 of Chap. 9 gives line-to-neutral surge impedances of a number of typical lines. The single-phase surge impedances are twice the values shown in this table.

21. Propagation Constant

Further study of the solution for a two-wire line shows that the phase and magnitudes of the voltage and current traveling toward the receiving end change as they progress along the line. The forward voltage and current at any point can be expressed as

$$E^+ = E_1^+ e^{(\alpha+j\beta)\Delta l} \quad (5a)$$

$$I^+ = I_1^+ e^{(\alpha+j\beta)\Delta l} \quad (5b)$$

where E_1^+ and I_1^+ are the values at some intermediate point on the line at a distance Δl toward the receiving end. Likewise, the voltage and current traveling in the opposite direction, E^- and I^- , change as they progress along the line, for

$$E^- = E_1^- e^{-(\alpha+j\beta)\Delta l} \quad (6a)$$

$$I^- = I_1^- e^{-(\alpha+j\beta)\Delta l} \quad (6b)$$

The quantity $\alpha+j\beta$ is the propagation constant of the line, which can be expressed as

$$\alpha+j\beta = \sqrt{ZY} = \sqrt{(R+j\omega L)(G+j\omega C)} \quad (7)$$

The real part of $\alpha+j\beta$ is an exponent that expresses the reduction of the amplitudes of the forward and reverse voltages and currents as they appear at various points along their respective directions of travel. The imaginary part expresses the phase shift of the voltages and currents that results from the finite time required for the waves to travel from one point to another on the line.

22. Standing Waves

The forward and reverse voltages (and currents) aid and oppose each other at various points along the line, depending upon their respective phase positions. The total voltage and the total current therefore exhibit maxima and minima at equally spaced points separated by a distance that is a function of the frequency, giving rise to the phenomenon of standing waves. The magnitudes of the maxima and minima are a function of the amount of energy reflected from the receiving end of the line.

Standing waves increase the losses in a line as compared with the losses obtained without reflection or standing waves. They also result in increased radiation of energy from the line and other usually undesirable effects.

23. Attenuation

The attenuation of a proposed channel is of prime importance in carrier application, because it determines the fraction of the transmitted energy available at the receiving end to overcome noise and interfering voltages.

If, as in practical open-wire lines at carrier frequencies, the shunt conductance G is negligible and R is small compared to $j\omega L$, the real part of the propagation constant (Eq. 7) can be expressed as

$$\alpha = \frac{R}{2Z_c} \text{nepers per unit of length} \quad (8a)$$

or

$$\alpha = \frac{4.34R}{Z_c} \text{decibels per unit of length.} \quad (8b)$$

The resistance R is the resistance of the conductors per unit of length at the frequency in question. Calculation of R is difficult for the usual transmission line using stranded conductors, because common skin effect formulas apply accurately only to round conductors. Formulas for stranded conductors have been developed, and these give good results for unweathered surfaces and straight parallel strands, but are subject to errors depending on the condi-

tion of the conductor surface and the twisting of the strands in an actual line.

Most of the literature on power-line-carrier transmission reports measured values of attenuation in excess of figures calculated from theoretical considerations. The differences in these cases appear too great to be accounted for by expected errors in the determination of skin effect. For this reason, it is the usual practice in power-line-carrier application to use attenuation figures based on measurements on actual lines, rather than calculated figures. A table of approximate attenuation figures is given in a later section of this chapter.

24. Line Input Impedance

The reverse voltage and current expressed by the second terms of Eqs. (1a) and (1b) result from reflection of the forward voltage and current at the receiving end of the line. Equation (1) shows that if the line is terminated at the receiving end in an impedance equal to its characteristic impedance, Z_c , so that $\frac{E_r}{I_r} = Z_c$, there is no reverse voltage or current; i.e., no reflection at the receiver terminal. Under these conditions the input impedance Z_i at the sending end of the line is the surge impedance Z_c , and the ratio of total voltage to total current everywhere along the line is equal to Z_c . Also, if the line is sufficiently long, the second terms of Eqs. (1a) and (1b) are at the sending end negligible in magnitude by comparison with the first terms, even though the line is not terminated in Z_c . In this case also the input impedance is Z_c . This latter condition is often approached in practical carrier applications on isolated untapped lines. Carrier transmitters and receivers do not ordinarily provide a termination equal to the surge impedance of a line, but most carrier channels are sufficiently long that the input impedance of an isolated line is for practical purposes the characteristic impedance.

A special case that must be considered is that of short tap or spur lines that bridge a line over which carrier energy is to be transmitted. The input impedance of such a line may be extremely low under certain conditions and may constitute practically a short circuit across the carrier channel.

Consider, for example, the case of a low-loss line, open-circuited at the receiving end, one quarter wavelength long at a certain frequency. Voltage of this frequency applied to the input terminals, upon arriving at the receiving end, is reflected toward the source unchanged in magnitude and polarity, and has travelled a total of one-half wavelength by the time it reaches the source. It is exactly 180 degrees out of phase with the voltage being impressed at that instant and practically neutralizes it. It is impossible, therefore, to establish an appreciable voltage across the input terminals of a low-loss quarter wavelength line, because the reflected voltage always opposes any voltage that may be impressed. Such a line therefore appears as practically a short circuit at the particular frequency at which it is a quarter wavelength long.

The same phase relations apply for a line that is any odd multiple of a quarter wavelength long. The greater the number of quarter wavelengths, however, the greater the total attenuation of the voltage along the path from the

source to the open end and back again, so that less and less of the input voltage is neutralized and the line appears to have progressively greater input impedance at the minimum points as its length is increased.

On the other hand, if an open-circuited low-loss line is half wave-length long, current arriving at the receiving end is reflected with reversed polarity. Upon returning to the sending end a full cycle after having entered the line, this reversed current directly opposes the current entering the line and practically neutralizes it at all instants of time. Thus, it is impossible to establish an appreciable current at the input terminals of such a line regardless of the voltage applied. In other words, the input impedance of a half wave-length open-ended line is extremely high. The input impedance of a line that is a multiple of a half wave in length depends upon the attenuation of the current wave along the path from sending end to receiving end and back again. The longer the line the lower is this impedance.

In the case of an open-ended line of a given length, as the frequency is varied over the normal carrier band from 50 to 150 kc, the input impedance of the line oscillates between maxima and minima at frequencies for which the line is half wave and odd-quarter-wave resonant, respectively. At a given frequency, as the length of a practical line is increased, similar maxima and minima occur, but each succeeding maximum and minimum point is closer to the surge impedance of the line. This is illustrated in Fig. 11,

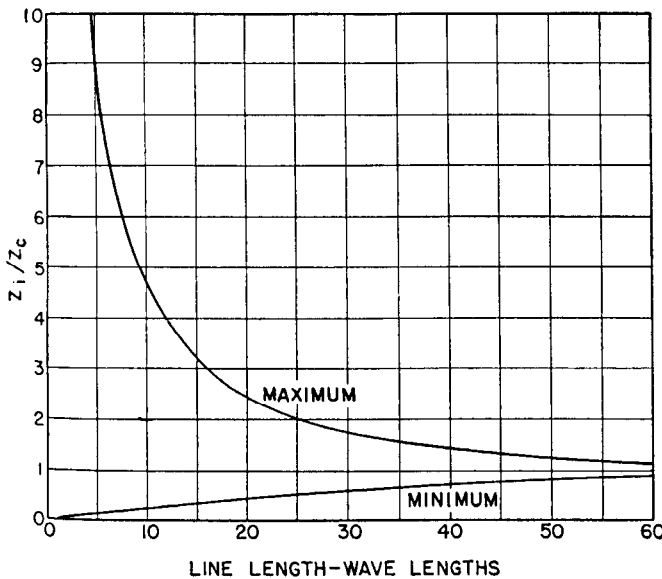


Fig. 11—Envelope of the minimum and maximum input impedance Z_i at 100 kc of a line with attenuation of 0.186 db per wavelength (0.1 db per mile).

which shows the envelope of the input impedance of an open-ended line, having an attenuation of 0.1 db per mile at 100 kc, as the length is increased.

In power systems a line actually terminated in an open circuit at carrier frequencies is rarely encountered. A much more common case is that of short spur or tap lines terminated in power transformers, which at carrier frequencies usually appear as a shunt capacitance of several hundred to several thousand ohms. The effect of a capacitance

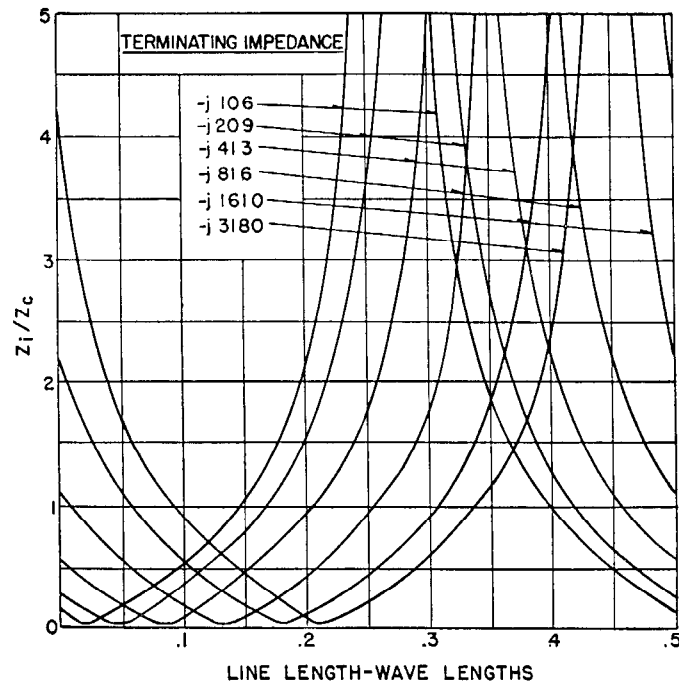


Fig. 12—Input impedance Z_i of a typical line with various capacitive reactance terminations.

termination is to make the line equivalent to a somewhat longer line terminated in an open circuit. For example, Fig. 12 shows the input impedance of a line of 730 ohms characteristic impedance as a function of length for various capacitive reactance terminations.

25. Propagation on Ground-Return Circuits

The equations for the propagation of energy over a circuit consisting of a single isolated conductor with ground return correspond exactly in form with Eqs. (1a) and (1b) for a two-wire circuit. In ground-return carrier transmission on power lines, however, the phenomena are complicated by the presence of the other conductors and the ground wires, because induced currents flow in these paths as a result of their coupling with the conductor to which the energy is initially applied. The equations for this case are much more complicated.

Chevallier has given a symmetrical-component treatment of ground-return carrier transmission on three-phase lines¹⁴. He resolves the applied line-to-ground voltage into positive-, negative-, and zero-sequence components and uses corresponding propagation constants and characteristic impedances with each. His results show that the presumably unused phase conductors actually play an important role as return conductors in line-to-ground transmission. In practical cases, at a distance of 50 miles or so from the terminals on long lines without ground wires, the amount of carrier current that flows in the ground is negligible in comparison with that returning to the source via the two opposite conductors in parallel.

The general equations derived by Chevallier include both the forward and reverse components of voltage and current for voltage applied in any manner to the line; i.e., phase-to-phase, phase-to-ground, or otherwise. Of greatest in-

terest is the case of line-to-ground coupling on long or properly terminated lines, in which reverse voltage and currents can be neglected. The equations are simplified in this case, and with carrier voltage E_s applied between phase one and ground, as shown in Fig. 13, the voltages to

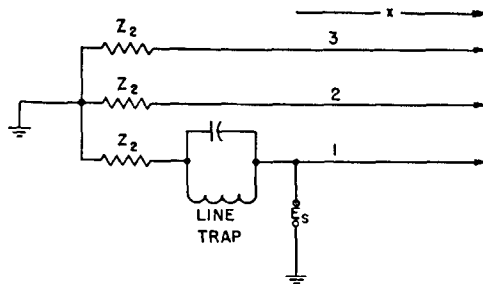


Fig. 13—Configuration assumed in discussion of propagation on ground return circuits. The impedances Z_2 may be lumped impedances or may be a continuation of the transmission line.

ground on phases 1, 2, and 3 at a distance x from the transmitting point are:

$$E_1 = \frac{E_s}{1+2Z'} e^{-k_0 x} + \frac{2Z'}{1+2Z} E_s e^{-kx}. \quad (9a)$$

$$E_2 = \frac{E_s}{1+2Z'} e^{-k_0 x} - \frac{Z'}{1+2Z} E_s e^{-kx}. \quad (9b)$$

$$E_3 = E_2. \quad (9c)$$

and the corresponding currents are:

$$I_1 = \frac{1}{Z_0} \frac{E_s}{1+2Z'} e^{-k_0 x} + \frac{2Z'}{Z(1+2Z')} E_s e^{-kx} \quad (10a)$$

$$I_2 = \frac{1}{Z_0} \frac{E_s}{1+2Z'} e^{-k_0 x} - \frac{1}{Z} \frac{Z'}{1+2Z} E_s e^{-kx} \quad (10b)$$

$$I_3 = I_2 \quad (10c)$$

In which

k_0 = zero-sequence propagation constant (propagation constant for voltage applied to all three phases in parallel, with ground return).

Z_0 = zero-sequence characteristic impedance (characteristic impedance of all three phases in parallel, with ground return).

k = Positive- or negative-sequence propagation constant (propagation constant for a three-phase carrier frequency wave; i.e., square root of the product of line-to-neutral impedance and line-to-neutral admittance.)

Z = Positive- or negative-sequence characteristic impedance, line to neutral.

$$Z' = \frac{Z}{Z_0} \frac{Z_0 + Z_2}{Z + Z_2}$$

Z_2 = Load impedance (to neutral) on phases 2 and 3 at coupling point. See Fig. 13.

The first term in each of these equations is a zero-sequence term. The attenuation of the zero-sequence terms is high on lines without ground wires, because of the high resistivity of the ground return path. These terms become negligible on long lines in comparison with the positive-

and negative-sequence terms at a certain distance from the coupling point, and propagation takes place almost entirely between the coupled phase and the other two. The return current divides equally between the latter.

It has been noted that the attenuation per unit of distance is greater on short line-to-ground channels than on long line-to-ground channels⁸. Equations (9) and (10) provide at least a partial explanation of these results.

At the receiving point the current in the two uncoupled phases causes a loss of energy in the terminating impedances of these phases beyond the receiving point. This loss and the corresponding loss in the terminating impedances on the opposite side of the transmitting point account for the extra attenuation noticed in long line-to-ground channels as compared with phase-to-phase channels, according to Chevallier's results.

26. Characteristic Impedance of Ground-Return Circuits

The characteristic impedance of a circuit consisting of a single conductor with ground return is

$$Z_c = 138 \log_{10} \frac{2h}{r} \quad (11)$$

where h is the height of the conductor above ground and r is its radius in the same units. Typical values for phase-to-ground carrier channels range from 400 to 600 ohms. The characteristic impedance of a transmission-line conductor with ground return is not greatly affected by the presence of the other conductors.

IV. NOISE VOLTAGE ON TRANSMISSION LINES

Since signal-to-noise ratio is the main criterion of the performance of a carrier transmission system, the noise level present at the receiving end of a carrier channel is equally as important to successful operation as the attenuation of the transmission path. The most important noise in a carrier system is that which originates in the power system itself; atmospheric noise is negligible, except that caused by nearby lightning strokes. The normal noise in a transmission system is the result of the presence of innumerable small arcs in dirty or defective insulators, poor joints, and the like. This condition is aggravated by wet weather, and is sometimes accompanied by corona discharge during such periods, with the result that noise usually increases to several times its normal amount. Noise also varies with the time of day under good weather conditions. Superimposed upon this normal or steady noise is the noise caused by switch operations, faults, etc.

27. Types of Noise^{18,21,22}

Noise from whatever cause can be classified under two general headings: random noise and impulse noise. Random noise has a continuous frequency spectrum, containing all frequencies in equal amounts. At the output of a receiver it produces a steady hissing or rushing sound. The rms amplitude of this type of noise at the output of a receiver is proportional to the square root of the bandwidth of the receiver; i.e., the noise power is proportional to the band-

width. The average and peak amplitudes are also proportional to the square root of the bandwidth.

Impulse noise is of far greater importance in carrier systems. It is produced when discrete, well-separated pulses exist at the input terminals of a receiver. If the pulses are irregular, the frequency spectrum is continuous and depends only slightly upon frequency. If the impulses are uniform and regularly spaced, the spectrum contains discrete frequency components separated by a frequency corresponding to the repetition rate. Power-line noise is essentially a combination of these two types of impulses, since basic repetition rates of 60 and 120 cycles are discernible along with random discrete pulses, all of irregular amplitude.

28. Response of a Receiver to Impulse Noise¹⁸

When a sharp impulse is applied to the input terminals of a receiver, the signal at the detector input is a damped oscillation having the natural resonant frequency of the preceding tuned circuits. The envelope of this oscillation, which represents the output of the receiver after detection, rises to a peak value at a certain time and then decays to zero. The greater the number of tuned circuits and the greater their *Q*, the more slowly the envelope of the oscillation rises to a maximum and the lower its peak value; i.e., the peak output is proportional to receiver bandwidth. However, the total area of the output signal envelope, and hence the average output, are independent of these factors. In practice, if the impulses are sharp and well separated, the rms output is independent of the shape of the impulses and is dependent only upon their areas, the gain of the receiver, and the square root of the receiver bandwidth. If the impulses are not well separated, so that in a receiver of a given bandwidth the resulting wave trains overlap, the response of the receiver simulates that for a combination of random noise and impulse noise. In some applications the peak output is of major importance, whereas in others the average or the rms output is the critical factor.

Thus, in specifying the characteristics of noise on transmission lines, it is necessary to state not only the relative amounts of random and impulse noise in a given bandwidth, but also the peak values of the impulses (or their statistical distribution) and the duration and spacing of the individual impulses. In order to evaluate the effect of this noise upon a given receiving system, it is necessary to know the receiver bandwidth and gain and the particular application involved. The number of tuned circuits and their *Q* determine the receiver bandwidth at a given frequency.

29. Measurement of Carrier-Frequency Noise on Power Lines

The accurate measurement of all the characteristics of carrier-frequency noise on transmission lines requires a considerable amount of equipment, including a noise meter of definite bandwidth, capable of measuring peak impulse amplitudes, and an oscilloscope to indicate the spacing and the duration of the impulses. In order to be significant, readings should be taken over a period of time sufficient to include both fair and rainy weather. As a result, actual test data of this type on carrier-frequency noise is ex-

tremely limited, and no typical figures for "quiet" or "noisy" lines have been established.

Figure 14 shows the results of one set of measurements made during fair weather on a 132-kv line that can be classified only as "relatively noisy" for carrier. These measurements were made with a Stoddart Type URM-6

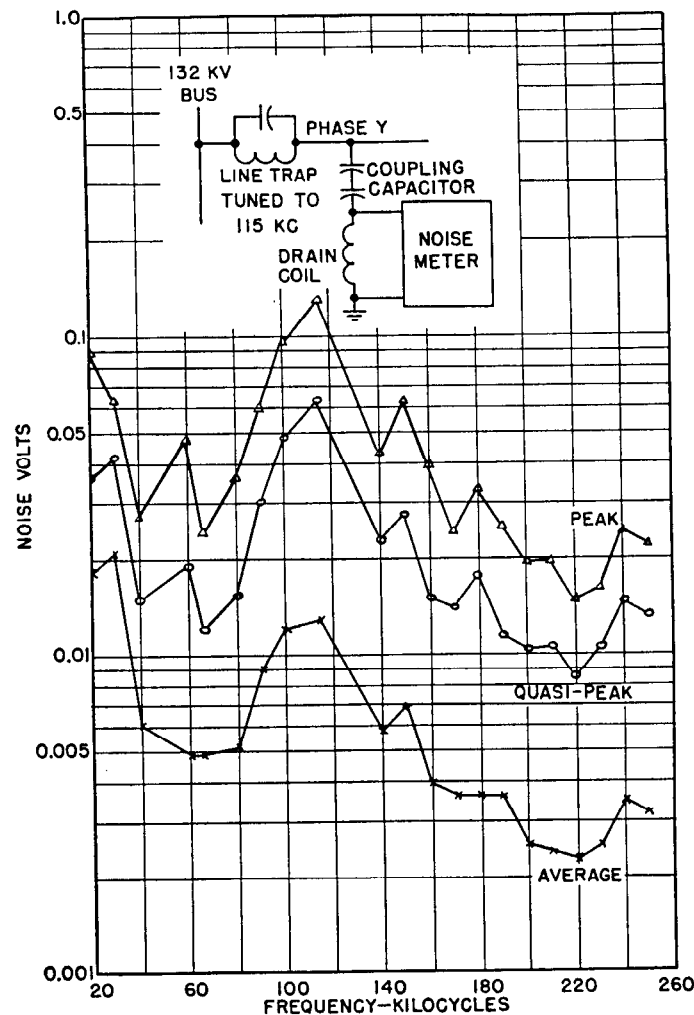


Fig. 14—Noise voltages as a function of frequency on a relatively noisy 132-kv line. The rise in the vicinity of 115 kc is probably accounted for by the presence of the line trap.

noise meter. The curves show that the peak values of noise on this line are far in excess of the average values, indicating that average-reading instruments do not give a true indication of the probable interfering effects of noise for all applications. A graphic record of quasi-peak values* over an extended time, including periods of rainy weather, gave the curves of Fig. 15, which indicate a relatively great increase in the noise under some conditions, with maximum quasi-peak values exceeding 100,000 microvolts for approximately 3 percent of the time.

*Quasi-peak readings are based on a fast detector output circuit charging time and a slow discharging time, and hence are a function of the peak amplitudes as well as the spacing of the impulses. The times are chosen so that the quasi-peak readings are approximately proportional to the interfering properties of impulse noise in aural reception of a-m signals.

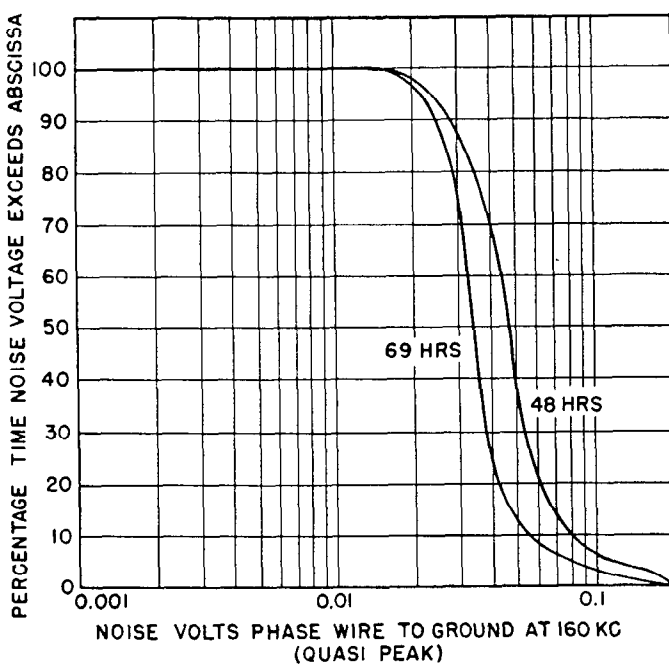


Fig. 15—Quasi-peak noise voltages at 160 kc taken over two extended periods on the same 132-kv line. Both periods included rainy as well as fair weather.

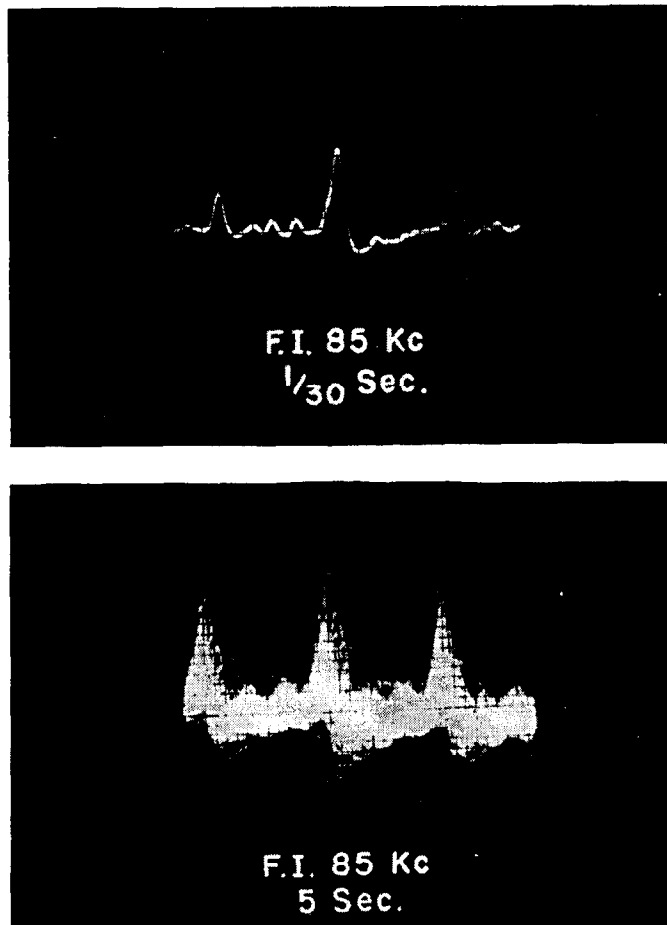


Fig. 16—Oscilloscope patterns of carrier noise at 85 kc with 1/30 second and 5 second exposures.

Cathode-ray oscilloscope patterns of the output of the detector of the noise meter used are shown in Fig. 16. These indicate irregularity in the pulses, even with 1/30-second exposures. The five-second exposure shows that although the basic system frequency is present in the amplitudes, the pulses occur almost at random throughout the cycle. It must be remembered that these pulses have undergone a smoothing and rounding effect as a result of the action of the tuned circuits in the noise meter and that the actual pulses at the input of the meter were sharper and of shorter duration than those shown in the photographs.

V. COUPLING AND TUNING EQUIPMENT AND CIRCUITS

In the early days of power-line carrier it was universal practice to couple the carrier equipment to the power line by a method known as antenna coupling. In this method the carrier equipment was connected to an isolated conductor, several spans long, on the same tower with the circuit to which coupling was to be effected. Eventually it was realized that the energy which found its way into the power line was transferred mainly through the capacitance between the antenna and the line, and this led to the development of compact capacitor units for coupling purposes. Such coupling capacitors are safer, easier to install, and are a more efficient coupling means than antennas. They also have the advantage that they can be used simultaneously in conjunction with potential devices to supply a voltage proportional to line voltage for the operation of protective relays and indicating instruments.

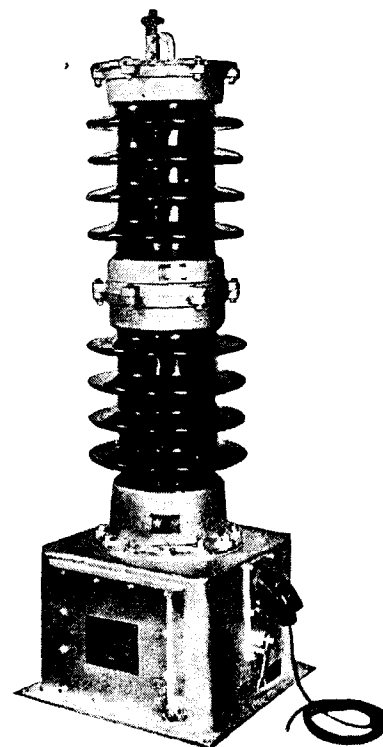


Fig. 17—Typical carrier coupling capacitor. This unit is rated at 115 kv and has a total capacitance of .00187 mfd.

30. Characteristics of Coupling Capacitors

A typical carrier coupling capacitor is shown in Fig. 17. The capacitor element proper is contained in a cylindrical porcelain housing with cast metal ends. The capacitor elements consist of a large number of individual working sections in series. Each working section is made up of an assembly of special paper and foil, non-inductively wound and impregnated.

Individual capacitor units are made up in several different voltage ratings, and one or more such individual capacitor units can be used in a stack to make up the complete coupling capacitance. The stack is mounted on a metal base that contains a grounding switch, a protective gap, and a carrier drain coil. These are connected as shown in Fig. 18. The purpose of the drain coil is to ground the

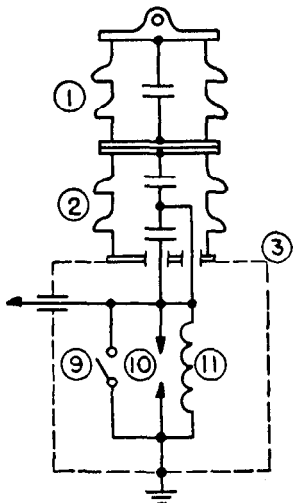


Fig. 18—Schematic of carrier coupling capacitor without potential device.

- (1) Coupling Capacitor
- (2) Multi-Unit Coupling Capacitor
- (3) Base Housing
- (9) Carrier Apparatus Grounding Switch
- (10) Carrier Apparatus Protective Gap
- (11) Carrier Drain Coil

capacitor terminal opposite the line terminal at 60 cycles and at the same time offer a high impedance at the carrier frequency. The grounding switch is used to by-pass the drain coil, providing a means of directly grounding the capacitor during inspection and maintenance of the coupling and tuning equipment. The gap protects the drain coil from excessive surge voltages during normal operation.

The capacitances of typical coupling capacitors of various standard voltage ratings are shown in Table 1, along with typical impulse and low-frequency test voltages. A typical power factor for coupling capacitors at carrier frequencies is 3 percent.

A diagram of a coupling capacitor with a potential device included in the base housing is given in Fig. 19. The potential device is essentially a transformer connected across a portion of the capacitance of the lower or base unit, deriving therefrom a voltage proportional to line voltage in accordance with the potential dividing proper-

TABLE 1—CHARACTERISTICS OF TYPICAL COUPLING CAPACITORS

System Voltage kv	Average Coupling Capacitance mfd.	Average Capacitance of Tap for In-Phase Potential Device mfd.	Low Frequency Test RMS kv		Impulse Test Crest kv, (+) or (-) 1.5×40μS Full Wave
			One Minute Dry	Ten Seconds Wet	
46	.004	.0205	110	100	250
69	.00275	.0225	165	145	350
92	.002	.0205	215	190	450
115	.00187	.0225	265	230	550
138	.00137	.0225	320	275	650
161	.00125	.0225	370	315	750
230	.00094	.0225	525	445	1050
287	.00075	.0225	655	555	1300

Note: If in-phase potential device is used, total capacitance for carrier is tap capacitance in series with coupling capacitance. If in-phase potential device is not used, tap capacitance is short-circuited.

ties of the capacitor string. A variable-reactance transformer is provided for adjusting the phase angle of the derived voltage, and a voltage-adjusting transformer is provided for adjusting its magnitude. The potential device is connected to the capacitor through a carrier-frequency choke coil that isolates the device from the capacitor at carrier frequencies.

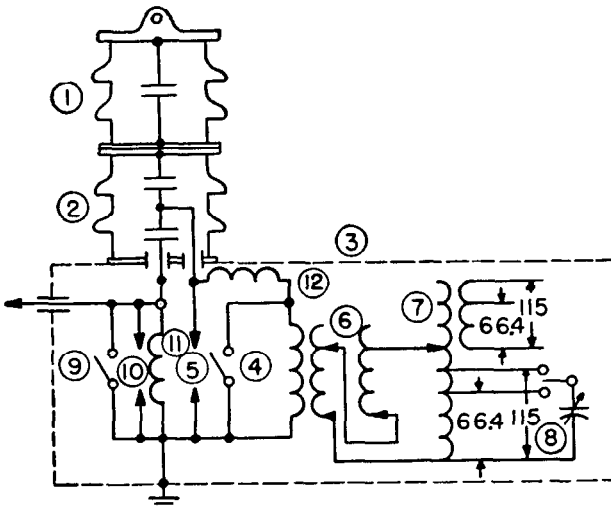


Fig. 19—Schematic of carrier coupling capacitor with potential device. A larger base than the one shown in Fig. 17 is used when the potential device is included.

- (1) Coupling Capacitor
- (2) Multi Unit Coupling Capacitor
- (3) Base Housing
- (4) Transformer Grounding Switch
- (5) Transformer Protective Gap
- (6) Variable Reactance Transformer
- (7) Voltage Adjusting Transformer
- (8) Power Factor Correction Capacitor
- (9) Carrier Apparatus Grounding Switch
- (10) Carrier Apparatus Protective Gap
- (11) Carrier Drain Coil
- (12) Carrier Choke Coil

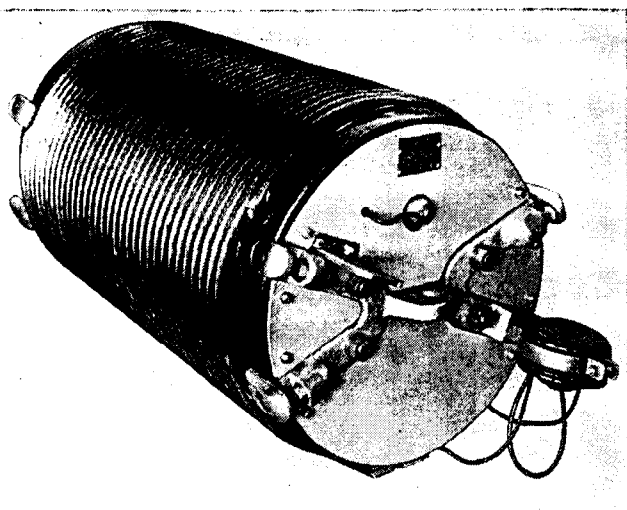


Fig. 20—Typical 400-ampere carrier line trap. (Type P-400).

31. Characteristics of Line Traps¹⁶

A line trap is a parallel resonant circuit tuned to offer a high impedance at a specific carrier frequency and inserted in series with one of the conductors of a transmission line. Line traps have negligible impedance at power frequencies and therefore do not affect normal power current.

A previous discussion in this chapter pointed out the deleterious effect that short spur or tap lines may have when bridged across a carrier channel. Such lines can be isolated from the carrier system by the insertion of line traps in series with one or more conductors of the spur line at its junction with the main line. Loops that offer alternate paths to the carrier current can be broken up by use of line traps. A line trap is always used at each end of a line section to which carrier relaying is applied. Their major purpose in this application is to prevent a nearby fault on an adjacent line section from short-circuiting the carrier channel and interrupting the transmission of a blocking signal to the opposite end of the line. In general, line traps provide a means of raising signal levels by confining the major portion of the carrier energy to its intended path and by isolating sources of high attenuation from the carrier circuit.

A typical carrier line trap is shown in Fig. 20. This unit is rated at 400 amperes at 60 cycles. The main coil is a heavy copper cable, capable of carrying the full power

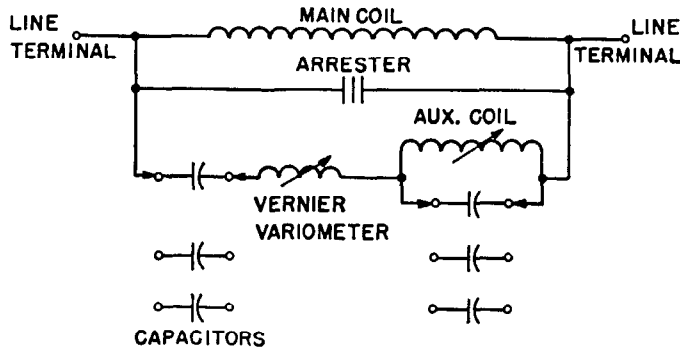


Fig. 21—Schematic of double-frequency line trap. (Type PDF-400).

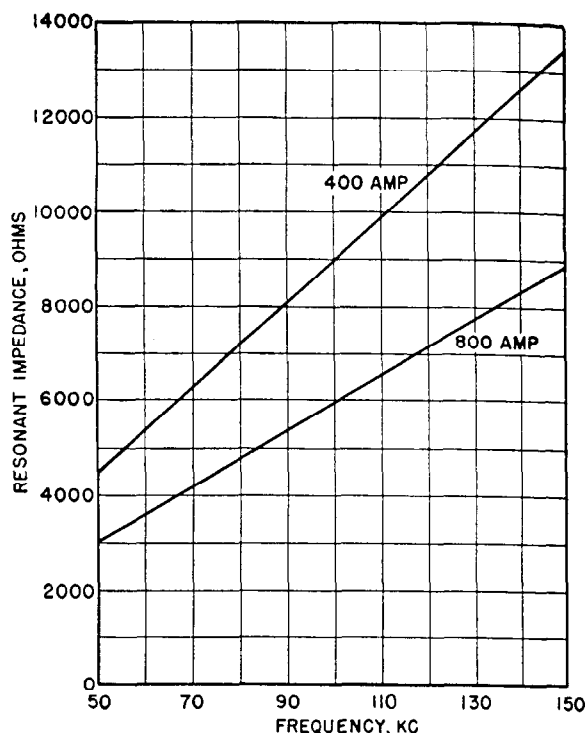


Fig. 22—Resonant impedance of typical 400- and 800-ampere line traps. The difference in impedance is due to the different inductances used in the two ratings.

current of the conductor into which it is inserted. This coil is wound on a porcelain cylinder, which also serves as a housing for the adjustable capacitor unit used to tune the coil to resonance at the desired frequency. A lightning arrester is provided across the trap to protect the capacitor unit from damage due to surges.

Manufacturers have standardized on 400 and 800 ampere ratings for line traps, and single- and double-frequency

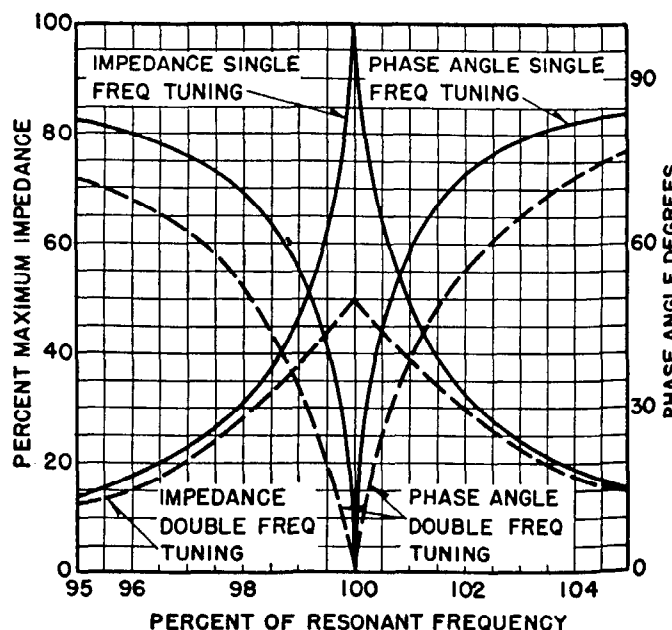


Fig. 23—Resonance curves of typical single- and double-frequency line traps.

models are available in both ratings. A schematic diagram for a double-frequency trap is shown in Fig. 21. The external appearance of a double-frequency trap is the same as that of a single-frequency trap of the same rating, because the extra circuits used to obtain the double-resonance characteristic are contained inside the main coil, which is the same in both cases.

The resonant impedances of typical 400- and 800-ampere line traps over the 50-150-kc band are given in Fig. 22. The difference in the two curves results from the difference in the inductances of the coils used in the two ratings. Figure 23 gives resonance curves for typical 400- and 800-ampere single-and double-frequency traps.

When a line trap is used to isolate a low-impedance circuit, the losses are not reduced to zero but to a value that is a function of the characteristic impedance of the carrier channel and the impedance of the trap in the vicinity of resonance. Figures 24 and 25 are curves of the losses in typical single- and double-frequency traps respectively when a line-to-ground channel of 500 ohms characteristic impedance is grounded through them. Losses in practical applications are somewhat less, depending upon the actual impedance of the offending circuit or device, and the losses shown by these curves should be taken as limiting values.

A single line trap at the end of a line-to-ground coupled channel does not materially reduce interference to channels on the same or nearby frequencies on lines beyond the trap, because it does not interrupt the current in the two un-

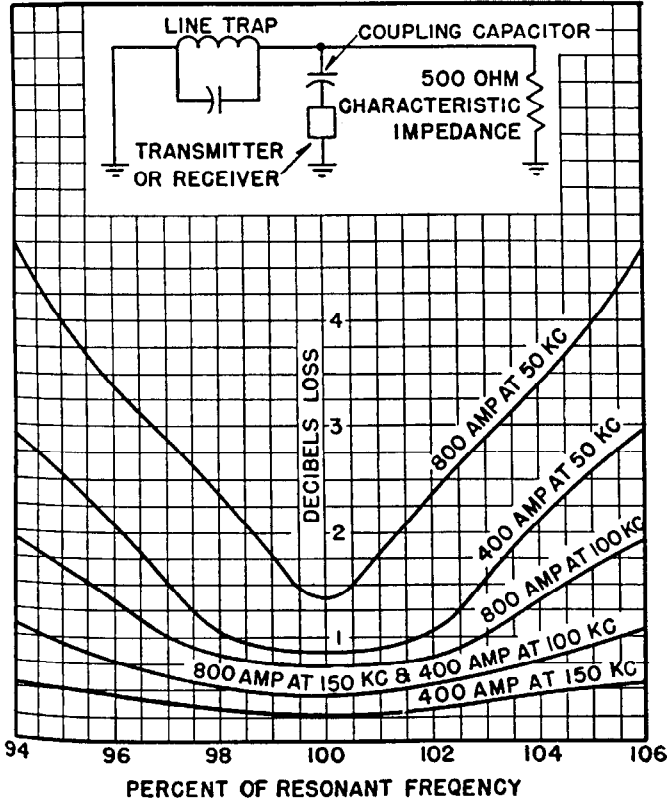


Fig. 24—Losses in typical 400- and 800-ampere single-frequency line traps when a line-to-ground carrier channel of 500 ohms characteristic impedance is short-circuited through them.

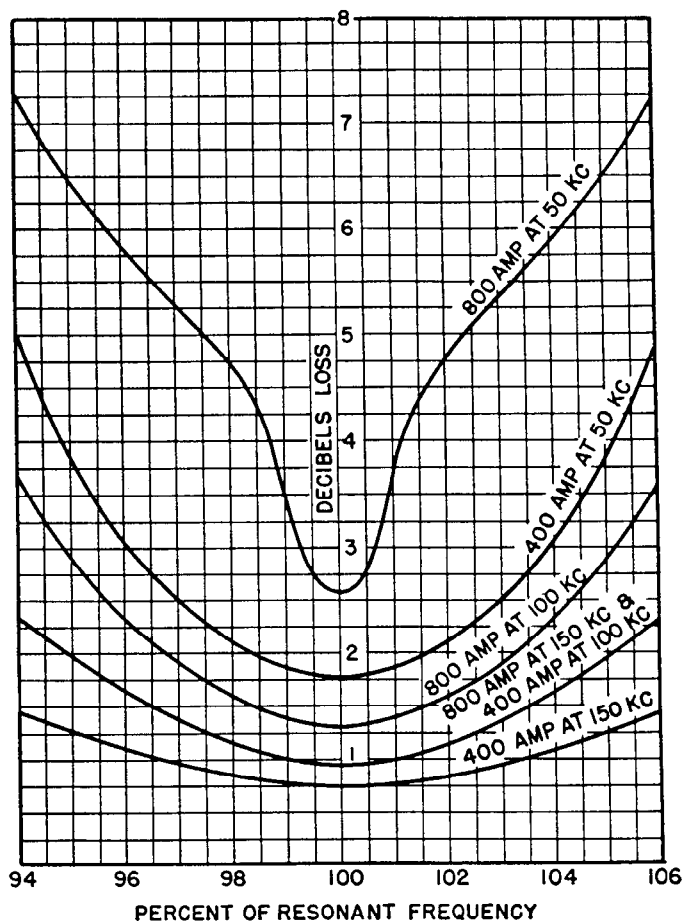


Fig. 25—Losses in typical 400- and 800-ampere double-frequency line traps when a line-to-ground carrier channel of 500 ohms characteristic impedance is short-circuited through them.

coupled phases. Two line traps, one in each phase conductor of an interphase coupled channel, are more effective in this regard. Even in this case, however, there is usually sufficient unbalance in the system at carrier frequencies to cause appreciable current in the unused conductor, with resulting interference to channels beyond the trap location. The installation of a line trap in each of the three phases of a line is the only effective way of isolating a channel for the purpose of reducing interference, regardless of the method of coupling used. For this method to be successful, there must be no important sources of coupling between circuits on opposite sides of the line traps. This means that these lines must extend in opposite directions from the trap location and must not be paralleled by untrapped lines. The degree of interference reduction obtained then is a function of the resonant trap impedance, the characteristic impedance of the lines in question, and the amount of coupling that remains between the ends of the circuits on opposite sides of the line traps.

32. Tuning Devices

The load resistances presented by power-transmission lines at carrier frequencies range from 400 to 900 ohms, and the reactances of coupling capacitors, which are effectively in series with this load, are appreciable and must be

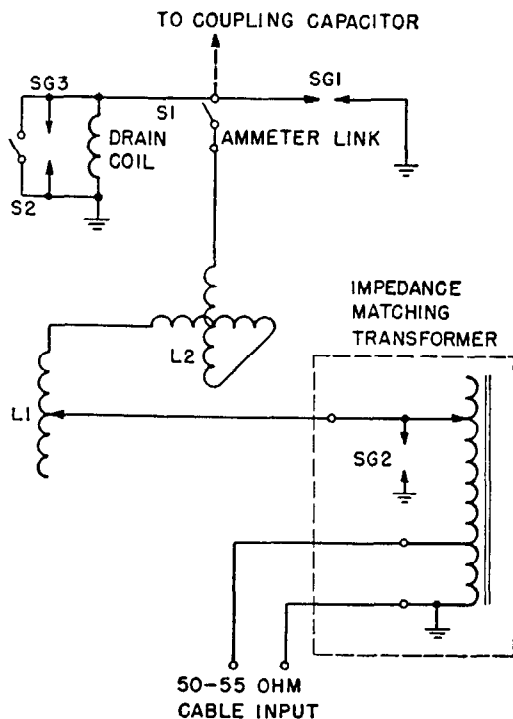


Fig. 26—Circuit diagram of single-frequency phase-to-ground line tuner. Switch S2, Gap SG3, and Drain Coil are omitted if included in coupling capacitor assembly.

compensated for if maximum coupling efficiency and a resistive load condition for the carrier transmitter are to be obtained. This compensation can be provided by placing in series with the capacitor an inductance that can be adjusted so that its reactance cancels the reactance of the coupling capacitance at the carrier frequency. The primary purpose of a line tuning unit is to furnish an adjustable inductance for this purpose. This inductance usually takes the form of a tapped main coil, which furnishes large steps in inductance, in series with a variometer that pro-

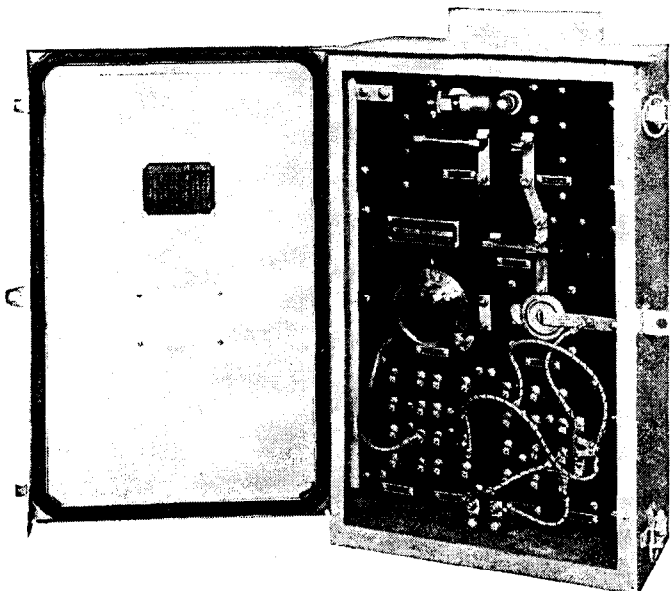


Fig. 27—Typical single-frequency phase-to-ground tuner.

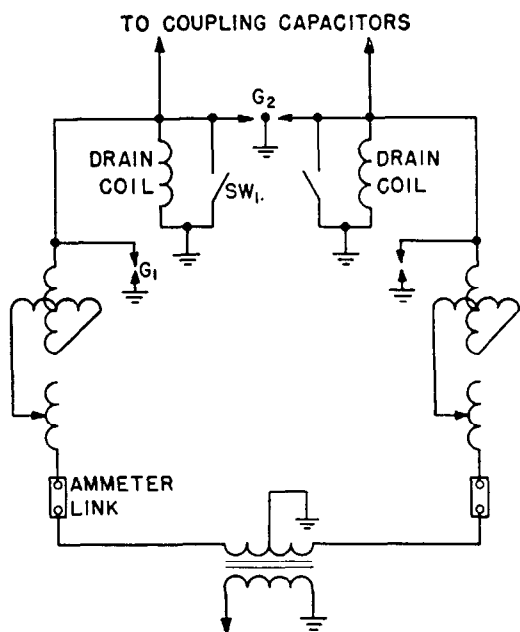


Fig. 28—Schematic diagram of an interphase single-frequency line tuner.

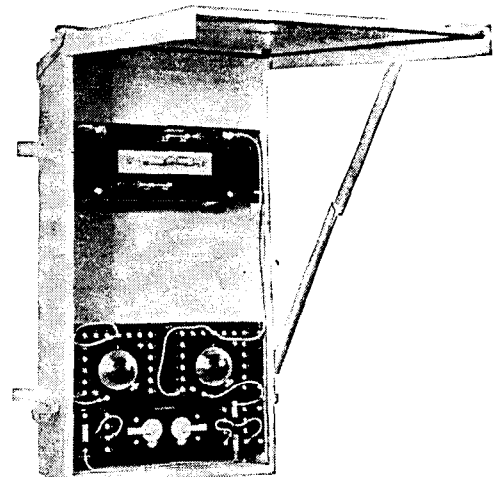


Fig. 29—A typical interphase line tuner.

vides a continuous range between tap values. Line tuners also include an impedance-matching transformer for transforming the characteristic impedance of the line to a value that properly terminates the coaxial cable commonly used between the carrier assembly and the line.

A schematic diagram of a typical single-frequency tuner, used to couple the carrier energy to a single phase conductor, is shown in Fig. 26. Figure 27 is a typical tuner of this type. Ground is used as the return circuit with this tuner. A protective gap is provided to prevent overvoltages from damaging the tuning inductances. The grounding switch is used to ground the lead from the coupling capacitor during inspection or adjustment of the tuner.

A phase-to-phase tuning unit is shown in Figures 28 and 29. In this unit two identical inductance coils and variometers are provided, one set for each capacitor. The

impedance-matching transformer is balanced to ground by means of a center tap on the line side.

33. Multi-Frequency Tuning

It is often necessary to provide for the coupling of more than one carrier frequency to a line at a given location. In such cases a worthwhile economy can be effected by the use of a multi-frequency tuning system, which permits a single coupling capacitor to be tuned to two separate carrier frequencies.

A schematic diagram of a two-frequency tuner for line-to-ground coupling is given in Fig. 30. The equipment consists essentially of two single-frequency tuners, in series

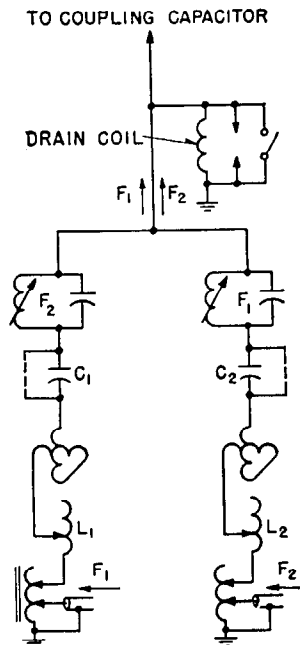


Fig. 30—Two-frequency line-to-ground tuning system with separate coaxial leads for each frequency.

with each of which a parallel-resonant trap circuit has been added. Each trap circuit is tuned to the carrier frequency which is to be passed through the tuning inductance in the opposite branch. Thus, if a frequency F_1 is to be passed through inductance L_1 , the trap circuit in series with the opposite branch is tuned to F_1 to prevent the carrier energy from being lost in that branch. Likewise, the trap circuit in series with the first branch is tuned to the opposite frequency F_2 to prevent loss of energy from source two. A photograph of a typical two-frequency tuner utilizing the system just described is shown in Fig. 31.

The trap circuits have appreciable reactance at frequencies off resonance, and for this reason the main series inductances cannot be finally tuned until the trap circuits have been individually adjusted to the proper frequencies. At frequencies below resonance, a trap circuit has inductive reactance that increases as the resonant frequency is approached. The branch that is to be tuned to the lower frequency, therefore, requires less inductance for overall series resonance than a single-frequency tuner used with

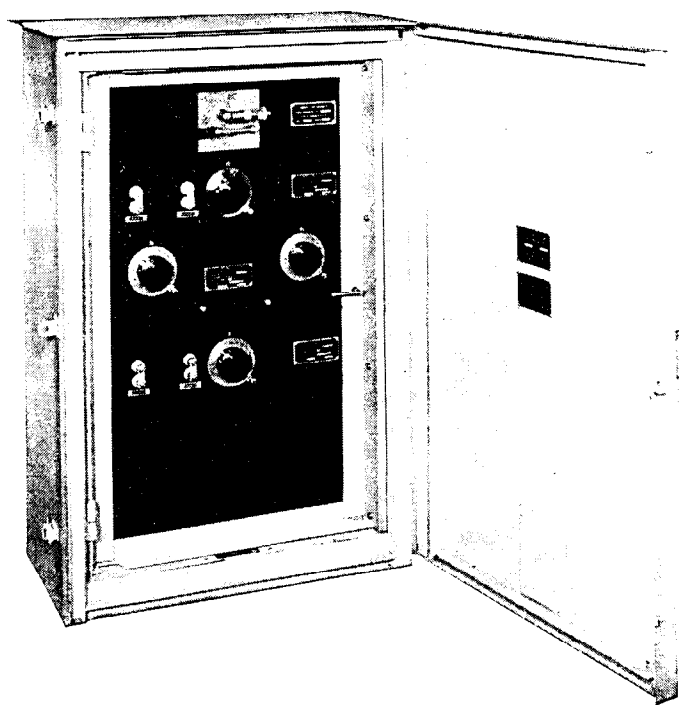


Fig. 31—A typical two-frequency line-to-ground tuning assembly of the type shown in Fig. 30.

the same coupling capacitor. Correspondingly, the branch that is to be tuned to the higher frequency requires more inductance than normal because the reactance of the associated trap circuit is capacitive. If the two frequencies are too close together, the additional reactances presented by the wave traps are so high that the overall series circuits cannot be tuned to resonance at the desired frequencies with ordinary tuning inductances. The separation required between the two frequencies depends upon the capacitance of the coupling capacitor and the inductance range available in the tuning inductances, but in general, the higher frequency must be at least 25 percent greater than the lower for satisfactory tuning with tuning inductances of the usual range. When the frequencies are too close to permit tuning as above, it is sometimes possible to obtain series resonance at the lower frequency by adding a fixed capacitor in series with the trap circuit to neutralize some of the excess inductive reactance obtained. This is the purpose of the fixed capacitors C_1 and C_2 shown in Fig. 30. It must be kept in mind that losses in the trap circuits increase rapidly as the frequency separation is reduced, however, so that every effort should be made to locate the channels in the spectrum with sufficient separation to avoid this expedient.

This system of multi-frequency tuning can be extended theoretically to handle as many separate frequencies as desired. For example, Fig. 32 illustrates a three-frequency system. In this case the trap circuits in each series leg are tuned to the frequencies of the opposite two legs. From a practical standpoint, however, it is generally inadvisable and uneconomical to attempt to tune a single capacitor to more than two frequencies. The complexity of the tuner and the difficulty involved in tuning it successfully to three

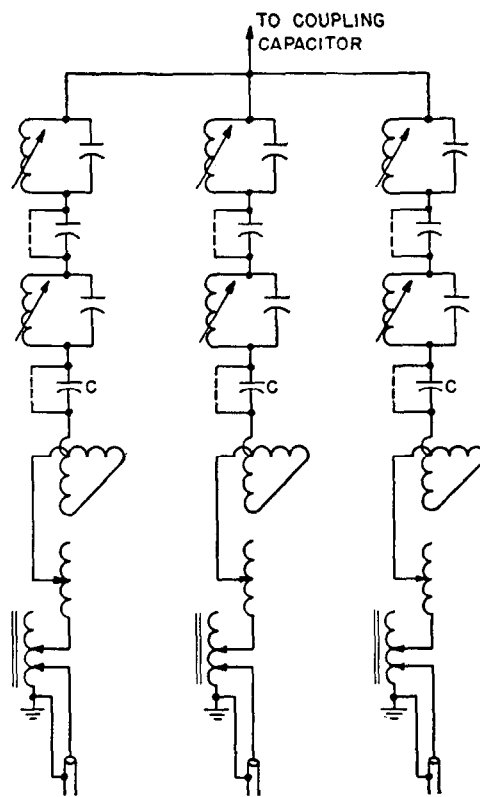


Fig. 32—Three-frequency tuning of a single coupling capacitor.

different frequencies nearly always outweighs any saving effected in equipment.

Another tuning circuit, which is series resonant to two frequencies and requires only a single co-axial lead, is shown in Fig. 33. The procedure for adjusting this circuit is to short-circuit the L_1C_1 combination and adjust L to series resonance with C at the higher of the two frequencies. With the short circuit removed, and with L_2 disconnected, L_1 and C_1 are then tuned to series resonance at the same frequency. L_1 and C_1 then effectively short circuit L_2 at the upper frequency, and its inductance, regardless of its value, has no effect at this frequency. At any lower fre-

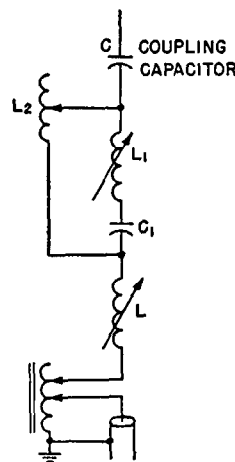


Fig. 33—A two-frequency tuning system requiring only a single coaxial lead.

quency, the L_1C_1 circuit shows a net capacitive reactance. This reactance is tuned in combination with L_2 to parallel resonance at a frequency intermediate between the upper and lower frequencies desired. Below this parallel resonant frequency, therefore, the $L_1C_1L_2$ combination appears inductive, the magnitude of the inductive reactance depending upon the intermediate frequency chosen. By varying this frequency by adjusting L_2 , the net inductive reactance of the $L_1C_1L_2$ combination in series with the main tuning inductance L can be made to tune the entire circuit to series resonance at the lower frequency.

If the double-frequency tuning scheme described above is used for coupling two transmitters to a line at a single location, trap circuits must be used at the transmitter output circuits to avoid the loading of one transmitter by the output circuit of the other when both work into a single coaxial cable.

34. Omission of Outdoor Tuning Equipment

On many carrier channels the terminal equipment is capable of operating through much greater attenuation than that introduced by the line itself. In such cases some economy in installation can be effected and greater convenience in making tuning adjustments can be provided by eliminating the usual outdoor tuning equipment and supplying equivalent units in the carrier assembly. In such cases the coaxial cable is usually connected directly to the coupling capacitor at the line terminal, as shown in Fig. 34. Some reduction in the resultant losses in the cable, due to the impedance mismatch at the junction of the cable and the capacitor, can generally be effected by using an impedance matching transformer at the coupling capacitor, as shown in Fig. 35. Such a transformer can make the terminating impedance equal in magnitude to the

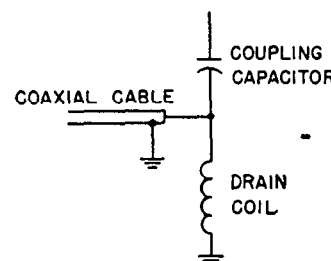


Fig. 34—Omission of outdoor tuner and matching transformer.

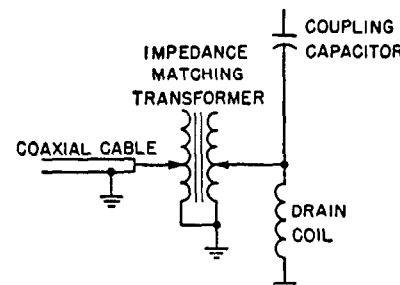


Fig. 35—Omission of outdoor tuner, matching transformer used to match absolute value of line and coupling capacitor impedance to coaxial cable impedance.

surge impedance of the cable, but it cannot compensate for the capacitive component of the combined line and coupling capacitor impedance.

The loss in a given length of coaxial cable in such installations is dependent upon the frequency involved, the reactance of the coupling capacitor, and the surge impedance of the line, as well as upon the characteristics of the coaxial cable itself. The curves of Fig. 36 show the mea-

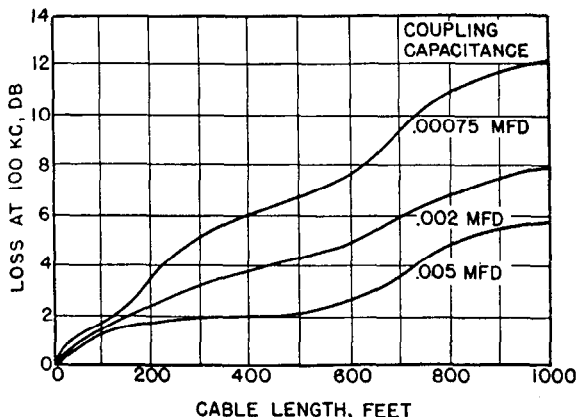


Fig. 36—Measured attenuation at 100 kc of various lengths of coaxial cable operating directly into 900-ohm resistive load through coupling capacitances shown. No impedance matching transformer used (Fig. 34).

ured db loss at 100 kc with various lengths of a typical coaxial cable, operating into a 900 ohm line through coupling capacitors of several different ratings. These curves apply for the case where no matching transformer is used at the coupling capacitor. For the case where a matching transformer is used, F. M. Rives¹⁵ has published similar data, giving the maximum length of coaxial cable permissible for given db losses at several different fre-

TABLE 2

Coupling Capacitance mfd.	Recommended Maximum Cable Lengths in Feet from Coupling Capacitor to Terminal Equipment Matching Transformer Used Without Tuning Equipment					
	For 1-db Attenuation			For 2-db Attenuation		
	50 kc	85 kc	150 kc	50 kc	85 kc	150 kc
.00075	150	180	200	300	350	410
.001	200	230	250	390	430	600
.0012	240	270	300	430	500	750
.0015	260	300	340	500	600	800
.002	360	390	460	680	800	1000
.003	450	450	475	900	1000	1000
.006	800	800	800	1000	1000	1000

quencies with various coupling capacitances. Table 2 is taken from Rives' paper.

The reactive and resistive components of the input impedance at the transmitter end of the coaxial cable vary radically with the frequency, the length of the cable, and

the terminating impedance in either of these systems. A conventional line tuner is not, in all cases, adequate to compensate for the reactances that may be encountered, nor are the impedance-matching transformers usually included in such tuners always capable of transforming the

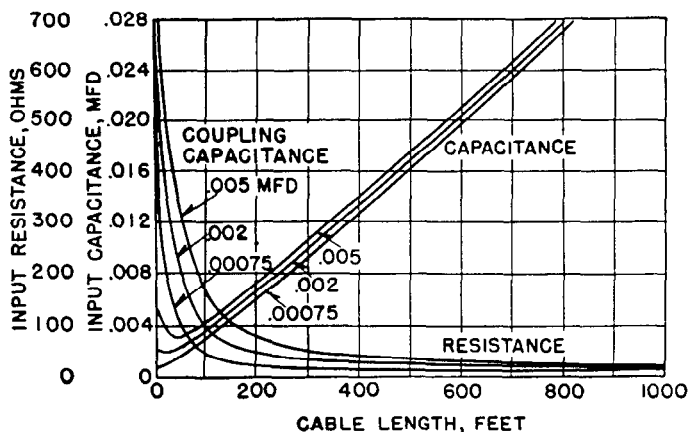


Fig. 37—Input resistance and capacitance ($R - jX_c$) at 100 kc of various lengths of coaxial cable operating directly into 900-ohm resistive load through coupling capacitances shown. No impedance matching transformer used (Fig. 34).

resistive component to the proper load resistance for the transmitter. Both the resistive and reactive components become very low as the length of the cable is increased up to a quarter wave. The input capacitance and resistance at 100 kc of a coaxial cable terminated in various capacitances and a 900-ohm line are shown in Fig. 37.

35. Carrier Coaxial Cable

It was common practice in the past to locate the carrier transmitter and receiver relatively close to the coupling capacitor and tuner, and to connect the assembly directly to the tuning inductance without impedance transformation at the tuner, as shown in Fig. 38. In such installations

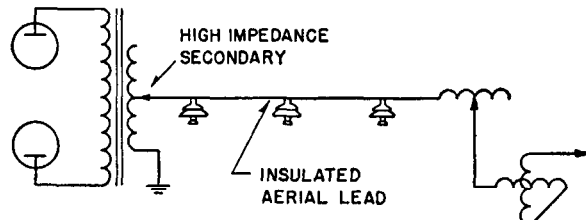


Fig. 38—Use of insulated aerial lead between carrier transmitter and outdoor tuner.

the lead between the carrier assembly and the tuner operates at line impedance level, and unless this lead is supported aerially and is well insulated, losses resulting from shunt conductance to ground becomes excessive in lengths over 100 feet or so.

Modern developments in solid-dielectric cables have resulted in practically complete abandonment of the practice of making the connection between the set and the tuner through a high-impedance lead. The losses in such cables, when they are properly terminated, is only about 0.5 db

per 1000 feet at carrier frequencies, and they can be run through conduit or buried directly in the ground without effect upon their performance.

The specification for a typical coaxial cable used in power-line carrier work is as follows:

The center conductor consists of a single-conductor 0.102-inch diameter (No. 10) soft-drawn, tinned copper wire. This conductor is covered with a continuous coating of 60 percent low-capacity rubber insulation making the outside diameter approximately 0.450 inch. Over this is a copper braid, equivalent in cross-section to the center conductor, made up of No. 30 tinned copper wire. Over this is a lead sheath $\frac{3}{64}$ inch thick with $\frac{3}{4}$ percent antimony. The outside diameter does not exceed 0.6 inch. The high-frequency loss does not exceed 0.32 decibel at 50 kilocycles, nor 0.60 decibel at 150 kilocycles. The surge impedance is approximately 60 ohms.

The measured characteristics of coaxial cable manufactured to these specifications were found to be as follows:

Surge impedance.....	61.1 $/ -0^{\circ}29'$ ohms
Propagation constant.....	0.568
Attenuation at 150 kc.....	0.429 db/1000 feet
Resistance.....	3.91 ohms/1000 feet
Inductance.....	110.1 mh/1000 feet
Shunt conductance.....	519 micromhos/1000 feet
Shunt capacitance.....	0.0295 mfd/1000 feet

Similar coaxial cables with synthetic rubber or plastic jackets, instead of lead, are also widely used. The electrical characteristics are about the same.

36. Methods of Coupling

There are a number of different ways of utilizing one or more conductors of a three-phase power line as conductors for carrier-frequency currents. Some of these are illustrated in Fig. 39. The simplest of these, and by far the most popular, is to use a single conductor of the power line as one leg of the carrier circuit, with ground as the return path (Fig. 39a). This system, commonly called "line-to-ground," "phase-to-ground," or "single-phase ground-return" coupling, requires less coupling equipment (coupling capacitors and tuners) than any of the other methods shown, and it is universally used for short-haul, point-to-point channels, such as for relaying. On lines not provided with ground wires, the attenuation of a circuit using this method of coupling is higher than an equivalent length of circuit using line-to-line coupling, particularly if ground characteristics are unfavorable. Line noise is also somewhat greater. However, modern practice favors line-to-ground coupling for all except the longest and most important carrier channels.

The coupling system shown in Fig. 39b is variously termed "line-to-line," "phase-to-phase," or "interphase" coupling. This system was at one time used almost exclusively in preference to line-to-ground coupling for communication channels and most telemetering channels of any length, but in recent years has given way to some extent to line-to-ground coupling. At first glance this system appears to have the advantage that one of the conductors can be grounded at any point without interrupting the continuity of the carrier channel. However, in the line-to-ground system there is often sufficient electrostatic

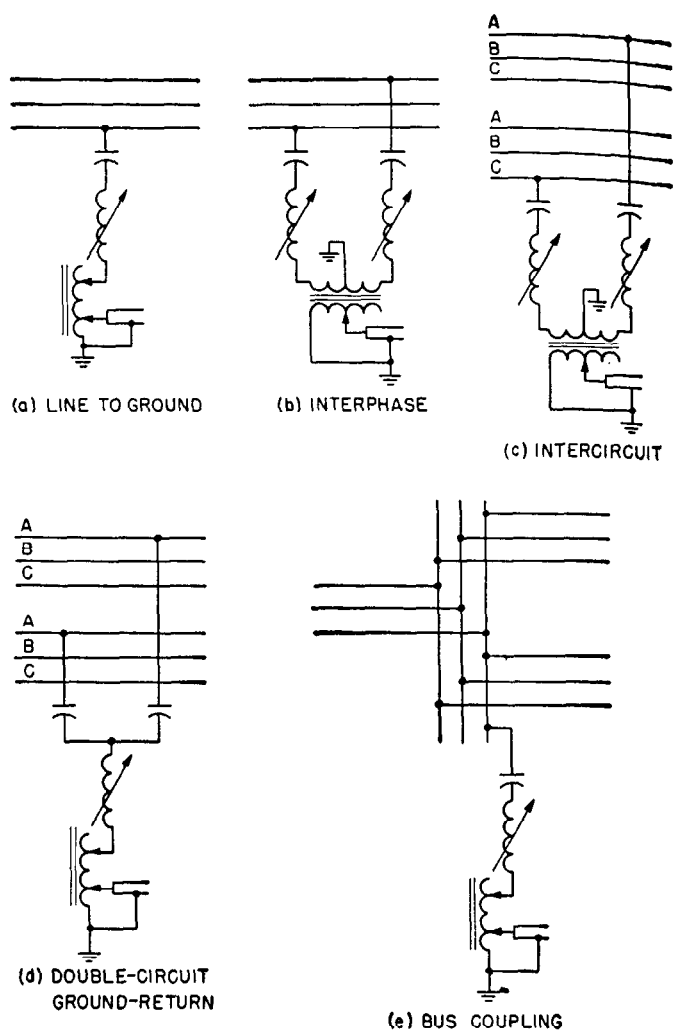


Fig. 39—Methods of line coupling.

and electromagnetic coupling between an open or grounded conductor and the two unaffected conductors to transfer enough energy around such a discontinuity to maintain a usable communication signal, provided the conductor is not opened or grounded closer than several hundred feet from the carrier terminal, and also provided that the channel normally operates with sufficient margin to take care of the increased signal-to-noise ratio. The secondary of the impedance-matching transformer used in the interphase system is usually center-tapped and grounded, and if one of the conductors is grounded close to the terminal, the output transformer may be partially short-circuited, resulting in a reduction of signal strength.

37. Inter-Circuit Coupling

If a double-circuit transmission line exists between carrier terminals, consideration can be given to several methods of coupling that increase carrier-circuit reliability under abnormal system conditions. One of these is intercircuit coupling, shown in Fig. 39c. With this type of coupling either circuit can be taken out of service and all three phases can be grounded at any point without interrupting the continuity of the carrier circuit. In intercircuit coupling, connection is made to one phase of one

circuit and to a different phase of the other. When both lines are in service and are bussed at both ends, this type of coupling is equivalent to interphase coupling. Inter-circuit coupling can be used only on a double-circuit line that cannot be sectionalized between carrier terminals.

38. Double-Circuit Ground-Return Coupling

In double-circuit ground-return coupling, Fig. 39d, the carrier signal is coupled to the same phase of the two circuits, and these operate in parallel under normal conditions with ground return. With this type of coupling either line can be taken out of service or sectionalized between terminals without interrupting the carrier channel. In fact, some installations use this type of coupling in which a portion of the intervening path between the terminals is a single-circuit line. It is generally possible with this type of coupling to ground one of the two circuits for maintenance without interrupting carrier service, provided the ground is not applied directly at the coupling capacitor location. Even in the latter case, if there is sufficient margin between the capability of the carrier sets and the normal attenuation of the circuit, it is often possible to keep the carrier channel in service.

39. Bus Coupling

Where it is desired to couple the carrier signal to several transmission lines simultaneously at a given location, bus coupling, Fig. 39e, is sometimes used. This system of coupling can be used either phase-to-ground or phase-to-phase. It is subject to several disadvantages, among them the fact that the opening of any circuit breaker on a given line between the two terminals, even at the terminals themselves, interrupts the carrier channel over that line. Also, if there are more than a few circuits connected to the bus, it may be impossible to locate a carrier frequency that can provide satisfactory operation under all system switching conditions, and the number of line traps required to isolate offending lines may eliminate the apparent economic advantage of bus coupling.

40. By-Passing of Carrier Signals

Carrier by-pass assemblies are used to provide a path for carrier energy around transformers, switches, circuit breakers, or other discontinuities that may exist in a carrier channel. By-pass assemblies consist essentially of one or more coupling capacitors and associated line tuning units. The capacitors are tuned to series resonance at the frequency or frequencies to be passed around the discontinuity. The following discussion specifically shows bypassing arrangements used with channels coupled line-to-ground, but it should be understood that similar arrangements utilizing twice the number of capacitors and tuning inductances can be applied on interphase channels.

41. Short By-Passes

The simplest type of by-pass assembly is that shown in Fig. 40, consisting of a single coupling capacitor and a single line tuner, both suspended in the line. This simple system is suitable only for bypassing transformers, regulators, and other such equipment that normally provides voltage on both sides of the by-pass assembly when either side

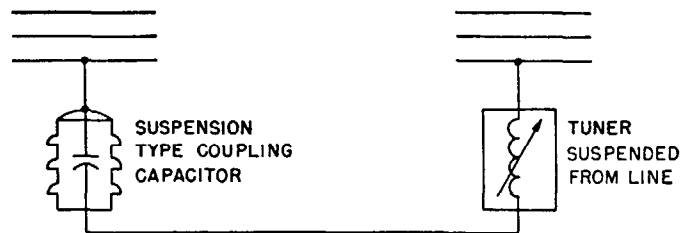


Fig. 40—Suspended by-pass arrangement.

is energized. It should never be used to bypass disconnect switches or circuit breakers, or to pass signals from a line of one voltage to a line of another voltage, except at transformation points, because the ungrounded coupling capacitor can supply dangerous amounts of charging current from the energized side of an open switch or breaker to the apparently de-energized line.

The simplest by-pass assembly suitable for general application as a short by-pass is that shown in Fig. 41.

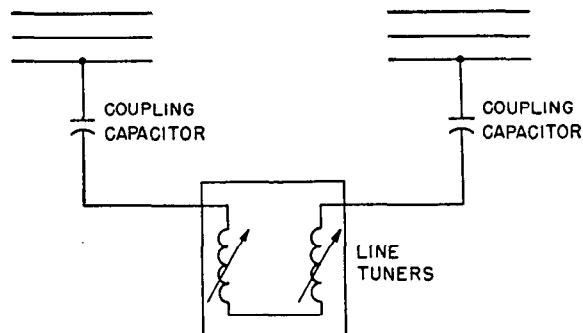


Fig. 41—Conventional short single-frequency by pass. One tuning inductance can be omitted in some cases.

Two coupling capacitors and a single tuning assembly, consisting of two tuning inductances, are used. The connections between the inductances and the capacitors are made with insulated aerial leads. No coaxial cable is employed. Since the leads between the capacitors and the tuning inductances operate at a high r-f potential, they must be extremely well insulated to prevent excessive losses due to shunt conductance. This system is not recommended for installations where the coupling capacitors are separated by more than 100 feet. The tuning inductances should be located as nearly midway between the coupling capacitors as possible.

For higher frequencies, or with lower-voltage lines where coupling capacitors of relatively higher capacitance are used, a single tuning inductance is often sufficient to tune both capacitors to resonance.

42. Long By-Passes

The most efficient of the commonly used by-pass arrangements is that shown in Fig. 42, in which a tuning inductance and impedance-matching transformer are located at each coupling capacitor, and coaxial cable is used as the link between them. With this arrangement the distance between the coupling capacitors can be as much as several thousand feet, depending upon the losses in the coaxial cable at the frequency involved.

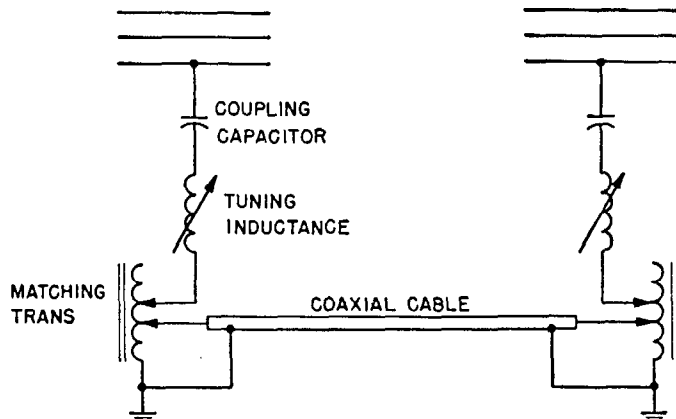


Fig. 42—Conventional long by-pass.

This type of by-pass actually amounts to two ordinary line tuning arrangements connected to operate into each other. If a carrier assembly is to be coupled into the line at the by-pass point, as might be desired on a multi-station communication system, the coaxial cable from each tuner is brought into the carrier assembly and connected to the low-impedance transmitter output tap usually provided for operation into two such cables in parallel. This arrangement is shown in Fig. 43.

This by-pass arrangement may be extended into a three-way system, as shown in Fig. 44, to pass signals from one line into two others. There is an inherent impedance mismatch in such a system at the junction of the three cables, as a result of the fact that each cable is terminated in one half its surge impedance. In addition to the 3-db loss in each direction due to the division of power between the two paths, there is a loss of about 0.5 db due to the mismatch at the junction.

43. Multi-Frequency By-Passes

All the multi-frequency tuning schemes shown in Figs. 30 to 33 can be applied in by-pass assemblies, so that more than one frequency can be passed. The arrangement shown in Fig. 30 is the easiest to tune and is the one most commonly used in such cases.

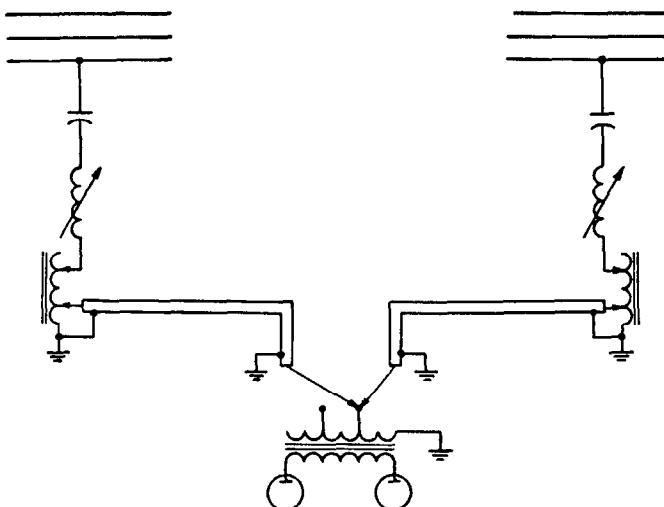


Fig. 43—By-pass with carrier terminal.

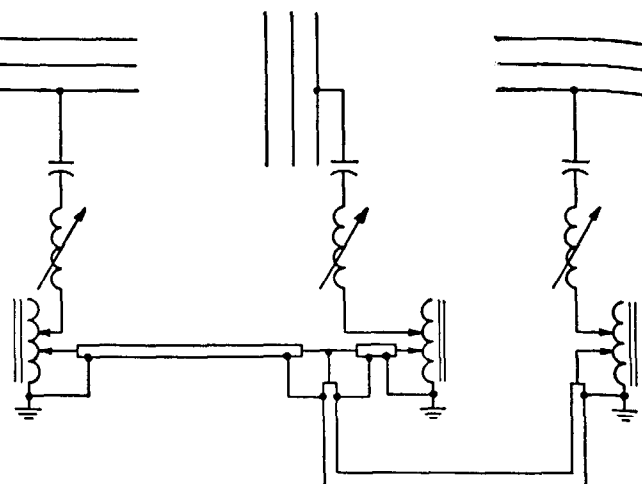


Fig. 44—Three-way by-pass.

Consideration has been given to the use of band-pass bypass circuits, such as that shown in Fig. 45. In this case the coupling capacitors form a portion of the series arms of a simple "T" section band-pass filter. Many other such arrangements are possible.

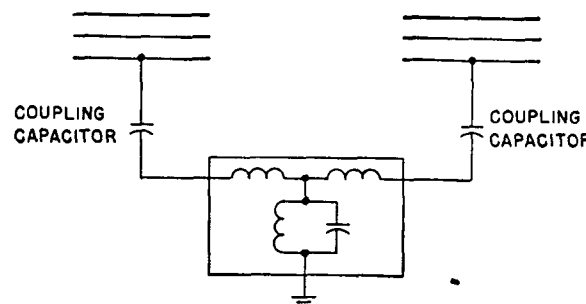


Fig. 45—Band-pass by-pass system.

VI. METHODS OF ESTIMATING CARRIER-CIRCUIT ATTENUATION

44. The Decibel

The decibel is a convenient unit for expressing the ratio between the power levels at two points in a communication system. This is because the actual ratios are often so large that their use is inconvenient on this account alone, and also because it is necessary to multiply the input and output power ratios for each individual component of the system to obtain the overall ratio. Losses and gains in decibels for individual components of a system can be added directly to give an overall loss or gain for the system.

The decibel is defined as 10 times the common logarithm of the power ratio, the ratio always being expressed as the quotient of the larger power by the smaller power; i.e.,

$$\text{db} = 10 \log_{10} \frac{P_1}{P_2} \text{ if } P_1 > P_2 \quad (12a)$$

or

$$\text{db} = 10 \log_{10} \frac{P_2}{P_1} \text{ if } P_2 > P_1. \quad (12b)$$

The ratio of two voltages or of two currents can be expressed in decibels as follows, provided that the impedances of the circuits in which these voltages or currents exist are the same:

$$\text{db} = 20 \log_{10} \frac{E_1}{E_2} \quad (13)$$

$$\text{db} = 20 \log_{10} \frac{I_1}{I_2}. \quad (14)$$

Convenient decibel figures to remember are that a 2 to 1 power ratio is 3 db, 3 to 1 is 4.8 db, and 10 to 1 is 10 db. From these figures the number of decibels corresponding to 4-to-1, 5-to-1, 6-to-1, 8-to-1, and 9-to-1 ratios and any decimal multiples of these ratios can be estimated quickly by simple mental addition.

45. Decibel Rating of Carrier Assemblies

It is common practice to rate carrier transmitter-receiver assemblies in terms of the maximum number of decibels of attenuation through which two similar assemblies can operate satisfactorily. Actually these ratings are based on the assumption of noise levels at the receiving location that can reasonably be expected on a normal power system, and the decibel rating has been assigned on the basis of providing a satisfactory but undefined signal-to-noise ratio. This practice in rating carrier equipment unduly penalizes it when applications on relatively quiet systems are contemplated, because most equipment is capable on quiet lines of operating through much more than its rated attenuation. As more is learned about the nature and the magnitude of carrier-frequency noise on power systems, it is reasonable to expect that more informative ratings based upon the transmitter power and the receiver sensitivity and the response of the latter to noises of a given character and magnitude will come into practice.

46. Losses in a Carrier Circuit

The most common sources of attenuation in a power-line carrier circuit are:

1. Losses in coaxial cable between carrier assemblies and tuning units.
2. Losses in tuning and coupling equipment.
3. Losses in by-pass equipment.
4. Losses in straightaway transmission lines.
5. Losses due to discontinuities in transmission lines.
6. Losses due to division of energy (a) in long branch circuits at transmitting points, and (b) in long branch circuits remote from transmitting points.
7. Losses due to low impedance presented by untrapped spur lines.
8. Losses due to simultaneous propagation over alternate paths.

The total attenuation in decibels for an entire circuit is the sum of the decibel losses for each part of the circuit. A discussion of the attenuation that can be expected from each of the above sources follows.

Losses in Coaxial Cable—In practice an attempt is usually made to match the characteristic impedance of the transmission line to the impedance of the coaxial cable used between the carrier assembly and the tuning unit. An

TABLE 3—APPROXIMATE LOSSES IN COAXIAL CABLE

Frequency, kc	Loss, db per 1000 ft.
20	0.2
50	0.32
100	0.5
150	0.6
300	0.9

impedance matching transformer is provided for this purpose in the tuning unit. The losses in typical coaxial cable as a function of frequency when properly terminated are shown in Table 3. Typical losses in coaxial cable operating directly into a 900-ohm line without impedance matching or tuning are shown in Fig. 36.

Losses in Tuning and Coupling Equipment—It is possible to calculate accurately the losses in a tuning and coupling circuit, provided that the Q's of the tuning inductance and the coupling capacitor and the characteristic impedance of the line are known. However, it is usually permissible for estimating purposes to assume a loss of one db for a simple tuner-capacitor combination working into an open-wire line.

Losses in tuning and coupling equipment working into a circuit of low characteristic impedance, such as a combination of several lines in parallel, or a power cable, are greater. An increase in coupling loss of one db can be assumed for each additional line at a transmitting point. In the case of power cables, an accurate calculation is desirable. The db attenuation of a single line tuner and coupling capacitor, applied to a power cable or other circuit of characteristic impedance Z_c , is

$$\text{db} = 10 \log_{10} \frac{Z_c + R_c(1 + Q_c/Q_L)}{Z_c} \quad (15)$$

in which R_c is the resistive component of the coupling capacitor impedance at the frequency considered, and Q_c and Q_L are the Q's of the capacitor and the tuning inductance, respectively. A Q of 50 to 80 is typical for tuning inductances in the 50-150-kc band. For estimating purposes, a Q of 30 can be used for coupling capacitors.

The coupling loss for receiving is independent of the number of branch circuits at the coupling point, since in this case the carrier equipment is the terminating device for the coupling circuit. For estimating purposes, a receiver coupling loss of 1.0 db can be used.

The attenuation figures given above are based on single-frequency line-to-ground coupling and for estimating purposes can be doubled for interphase coupling. In the latter case, however, the characteristic impedance of the line is greater and the actual difference in attenuation is somewhat less.

The losses in two-frequency tuners are higher than those in simple single-frequency tuners. No accurate figures can be given, because the additional losses depend critically upon the Q's of the inductances and the separation of the two frequencies involved. For a separation of 25 percent or more of the higher frequency, a loss of 2 db at each frequency can be used for estimating purposes on line-to-ground channels, or 4 db on interphase channels.

Losses in By-Pass Equipment—The losses in bypassing equipment are at least twice those of coupling equipment at a carrier terminal because two sets of coupling capacitors and tuners are involved. An interphase by-pass involves four times as much coupling equipment as a line-to-ground terminal, and the losses in this case can be assumed to be about four times as great, or 4 db. Losses in the coaxial between the two tuners must be added to these figures.

A factor that can increase the apparent loss in by-pass on a phase-to-ground circuit is that the carrier energy in a phase-to-ground channel tends to use the idle phases of the line as a return path. Since only the phase to which the carrier is directly coupled is normally by-passed, the opening of a by-passed circuit breaker interrupts the return path offered by the other two phases, and a greater increase in attenuation than that indicated by the loss figures previously given may be experienced. This is particularly true of phase-to-ground channels on lines not provided with ground wires.

In circuit-breaker by-pass installations involving long coaxial cable runs, it is occasionally found that the attenuation of the overall circuit is greater when the breakers are closed than when they are open. This can be explained as a case of attenuation due to simultaneous propagation over alternate paths, to be discussed presently. A remedy usually effective in this case is to reverse the phase of the current traveling through the by-pass circuit by reversing the connections to the impedance matching transformer in one of the tuners.

Losses in Transmission Lines—The attenuation of a straightaway transmission line at carrier frequencies is subject to many factors, such as the voltage of the line, which affects its construction and its insulation level, the type and the condition of the conductors and the insulators, the presence or absence of ground wires, the method of coupling used, weather conditions, and so forth. For this reason the attenuation figures given in Table 4 are neces-

sary only for overhead power circuits.

Losses Due to Discontinuities in a Line—Any series or shunt impedance or physical condition at a given point in a line that causes the impedance seen looking into the line just ahead of the point in question to be different from the characteristic impedance of the line up to that point constitutes a discontinuity in the line. Discontinuities give rise to reflections and standing waves that cause increased losses in the line up to the discontinuity. In addition to these losses there may be losses in the device causing the discontinuity, with the net result that a discontinuity is a source of additional attenuation in a carrier channel.

When a discontinuity as defined above exists close to a transmitting point, so that a large fraction of the reflected energy returns to the transmitter, the line does not present its surge impedance as a load to the transmitter and may in fact present an impedance that is highly reactive in nature. In such cases it is necessary to compensate for the reactive portion of the line impedance by proper adjustment of the line tuner and to match the resulting resistive component of the load, which may be higher or lower than the characteristic impedance, by adjustment of the taps of the impedance-matching transformer in the tuner. Although the losses in the short section of line up to the discontinuity are greater than if the line were properly terminated, the increase is not serious except in extreme cases, and the only major loss, if any, is that in the device causing the discontinuity.

On the other hand, when a discontinuity exists at an intermediate point in a channel, sufficiently far from the transmitting point so that essentially the characteristic impedance of the line is presented to the transmitter, the loss in the line resulting from reflection at the discontinuity may be considerable.

Thevenin's theorem (see Chap. 10) suggests a general method of calculating the loss due to any discontinuity, either shunt or series, that exists in a carrier channel at a

TABLE 4—APPROXIMATE CARRIER ATTENUATION OF OVERHEAD POWER CIRCUITS

Line Voltage kv	Approximate Attenuation db per Mile									
	Phase-to-Phase Coupling					Phase-to-Ground Coupling				
	20 kc	50 kc	100 kc	150 kc	300 kc	20 kc	50 kc	100 kc	150 kc	300 kc
230	.03	.05	.075	.107	.2	.04	.062	.094	.13	.25
138	.041	.065	.09	.12	.215	.051	.081	.113	.15	.27
115	.05	.075	.102	.135	.27	.062	.094	.130	.16	.34
69	.055	.08	.11	.145	.29	.069	.100	.137	.18	.36
34.5	.073	.10	.13	.18	.38	.094	.125	.16	.22	.47
13.8	.12	.15	.18	.215	.45	.15	.19	.22	.27	.56

sarily only approximately correct. The figures for phase-to-ground coupling are 1.25 times those given for interphase coupling. On short lines (up to 50 miles) the attenuation may be greater, and on long lines it may be less, but the factor of 1.25 represents a good average. The figure of 0.1 db per mile is frequently used for preliminary estimat-

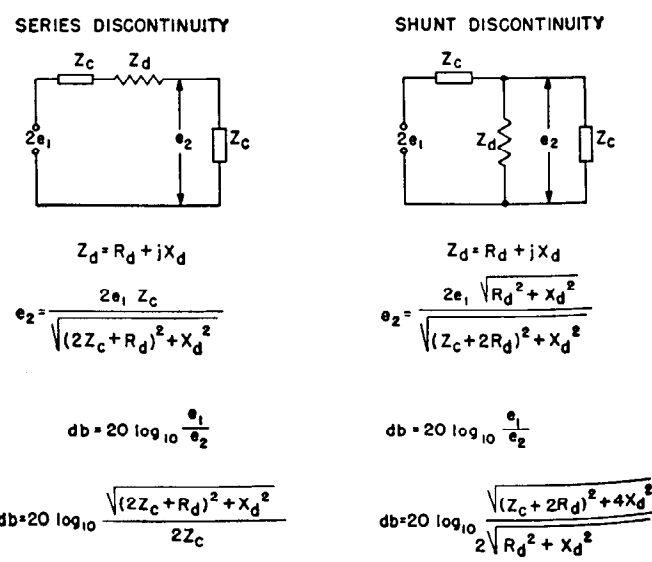


Fig. 46—Derivation of equations for loss due to series and shunt discontinuities in a long line.

point sufficiently remote from the transmitter. If the line were open circuited just ahead of the discontinuity, the voltage that would exist at the open circuited terminals would be twice the voltage that would exist across the line if it were continuous; i.e., if there were no discontinuity. Furthermore, if the line were short circuited at the transmitting point, the impedance seen looking into the open-circuited terminals back toward the remote source would be the characteristic impedance of the line. The system up to the discontinuity can be represented therefore by a voltage equal to twice the voltage that would exist with no discontinuity, in series with a resistance equal to the characteristic impedance of the line. If the discontinuity is a series impedance, it is placed in series with the characteristic impedance of the line beyond the discontinuity. If it is a shunt discontinuity, it is placed across the characteristic impedance of the line, and the combination is applied to the terminals of the equivalent network. These connections are illustrated in Fig. 46. The resulting loss, which includes the loss due to reflection as well as that in the device causing the discontinuity, is then expressed for a series discontinuity as

$$db = 20 \log_{10} \frac{\sqrt{(2Z_c + R_d)^2 + X_d^2}}{2Z_c} \quad (16)$$

and for a shunt discontinuity as

$$db = 20 \log_{10} \frac{\sqrt{(Z_c + 2R_d)^2 + 4X_d^2}}{2\sqrt{R_d^2 + X_d^2}} \quad (17)$$

In both of these equations

R_d = Resistive component of impedance of discontinuity

and X_d = Reactive component of impedance of discontinuity.

In the derivation of these equations it is assumed that the characteristic impedance of the line is the same on both sides of the discontinuity.

Losses Due to Long Branch Circuits—When a carrier transmitter is coupled to a power system at a point from which several long untrapped transmission lines radiate, the load impedance presented to the carrier equipment is the parallel of the characteristic impedances of the lines involved. The impedance matching transformer in the line tuner can usually be adjusted so that this impedance is transformed to load the transmitter properly, so that there is no reflection loss. However, the division of the energy

TABLE 5—LOSSES DUE TO LONG BRANCH CIRCUITS AT TRANSMITTING POINTS

1 additional circuit	3.0 db
2 additional circuits	4.8 db
3 additional circuits	6.0 db
N additional circuits	$10 \log_{10} (N+1) \text{ db}$

among the several circuits in effect constitutes an attenuation of energy along the desired path. If the characteristic impedances of all the lines involved are the same, the losses at a transmitting terminal in this case are as shown in Table 5. It should be noted that these losses are correct for a transmitting terminal only. If one or more long un-

trapped lines radiate from an intermediate point in a carrier channel, or from a receiving point, there is a loss due to reflection as well as a loss due to division of the energy among the circuits. Treatment of this case as a shunt discontinuity, by methods previously outlined, yields the results given in Table 6.

TABLE 6—LOSSES DUE TO LONG BRANCH CIRCUITS REMOTE FROM TRANSMITTING POINTS

1 additional Circuit	3.5 db
2 additional Circuits	6.0 db
3 additional Circuits	8.0 db
N additional Circuits	$20 \log_{10} \left(\frac{N+2}{2} \right) \text{ db}$

Losses Due to Short Untrapped Branch Lines—As contrasted with the long branch lines just considered, short untrapped spur lines (in general, lines less than 50 miles in length) may present shunt impedances differing radically from the characteristic impedance of the line. If the terminating impedance and the length of a spur line are known accurately, it is feasible to calculate the impedance such a spur line presents at its input terminals at a given frequency. This impedance can then be considered as a shunt discontinuity and treated by the method previously given. Fig. 12 shows the absolute value of the input impedance of a typical line ($Z_c = 730$ ohms, attenuation 0.186 db per wavelength) as a function of various capacitive reactance terminations.

Data on the carrier frequency impedance of power transformers and other terminating devices are not generally available, however, and it is not usually possible to calculate the input impedance of a spur line. If after installation of the equipment a carrier frequency cannot be chosen that will maximize the spur-line impedance, it may be necessary to install line traps to isolate the spur line from the carrier channel. In this case the effect of the spur line upon the attenuation is reduced to a low value, depending upon the characteristics of the line trap.

Losses Due to Simultaneous Propagation Over Alternate Paths—A carrier channel that includes two alternate paths may suffer attenuation due to out-of-phase arrival at a common point of signals traveling over the two paths. The magnitude of this attenuation is highly variable, depending upon the nature of the two paths, their relative individual attenuations, and the frequency used. Limiting attenuation figures can be established, however, for certain cases in which one or both of the alternate paths are long (over 50 miles).

If both paths are long, there is a loss of 0.5 db at the branch point due to reflection. The relative amplitudes and the phase of the two signals arriving at the junction of the paths determines the additional attenuation. Specific cases are as follows:

Equal Amplitudes, In-Phase Arrival—Reflection losses of 0.5 db at junction and at branch point due to impedance mismatch. Total attenuation from branch point to junction 1.0 db plus attenuation of one path.

Equal Amplitudes, Out-of-Phase Arrival—Cancellation of voltage at junction, infinite attenuation. This is an unlikely condition because two long alternate paths having

exactly the same attenuation are rarely encountered. The attenuation may still be large in practical cases, however, as pointed out below.

Unequal Amplitudes, In-Phase Arrival—Maximum loss at junction 3.5 db. Total maximum loss 3.5 db at branch point due to reflection and division of energy, plus 3.5 db maximum at junction, plus attenuation of shorter path. These maximum losses are based on complete attenuation of the signal in the longer path.

Unequal Amplitudes, Out-of-Phase Arrival—Minimum loss at junction 3.5 db, increasing with decreasing differ-

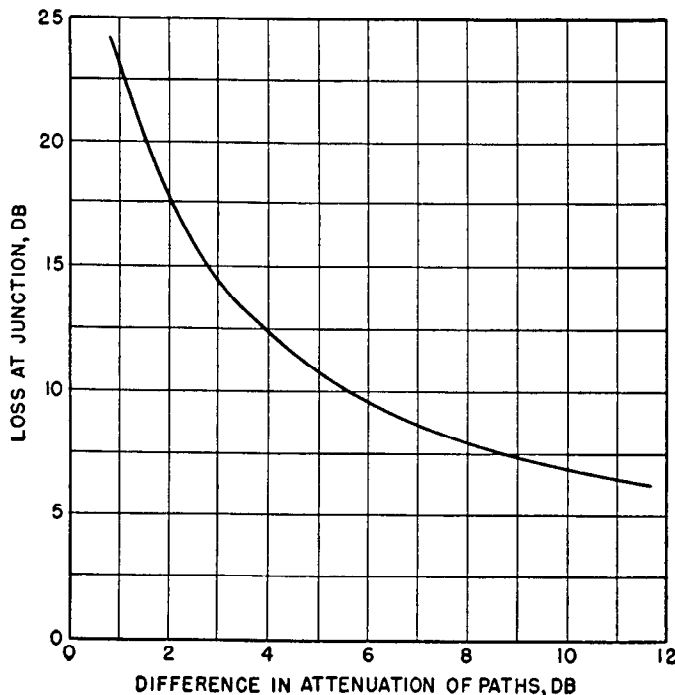


Fig. 47—Loss due to out-of-phase arrival of signals at a junction of two long alternate paths. This curve gives loss at the junction only and does not include the loss at the branching point or the loss in the paths themselves. The junction is assumed to be terminated by a single line which is a continuation of the channel.

ence in attenuation of the two paths, as shown in Fig. 47. To these losses must be added 0.5 db loss at the branch point due to reflection and 3 db due to division of energy, plus the attenuation of the shorter path.

If both paths are short and of unequal length, the attenuation may be very great, particularly if one of the paths is a half wavelength longer than the other.

In general, if the frequency cannot be adjusted after installation to avoid out-of-phase arrival at a junction, it may be necessary to resort to the use of line traps to eliminate alternate paths. A long alternate path, when trapped at one end only, reduces to the case of a single long branch circuit, for which the attenuation is 3.5 db. A short alternate path may require trapping at both ends for reduction of the attenuation to an acceptable value, because a trap installed at one end only may reduce the situation to that of a short untrapped spur line, for which the attenuation may still be excessive.

47. Example of Calculation of the Total Attenuation of a Typical Carrier Circuit

The typical system of Fig. 48 will be used to illustrate the application of the principles just discussed in estimating the attenuation of a carrier channel. In this example a 100 kc line-to-ground-coupled carrier channel is to be established between Stations A and C, and the losses are to be estimated for transmission in each direction.

At Station A there are three long circuits on the 138-kv bus in addition to the circuit over which carrier is to be transmitted. These cause a loss of 6 db because of division of the energy among the total of four circuits (Table 5). They also cause an additional coupling loss because the coupling circuit is working into a load impedance lower than normal line characteristic impedance. This additional coupling loss is estimated at 1 db for each additional circuit, or 3 db, plus the normal 1 db coupling loss.

All line losses are estimated from Table 4.

The branch circuit loss at Station B is 6 db, as given by Table 6, because this station is remote from the transmitting point.

The by-pass loss at Station C is twice the loss of a terminal coupling circuit, or 2 db, plus 0.5 db loss for 1000 feet of coaxial cable at 100 kc (Table 3).

The loss in the trap on the short line out of Station C is approximately 0.5 db, as shown in Fig. 24 for a 400-ampere trap terminated in zero impedance.

There is an alternate path between Station C and Station D which has approximately 7 db greater attenuation than the direct path. From Fig. 47 the maximum possible loss, which would occur with out-of-phase arrival of the signals at Station D, is estimated as 8.5 db. To this must be added a loss of 3 db due to division of energy between the alternate paths at Station C, plus a reflection loss of 0.5 db at this point, a total attenuation of 12.0 db due to the presence of the alternate route. These figures do not include the 5.5 db attenuation of the direct path, which is added separately.

The long line extending beyond Station D serves as a terminating impedance for the circuit. Most modern carrier transmitter-receiver assemblies present an impedance of 5 to 10 times the load impedance into which they are intended to work, and as a result they do not serve to terminate a line in its characteristic impedance. If the line beyond Station D were not present, there would be a slight gain in voltage received at Station D because of the high terminating impedance.

There is an estimated 1 db coupling loss for receiving at Station D, plus 0.25 db coaxial cable loss. The total attenuation of the channel for transmission from Station A to Station D is the sum of all the losses discussed. These are summarized and added in Fig. 48, giving a total attenuation of 52.2 db for the channel.

For transmission from Station D to Station A, there is a 4.8 db loss at Station D due to division of energy among the three lines on the bus, and an increase of 2 db in the coupling loss. The additional loss due to the alternate path in this case is 8.5 db at Station C. At Station A, one of the branch lines can be considered as a continuation of the main line. The other two branch lines cause 6 db attenuation, partly due to reflection and partly due to division of

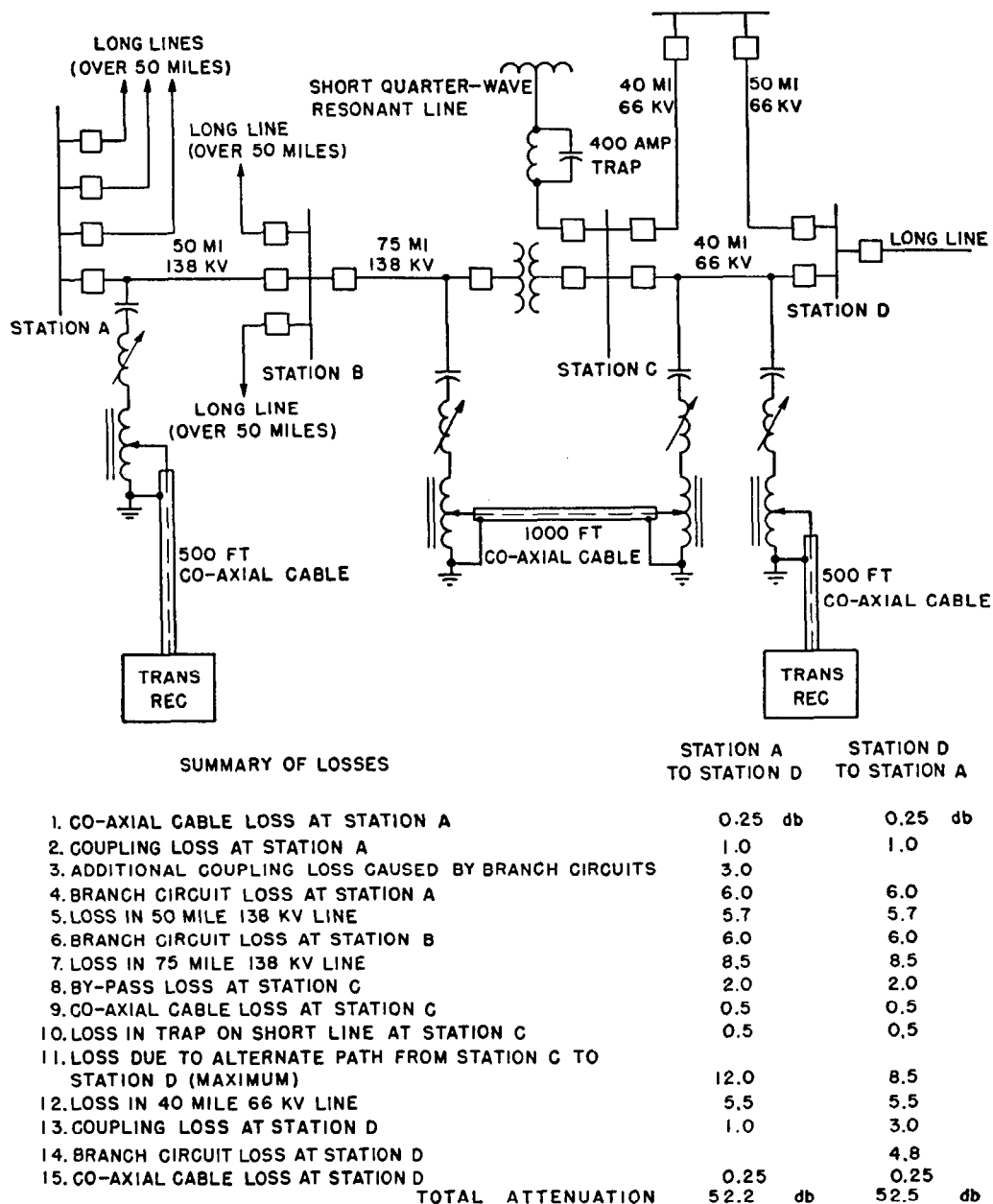


Fig. 48—Typical system assumed for example of calculation of losses, and summary of attenuation in each direction.

energy. The coupling loss for receiving is estimated as 1 db. All other losses in the channel are the same as for transmission from Station A to Station D. The total attenuation of the channel for transmission from D to A is therefore 52.5 db.

alternate paths, and other causes of high attenuation are eliminated from the channel by means of line traps. A clean, well-trapped channel delivers a reliable signal at the receiving point on any carrier frequency that may be available for use, regardless of system switching conditions.

As a result of the crowding of the carrier frequency spectrum on most interconnected power systems in this country, it is seldom that any appreciable latitude is available in the choice of a frequency for a new channel. Where a choice is available, however, it is sometimes possible to install carrier equipment on a system with little or no trapping and to experiment with different frequencies until one is found which permits successful transmission between the carrier terminals under all anticipated system switching conditions. In this case the carrier energy is "broad-

GENERAL CONSIDERATIONS IN APPLYING CARRIER SYSTEMS

48. Trapped Channels vs. Broadcast Systems

From the discussion just given of the sources of attenuation to carrier in a power system, it is evident that successful operation of a proposed carrier channel on a specified frequency can be assured only if spur lines, short

cast" throughout the power system, and the signal delivered to the intended receiving point is inherently weaker and less reliable than that delivered over a clean channel. Frequently it is impossible to find on a complicated system a frequency that permits successful operation of a "broadcast" type of channel. In this case it is necessary to seek out the sources of high attenuation and to isolate them one by one until a workable channel is obtained on an available frequency.

It is clear, therefore, that a trapped channel is preferable to a broadcast type of channel from the standpoint of reliability, ease of application, improved signal-to-noise ratio, and reduced interference to neighboring systems.

49. Frequency Assignments and Separations

One of the most important problems in the application of carrier equipment is the determination of the minimum frequency separation required between channels on the same system and the assignment of frequencies to new channels in a manner that permits maximum conservation of the available spectrum space.

In general, it is advisable to assign the lower frequencies in the spectrum to long-haul communication and telemetering channels, and to use the higher frequencies, which are attenuated more rapidly, for short channels. Relaying channels in particular are well suited to operation on the higher frequencies because they are always trapped at both ends and extend over only one line section. There are cases of successful application of relaying systems on identical frequencies on well-separated line sections on the same power system.

The frequency separation required between carrier channels on a power system is a function of a number of factors, such as the selectivity of the receivers employed, the relative strengths of desired signals and interfering signals at a receiving point, the type of modulation used, and the purposes for which the channels are applied. The last factor determines approximately the signal-to-interference ratio that can be tolerated. For these reasons no generally applicable figures for required separations can be given and each case must be considered individually.

Other factors being equal, single sideband channels can be spaced closer together in the spectrum than channels using other types of modulation. This results primarily from the increased receiver selectivity permissible in the reception of single sideband signals. The narrow bandwidth occupied by single sideband channels is also an important factor in determining required frequency separations between them and other types of channels, although the selectivity of the receivers used in the other channels is the limiting factor in determining the permissible reduction of the separation in this case.

The signal-to-interference ratio acceptable in a given type of service is to some extent a matter of opinion, and in addition it depends critically upon the adjustment of the equipment in most applications. Hence it is difficult to set down specific figures for various cases. Discussion of a few of the considerations involved, however, will aid in establishing acceptable figures for a given application, and Table 7 can be used as a guide.

In telegraph-type channels, in which the operation or

TABLE 7—RATIO BETWEEN MINIMUM SIGNAL RESPONSE AND MAXIMUM INTERFERENCE RESPONSE ON CARRIER RECEIVERS FOR VARIOUS APPLICATIONS

†Keyed Carrier Telemetry	†Carrier Relaying or Supervisory Control	Tone Telemetering	*Voice Communication
15 db	20 db	15 db for a single received tone, $(15 + 20 \log_{10} N)$ db for multiple tones, where N is the number of tones.	15 db minimum on automatic simplex systems. 10 db tolerable for short periods on other systems. 20 db good 30 db excellent

†Receiver sensitivity set so that receiver detector is barely saturated on minimum signal.

*Receiver sensitivity set so that minimum signal is at lower end of ave range. On automatic simplex systems, no greater transfer unit r-f sensitivity should be used than that required to give reliable operation on minimum signal.

non-operation of a receiving relay is the criterion of the effect of interference, it is necessary only to allow a reasonable margin of safety for relay drop-out in specifying the maximum interference level. A 2 to 1 ratio is a reasonable margin for telemetering purposes. If the telegraph receiver sensitivity is set so that the *minimum* expected value of the desired signal just causes saturation of the detector plate current, the maximum response of the receiver to an interfering signal should not exceed half the relay drop-out current. In the usual saturated-detector type receiver, this ratio is 12 to 15 db.

Although the same type of equipment is used for relaying purposes and frequently for supervisory control, the consequences of an incorrect relay operation in these applications are more serious and hence an additional factor of safety of 5 db has been allowed in Table 7 for these functions.

In tone telegraph service, such as tone telemetering, the carrier signal is normally on continuously, and the receiver sensitivity setting is not so critical, provided that the receiver operates on the flat portion of the ave (automatic volume control) characteristic over the entire range of variation in signal strength. The maximum signal-to-interference ratio that can be tolerated for a received carrier modulated 100 percent by a single tone is the same as that for keyed carrier reception, or 15 db, because the saturation characteristics of tone receivers are similar to those of saturated-detector carrier receivers. Additional margin must be allowed for modulation by more than a single tone, however, because the permissible percentage of modulation by each tone is reduced as the number of tones is increased. This is equivalent to a reduction of signal strength at the input of the tone receivers, and their sensitivities must be increased accordingly. Hence a formula which provides an allowance for additional tones is given in Table 7.

It is difficult to give actual figures for voice communication circuits, because there are widely different opinions as to what constitutes a "usable" channel or a "good" channel. Although it is possible to convey intelligence over a

voice channel in which the signal-to-interference ratio is nearly unity, a ratio of 10 db is about the minimum that can be tolerated for any length of time. A 20-db ratio is considered good and a 30-db ratio excellent by most users. The nature of the interference also is a factor on communication channels. For example, the psychological effect of speech interference of a given level is greater than that of interference of other types at the same level.

In automatic simplex channels, there must be adequate margin between the response of the receiver to the desired signal and its response to the interfering signal when the desired signal is absent, to permit reliable operation of the transfer unit. In such systems the receiver sensitivity should be set so that desired signals just cause operation on the flat portion of the avc characteristic when allowance is made for maximum attenuation. A minimum of 10 db difference between response to interference and response to such signals should then be allowed. Because of residual avc action, this requires about 15-db attenuation of the interference in typical receivers. Hence, automatic simplex channels should not be expected to operate reliably with smaller signal-to-interference ratios than 15 db.

The first step in the process of estimating required frequency separation is to calculate the relative strengths of the desired and undesired signals at the receiving point or points. This can be done by methods outlined in the sections of this chapter devoted to estimating attenuation. The relative carrier powers of the signals at the receiver are the original transmitter carrier outputs reduced by the attenuation of the respective paths of the signals to the receiving point in question. This establishes a signal-to-interference ratio at the receiver input terminals. The difference between this ratio and the required signal-to-interference ratio must be made up by the selectivity of the receiver. The separation required for this purpose can be determined by reference to the selectivity curve of the receiver at the particular frequency in question. Consideration must be given to the bandwidth of the interfering signal. This depends upon the type of service for which it is employed and the modulation system used. For example, an interfering a-m voice communication signal occupies a bandwidth extending approximately 3 kilocycles on each side of the carrier frequency and requires correspondingly greater separation from the desired signal than a carrier signal which is keyed for telemetering purposes and occupies a band of only a few cycles on each side of the carrier frequency. If the interfering channel is a single sideband voice channel, its bandwidth extends three kilocycles below the carrier frequency if the lower sideband is used, or three kilocycles above it if the upper sideband is transmitted. The suppression of the unused sideband can be assumed to be a minimum of 20 db.

The following is an example of the use of the principles discussed in determining required frequency separation for a typical case:

On a 100-kc voice communication channel having 50-db attenuation under extreme conditions, transmitter carrier power is 25 watts, and a receiver having the selectivity curve of Fig. 49 is used. A new a-m voice channel is to be added to the system. The transmitters in the new system will have a carrier output of 2.5 watts and the minimum attenuation between

any transmitter of the new channel and any receiver of the original channel is 10 db. What is the minimum frequency separation required to give a 20 db signal-to-interference ratio in the original channel?

The signal to interference ratio at the input terminals of the receiver is minus 30 db (10 db difference in transmitter power and 40-db difference in attenuation). Therefore 50 db of interference rejection is required for a 20-db signal-to-interference ratio. According to Fig. 49, signals

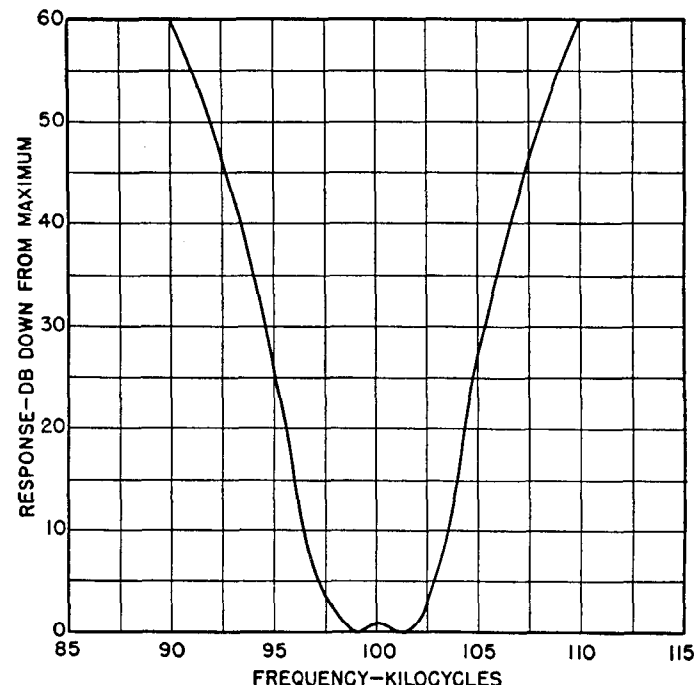


Fig. 49—Typical a-m receiver selectivity curve.

at 108 kc and at 92 kc are attenuated by this amount when the receiver is tuned to 100 kc. Allowing 3 kilocycles for sideband components of the interfering signal, the minimum separation of the carrier frequency of the new channel from that of the original channel is 11 kc above it or 11 kc below it. These are safe figures for either duplex or automatic simplex channels, provided that in the latter case the receiver sensitivity is adjusted properly. By a similar process, the separation required to provide a 20-db signal-to-interference ratio in the new channel can be estimated. Either the figures so obtained or those previously calculated, whichever are the larger, determine the separation required to maintain a minimum of 20-db signal-to-interference ratio in both channels.

50. Signal-to-Noise Ratio

Minimum tolerable signal-to-noise ratios for various carrier applications parallel closely the values of minimum signal-to-interference ratios given in Table 7, provided that the proper characteristic of the noise (e.g. peak amplitude, average amplitude, etc.) is considered in establishing these ratios for each application. The receiver bandwidth also must be considered in most applications, because noise response is usually a function of bandwidth.

In keyed-carrier telemetering applications, the average rectified noise output of the receiver is a measure of the

interfering properties of the noise. For impulsive interference with pulses separated sufficiently to prevent overlapping of the resulting wave trains, the average output is independent of the receiver bandwidth, and hence bandwidth does not enter into the picture in such applications. The area of the impulses is the major determining factor.

The same comments apply to carrier relaying, although in this case trouble from noise is not likely to be encountered. Because of the limited extent of carrier relaying channels, and the fact that they are always trapped at both ends, signal-to-average-noise ratios at receiving points are practically always far above the 20-db minimum. A possible exception is the case of three-terminal lines in which one leg of the circuit is approximately an odd number of quarter wavelengths at the frequency used.

For supervisory control by keyed carrier, the 20-db ratio given by Table 7 should be maintained between minimum signal and average noise.

In tone telegraphic functions (e.g. telemetering) the narrow bandwidth of the tone receivers reduces their response to random noise to negligible amounts. In addition to this factor, the wave trains resulting from impulsive noise with 60- or 120-cycle pulse-frequency overlap to a considerable extent in tone receivers of the usual narrow bandwidth. Under these conditions the average rectified noise output is less than that obtained with broadly tuned circuits. The actual reduction is a function of the bandwidth of the tone receivers, which in turn is usually a function of the tone frequency itself. However, the formula given in Table 7 can be used as a guide to the maximum permissible signal-to-noise ratio, and the additional noise reduction due to overlapping of the wave trains can be taken as a safety factor.

In carrier communication applications, the type of system used determines which noise characteristic is most important. In automatic simplex systems, operation of the transfer unit occurs when the peak value of the noise equals the r-f sensitivity setting of the unit. Although momentary operation of the transfer unit on extremely high isolated peaks occurring not oftener than once or twice a minute should not be objectionable, the signal-to-peak-noise ratio for noise peaks occurring more frequently should not exceed the 15 db shown in Table 7.

Quasi-peak noise levels are representative of the interfering effects of noise in duplex and manual simplex carrier communication channels. The figures of Table 7 can therefore be used as the maximum permissible signal-to-quasi-peak noise ratios in these systems for various grades of service.

Because it is not ordinarily possible to reduce appreciably the noise level present at a given receiving point in a carrier system, the only practical way to improve signal-to-noise ratio is to raise the signal level at the receiving point. It is not usually feasible to raise signal levels by increasing the transmitted power, because appreciable gains in terms of decibels require inordinately large increases in power. For example, to raise the signal level from a 10-watt transmitter by 20 db requires an increase to 1000 watts, or 100 times the original power. A much more practical solution is to reduce the channel attenuation by judicious application of line traps to eliminate short taps or spur lines and alternate paths.

REFERENCES

Carrier Equipment and Applications

1. "Modern Power-Line Carrier Equipment," E. L. Harder, *Westinghouse ENGINEER*, July 1944, pp 98-104.
2. "Power-Line Carrier Communication," R. C. Cheek, *Westinghouse ENGINEER*, September, 1947, pp 151-154.
3. "The Applications of Power-Line Carrier," R. C. Cheek, *Power Plant Engineering*, Nov. 1945, pp 76-81.
4. "A Versatile Power-Line Carrier System," H. W. Lensner and J. B. Singel, *AIEE Transactions*, Vol. 63, 1944.
5. "A Simple Single-Sideband Carrier System," R. C. Cheek, *Westinghouse ENGINEER*, November 1945, pp 179-183.
6. "A New Single-Sideband Carrier System for Power Lines," B. E. Lenehan, *AIEE Transactions*, Vol. 66, November 1947.
7. "The Combination of Supervisory Control with Other Functions on Power-Line Carrier Channels," R. C. Cheek, W. A. Derr, *AIEE Transactions*, Vol. 64, May, 1945, pp 241-246.
8. "Power-Line Carrier," F. S. Mabry, *Industrial Electronics Reference Book*, Chapter 25, pp 442-456, John Wiley & Sons, New York, 1948.

Modulation Systems

9. "Frequency Modulation for Power-Line Carrier Current," E. W. Kenefake, *AIEE Transactions*, Vol. 62, 1943, pp 616-620.
10. "A Comparison of the Amplitude Modulation, Frequency Modulation, and Single Sideband Systems for Power-Line Carrier Transmission," R. C. Cheek, *AIEE Transactions*, Vol. 64, May 1945, pp 215-220.
11. "Power-Line Carrier Modulation Systems," R. C. Cheek, *Westinghouse ENGINEER*, March 1945, pp 41-45.

Transmission Theory and Carrier Channel Application

12. *Communication Engineering* (book), W. L. Everitt, McGraw-Hill Book Co., New York, 1937.
13. *Electrical Transmission of Power and Signals* (book), Edward W. Kimball, John Wiley & Sons, New York, 1949.
14. "Propagation d'ondes haute fréquence le long d'une ligne triphasée symétrique," A. Chevallier, *Rev. Gen de l'Electricité*, Vol. LIV, January 1945.
15. "Application of Carrier to Power Lines," F. M. Rives, *AIEE Transactions*, Vol. 62, 1943, pp 835-844.
16. "Power-Line Carrier Channels," M. J. Brown, *AIEE Transactions*, Vol. 64, May 1945, pp 246-250.
17. "Operation of Power-Line Carrier Channels," H. W. Lensner, *AIEE Transactions*, Vol. 66, November, 1947.

Noise and Noise Measurement

18. Survey of Existing Information and Data on Radio Noise Over the Frequency Range 1-30 Mc/s. H. A. Thomas, R. E. Burgess, Special Report No. 15, Radio Research, Department of Scientific and Industrial Research, National Physical Laboratory, London, 1947.
19. "Selective Circuits and Static Interference," *Bell System Technical Journal*, Vol. 4, 1925, pp 265-279.
20. "Frequency-Modulation Noise Characteristics," M. G. Crosby, *Proceedings IRE*, Vol. 25, 1937, pp 472-514.
21. "An Experimental Investigation of the Characteristics of Certain Types of Noise," K. G. Jansky, *Proceedings IRE*, Vol. 27, 1939, pp 763-768.
22. "A Study of the Characteristics of Noise," V. D. Landon, *Proceedings IRE*, Vol. 24, 1936, pp 1514-1521.
23. "Methods of Measuring Radio Noise," Joint Committee on Radio Reception of EEE, NEMA, and RMA, EEE Publication G9, NEMA Publication No. 107, February 1940.
24. "Proposed American Standard Specification for a Radio Noise Meter—0.15 to 25 Mc/s." ASA Sectional Committee on Radio-Electrical Coordination, ASA C 63.2—1949.

CHAPTER 13

POWER-SYSTEM STABILITY

BASIC ELEMENTS OF THEORY AND APPLICATION

Original Authors:

R. D. Evans and H. N. Muller, Jr.*

Revised by:

J. E. Barkle, Jr. and R. L. Tremaine

THIS chapter presents a general introduction to the power-system stability problem including definitions of basic terms, useful physical and analytical concepts, methods of calculation of steady-state and transient stability problems for simplified systems, and the extensions necessary for the application of these principles to practical systems. Short-cut methods for estimating permissible transmission-line loading, and the transient stability performance of common systems are presented. Means of improving system stability are discussed. Examples of steady-state and transient stability calculations appear throughout the chapter.

On commercial power systems, the larger machines are of the synchronous type; these include substantially all of the generators and condensers, and a considerable part of the motors. On such systems it is necessary to maintain synchronism between the synchronous machines under steady-load conditions. Also, in the event of transient disturbances it is necessary to maintain synchronism, otherwise a standard of service satisfactory to the user will not be obtained. These transient disturbances can be produced by load changes, switching operations, and, particularly, faults and loss of excitation. Thus, maintenance of synchronism during steady-state conditions and regaining of synchronism or equilibrium after a disturbance are of prime importance to the electrical utilities. Electrical manufacturers are likewise concerned because stability considerations determine many special features of apparatus and under many conditions importantly affect their cost and performance. The characteristics of virtually every element of the system have an effect on stability. It introduces important problems in the coordination of electrical apparatus and lines in order to provide, at lowest cost, a system capable of carrying the desired loads and of maintaining a satisfactory standard of service, both for steady-state conditions and at times of disturbances.

The problem of system stability had its beginning when synchronous machines were first operated in parallel or in synchronism. It was early recognized that the amount of power that can be transferred from one synchronous machine to another is limited. This amount of load is known as the stability limit, and when it is exceeded, the machine acting as a generator "over speeds" and the machine acting as a motor "stalls."

As power systems developed, it was found with certain

machines, particularly with certain systems connected through high-reactance tie lines, that it was difficult to maintain synchronism under normal conditions and that the systems had to be separated in the event of faults or loss of excitation. Various emergency conditions occasionally made it necessary to operate machines and lines at the highest practicable load; under these conditions stability limits were found by experience. Subsequently, it became apparent that many of the interruptions to service were the result of disturbances that caused loss of synchronism between various machines and that, by modifying the system design, layout, or operation, it was possible to provide a better standard of service.

The early analytical work on system stability was directed to the determination of the power limits of synchronous machines under two conditions: first, the pull-out of a synchronous motor or generator from an infinite bus; and second, the pull-out or stability limit for two identical machines, one acting as a generator and the other acting as a motor. However, the principal developments in system stability did not come about as an extension of synchronous-machine theory, but as the result of the study of long-distance transmission systems.

The modern view of the stability problem dates from the 1924 Winter Convention of the American Institute of Electrical Engineers when a group of papers† called attention to the importance of the problem and presented the results of the first laboratory tests¹ on miniature systems proportioned to simulate a power system having a long transmission line. Another important step was taken in 1925 when the first field tests^{4,5} on stability were made on the system of the Pacific Gas and Electric Company. Much additional practical information⁹ on the problem was obtained by transient recording apparatus, first installed on the system of the Southern California Edison Company. Initially the studies of the problem were restricted principally to the determination of whether certain layouts, proposed for the longer transmission projects, were actually capable of transmitting the desired amount of power under steady-state conditions. Subsequently, it was found that the more important phase of the problem was in the determination of system layouts and loads that would insure satisfactory operating characteristics at times of various transient disturbances arising from load changes, switching operations, and circuit faults with their subsequent isolation. During the ten-year period from 1924 to 1933, the theory of system stability was carefully investi-

*H. N. Muller, Jr. was the original author of "System Stability—Examples of Calculation," which has been included in Chapter 13 in this revision.

†AIEE Transactions, vol. 43, pp. 16-103, 1924.

gated. During this work there were proposed many new methods of improving the stability of systems as discussed in the latter part of this chapter. Since that time considerable experience has been obtained with methods of analyzing stability and with new methods of improving stability, with the result that the subject is now considered to be on a basis that is satisfactory from the standpoint of theory and practice.

The notation used throughout this chapter is as follows: E represents a vector quantity and may be expressed in terms of rectangular coordinates or in polar form. \bar{E} represents the magnitude or scalar value of vector E . Thus,

$$E = \bar{E}(\cos \theta + j \sin \theta) = \bar{E}e^{j\theta} = \bar{E}/\theta$$

I. BASIC CONCEPTS OF STABILITY

1. Essential Factors in the Stability Problem

The essential factors in the stability problem are illustrated in connection with the two-machine system shown schematically in Fig. 1. The various elements of the sys-

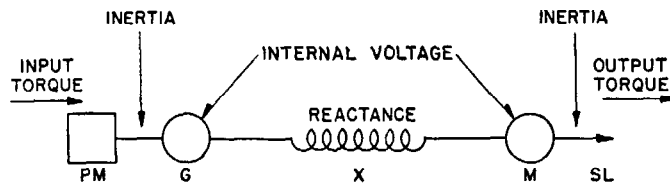


Fig. 1—Basic diagram for the two-machine stability problem.

- PM—Prime mover.
- G—Synchronous generator.
- X—Reactance line.
- M—Synchronous motor.
- SL—Shaft load.

tem, prime mover, synchronous generator, reactance line, synchronous motor, and the shaft load, are indicated. There are seven essential factors affecting stability. These are of two kinds, mechanical and electrical. The essential mechanical factors are:

1. Prime-mover input torque.
2. Inertia of prime mover and generator.
3. Inertia of motor and shaft load.
4. Shaft-load output torque.

The essential electrical factors are:

1. Internal voltage of synchronous generator.
2. Reactance of the system including:
 - a. Generator
 - b. Line
 - c. Motor.
3. Internal voltage of synchronous motor.

In the foregoing discussion, losses have been ignored and this is permissible since losses do not affect the phenomena except to introduce damping for which allowance can easily be made after the character of the system oscillations is understood. To introduce damping at the outset would obscure the character of the essential phenomena involved.

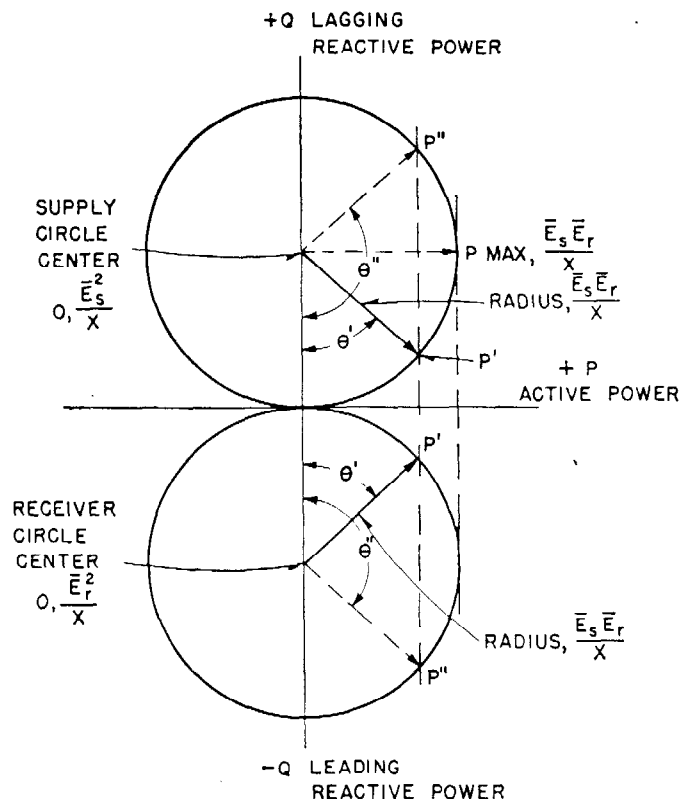


Fig. 2—Elementary power-circle diagram for line reactance X , voltages E_s and E_r , system of Fig. 1.

2. Power-Circle Diagrams and Power-Angle Diagrams

The performance characteristics of the simple two-machine power-transmission system, Fig. 1, are readily shown by power-circle diagrams and power-angle diagrams as given in Figs. 2 and 3 respectively. The diagrams are based on methods described in Chap. 9 and are reducible to the simple form shown because they depend, in the absence of loss, merely upon the four factors \bar{E}_g , \bar{E}_m , θ and X . The equation relating power transfer in a three-phase system is as follows:

$$P = \frac{\bar{E}_g \bar{E}_m}{X} \sin \theta \quad (1)$$

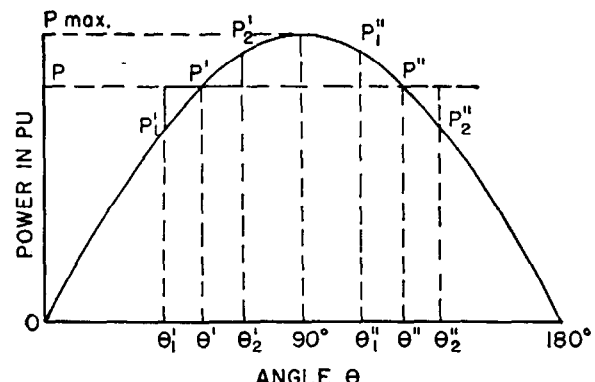


Fig. 3—Elementary power-angle diagram, system of Fig. 1.

where:

P = three-phase power transferred in watts.

\bar{E}_g = internal voltage of generator (line-to-line volts).

\bar{E}_m = internal voltage of motor (line-to-line volts).

X = reactance between generator and motor internal voltages, ohms per phase.

θ = angle by which the internal voltage of generator leads the internal voltage of motor.

When per-unit values of voltages and reactance are used in Eq. (1), the power transferred is obtained as a per-unit quantity referring to the kva base being used. Thus, the three-phase power flow in kilowatts would be the per-unit value multiplied by the kva base.

3. Meaning of Stability Terms

The terms "stability" and "maintenance of synchronism" are quite frequently used interchangeably. However, a system consisting of a synchronous generator, a reactance line, and an induction motor may become unstable but cannot lose synchronism. Nevertheless, system stability is, ordinarily, of importance only when it deals with the conditions of stable operation between synchronous machines. The problem is of importance, primarily from the standpoint of the maximum amount of power that can be transmitted without instability being incurred under steady-state conditions or as a result of circuit changes or faults. The terms "stability" and "power limit" are also frequently used interchangeably. However, a simple system consisting of a generator, a reactance line, and a resistance load has a definite power limit without having a stability limit.

Stability can be formally defined as follows:

Stability when used with reference to a power system, is that attribute of the system, or part of the system, which enables it to develop restoring forces between the elements thereof, equal to or greater than the disturbing forces so as to restore a state of equilibrium between the elements.*

Stability applies to both steady-state and transient conditions on a power system. The distinction between them depends upon whether the stability applies to a condition that includes a transient disturbance. Certain automatic devices, such as voltage regulators, have a bearing on the stability conditions. If such devices are used this fact should be indicated as follows: steady-state stability with automatic devices.

Stability limit for a system with synchronous machines can be considered the same as the power limit, and is defined as:

A *Stability Limit* is the maximum power flow possible through some point in the system when the entire system or the part of the system to which the stability limit refers is operating with stability.*

Criterion of Stability—There are several criteria for the determination of the conditions establishing stability that are needed in connection with the analysis of complicated systems. These criteria can be stated as follows:

*American Standard Definitions of Electrical Terms, ASA-C42-1941.

A power-transmission system operating under specified circuit and transmitted load conditions is said to be stable if, when displaced from these conditions by any small arbitrary forces, the system upon removal of these forces develops restoring forces tending to return it to the original conditions.

The arbitrary displacement can be made in several ways, the most convenient of which is a small arbitrary increase in the angular displacement.

4. Application of the Criterion of Stability

The application of the definition of stability and the criterion of stability will now be considered in connection with the system of Fig. 1. Examination of Figs. 2 and 3 shows that solutions are obtained for the points corresponding to the power P' at the angle θ' and also to the power P'' at the angle θ'' . In the absence of loss, the amounts of sending and receiving power are equal and P' and P'' are equal.

In applying the criterion of stability, the system is assumed to be subjected to a slight arbitrary reduction in angle between internal voltages from θ' to θ_1' in Fig. 3, and the power transferred from the generator to the motor is correspondingly reduced from P' to P_1' . The input and output torques, Fig. 1, remain constant and are equal to each other and to P in Fig. 3 since the system is assumed to have no loss. The prime-mover input power P is now greater than the electrical output power P_1' , resulting in acceleration of the generator rotor which tends to increase the angle between the sending and receiving ends of the system. At the receiving end, the electrical input to the motor P_1' is now less than its mechanical output P and this difference in power decelerates the motor, which also tends to increase the angle between the sending and receiving ends. Thus the arbitrary reduction of the angle between the internal voltages of the generator and motor from θ' to θ_1' reduced the electrical power transferred through the system and resulted in the development of restoring forces tending to increase the angle between the internal voltages and return the system to the original angle θ' . Since losses have been omitted, the angle between the internal voltages would oscillate about the value θ' , but in a practical system where losses are always present, this oscillation would be damped and the system would eventually return to the original angle.

Next, assume that the system is subjected to a slight arbitrary movement increasing the angle from θ' to θ_2' . Under this condition the output of the generator P_2' is greater than its input, which corresponds to P . The difference in input and output decelerates the generator and thus tends to reduce the angle between the sending and receiving ends. Similarly, since losses are neglected, the input to the motor is greater than its shaft load with the result that the motor accelerates and thus tends also to reduce the angle between the sending and receiving ends. The arbitrary displacement of the system, by a small amount from the solution at the angle θ' in such a direction as to increase the angle, creates restoring forces to return the system to the original operating point.

It has been shown that if the system operating at the angle θ' is subjected to small disturbing forces, then regardless of the direction of the small disturbing forces, when

these forces are removed the system develops restoring forces in such a direction as to return the system to the original angle between the internal voltages of the generator and motor. Therefore, the mathematical solution corresponding to the power P' and the angle θ' constitutes a stable operating point, since any tendency for the system to drift away from the operating point θ' develops adequate restoring forces.

Critical Point in System Oscillation—Consider next the operation at the point defined by the angle θ'' and the power P'' . Assume the condition with the angle θ'' increased to θ_2'' . Under this condition the output of the generator and input of the motor are decreased to P_2'' , so that the output of the generator is less than its input, and the input of the motor is less than its output or shaft load. These circumstances produce forces that accelerate the generator and decelerate the motor, and increase further the angle by which the generator leads the motor. The changes in force are such as to augment the change in angle with the result that the system pulls out of step, that is, the system becomes unstable. Apply next this same criterion for the condition of a slight reduction in the angle below θ'' . For θ_1'' the electrical output of the generator is greater than its mechanical input and the electrical input to the motor is greater than its mechanical output or shaft load. The change in the angle between internal voltages in the system slows down the generator and speeds up the motor. Both of these changes cause the system to reduce still further the angle between the internal voltages. Thus the solution corresponding to the angle θ'' and the power P'' is said to be an unstable solution since a slight departure from that point sets up forces to augment the change in that same direction instead of restoring the condition to the original point of solution. However, in the case of movement back from the point corresponding to the angle θ'' , the system further reduces the angle and moves in the direction of the stable operating point at θ' . The system will develop forces causing it to move in the direction of θ' for all angles between θ'' and θ' .

Thus the point corresponding to the angle θ'' is the *critical point in system oscillation* for given internal voltages, reactance, and power-flow conditions. If the system has a stable solution at θ' , it can withstand system disturbance that causes it to oscillate on either side of this angle up to θ'' . If that angle is exceeded, the system will lose synchronism. If that angle is not reached, the system will oscillate about θ' and because of losses it will come into equilibrium at that angle.

5. Steady-State Stability Limit

For the simple two-machine transmission system illustrated in Fig. 1, the steady-state stability limit is given by the maximum power obtained from either the power-circle diagram or the power-angle diagram of Figs. 2 and 3. The steady-state stability limit of a system without loss occurs at the angle of 90 degrees between sending and receiving ends as shown by these diagrams or as readily obtained from Eq. (1). The steady-state limit for a three-phase system is given by

$$P_{\max} = \frac{\bar{E}_g \bar{E}_m}{X} \quad (2)$$

which gives the maximum power in watts when the voltages are expressed as line-to-line volts and the reactance as ohms per phase, or the maximum power in per unit when per-unit voltage and reactance are used. If the criterion of stability is applied, (1) for all load conditions with the power and angle less than those corresponding to the 90-degree limit, the system will be inherently stable; whereas (2) for all loads at angles greater than 90 degrees the system will be unstable. The 90-degree load point for a system without loss is the *critical load* or the maximum value of all steady-state operating points that are inherently stable.

There is a single steady-state stability limit for specified circuit, impedance, and internal voltage conditions. It follows, therefore, that if the excitation of either or both machines is changed so as not to correspond to the internal voltages assumed, the stability limit will be correspondingly changed. Loss of field results, of course, in reducing the synchronizing power to zero. The machine that loses its excitation pulls out of synchronism with the other synchronous machines and operates as an induction machine. Whether the system is stable or unstable as a combination of synchronous and induction machines is determined in part by the characteristics of the induction machines.

6. Transient-Stability Limit

Transient stability refers to the amount of power that can be transmitted with stability when the system is subjected to an "aperiodic disturbance." By *aperiodic* disturbance is meant one that does not come with regularity and only after intervals such that the system reaches a condition of equilibrium between disturbances. The three principal types of transient disturbances that receive consideration in stability studies, in order of increasing importance, are:

1. Load increases.
2. Switching operations.
3. Faults with subsequent circuit isolation.

The basic power-angle diagrams give an adequate picture of the stability phenomena encountered in each of these disturbances.

Load Increases can result in transient disturbances that are important from the stability standpoint if (1) the total load exceeds the steady-state stability limit for spe-

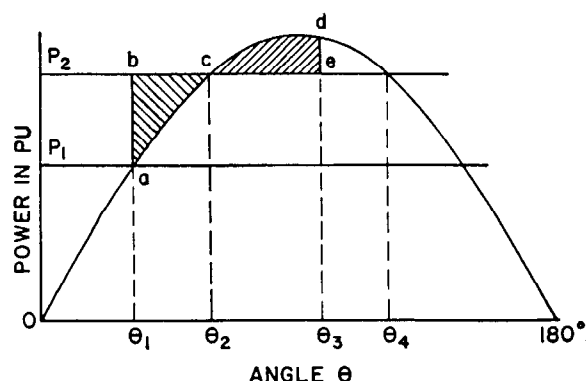


Fig. 4—Power-angle diagram for analyzing load increases.

cific voltage and circuit reactance conditions, or (2) if the load increase sets up an oscillation that causes the system to swing beyond the *critical point* from which recovery would be impossible, as pointed out previously. Consider a system operating under the conditions shown in Fig. 4 with the load P_1 at the angle θ_1 and the prime-mover input and shaft output abruptly increased to P_2 . Because of the inertia of the rotating machines, the internal voltages of the generator and motor do not immediately swing to θ_2 , which would permit transfer of power P_2 . Instead, the initial differences of power input and output are used in accelerating the generator and in decelerating the motor rotating elements. Both of these changes cause the rotors to depart from synchronous speed and to increase their angular differences. Thus when the system reaches θ_2 , the generator is traveling above synchronous speed and the motor below synchronous speed. The difference in the stored energy cannot instantly be absorbed and as a result the system overshoots θ_2 and reaches some larger angle as θ_3 , such that the shaded area cde is equal to the area abc . Neglecting losses, these two areas can be taken as equal³. The oscillation will not exceed the angle θ_3 , and because of losses in an actual system, equilibrium will ultimately be reached at θ_2 . In the case illustrated in Fig. 4 the system oscillates to the angle θ_3 , which is greater than 90 degrees but is stable because θ_3 is less than θ_4 , the critical angle for the load P_2 . With a somewhat larger total load or with a greater increment of load, the maximum point reached in the oscillation would be greater than θ_3 shown in the diagram. With increasingly severe conditions, a point is reached where the critical angle is equaled and this represents the transient limit for the load increase. The amount of load increase that a system can withstand depends upon the steady-state limit of the system and the initial operating angle. Figure 5 shows the total permissible sudden increase in amount of power that can be absorbed with stability, expressed as a percentage of the steady-state stability limit of a system without loss and plotted as a function of the angle between internal voltages.

Switching Operations—The transient-stability limits

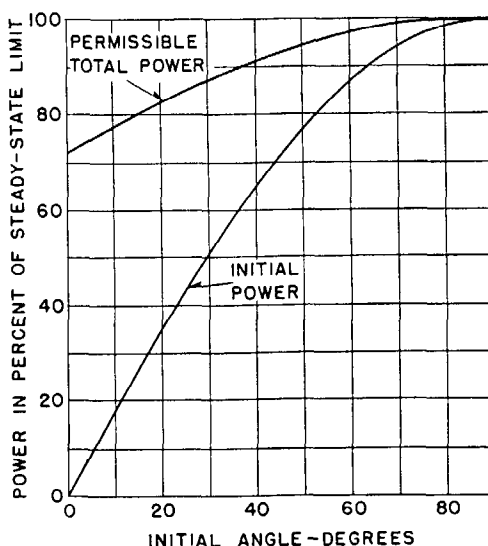
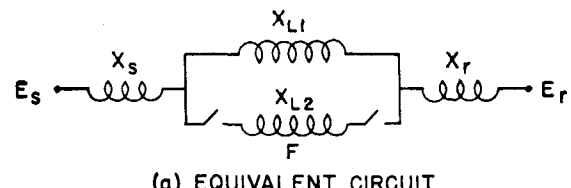
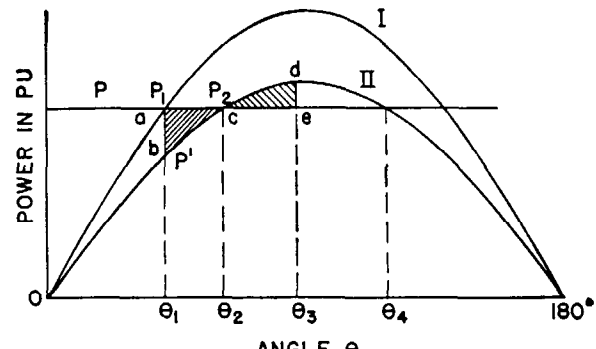


Fig. 5—Permissible load increase vs. initial-angle curve.

for switching operations can be investigated in a similar manner using the equal-area criteria³ that have been applied for the determination of the transient limit for load increases. In the case of switching operations there are, however, two power-angle diagrams that require consideration: (1) the power-angle diagram for the initial condition, (2) the power-angle diagram for the final condition, that is, the condition after the switching operation has taken place. Figure 6 (a) indicates a system with two lines initially in service; Fig. 6 (b) shows two power-angle diagrams, Curve I applying to the initial circuit-condition and Curve II applying to final circuit-condition. The diagram shows the transmitted power P , the initial operating condition at the angle θ_1 and the power P_1 , and the final operating condition at θ_2 and P_2 . The moment the switching operation takes place the electrical output is reduced from P_1 to P' . This change produces an increment power of magnitude $(P - P')$, which is available for accelerating the generator and decelerating the motor, both changes tending to increase the angle between the sending and receiving machines. Thus, the two machines depart



(a) EQUIVALENT CIRCUIT



(b) POWER-ANGLE DIAGRAM

Fig. 6—Power-angle diagram for analyzing transients due to switching operations.

from synchronous speed, accelerating and decelerating forces increasing the angle from θ_1 to θ_2 . At this point the generator rotor is traveling above synchronous speed and the motor rotor below synchronous speed with the result that both rotors tend to overshoot θ_2 and to reach θ_3 , such that the area abc is equal to the area cde . At θ_3 , the energy stored above and below synchronous speed has been absorbed and since the instantaneous power output of the generator and input of the motor are greater than the prime-mover input and shaft loads, respectively, restoring forces are developed that cause the system to oscillate about θ_2 and reach a condition of equilibrium because of losses in a practical system.

The amount of power transferable without loss of synchronism depends upon (1) the steady-state stability limit

for the condition after the switching operation takes place and upon (2) the difference between initial and final steady-state operating angles. The stability limits for switching operations are lower for the larger amount of the final circuit reactance and for the greater percentage change in the circuit reactance.

Faults and Subsequent Circuit Isolations—The third and most important type of transient disturbance arises from application of faults and the subsequent circuit changes required to isolate the fault. For such disturbances three or more circuit conditions require consideration: (1) the initial condition, immediately prior to the fault, (2) the condition during the fault, and (3) the condition subsequent to the isolation of the fault. Additional conditions are required to cover the cases in which the fault is isolated in two or more steps, such as would be produced by the disconnection of a line section by sequential switching. Additional steps would be required to take care of the case of a high-speed reclosing breaker, which first disconnects a faulted line and suppresses the arc, and subsequently restores the line to the original circuit connection. However, the procedure to be followed in the more complicated cases will become evident from consideration of the simpler case.

Consider a transmission system similar to Fig. 6 (a) but with one line subjected to a fault at an intermediate point. The power-angle diagram for the case with the two lines in service is indicated in Fig. 7 by the Curve I, which

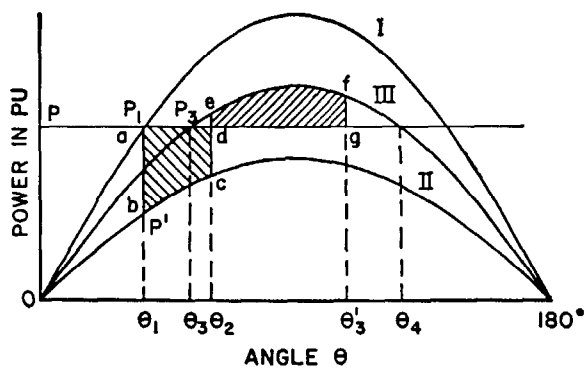


Fig. 7—Power-angle diagram for analyzing transient disturbances due to faults with subsequent circuit isolation. See Fig. 6 (a).

intercepts the line of transmitted power at the angle θ_1 and the power P_1 . Upon application of the fault the amount of power transferable from one end to the other is reduced. If the fault were a zero-impedance fault on all lines the power transmitted would be reduced to zero. However, if, as is usually the case, the fault is not a zero-impedance fault on all lines, some power can be transmitted from the sending to the receiving ends. This case is assumed in the diagram of Fig. 7 and is indicated by the Curve II passing through the points b and c . The power-angle diagram for the final condition with the faulted line switched out of service is shown by the Curve III that passes through the line of transmitted power at the angle θ_3 and the power P_3 . Upon application of the fault, the power output of the generator and the power input to the motor are reduced

from P to P' , the difference in power ($P - P'$) being absorbed in accelerating the generator and decelerating the motor. For the severe type of fault shown, the system would pull out of step if the fault were not promptly cleared. Assume, however, that the fault is cleared by the time the system swings to θ_2 . At this point, transfer is made to the final circuit condition, Curve III. The power-angle diagram shows that the power output of the generator exceeds the input, with the result that the generator rotor is decelerated and that the motor is accelerated. However, because of the energy stored in the machine rotors above and below synchronous speed the system continues to swing to some larger angle, such as θ'_3 , so that the area $defg$ is equal to the area $abcd$. Thus, θ'_3 is the maximum point reached in the system oscillation using the same equal-area criteria discussed in connection with other types of transient disturbances. The system oscillates about the angle θ_3 and because of losses will ultimately come to equilibrium at that angle.

If the severity of the fault is increased, as indicated by the reduction in amount of power that can be transmitted during the fault condition, or if the duration of the fault is increased as indicated by a larger θ_2 , or if the power-angle diagram for the final condition has a lower maximum, the largest angle during the system oscillation is increased beyond θ'_3 and under some conditions would reach the critical angle θ_4 for the transmitted power under the final circuit condition. When this condition is met the transient-stability limit for the condition is said to be reached.

The nature of transient disturbances incident to faults can be examined further in connection with the use of quick-reclosing breakers as illustrated in Fig. 8. Two cases are considered, namely, a single-circuit case shown in (a) and a double-circuit case shown in (b). In both cases, the faulted line is de-energized to suppress the arc in the fault and reclosed after an interval for the purpose of insuring stability. These switching operations provide a succession of power-circuit conditions and a corresponding set of power-angle diagrams as can be seen by a detailed examination of Fig. 8. The conditions necessary for maintaining stability are also stated in terms of the stored-energy relations as shown by corresponding areas on the power-angle diagram.

No method has been given for the determination of the angles, θ_2 in Fig. 7, or θ_2 and θ_3 in Figs. 8 (a) and (b), which define the condition for which the fault is removed or the circuit switched. From a practical standpoint the circuit change is not made in accordance with the angular difference between the sending and receiving ends; instead it is made as a function of time measured from fault application, the duration being that required for the operation of protective relays and circuit breakers. This time can be calculated by a step-by-step process to determine the changes in accelerating force, the changes in velocity, and the changes in angles. Thus, the determination of the angle-time relations constitutes one of the important steps in transient-stability calculations and will receive considerable attention in subsequent sections.

For a power system with machines of assumed constant internal voltages, with circuits of assumed reactances, and with losses neglected, there is only one steady-state limit.

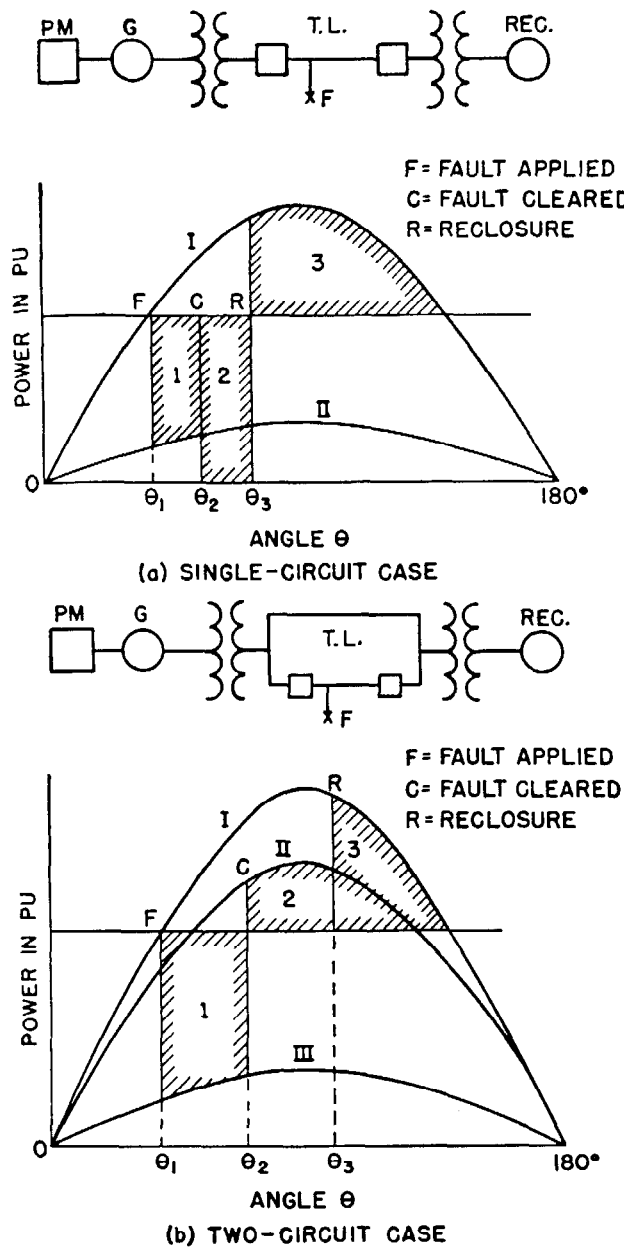


Fig. 8—Power-angle diagram for reclosure.

- (a)—Single-circuit case
 - Curve I for normal circuit
 - Curve II for fault condition ($2L - G$)
 - For stability, areas (1 plus 2) \leq area 3
- (b)—Two-circuit case
 - Curve I for two lines (normal)
 - Curve II for one line (normal)
 - Curve III for fault ($2L - G$)
 - For stability, area 1 \leq areas (2 plus 3)

However, for the transient-stability calculations there are many conditions depending upon the character of the transient under consideration. For example, for load increases, the transient-stability limit depends upon the initial load and the increment of load. For the switching operation, the transient limit depends upon the stability limit for the final circuit condition and upon the initial



Fig. 9—The mechanical model (set up for a system with two generators and an intermediate synchronous condenser).

operating angle. The transient limit for the simplest condition involving a fault on a system with subsequent circuit isolation depends upon the initial operating angle, the severity of the fault and its duration, and the stability limit for the system after the fault is cleared. It becomes necessary, therefore, when giving a transient-stability limit of a system to define the conditions under which the limit applies.

7. The Mechanical Analogy of a Power-Transmission System

The definitions of stability given in Sec. 3 and the subsequent discussions have been given in terms of equilibrium of the power-transmission system. Equilibrium phenomena are ordinarily visualized in terms of a static system in mechanics. However, the discussion of the familiar static systems cannot directly be applied to the complicated electro-mechanical system employed in power transmission. Furthermore, the actual system involves dynamic rather than static equilibrium. To circumvent this difficulty a mechanical analogy, which has properties corresponding to the actual dynamic electro-mechanical system, has been devised.

The most convenient means of visualizing the basic phenomena of a power-transmission system is the mechanical analogy developed by S. B. Griscom⁶ and shown in Figs. 9 and 10. The mechanical analogy or mechanical model, as the device is more commonly called, consists essentially of two rotatable units mounted on a common shaft and provided with lever arms, which are connected at their outer ends by a spring. One of these rotatable elements is designated as the generator element and the other as the motor element. Each of these elements is provided with means for applying torque in such a way as to stretch the spring connecting the lever arms.

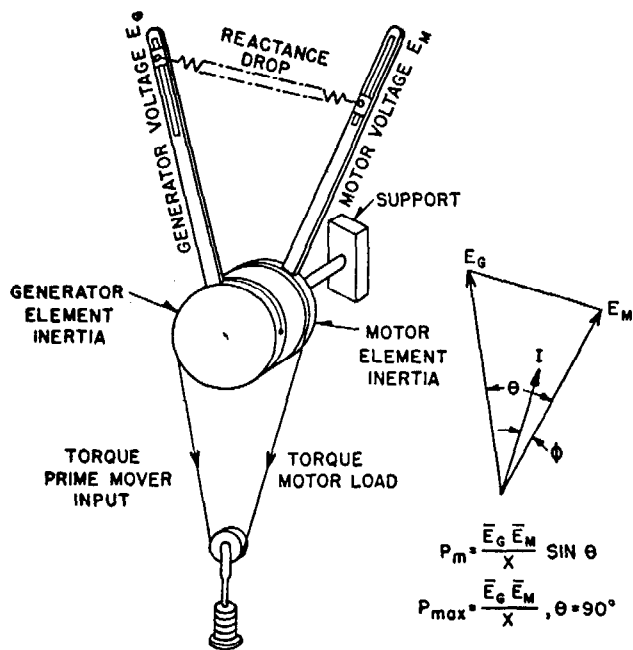


Fig. 10—The mechanical analogy for power-system stability.

Mechanical Model

1. Radial distance from pivot to any point on spring.
2. Length of spring.
3. Tension of spring, proportional to its length.
4. Torque of either arm = product of the length of the arm and component of spring tension perpendicular to arm.
5. Product of the length of the arm and component of spring tension along the radius at any point.
6. Angle between any two points on the spring.

Power-Transmission System

- | | |
|---|----------------------|
| Line voltage at corresponding point. | Line reactance drop. |
| Line current. | Active power. |
| | Reactive power. |
| Phase displacement of voltages at the corresponding points of the system. | |

The correspondence between the various mechanical and electrical factors of the mechanical model and the power-transmission system is shown in connection with Fig. 10. The mechanical model is stationary for the normal synchronous frequency, and the power-flow relations are represented by torques. Movement of the model corresponds to oscillations of the power system with respect to normal synchronous speed. Thus, the model shows only the changes in movement that are significant from the standpoint of stability. The mechanical model has a power limit occurring at an angle of 90 degrees between the lever arms of a two-machine system. The model is also proportioned so as to simulate transient conditions as well as steady-load conditions. The mechanical model can be extended by the addition of rotatable elements and additional springs so as to simulate complicated power systems. For example, a transmission system with an intermediate synchronous condenser can be represented by the aid of the third element of Fig. 9 with the addition of a spring from the lever arm of the third element to the appropriate point on

the spring connection between the other two rotatable elements.

The mechanical model has been used for the calculation of actual stability problems but the a-c network calculator method is more convenient. Thus, the mechanical model is now employed in its original function of providing the best qualitative method of visualizing the essential phenomena in the power-system stability problem. Sufficient information has been given to enable one mentally to set up the mechanical model for the corresponding system condition and to study its performance for various steady-state and transient conditions. While an actual model is of considerable assistance, the mechanical analogy is useful even though no model is available. It is suggested that the mechanical analogy should be considered in connection with the entire discussion of this chapter, particularly in connection with multi-machine problems, such as those involving an intermediate synchronous condenser, since it frequently happens that some particular point is more readily grasped from the consideration of the model than of the actual system.

II. REPRESENTATION OF SYSTEM FOR STABILITY CALCULATIONS

In discussing methods for calculating stability, it is convenient to consider first the case involving two synchronous machines, and, subsequently, those involving three or more machines. In the previous part the stability phenomena were discussed in terms of the two-machine system reduced to its elements with the electrical system represented by two internal voltages and one reactance between them. In practical systems, even for the two-machine case, it is necessary to consider other factors, such as:

1. Representation of system-impedance elements.
 - a. Series branches with resistance.
 - b. Shunt branches.
 1. Shunt capacitance.
 2. Shunt loads.
 3. Faults.
2. Initial operating conditions.
3. Representation of machines including the effects of regulators and exciters.

8. Representation of System-Impedance Elements

A typical layout for a two-machine transmission system is shown in Fig. 11. This system is assumed to have series resistances, shunt capacitances, shunt loads, maintained voltages at sending and receiving buses, and to be subjected to an unbalanced fault at point F on line 2, which is subsequently disconnected to isolate the fault.

In a practical system it is frequently necessary to consider the effect of resistance and of shunt capacitance, since these are always present in transmission lines. Since voltage is normally maintained on the sending and receiving buses, it is convenient to obtain the equivalent constants for the intervening part of the system. This can be done by the use of the generalized equivalent π network or the general circuit constants for the transmission line as described in Chaps. 9 and 10. In either case, it is possible

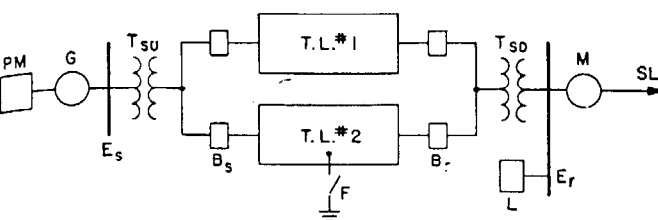


Fig. 11—Typical two-machine stability problem.

Notation: See Fig. 1; also the following:

T_{su} —Step-up transformer.

T_{sd} —Step-down transformer.

T.L. #1, T.L. #2—Transmission lines.

B_s, B_r —Breakers.

F—Fault.

E_s, E_r —Voltages at regulated buses.

L—Shunt load.

to derive power-circle diagrams and power-angle diagrams on the basis of the network intervening between buses, which have maintained voltages E_s and E_r . When loss is taken into account there is a difference between the sending and receiving power, as can be seen from Fig. 14. For this reason, power-angle relations for the two ends are no longer identical as assumed in Sec. 3. The method of taking this fact into account will be discussed subsequently in Sec. 23, Step-by-Step Procedure.

When loss or intermediate loads are present in a power transmission system, the maximum amounts of power at the sending and receiving ends occur at different angular displacements. If under steady-state conditions the prime-mover input corresponds to maximum input to the motor, two interesting phenomena occur if the shaft load is slightly increased. The motor slows down in any event, but the generator (1) may pull out of step with the motor and overspeed or (2) may stay in synchronism with the motor and slow down with it, depending upon the relative inertias of generator and motor. These phenomena, while of considerable theoretical interest*, are of little practical interest, except as indicative of margins, because the important load condition corresponds to the maximum delivered power and that is not dependent upon the relative inertia characteristics.

9. Representation of Shunt Loads

On a system that contains only two large synchronous machines requiring individual consideration, the various other loads may have different characteristics from the standpoint of changes in real and reactive components with change in voltage. It is usually permissible to assume for small synchronous motors and induction motors that the kilowatt load is independent of the voltage. Synchronous-converter load is assumed to vary in proportion to the square of the voltage. Lighting load is often assumed to vary as the square of the voltage, but it is more accurate to assume that the change is according to the 1.8 power of the voltage ratio³². The changes in reactive kva with voltage are widely different for these different typical loads, as shown in Fig. 12.

From a practical standpoint, it is not feasible to consider

*For further study of these phenomena see Reference 10 or 36.

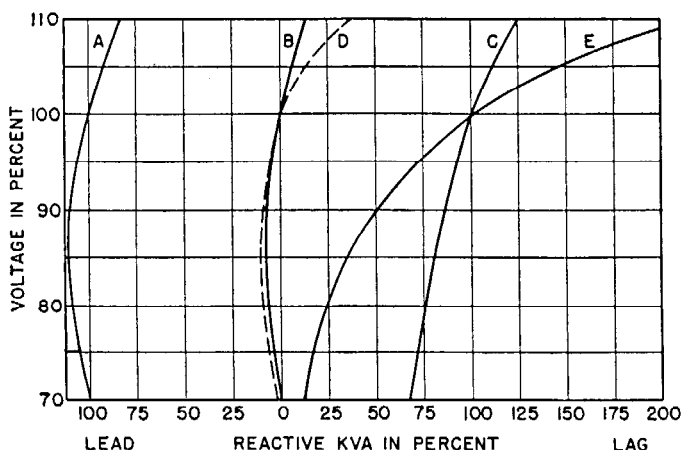


Fig. 12—Reactive Kva-Voltage characteristics of typical loads.

Curve	Description	Reactive Kva Base
A	100-kva synchronous motor 80 percent power-factor	60 kva
B	100-kva synchronous motor 100 percent power-factor	100 kva
C	15-hp induction motor, 80 percent load, 90 percent power-factor	5 kva
D	1000-kw synchronous converter	1000 kva
E	Transformer magnetizing Value at 100 per- cent voltage	

a large number of small shunt loads; instead, it is permissible to use a single composite load curve. To determine such a load characteristic an effort should be made to obtain the segregation of the principal types of load carried by the system under the conditions for which the stability characteristics are to be investigated. Table 1 gives a typical segregation of peak loads.

TABLE 1—SEGREGATION OF TYPICAL SHUNT LOADS

Induction Motor.....	60%
Synchronous Motor.....	10%
100% Power-Factor.....	5%
80% Power-Factor.....	5%
Synchronous Converter.....	5%
Lighting and Heating.....	25%

By combining the real and reactive components of loads from segregations similar to that of Table 1 and with reactive kva variations similar to those of Fig. 12, it is possible to arrive at a composite load characteristic curve, such as shown in Fig. 13, which includes 15 percent exciting kva. This figure shows the variations in both the real and reactive components of load with change in voltage using the real component at normal voltage as reference. The dotted curve of Fig. 13 shows the variation for a constant shunt-impedance load. Figure 13 also shows points on the power-voltage and reactive kva-voltage curves for 100 percent and 90 percent voltage obtained from tests on the Brooklyn Edison Company's system[†]. These tests showed for a 10 percent reduction in voltage that the power was reduced to 87 percent and the reactive kva to 80.6 percent of the corresponding values at normal voltage. These are

[†]System Load Swings, by Bauman, Manz, McCormack, and Seeley, *AIEE Transactions*, Vol. 60, 1941, p. 541, Disc., p. 735.

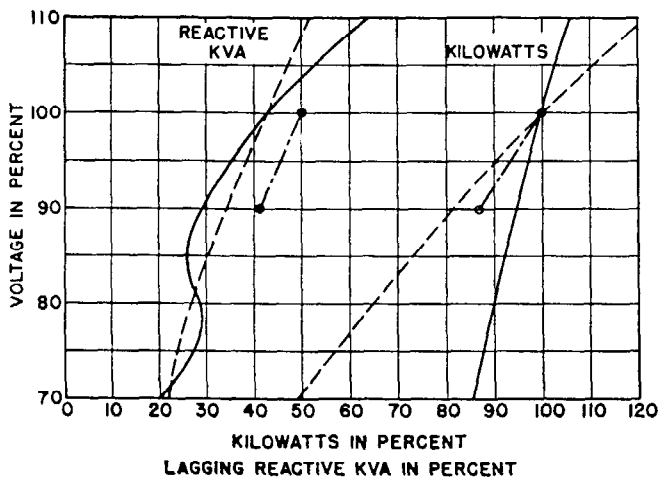


Fig. 13—Variation of composite load with voltage.

— Composite load based on Fig. 12.
 - - - Constant impedance.
 - - - (Bauman, Manz, McCormack and Seeley.) Normal kilowatts equal 100 percent.

to be compared with 81 percent, which would be obtained with a constant-impedance load of the corresponding power factor. The variations in load voltages usually are not great because they are maintained by local generators and synchronous condensers equipped with voltage regulators. This fact permits the relatively crude approximation of constant-impedance loads to give satisfactory results for the majority of cases.

10. Representation of Faults

In this discussion of stability, symmetrical systems only have received consideration. However, the majority of faults on power systems are not balanced three phase. As a consequence, the individual phase voltages are considerably unbalanced, and the voltage of neither the faulted nor unfaulted phase (or phases) is a measure of the voltage available for through power transmission. Instead, the positive-sequence voltage is the representative quantity.

In Fig. 21 of Chap. 2, interconnections between the sequence networks are given for various types of faults at a single location. When the sequence networks, as viewed from the point of fault, are thus interconnected to represent a particular type of fault, correct positive-sequence voltages and currents will exist at all points in the positive-sequence network (the original balanced network). Since only the positive-sequence quantities are to be used, all of the interconnected network except the positive-sequence network can be reduced to a single impedance*, which simplifies calculations. This impedance is, as the above discussion shows, a function of the negative- and zero-sequence impedances as measured from the point of fault, and varies with the type of fault. Thus, for a single line-to-ground fault this impedance is $(Z_2 + Z_0)$ connected from the point of fault to the neutral of the system; and for a double line-to-ground fault, it is $\left(\frac{Z_2 Z_0}{Z_2 + Z_0}\right)$, that is, Z_2 and

Z_0 in parallel, connected from the point of fault to the neutral. Thus the stability problem involving an unbalanced fault at a single location is reduced to one involving an equivalent three-phase symmetrical system. The original balanced network gives the desired positive-sequence quantities at all points when this equivalent impedance is connected to it†.

The physical interpretation of this method of handling unbalanced faults is helpful‡. The power and reactive kva consumed in the negative- and zero-sequence networks are generated in the machines as positive-sequence quantities and are transmitted through the system to the fault location. There these quantities are converted by the asymmetry of the fault to negative- and zero-sequence quantities which are fed back into the system and consumed as $R I^2$ and $X I^2$ for negative- and zero-sequence except for the effect produced by negative-sequence torques in machines. As pointed out in Chap. 6, the negative-sequence input to the rotor of a machine is consumed half in $R_2 I_2^2$ losses and half in negative-sequence torques. These torques tend to drive the machine in a direction opposite to that of its normal rotation. The accurate method of considering this effect is, of course, to modify appropriately the mechanical input to the machine. The negative-sequence resistance for typical machines is given in Table 4 of Chap. 6.

11. Determination of Initial Operating Conditions

Frequently in stability studies only part of the initial operating conditions are defined or are known. Consequently, to determine the initial conditions, calculations and frequently additional assumptions are necessary. Usually the delivered power and maintained voltages at sending and receiving buses are known. In addition, the characteristics of the transmission line, step-up and step-down transformers are known, although sometimes the kva capacity of the latter must be adjusted. For the determination of the initial operating conditions the use of the power-circle diagram is frequently advantageous because the bus voltages are usually known or can be assumed since they are subjected to relatively narrow variations. A particular method of using the power-circle diagram to assist in the determination of the initial operating conditions will now be described in connection with the system outlined in Fig. 11. The operating conditions of that part of the transmission system, including step-up and step-down transformers, between the sending and receiving buses whose voltages E_s and E_r are maintained, can conveniently be shown by the power-circle diagram of Fig. 14. The center of the receiving circle for the transmission line with transformers is plotted at the point C_r and of the sending-end circle at the point C_s . The positions of the

*This method is actually applicable to all types of unbalances, including open conductors and multiple faults at separate locations. For example, for the case of two conductors open, the equivalent impedance is the sum of the negative- and zero-sequence impedances as viewed from across the open, connected across the open of the positive-sequence network, i.e., an impedance between two points of the positive-sequence network. Referring to Chap. 2, Fig. 21 (p), impedances (X_2 to Y_2) plus (X_0 to Y_0) connected from X_1 to Y_1 .

†Page 324 of Reference 27.

*Appendix III of Reference 5 and Reference 27.

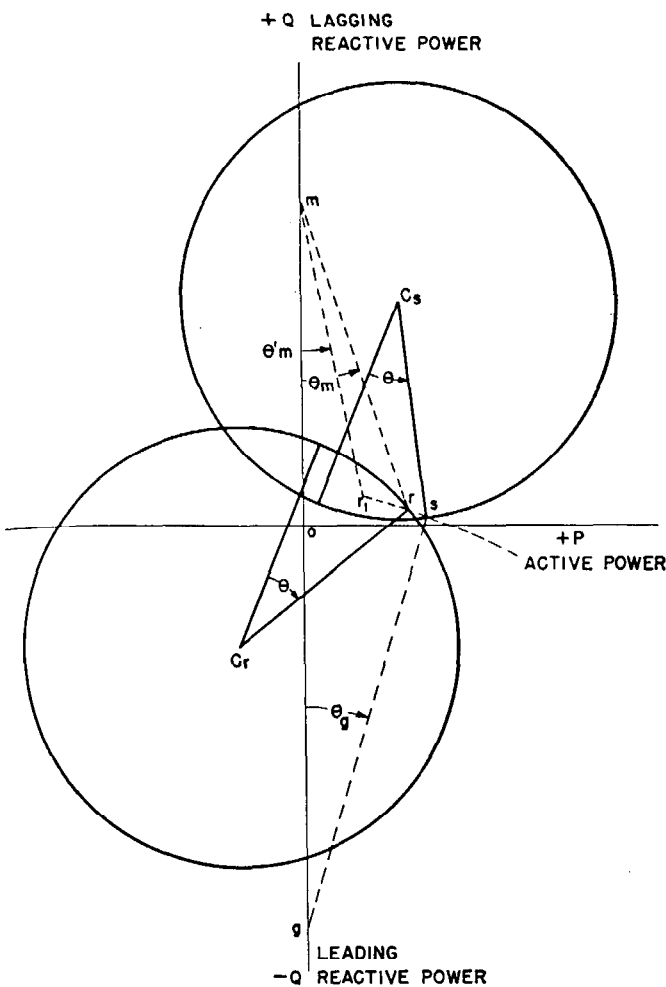


Fig. 14—Diagram illustrating the use of power-circle diagrams to determine initial conditions of internal voltages and overall angles on a system with maintained terminal voltages.

radii of these circles for zero difference in phase position between sending and receiving voltages are shown as the reference position for the angle θ . For a typical operating condition the receiver load is represented by a point in the receiver circle at r and at the angle θ with respect to the zero position of the radius vector. The corresponding sending-end power and reactive-kva quantities are shown at the point s also at the angle θ with respect to the zero position of the radius vector for the sending-end circle.

The output of the synchronous generator supplying the transmission line is completely defined by the real and reactive kva and terminal voltage. If the equivalent reactance of the generator is known, the internal voltage can readily be computed from the terminal conditions in the usual manner. It is a simpler matter usually to plot parts of another circle diagram for the synchronous generator considering it as a reactance line for which the receiver conditions are completely defined. Ordinarily, the resistance loss is negligible in comparison with the reactive kva with the result that the center of the generator circle diagram is located on the Y -axis. The center of the receiver circle for the generator is located at the point g , which is numerically equal to the generator short-circuit

kva computed on the basis of the terminal voltage and equivalent machine reactance. The internal voltage in magnitude and phase position becomes immediately available from the circle diagram, since the receiver conditions for the generator must equal the sending-end conditions for the line. The phase position is given by the angle θ_g measured between the radius $g-s$ and the line of centers $g-o$. Since terminal conditions at s must be satisfied, the magnitude of the internal voltage of the generator is given by the relation:

$$\bar{E}_g = \frac{\text{distance } g \text{ to } s}{\text{distance } g \text{ to } o} \bar{E}_s \quad (3)$$

Similarly, the internal voltage of the synchronous motor can be obtained from its real and reactive-kva input and its terminal voltage. The center of the sending circle for the motor is located at the point m . The phase position of the internal voltage with respect to the terminal voltage is given by the angle θ_m . The magnitude of the internal voltage of the motor is:

$$\bar{E}_m = \frac{\text{distance } m \text{ to } r}{\text{distance } m \text{ to } o} \bar{E}_r \quad (4)$$

The effect of shunt load, such as shown at the receiver bus in Fig. 11, can be taken into account in several ways. For example, the shunt load can be added to the transmission system and considered as a part of it. Another method is to subtract the shunt load from the receiver, which assumption would modify the input to the synchronous motor by the amount shown graphically by changing the load point from r to r_1 . The effect of this shunt load on the magnitude and phase position of the internal voltage of the motor can readily be computed for the load at r_1 in a manner similar to that previously described for the load at r .

The method of using the circle diagrams illustrated in Fig. 14 provides a convenient method of obtaining the internal voltages of machines both in magnitude and phase position. The total difference in angle between these voltages is, of course, equal to the sum of the machine and line angles, that is, the sum of θ_g , θ and θ_m . This method of using the power-circle diagram is particularly applicable for those problems in which the voltages are maintained at sending or receiving buses or at other points in the system through the use of voltage compensators.

12. Representation of Machines

Previously, it has been indicated that a synchronous machine can be represented in stability studies by an appropriate reactance and a corresponding internal voltage. Two reactances are commonly used, viz.:

1. An equivalent synchronous reactance for steady-state stability.
2. Transient reactance for transient stability.

The internal voltages associated with these reactances are determined from the terminal voltage and the voltage drop due to the load currents flowing through the machine reactance.

In the case of steady-state stability, the value used for the equivalent synchronous reactance depends upon the

method of calculation being used. This is discussed in detail in Sec. 14 where methods of steady-state stability calculation are described.

In transient-stability studies, the internal voltage is the vector sum of the terminal voltage and the transient-reactance voltage drop due to the load currents just prior to the disturbance.

III. STEADY-STATE STABILITY CALCULATIONS

In this part the general problem of steady-state stability calculation is discussed in detail and specific examples given to illustrate each method of calculation. Particular attention is given the problem of calculating the power limit of the synchronous generator connected to a system. The power limit in this case is commonly called the "pull-out power" or the "pull-out torque."

The pull-out power as discussed herein refers to a steady-state stability condition, which is initially of a transient character but must be endured long enough to bring it into the classification of steady-state stability. Tripping of a loaded generator, loss or reduction of the excitation of a generator, or the tripping of a tie line supplying power to the system illustrate that pull-out power or maximum power output of the generators involved is important. The pull-out power of a generator is calculated from the inherent characteristics of the generator, which are governed by such factors as air-gap length, demagnetizing effect of the stator on the rotor, degree of saturation, reactance, and short-circuit ratio. For modern machines if the short-circuit ratio is specified, the other factors usually have a fairly definite range of values, so that short-circuit ratio is the best single index of inherent steady-state stability of a generator.

The power equations in the following sections are written in terms of single-phase quantities. Thus, when the voltages are written as line-to-neutral volts and the reactances as ohms per phase, the power obtained from the equations is single-phase power. It should, of course, be multiplied by three to obtain the three-phase power. If all line-to-neutral voltages are multiplied by $\sqrt{3}$ and expressed as line-to-line volts, the equations give three-phase power directly. The equations can be used without alteration when the work is done using per-unit values.

13. Effect of Saliency on Steady-State Stability

The steady-state performance of a system containing unsaturated salient-pole machines can be calculated by the two-reaction method discussed in Chap. 6, particularly in connection with Figs. 12, 14, and 15. These diagrams are similar to that of Fig. 15 of this chapter, except that the notation has been changed from machine form to circuit form. For this diagram the relations of voltage and current in terms of the machine angles were previously derived or may be written by inspection as follows:

$$\bar{E}_d = \bar{E}_t \cos \theta + x_d \bar{I} \sin (\theta + \phi) \quad (5)$$

$$0 = -\bar{E}_t \sin \theta + x_q \bar{I} \cos (\theta + \phi) \quad (6)$$

$$\bar{I} = \frac{\bar{E}_d - \bar{E}_t \cos \theta}{x_d \sin (\theta + \phi)} \quad (7)$$

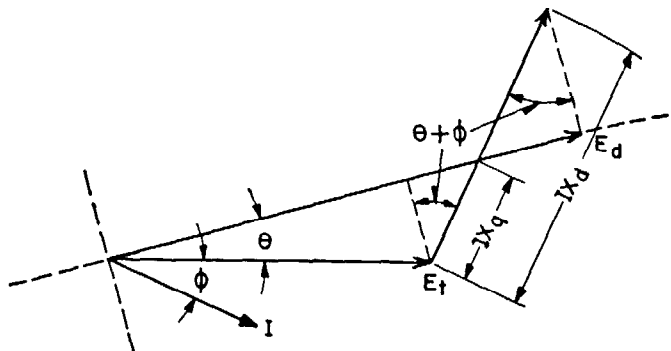


Fig. 15—Vector diagram for salient-pole synchronous machine based on two-reaction method.

- E_t —Terminal voltage (phase-to-neutral—rms).
- E_d —Excitation voltage due to flux in direct axis.
- I —Armature current (line-rms).
- θ —Displacement angle.
- ϕ —Power-factor angle.

$$\bar{I} = \frac{\bar{E}_t \sin \theta}{x_q \cos (\theta + \phi)} \quad (8)$$

where x_d and x_q are direct- and quadrature-axis synchronous reactances. Equation (5) is based on the relations in the quadrature axis for which excitation voltage E_d is provided by flux in the direct axis. Equation (6) is based on the relation in the direct axis for which there is no excitation voltage, as is almost invariably the case. The corresponding current equations are given by (7) and (8). The expression for three-phase power in terms of terminal and excitation voltages can be obtained by eliminating I and ϕ from Eqs. (5), (6), and (8) with the result

$$P = 3 \frac{\bar{E}_t \bar{E}_d}{x_d} \sin \theta + 3 \frac{\bar{E}_t^2 (x_d - x_q)}{2x_d x_q} \sin 2\theta$$

which becomes

$$P = \frac{\bar{E}_t \bar{E}_d}{x_d} \sin \theta + \frac{\bar{E}_t^2 (x_d - x_q)}{2x_d x_q} \sin 2\theta \quad (9)$$

when the voltages are expressed as line-to-line voltages. All voltages are line-to-line values in the remainder of this section. The power limit for a single salient-pole machine connected to an infinite bus of maintained voltage \bar{E}_t can be obtained directly from Eq. (9). In a salient-pole machine the steady-state power limit is reached at an angle considerably less than 90 degrees. For the non-salient pole machine the quadrature-axis reactance x_q is equal to the direct-axis reactance x_d , which relation reduces the maximum power from Eq. (9) to the familiar form previously derived for the transmission line and given in Eq. (2).

$$P = \frac{\bar{E}_t \bar{E}_d}{x_d} \quad (10)$$

With two identical salient-pole synchronous machines at equal excitation, one acting as a generator, and the other as a motor, the terminal voltages and currents are in phase causing the angle ϕ to be zero. The power relation for this condition can be stated in terms of the terminal

voltage as given in Eq. (11) or in terms of the excitation voltage as given by Eq. (12).

$$P = \frac{\bar{E}_t^2}{x_q} \tan \theta \quad (11)$$

$$P = \frac{\bar{E}_d^2 \sin 2\theta}{x_q \left(\cos^2 \theta + \frac{x_d}{x_q} \sin^2 \theta \right)^2} \quad (12)$$

The maximum power that can be delivered by a system consisting of two identical salient-pole machines directly connected and operating at equal excitation is obtained from Eq. (13).

$$P = \frac{1}{2} \frac{\bar{E}_t^2}{x_d} F(\theta, x_d, x_q) \quad (13)$$

for which the value of the function $F(\theta, x_d, x_q)$ is plotted in Fig. 16. As a matter of interest the total angle between synchronous machine rotors, 2θ , at the point of pull-out is

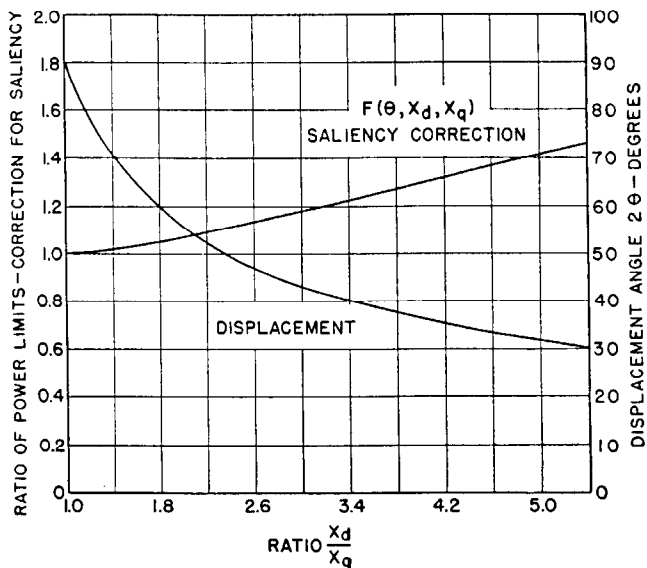


Fig. 16—Effect of saliency on power limit and total displacement angle for two identical machines operating at equal fixed excitation adjusted to maintain constant terminal voltage. Saliency effect plotted as ratio of power limit for various ratios x_d/x_q to values based on x_d alone.

also plotted in this figure. It will be noted that for $x_q = x_d$, Eq. (13) is identical in form with that previously derived for the steady-state stability limit and that the maximum power occurs at an angle of 90 degrees between the two machines and with an internal voltage equal to $\sqrt{2}$ times the terminal voltage. By using the internal voltages and the total reactance the same power expression would be obtained as previously given in terms of terminal voltage and the reactance of a single machine. Figure 16 is also useful as indicating the correction in the stability limit, which must be made because of the effect of saliency.

Example 1. Two salient-pole machines directly connected, three-phase, 2200 volt, 210 kva, operated at 1150 volts to avoid effects of saturation, with reactances of $x_d = 31.4$ ohms, $x_q = 8.83$ ohms. The stability limit as determined from the

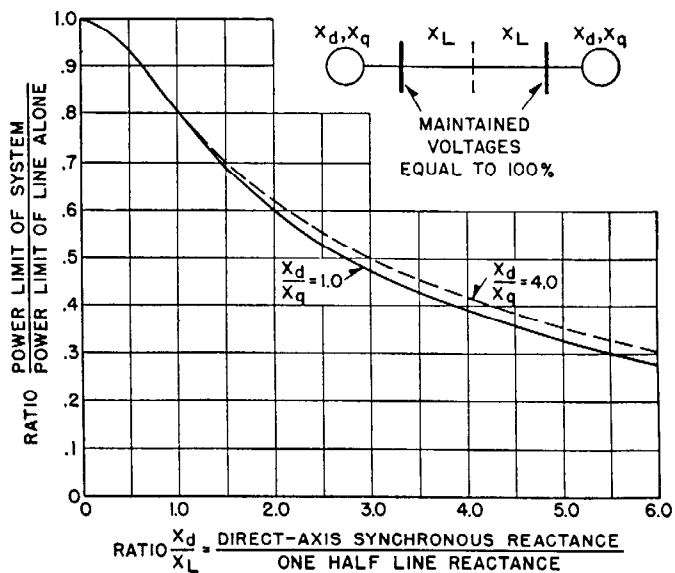


Fig. 17—Effect of machine reactance on power limits of transmission system with identical machines and fixed excitation. Curves plotted in terms of the reactance x_d and x_q of each machine and X_L of one-half of line.

terminal voltage and the direct-axis synchronous reactance only, using Eq. 13 with $x_q = x_d$, gives 42.3 kw. Using the correction factor obtained from Fig. 16, the stability limit considering the effect of saliency was calculated to be 52 kw. Actual tests made on these machines gave 52 kw.

The effect of saliency on the power limit of a transmission system is illustrated in Fig. 17. In this case the transmission system is assumed to consist of two identical machines, one operating as a generator and the other as a motor, with equal fixed excitation adjusted to maintain 100 percent terminal voltages as indicated in the insert of the figure. The power limits for such a system can conveniently be expressed in terms of the limit of the line alone. In Fig. 17 the solid-line curve is plotted for non-salient pole machines, i.e., with $x_q = x_d$; the dotted-line curve is plotted for a salient-pole machine for the relatively large ratio of x_d/x_q equal to four. The effect of saliency is small even for a ratio of x_d/x_q as high as four. For ratios of x_d/x_q between one and four the values will lie relatively close to the solid-line curve as the curve for saliency correction given in Fig. 16 suggests.

The foregoing discussion has presented sufficient formulas to permit the analysis of the difference in stability limits resulting from the saliency effect obtained by the two-reaction method in comparison with the results obtained by using the direct-axis reactance only. The reactances of synchronous machines given in Table 4 of Chap. 6 show that the ratio of x_d/x_q varies from one to an upper limit of approximately four. Under practical operating conditions this ratio is greatly reduced because of the effects of saturation. Furthermore, the power systems for which the steady-state stability limits are important almost invariably involve circuit elements that introduce impedance between the machines and which result in an important reduction in the effective ratio of the direct- and quadrature-axis reactances.

14. Effect of Saturation on Steady-State Stability

The effect of saturation on the equivalent synchronous reactance and corresponding internal voltage of synchronous machines is generally much more important than that of saliency. These effects from the stability standpoint are determined from the terminal voltage, power and reactive kva output, and the excitation characteristics of the machines as determined by test, or by recognized methods of calculating the regulation of synchronous machines as described in Chap. 6.

There are several methods of including the effects of saturation in the determination of pull-out power of a generator. The most accurate of these uses the voltage behind Potier reactance, E_p , to adjust the saturation of the ma-

chine at the pull-out point. This method of solution is described below along with some simplified methods of calculation. The results obtained by using the various methods are compared over a range of conditions to illustrate those cases where the simplified methods can be used with acceptable accuracy.

Potier Voltage Method—This method is best understood if the analysis is considered on the basis of the two existing operating conditions: the initial operating condition, and the pull-out operating condition. In Fig. 18 (a) is illustrated a generator G connected through its own reactance x_g to a terminal bus, which in turn is connected to an assumed infinite bus in the system through the equivalent external reactance x_e . The reactance x_e is the reactance of the system between the generator terminals and the infinite bus reduced to a single equivalent reactance. The internal voltage of the generator is represented by E_{int} .

The vector diagram for the system during the initial operating conditions prior to pull out is given in Fig. 18 (b). It is necessary, of course, to express all vector quantities on a common base, and the most convenient method of doing so is to use the per-unit system with the generator rating as a base. This is equivalent to referring to all voltages in terms of the generator field excitation required to produce them. The generator rated voltage, current, and kva are used for the base in expressing the voltages, currents, and reactances, respectively, as per-unit quantities. On this basis, 1.0 per-unit power converted to kilowatts is equal to the generator kva rating.

Referring to Fig. 18 (b), the following equations can be written. The infinite bus voltage E_r is the generator terminal voltage minus the drop through the external reactance,

$$E_r = E_t - Ix_e \quad (14)$$

The voltage behind Potier reactance E_p is equal to the terminal voltage plus the Potier reactance drop,

$$E_p = E_t + Ix_d \quad (15)$$

The internal voltage E_{int} of the generator is equal to the terminal voltage plus the drop through the generator unsaturated synchronous reactance,

$$E_{int} = E_t + Ix_d \quad (16)$$

The saturation curve of the generator is shown in Fig. 19 plotted in per unit. Rated generator voltage is used as 1.0 per-unit voltage, and the field current necessary to produce rated voltage on the air-gap line is 1.0 per-unit field current. The saturation \bar{S} is the difference between the excitation required to produce \bar{E}_p on the no-load saturation curve and the excitation required to produce \bar{E}_p on the air-gap line. The excitation voltage \bar{E}_x , which is equivalent to the total field current under the initial load condition, is the internal voltage plus the saturation,

$$\bar{E}_x = \bar{E}_{int} + \bar{S} \quad (17)$$

The power transferred from the generator to the infinite bus is

$$P = \frac{\bar{E}_{int} \bar{E}_r}{x_g + x_e} \sin \theta \quad (18)$$

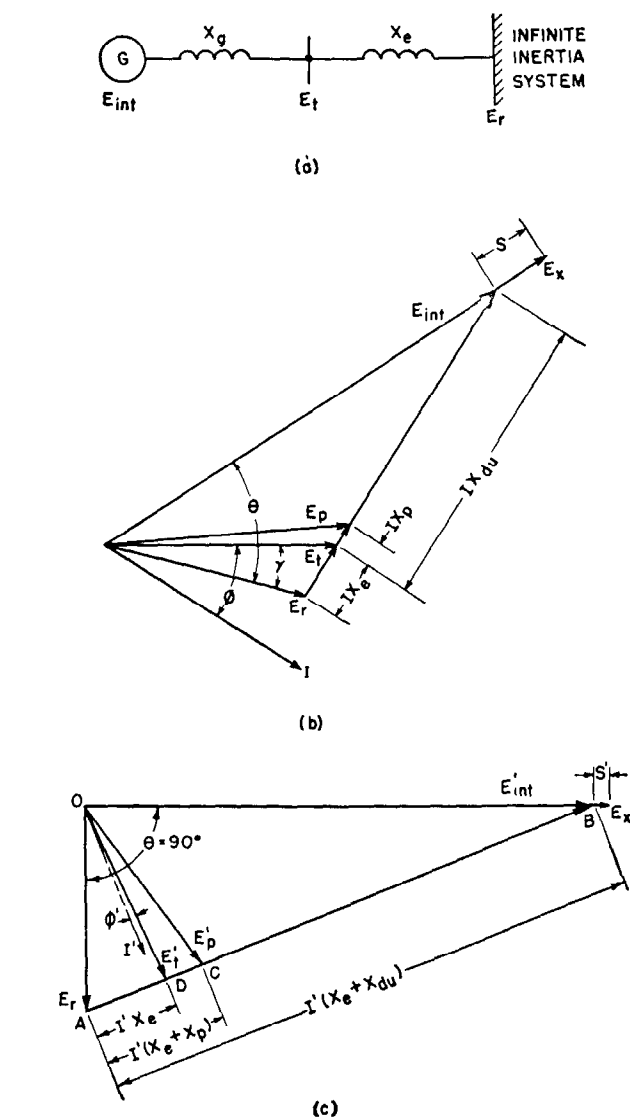


Fig. 18—Vector diagrams for initial-load and pull-out conditions.

- (a)—Equivalent representation of generator and external system.
- (b)—Vector diagram of system with generator loaded with rated kilowatts, power factor and voltage.
- (c)—Vector diagram at pull out with θ increased to 90 degrees and E_x and E_r equal to initial-load values in (b).

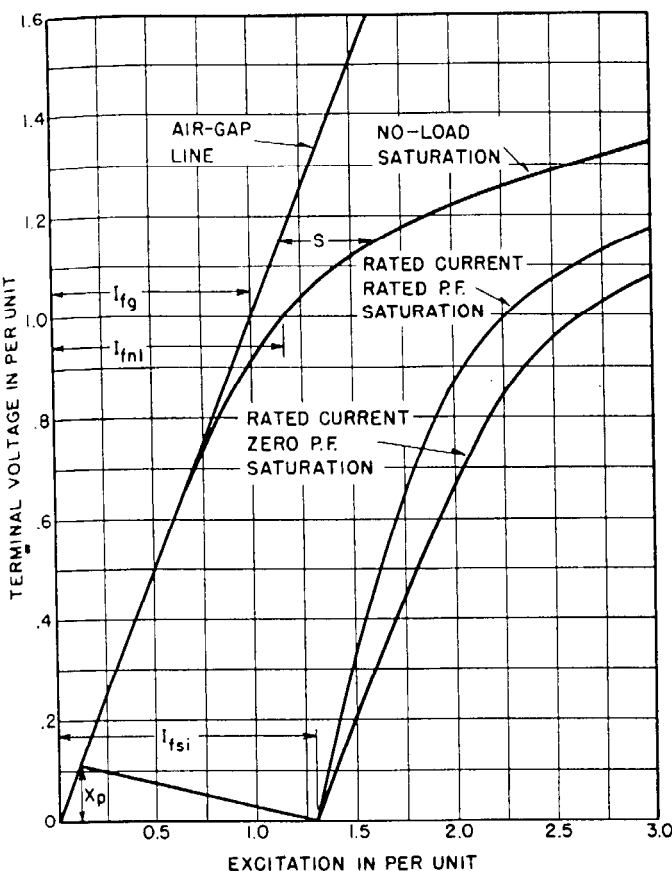


Fig. 19—Saturation curve of 60 000-kilowatt, 13 800-volt, 0.85-power factor generator used in the example of steady-state stability calculations.

where

$x_g = x_d$, the generator unsaturated synchronous reactance.

θ = Angle between E_r and E_{int} .

The generator power output is, of course, also found from the equation

$$P = \bar{E}_t \bar{I} \cos \phi \quad (19)$$

Under the hypothesis of constant excitation in the transition from the initial load condition to the pull-out condition, the excitation voltage \bar{E}_x remains constant. The infinite bus voltage \bar{E}_r is also assumed to remain constant, so that these two voltages and the reactances x_g , x_p , and x_e and the angle θ are the only quantities known at the time of pull out, and the internal voltage at pull out E'_{int} must be determined.

The vector diagram of the system at the time of maximum power transfer is given in Fig. 18 (c). The excitation voltage \bar{E}_x is used as the reference vector and is equal in magnitude to the value calculated for the initial load condition. The angle θ is 90 degrees, so the infinite bus voltage E_r lags E_x by that angle. Expressions for the remainder of the vector diagram are

$$\bar{E}'_{int} = \bar{E}_x - \bar{S}' \quad (20)$$

$$I'(x_d + x_e) = E'_{int} - E_r \quad (21)$$

$$I' = \frac{E'_{int} - E_r}{x_d + x_e} \quad (22)$$

$$E'_t = E_r + I' x_e \quad (23)$$

$$E'_p = E_r + I'(x_e + x_p) \quad (24)$$

A method of successive approximations must be used to determine the value of \bar{S}' which leads to the correct solution of the vector diagram. First, a value is assumed for \bar{S}' and Eqs. (20), (21), (22), and (24) are used to calculate E'_p . The actual value of \bar{S}' is found from the saturation curve at a voltage equal to \bar{E}'_p and is compared with the assumed value. The assumed value is then adjusted until the actual value found by repeating the calculation of \bar{E}'_p is equal to the assumed value. Usually, two approximations yield a sufficiently accurate answer. When the correct values of \bar{S}' and \bar{E}'_{int} are found, the pull-out power can be calculated by

$$P_{max} = \frac{\bar{E}'_{int} \bar{E}_r}{x_d + x_e} \quad (25)$$

or

$$P_{max} = \bar{E}_t \bar{I}' \cos \phi' \quad (26)$$

The application of the Potier voltage method is illustrated with an example in which G in Fig. 18 (a) is a 60 000-kw, 70 588-kva, 13 800-volts, 0.85-power factor, hydrogen-cooled turbine generator. The saturation curve of the generator is shown in Fig. 19. The equivalent system reactance x_e is 0.25 per unit on the generator rating of 70 588 kva. During the initial load conditions, the generator is assumed to be carrying 60 000 kw at 0.85 lagging power factor with its terminal voltage E_t maintained at rated value. The initial load data can be written as follows, using the generator rating as a base:

$$E_t = 13 800 \text{ volts} = 1.0 + j0.0 = 1.0 / 0^\circ \text{ per unit.}$$

$$\text{kW output} = 60 000 \text{ kw} = 0.85 \text{ per unit.}$$

$$\text{kVA output} = 70 588 \text{ kva} = 1.0 \text{ per unit.}$$

$$I = 0.85 - j0.527 = 1.0 / -31.8^\circ \text{ per unit.}$$

$$\phi = 31.8^\circ.$$

$$x_p = 0.25 \text{ per unit.}$$

The required generator constants can be determined from the saturation curve:

$$x_d = \frac{I_{fci}}{I_{fg}} = \frac{1.30}{1.00} = 1.30 \text{ per unit}$$

where

I_{fci} = Field current required to produce rated armature current with a three-phase short circuit at the generator terminals.

I_{fg} = Field current required to produce rated voltage on the air-gap line.

The Potier reactance x_p is determined from the Potier voltage triangle as shown in Fig. 19 and is

$$x_p = 0.11 \text{ per unit.}$$

Referring to the vector diagram in Fig. 18 (b) and using Eqs. (14), (15), and (16),

$$\begin{aligned}
 E_r &= (1.0+j0.0) - (0.85-j0.527)(j0.25) \\
 &= 0.8682-j0.2125 = 0.894 / -13.77^\circ \\
 \gamma &= 13.77^\circ \\
 E_p &= (1.0+j0.0) + (0.85-j0.527)(j0.11) \\
 &= 1.058+j0.0935 = 1.062 / 5.06^\circ \\
 E_{int} &= (1.0+j0.0) + (0.85-j0.527)(j1.30) \\
 &= 1.685+j1.105 = 2.015 / 33.25^\circ \\
 \theta - \gamma &= 33.25^\circ \\
 \theta &= 33.25^\circ + 13.77^\circ = 47.02^\circ
 \end{aligned}$$

From the saturation curve at a voltage equal to $\bar{E}_p = 1.062$ per unit, the saturation S is 0.254 per unit, and from Eq. (17)

$$\bar{E}_x = 2.015 + 0.254 = 2.269$$

The above results can be used in Eq. (18) as a check to determine the accuracy of the calculations thus far:

$$\begin{aligned}
 P &= \frac{(2.015)(0.894)}{1.30+0.25} \sin 47.02^\circ \\
 &= 0.8504 \text{ per unit.}
 \end{aligned}$$

The vector diagram for the pull-out condition is shown in Fig. 18 (c), and using E_x as a reference, the following quantities are known:

$$\begin{aligned}
 E_x &= 2.269 / 0^\circ = 2.269 + j0.0 \\
 E_r &= 0.894 / -90^\circ = 0.0 - j0.894 \\
 \theta &= 90^\circ
 \end{aligned}$$

Examination of the vector diagram reveals that \bar{E}_p' can be estimated by drawing the line $\bar{A}\bar{B}$, assuming S' equal to zero, i.e., $\bar{E}'_{int} = \bar{E}_x$. The location of point C can be found from

$$\bar{AC} = \frac{x_e + x_p}{x_e + x_d} (\bar{AB})$$

The vector \bar{OC} is equal to E_p' , the voltage behind Potier reactance, and can be used to determine a value for the first approximation of S' . Following this procedure, S' is assumed to be 0.10 per unit. From Eqs. (20), (21), (22) and (24),

$$\begin{aligned}
 E'_{int} &= (2.269 + j0.0) - 0.10 \\
 &= 2.169 + j0.0 = 2.169 / 0^\circ \\
 I'(x_d + x_e) &= 2.169 + j0.894 = 2.347 / 22.4^\circ \\
 I' &= \frac{2.169 + j0.894}{j1.30 + j0.25} \\
 &= 0.577 - j1.400 = 1.514 / -67.6^\circ \\
 E'_p &= (0.0 - j0.894) + (0.577 - j1.400)(j0.36) \\
 &= 0.504 - j0.686 = 0.852 / -53.73^\circ
 \end{aligned}$$

From the saturation curve at $\bar{E}_p' = 0.852$ per unit, $S' = 0.057$ per unit which shows that the first approximation was too high. A lower value, therefore, should be assumed for the second approximation, but observe that decreasing the value of S' slightly increases the value of \bar{E}_p' . Thus, S' is assumed as 0.06 per unit for the second approximation.

$$\begin{aligned}
 E'_{int} &= 2.209 + j0.0 = 2.20 / 0^\circ \\
 I'(x_d + x_e) &= 2.209 + j0.894 = 2.385 / 22.0^\circ \\
 I' &= 0.577 - j1.425 = 1.538 / -68.0^\circ \\
 E'_p &= 0.513 - j0.686 = 0.857 / -53.2^\circ \\
 S' \text{ (from saturation curve)} &= 0.06 \\
 E'_t &= (0.0 + j0.894) + (0.577 - j1.425)(j0.25) \\
 &= 0.356 - j0.750 = 0.830 / -64.6^\circ
 \end{aligned}$$

The pull-out power for the assumed conditions is found from Eq. (25)

$$P_{max} = \frac{(2.209)(0.894)}{1.30+0.25} = 1.274 \text{ per unit}$$

or from Eq. (26) where

$$\begin{aligned}
 \phi' &= 68.0^\circ - 64.6^\circ = 3.40^\circ \\
 P_{max} &= (0.830)(1.538) \cos 3.40^\circ = 1.274 \text{ per unit}
 \end{aligned}$$

The pull-out power in kilowatts is

$$P_{max} = (1.274)(70\ 588) = 89\ 930 \text{ kw.}$$

Many different initial operating conditions might be used to represent the system in a practical calculation. In the above example, where the generator terminal voltage was assumed as 1.0 and the kw load as 0.85, the margin obtained between the operating condition and the pull-out condition was $1.274 - 0.85$ or 0.424 per unit which is equivalent to 29 930 kw. The generator kw load, therefore, could be increased approximately 50 percent before the machine would pull out of step with the system. There may be other considerations such as turbine capability or generator heating that limit the load to some value below the maximum permissible power from the stability standpoint. If other initial operating conditions are assumed, the excitation voltage is, of course, changed, and the pull-out power differs from that obtained in the above example.

Synchronous Reactance Method—In this simplified method of steady-state stability calculation, the generator is represented by a reactance equal to the unsaturated synchronous reactance, x_d , and an internal voltage equal to the voltage behind unsaturated synchronous reactance, as determined by the initial load conditions. This voltage, E_d , is the same as E_{int} determined in Eq. (16). It is evident, therefore, that this method of calculation does not take into account the increase in E_{int} caused by the reduced saturation when the pull-out point is reached, and the maximum power so obtained is less than that given by the Potier voltage method. The maximum power equation becomes

$$P_{max} = \frac{\bar{E}_d \bar{E}_r}{x_d + x_e}$$

$$\text{where } E_d = E_t + Ix_d$$

calculated for the condition prior to pull out.

From the calculations in the example above,

$$\begin{aligned}
 \bar{E}_{int} &= \bar{E}_d = 2.015 \text{ per unit} \\
 \bar{E}_r &= 0.894 \text{ per unit} \\
 P_{max} &= \frac{(2.015)(0.894)}{1.30+0.25} = 1.162 \text{ per unit.}
 \end{aligned}$$

Short-Circuit Ratio Method—The short-circuit ratio (*SCR*) of a generator can be obtained from the saturation curve

$$SCR = \frac{I_{fn1}}{I_{fs1}} \quad (27)$$

where

I_{fn1} = Field current required to produce rated voltage on the no-load saturation curve.

I_{fsi} = Field current required to produce rated armature current with a three-phase short circuit at the generator terminals.

In this method of calculation, the generator reactance x_g is represented by the reciprocal of the generator short-circuit ratio,

$$x_g = \frac{1}{SCR}$$

The quantity $\frac{1}{SCR}$ is roughly equivalent to the generator unsaturated synchronous reactance, differing only in the fact that it takes into account a certain amount of saturation. The saturation included is that existing at rated voltage on the no-load saturation curve, and if this value of saturation is designated S_{nl} , it can be shown that

$$\frac{1}{SCR} = x_a \left(\frac{1}{1+S_{nl}} \right)$$

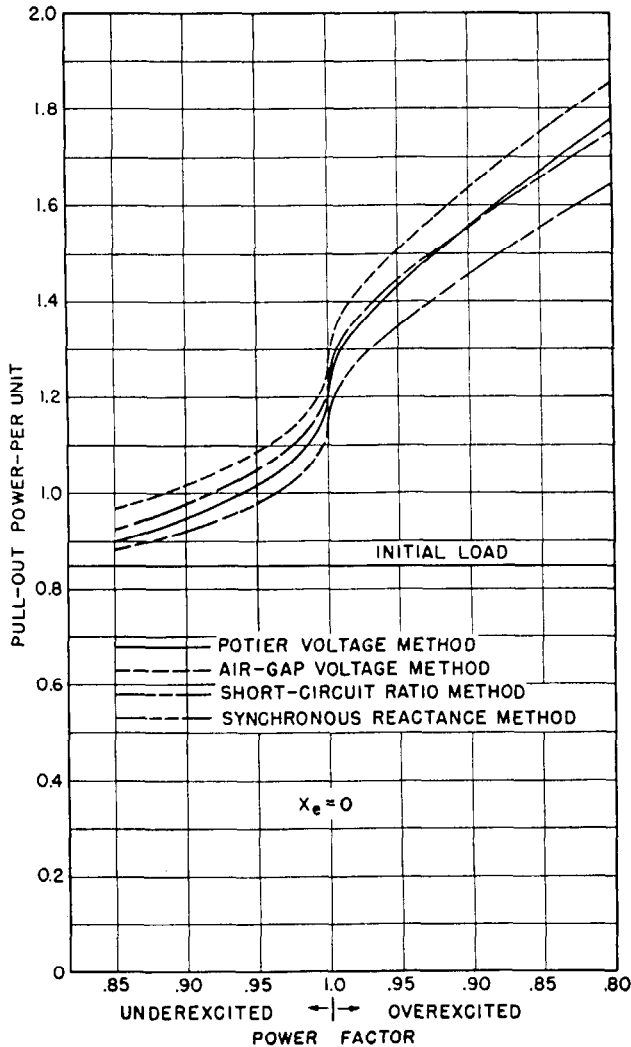


Fig. 20—Comparison of four methods of calculating pull-out power.
 $x_e = 0$ per unit

Initial load equal to 60 000 kw or 0.85 per unit at various power factors with terminal voltage E_t equal to 13 800 volts or 1.0 per unit.

In this method, therefore, a certain amount of correction for saturation at pullout is obtained, but it is a constant approximation, whereas the true saturation is variable depending on the operating conditions.

Internal voltage is calculated for the initial operating conditions from

$$E_{int} = E_t + I \left(\frac{1}{SCR} \right)$$

and the magnitude of the internal voltage at the pull-out point is assumed equal to the value so calculated. The maximum power equation is

$$P_{max} = \frac{\bar{E}_{int} \bar{E}_r}{\frac{1}{SCR} + x_e}$$

Applying this method to the example, the short-circuit ratio is found from the saturation curve and Eq. (27),

$$SCR = \frac{1.16}{1.30} = 0.892$$

$$x_g = 1.121 \text{ per unit}$$

$$E_{int} = (1.0 + j0.0) + (0.85 - j0.527)(j1.121) \\ = 1.591 + j0.953 = 1.854 / 30.9^\circ$$

$$P_{max} = \frac{(1.854)(0.894)}{1.121 + 0.25} = 1.209 \text{ per unit.}$$

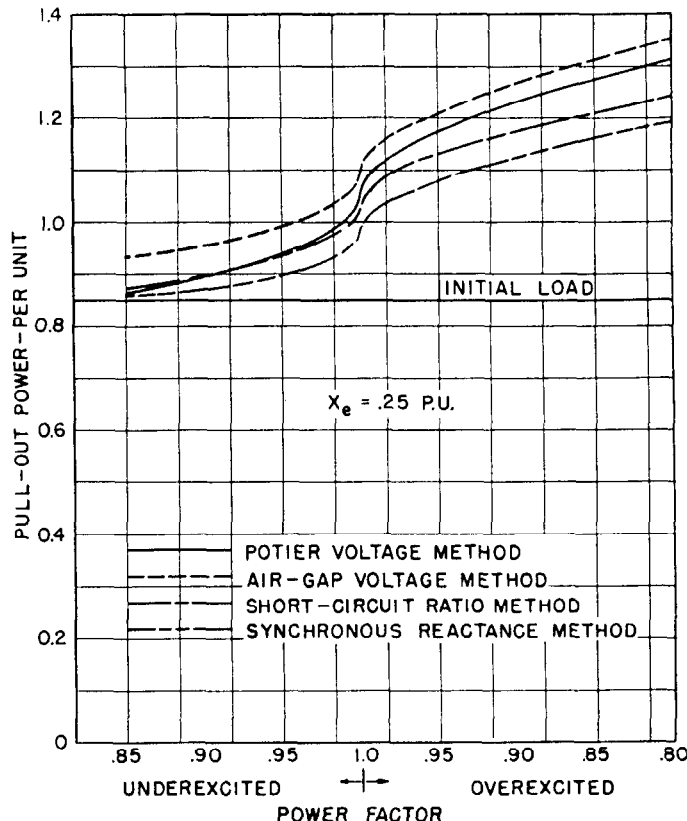
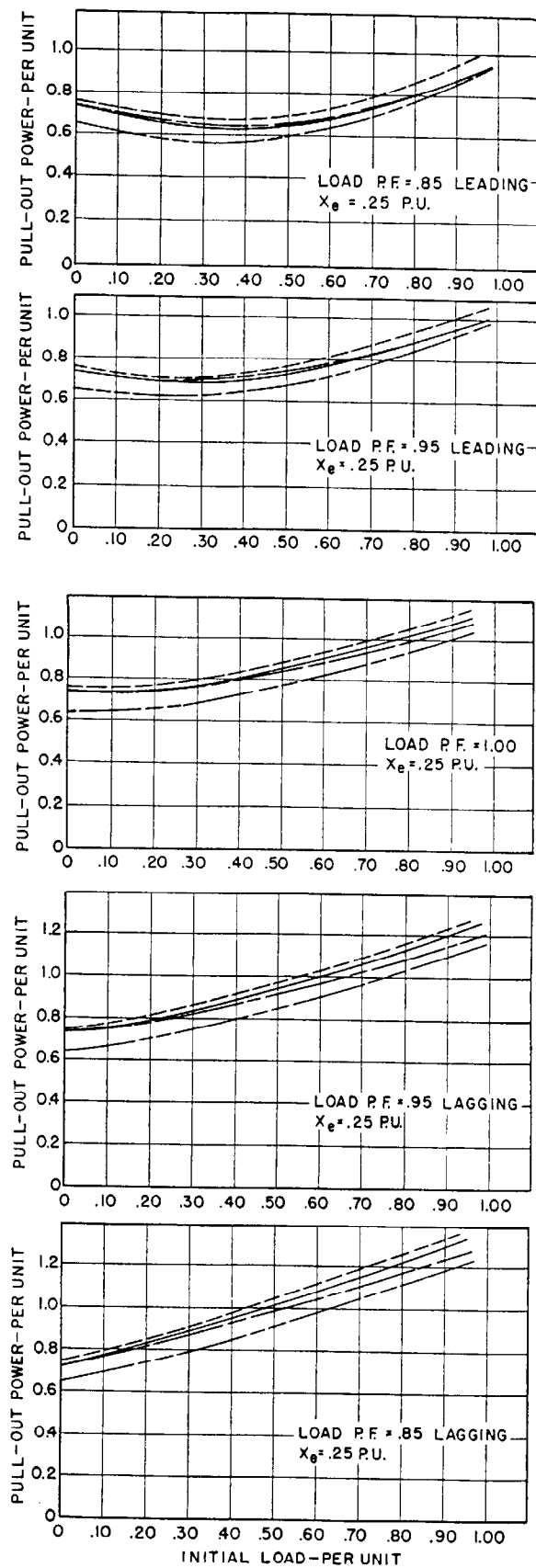
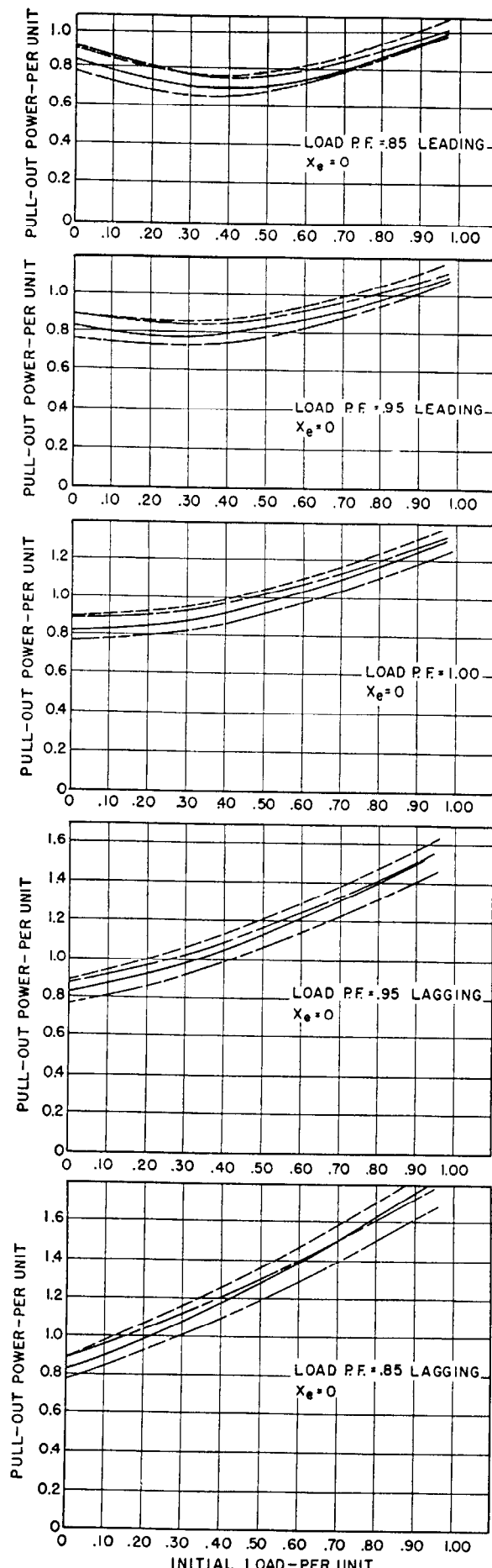


Fig. 21—Comparison of four methods of calculating pull-out power.
 $x_e = 0.25$ per unit

Initial load equal to 60 000 kw or 0.85 per unit at various power factors with terminal voltage E_t equal to 13 800 volts or 1.0 per unit.



————— POTIER VOLTAGE METHOD
 - - - - AIR-GAP VOLTAGE METHOD
 - - - - - SHORT-CIRCUIT RATIO METHOD
 - - - - - - SYNCHRONOUS REACTANCE METHOD

Fig. 22—Comparison of four methods of calculating pull-out power. Each curve is calculated for an initial-load condition of various kilowatts at the indicated power factor with the terminal voltage equal to 1.0 per unit.

Air-Gap Voltage Method—The use of the air-gap line voltage to represent the internal voltage of a generator in a steady-state stability study is based on the fact that there is usually little saturation existing at the time of pull out. The air-gap line voltage which is used is that voltage read on the air-gap line at a value of excitation equal to that required for the initial load condition. When expressed in per unit, this voltage is equal to the excitation voltage \bar{E}_x obtained in Eq. (17). The unsaturated synchronous reactance x_d is used to represent the generator reactance x_g . Thus, if there is any saturation in the machine at pull out, this method uses a voltage which is too high by the amount of the saturation to represent the internal voltage. The maximum power equation for this method is

$$P_{\max} = \frac{\bar{E}_{\text{int}} \bar{E}_r}{x_d + x_e}$$

where

$\bar{E}_{\text{int}} = \bar{E}_x$ = Voltage read on air-gap line at the field excitation required to produce the terminal voltage under conditions of load.

In the example above, \bar{E}_x was found to be 2.269 per unit, and the maximum power is

$$P_{\max} = \frac{(2.269)(0.894)}{1.30 + 0.25} = 1.309 \text{ per unit.}$$

Comparison of Methods—Results obtained by calculating the pull-out power for a given kilowatt load at various power factors using the four methods are compared in Figs. 20 and 21. The 60 000-kw generator described in the example above was used in making the calculations. In all cases, the generator was assumed to be carrying 60 000 kilowatts at the specified power factor and with the terminal voltage maintained at rated value during the initial load condition. In the transition to the pull-out point, the infinite-bus voltage was assumed constant at the value calculated for the initial load condition. Figure 20 shows the results with the external reactance $x_e = 0$, and in Fig. 21, $x_e = 0.25$ per unit.

In all cases, the air-gap voltage method gives the highest value of pull-out power. This is to be expected since this method assumes no saturation at pull out and uses a voltage higher than actual to represent the generator internal voltage. The synchronous-reactance method, on the other hand, assumes that the saturation at pull out is equal to the saturation existing under the initial load condition and, consequently, represents the generator internal voltage by a voltage lower than the true value. The synchronous-reactance method, therefore, gives the lowest results in all cases. The actual value of pull-out power must be between the values obtained by these two methods, since one method considers no saturation while the other considers a high value of saturation.

The Potier-voltage method and the short-circuit ratio method give results within the limits set by the air-gap voltage and synchronous-reactance methods. Based on modern synchronous machine theory, the results of the Potier-voltage method are more accurate, because the saturation at pull out is adjusted to the proper value. The short-circuit ratio method gives results that compare

closely with the Potier-voltage method over the range of conditions studied.

A summary of a large number of calculations of pull-out power for the sample machine is given in Fig. 22. To obtain the data in each curve the generator power factor and terminal voltage were held constant for the initial load condition, while the generator load in kilowatts was varied. Study of these curves shows close agreement between the four calculating methods over the range of conditions included. Of particular interest is the fact that the result obtained by the short-circuit ratio method exceeded that obtained by the air-gap voltage method at low leading power factor and reduced load.

Extension of the Potier-Voltage Method—The Potier-voltage method as described above may appear to be a long and tedious procedure when a large number of conditions are being studied. The equations can, however, be modified for certain specific conditions and the calculations are then greatly simplified.

Frequently, it is desired to know the magnitude of field current or excitation voltage that must be maintained to prevent a generator from pulling out of synchronism. It has been shown that the pull-out power is a direct function of the excitation voltage less the saturation. A generator will pull out of synchronism when carrying a given kilowatt load if the excitation voltage is reduced below a certain minimum value. A curve of pull-out power as a function of excitation voltage is easily derived by the Potier-voltage method.

The first step in the procedure is to assume a value of pull-out power, P_{\max} , and determine the magnitude of internal voltage required to deliver that power by solving Eq. (25) for \bar{E}'_{int} :

$$\bar{E}'_{\text{int}} = \frac{P_{\max}}{\bar{E}_r} (x_d + x_e) \quad (28)$$

Referring to the vector diagram in Fig. 18 (c), two equations can be written:

$$-j\bar{E}_r + jI'(x_d + x_e) = \bar{E}'_{\text{int}} + j0 \quad (29)$$

$$E_p' = -j\bar{E}_r + jI'(x_e + x_p) \quad (30)$$

Solving for I' in Eq. (29) and substituting in Eq. (30),

$$E_p' = \sqrt{\bar{E}'_{\text{int}}^2 \left(\frac{x_p + x_e}{x_d + x_e} \right)^2 + \bar{E}_r^2 \left(\frac{x_p + x_e}{x_d + x_e} - 1 \right)^2}$$

Letting

$$K = \frac{x_p + x_e}{x_d + x_e} \quad (31)$$

$$\bar{E}_p' = \sqrt{\bar{E}'_{\text{int}}^2 K^2 + \bar{E}_r^2 (K - 1)^2} \quad (32)$$

In terms of the pull-out power, Eq. (32) converts to

$$\bar{E}_p' = \sqrt{\frac{P_{\max}^2}{\bar{E}_r^2} (x_p + x_e)^2 + \bar{E}_r^2 (K - 1)^2}. \quad (33)$$

Using Eq. (28), therefore, the internal voltage is determined, and \bar{E}_p' , the voltage behind Potier reactance, is determined by using either Eq. (32) or Eq. (33). The saturation \bar{S}' is then read from the saturation curve at a voltage equal to \bar{E}_p' and added to the internal voltage to obtain the

excitation voltage as in Eq. (17). As pointed out previously, it is desirable that all calculations be done using per-unit values. When this is done, the excitation voltage obtained is in reality the per-unit field current required by the machine. The actual value of field voltage required can be obtained by multiplying the field current by the field resistance properly adjusted to take into account temperature effects.

As an example, this procedure can be applied to the 60 000-kw generator used above, and the field current determined for a maximum power of 1.25 per unit with the infinite bus voltage \bar{E}_r , equal to 1.0 per unit and the external reactance equal to 0.25 per unit. From Eq. (28),

$$\bar{E}'_{int} = \frac{1.25}{1.0} (1.30 + 0.25) = 1.937 \text{ per unit.}$$

$$K = \frac{0.11 + 0.25}{1.30 + 0.25} = 0.2323.$$

From Eq. (32)

$$\bar{E}'_p = \sqrt{(1.937)^2(0.2323)^2 + (1.0)^2(0.2323 - 1.0)^2} = 0.890 \text{ per unit.}$$

From the saturation curve, S' is 0.074 per unit, and the required excitation voltage or field current is $1.937 + 0.074 = 2.011$ per unit. One per unit field current on this generator is 332 amperes, so that the field current required would be 668 amperes, and the field voltage would be this current multiplied by the field resistance.

The results of a number of calculations of this type on the sample machine are plotted in Fig. 23 for three values of external reactance, to illustrate the manner in which the data can be presented. Because these curves give the value of field current for pull out, it is obvious that the generator

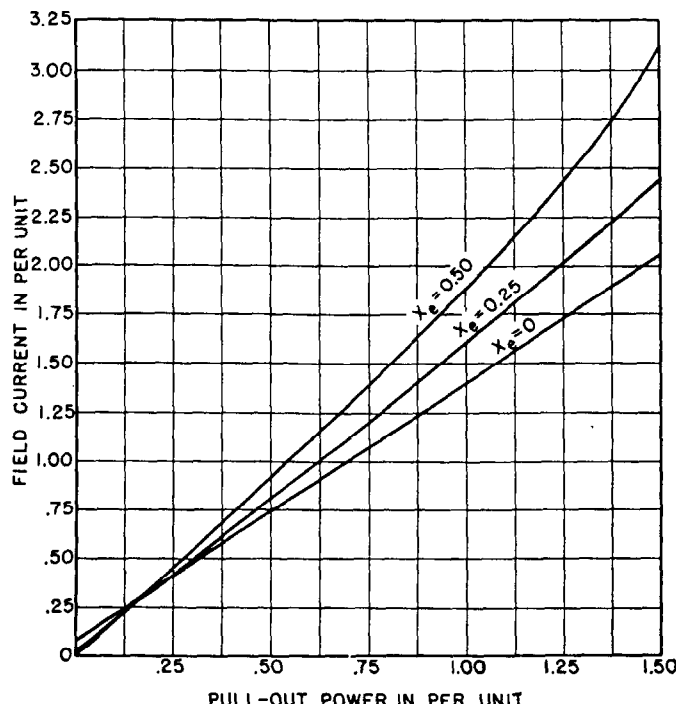


Fig. 23—Variation of pull-out power as generator field current is changed; calculated by Potier-voltage method with infinite bus voltage $E_r = 1.0$ per unit.

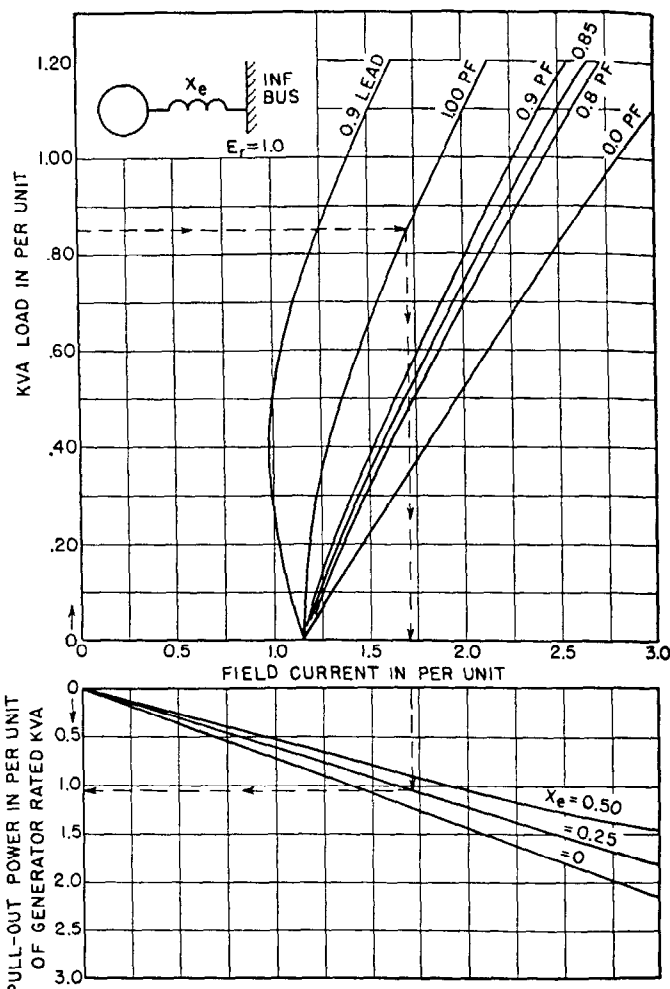


Fig. 24—Estimating curve for determining the pull-out power of an AIEE-ASME standardized turbine generator as a function of kva load and power factor.

1.0 per unit kva load = generator rated kva.

1.0 per unit Pull-out Power = generator rated kva.

1.0 per unit field current = field current required for rated voltage on air-gap line.

Find the point corresponding to the initial kva load on the upper ordinate and trace horizontally to the proper power factor line. Drop vertically to read field current on the abscissa and to intersect with proper external-reactance curve. Pull-out power is read on the lower ordinate. For 0.85 p.u. initial kva load at 1.0 pf., the pull-out power is 1.05 per unit and the field current is 1.72 per unit as found by following the dotted arrows. See text regarding accuracy of curves.

should be operated so as to maintain the field current high enough above the value indicated for the load being carried to provide sufficient pull-out margin. Methods of controlling the minimum excitation under voltage-regulator control and assuring sufficient field current for all kilowatt loads are discussed in Chap. 7.

Estimating Curves—The ASME-AIEE standardized designs of turbine generators are described in Chap. 6. These generators are designed for a rated power factor of 0.85 and a nominal short-circuit ratio of 0.80. The curve in Fig. 24 has been prepared for the purpose of quick-esti-

mating the pull-out power for these machines. The procedure for using the curve is explained in the caption.

In using the curves of Fig. 24, the conditions for which they are plotted should be considered. The upper curves of kva vs. field current for various power factors are plotted for 100 percent generator terminal voltage. The lower curves of pull-out power vs. field current for various external reactances are plotted for 100 percent voltage on the infinite bus. The infinite-bus voltage and generator terminal voltage are equal only when the external reactance x_q is zero. Therefore, the curves give correct results when the generator is connected directly to the infinite bus with no external reactance and with the terminal voltage at rated value.

For values of external reactance other than zero, the generator terminal voltage is more or less than 100 percent, depending on the power factor of the load current. The upper curves do not give the correct value of field current for these conditions, but the results are of acceptable accuracy for small variations in generator terminal voltage. The pull-out power obtained for conditions with external reactance, however, should be considered as approximations.

The curve is also closely applicable for quick-estimating the pull-out power of turbine generators in general, especially those having normal characteristics. If the per-unit field current is determined for the load being carried, the lower set of curves of pull-out power vs. per-unit field current can be used to determine the pull-out power with increased accuracy for non-standardized generators.

IV. TRANSIENT-STABILITY CALCULATIONS— TWO-MACHINE SYSTEMS

In this part, system components entering into transient-stability calculations and the step-by-step method of making transient-stability calculations are discussed.

15. Effect of Saliency on Transient Stability

The transient performance of a system containing salient-pole machines can be calculated by the two-reaction method discussed in Chap. 6. A vector diagram for the two-reaction method expressed in circuit notation is shown in Fig. 25. This is the most commonly used diagram since in stability studies salient-pole machines are usually encountered and for these the quadrature-synchronous and the quadrature-transient reactances are equal, i.e., $x_q = x_q'$. The power output can be expressed in terms of the terminal voltage, current, the angle θ' , and \bar{E}_d' , which corresponds to the actual flux in the direct axis. The expressions are identical with those given in Eqs. (5) to (13) inclusive, with the exception that transient reactance x_d' must be substituted for synchronous reactance x_d and that \bar{E}_d' must be substituted for \bar{E}_d .

The range of transient-reactance values is given in Table 4 of Chap. 6. In salient-pole machines the quadrature-axis transient reactance is considerably higher than the direct-axis transient reactance.

For commercial salient-pole machines the ratio of x_q' to x_d' is usually greater than 2.0. For turbine generators the quadrature-axis transient reactance is for solid rotors about

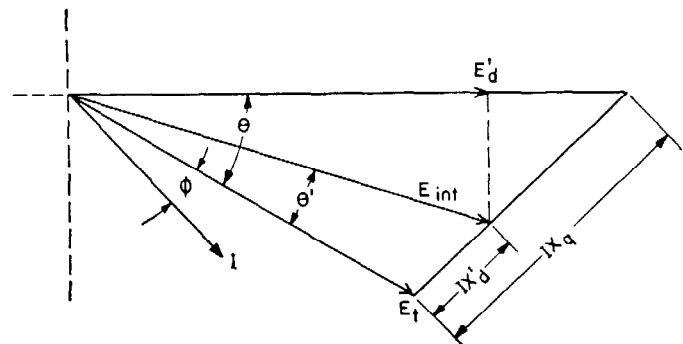


Fig. 25—Vector diagram of salient-pole generator for transient stability.

E, I —Terminal voltage and armature current (phase-to-neutral).

E_{int} —Internal voltage, the voltage back of direct-axis transient reactance x_d' .

E_d' —Voltage due to flux in the direct axis.

θ —Displacement angle between rotor position and terminal voltage.

θ' —Displacement angle between internal voltage and terminal voltage.

the same as the direct-axis transient reactance, but for laminated rotors it varies from approximately 50 percent greater than the direct-axis transient reactance to a value approaching the quadrature-axis synchronous reactance. To generalize on the quadrature-axis transient reactance of turbine generators is impractical because of the complex character of the magnetic circuits in such machines.

The power-angle curve, used in transient-stability studies of systems with salient-pole machines, consists of a fundamental component and a second-harmonic component. From Eq. (9) when modified for transient conditions, since x_q' is greater than x_d' , the maximum power is seen to occur for angles greater than 90 degrees. This condition is to be contrasted with that shown for steady-state conditions using synchronous reactances. The difference, of course, follows because the sign of the second-harmonic term is dependent upon the difference between the direct- and quadrature-reactances as Eq. (9) shows.

In stability studies it is rather difficult to carry out analytical calculations using the two-reaction method* on systems with more than two machines. As a practical matter, it is sufficiently accurate to use a method based on the round-rotor theory in which the machine is represented by the direct-axis transient reactance and an internal voltage equal to the terminal voltage plus transient-reactance drop for the condition immediately preceding the transient. This transient-reactance drop and the corresponding internal voltage E_{int} are shown in Fig. 25. Under ordinary conditions, there will not be any large difference in the magnitude of the internal voltage E_{int} and the voltage E_d' due to flux in the direct axis. Consequently, the funda-

*See Sec. 37 of this chapter for a discussion of such a method.

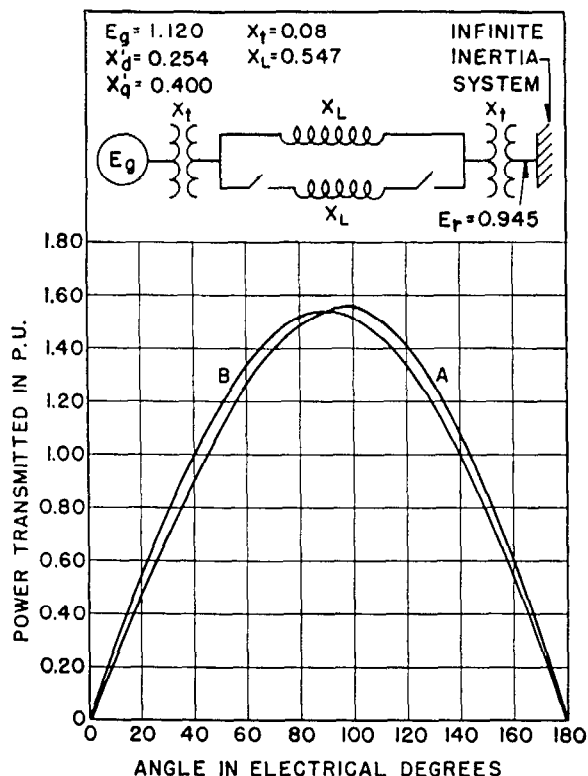


Fig. 26—Effect of saliency on transient stability for system shown in insert with both lines in service.

- A—Power-angle diagram based on initial load of 0.833 per unit—two-reaction theory.
- B—Power-angle diagram based on same initial load—round-rotor theory using same direct-axis transient reactance and corresponding internal voltage.

mental component of the power-angle curve is substantially the same in magnitude whether the round-rotor method or the two-reaction method is used.

Consider a simple transmission system*, such as shown in the insert of Fig. 26. Power-angle diagrams for this system have been calculated by the round-rotor and the two-reaction methods using the same values for x_d' in the machine and for the reactances of the remainder of the system. These power-angle diagrams for initial machine-conditions corresponding to a steady transmitted load of 0.833 per unit are shown in Fig. 26. In this case there is a difference of one percent in the power limit, the larger being obtained by the two-reaction method. The areas in the power-angle diagram for the initial output of 0.833 per unit are somewhat greater for the two-reaction method than for the round-rotor method. Furthermore, with the two-reaction method an appreciably greater percentage of this area occurs at a greater angle than with the round-rotor method. The power-angle curves show that the round-rotor method gives a conservative stability limit for the usual transient conditions. This is illustrated by Fig. 27 which is based on the system of Fig. 26 subjected to a double line-to-ground fault at the sending end. In this figure two curves are given for the stability limit plotted as a function

*This is identical with the system used in the single-machine problem, Sec. 24.

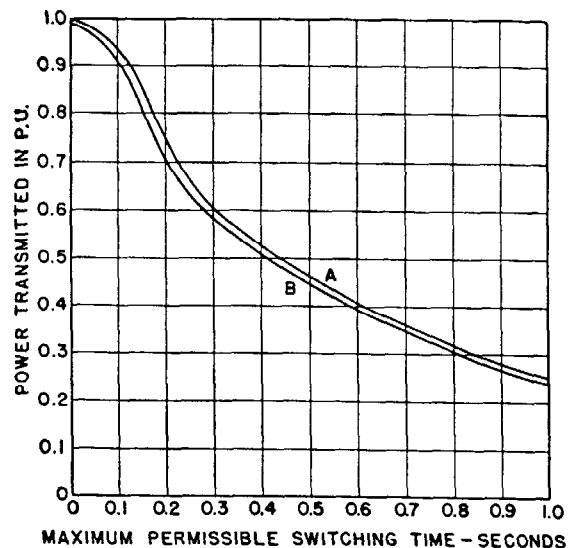


Fig. 27—Effect of saliency on permissible switching time—simultaneous clearing of line-section with double line-to-ground fault at sending end of system shown in Fig. 26.

- A—Two-reaction theory.
- B—Round-rotor theory.

of the duration of fault using both the round-rotor and two-reaction methods. These curves show that there is little difference in the stability limit or the permissible switching time, but the values are somewhat greater when calculated by the two-reaction method. If salient-pole machines were used at both ends of the system, the effect of saliency would be of greater importance. However, for the majority of problems the round-rotor method is satisfactory because it gives a conservative stability limit and is preferable because the calculations are much simpler.

16. Effect of Saturation on Transient Stability

Machine saturation affects transient stability by reducing the magnitude of transient reactances. As brought out in Chap. 6, the unsaturated transient reactance is rarely useful. The two commonly available and useful values of transient reactance are (1) the "rated-current value" obtained by short-circuiting a machine at the appropriate reduced excitation, and (2) the "rated-voltage value" obtained by short circuiting the machine from no load but with excitation corresponding to rated voltage. The difference in these reactances results from saturation arising from the difference in excitation, the higher value being for the lower excitation. The rated-voltage value is the one commonly used for short-circuit calculations and, therefore, is generally available. Actually the variation in the value of transient reactance caused by saturation is not large and it is preferable in stability studies to use a conservative, that is, the higher value. It is possible to include the effect of saturation in the estimate of the transient reactance corresponding to the particular excitation and of armature current as discussed in Chap. 6. Practically,

however, there is little difference for the range of currents commonly encountered. For this reason it is usually sufficiently accurate to use the "rated-current value."

17. Dynamic Stability with Automatic Devices

When synchronous machines are operated with voltage regulators, the stability limits of the system are importantly changed from the values which obtain for hand control. This phenomenon has been designated "dynamic stability with automatic devices." Dynamic stability on power systems is made possible by the action of voltage regulators that are capable of increasing or decreasing flux within a machine at a faster rate than that caused by the system in falling out of step. When the inherent stability limit is exceeded, both the mechanical system and the electrical system are maintained in a continuous state of oscillation through the development of restoring forces equal to or greater than the disturbing forces.

This conception of dynamic stability was first recognized by E. B. Shand, but at the time it was not thought to lie within the range encountered with commercial equipment. Subsequently, Evans and Wagner* demonstrated by analytical methods and by miniature-system tests that substantial improvement in stability limits could be obtained by making use of this phenomenon. Their tests, reported in 1926, showed that the stability limits of a transmission system with a 200-mile transmission line could be increased 25 percent by this method. Later Doherty⁷ and Nickle made tests for the special and rather academic condition of two machines directly connected, which showed that the limits could be increased about 300 percent by the same means. These two tests are actually quite comparable when the effects of line reactances are considered.

Dynamic stability with automatic devices can be considered as a problem in transient stability, making use of the machine air-gap flux and a reactance intermediate between the familiar synchronous and transient reactances. With ideal excitation systems, that is, with voltage regulators without time lag, with high frequency of operation, and with unlimited exciter range and response, the stability limit would be determined by the transient reactance. From a practical standpoint the exciter response is not sufficiently fast to approach closely the ideal condition. More important, however, is the inability of the regulator to approximate the ideal characteristics because of the time delay and the finite steps of regulator action, and delay in the anti-hunting feature. This provides a definite limit to the increase in the stability limit resulting from regulator action. Nevertheless, for the system consisting of two machines, as described in Ex. 1 of Sec. 13, operating at equal excitation and constant terminal voltage under the control of a voltage regulator, the stability limit was raised with automatic devices from 52 to 183 kilowatts. The importance of the increase in stability limits due to the operation of automatic devices is, of course, greatly reduced when appreciable reactance is introduced between the sending and receiving systems. For example, Fig. 28 shows the effect of introducing line reactance between the two machines just described.

*Reference 5; test results reported in closing discussion.

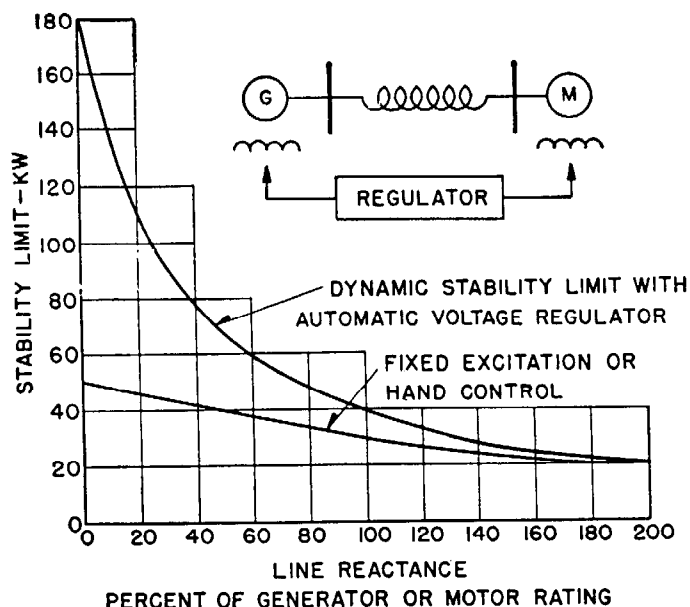


Fig. 28—Comparison of stability limit with automatic voltage regulator and limit with fixed excitation or hand control. Shows gain due to "Dynamic Stability."

bility,⁸ reference should also be made to the second part of Sec. 47 under Excitation Systems.

18. Hunting of Synchronous Machines

The hunting of synchronous machines can arise from phenomena closely related to system stability. In the early stages of power-system development it was difficult to differentiate between hunting and instability. The term "hunting" is now commonly restricted to two phenomena, which may be designated as

- (1) Hunting from spontaneous action, and
- (2) Hunting from pulsating torques.

The first of these phenomena was observed in connection with the operation of synchronous converters when supplied over "shoe-string lines." It was found that the hunting could be overcome (1) by limiting the resistance drop of these lines to a certain percent of the total reactance drop, or (2) by the use of suitable damper windings. Spontaneous hunting is still encountered occasionally, principally in connection with high-resistance lines or in connection with series capacitors as a result of which the resistance sometimes becomes relatively large through the neutralization of inductive reactance. The phenomenon of spontaneous hunting is now well understood, and the conditions under which it can occur can now be expressed in mathematical form.¹⁹

The hunting that results from pulsating torques is a phenomenon which today is of much less importance than it was when reciprocating types of prime movers were used. These pulsations have been minimized by the use of greater inertia and the use of damper windings. The development of the continuous-torque prime movers of the turbine type for both steam and hydro-electric installations substantially eliminated the problem in connection with these prime movers. At present the problem is occa-

sionally encountered in connection with Diesel-engine prime movers or with certain types of pulsating loads. The phenomenon may be analyzed by methods outlined in this chapter for a study of transient stability by using the known pulsating-torque characteristic of the prime mover or of the load, and the electro-mechanical equations or the electric-circuit equivalents.

Natural Frequency of Synchronous Machines*—The natural frequency of undamped electro-mechanical oscillation for a synchronous machine connected to an infinite bus and shaft-connected to reciprocating machinery is given by

$$f_n = \frac{35200}{n} \sqrt{\frac{P_r f}{WR^2}} \quad (34)$$

where

f_n = Natural frequency in cycles per minute.

n = Speed of machine in revolutions per minute.

P_r = Synchronizing power as defined below.

f = Frequency of circuit in cycles per second.

WR^2 = Moment of inertia of synchronous machine and shaft-connected prime mover or load, in lbs-ft².

The synchronizing power is the power at synchronous speed corresponding to the torque developed at the air gap between the armature and field. The synchronizing coefficient P_r is determined by dividing the shaft power in kw by the corresponding angular displacement of the rotor in electrical radians. P_r , therefore, is expressed in kw per electrical radian. The displacement angle of the rotor for a given current and power factor is

$$\delta = \tan^{-1} \frac{\bar{I}x_q \cos \phi}{E_t + \bar{I}x_q \sin \phi}$$

where

δ = Rotor displacement angle in electrical radians.

\bar{I} = Per-unit armature current.

E_t = Per-unit armature terminal voltage.

ϕ = Power-factor angle.

x_q = Per-unit quadrature-axis synchronous reactance.

The value of P_r determined by this method is quite generally applicable for predicting operation at full load, particularly where the amplitude and frequency of the power pulsations are low. The value of P_r at no load with the field excitation corresponding to normal open-circuit voltage may be taken as normal rated kva divided by x_q . The variation of P_r from no load to full load is approximately linear when the terminal voltage and power factor are held constant.

19. Governors

At present, prime movers for waterwheel and turbine generators are under the control of governors that respond to variation in speed or frequency. Some prime movers are operated on a mechanically-limited valve opening or "block" and an adjustment of the governor for that particular unit to regulate for a frequency somewhat above the system so that the unit operates to give the maximum prime-mover input corresponding to the de-

sired block. A governor under such a setting is, of course, operative to limit overspeed, the control becoming effective at a frequency slightly above the normal frequency. Governors are relatively slow in action with respect to the time elements which are important from the standpoint of power-system oscillations. For this reason governors are usually not important from the standpoint of transient stability. In the case of hydro-electric plants, because of the large amount of energy stored in the water column it is impracticable for the governor to limit rapidly the prime-mover input, although by-passing action can be effected more rapidly. Proposals for faster action have been made, but by-passing arrangements as built are too slow to be beneficial from the standpoint of stability. In the case of steam turbines, there is somewhat greater possibility of control. However, in many plants the amount of energy stored in the steam in the piping and various high- and low-pressure units, limits the benefits that might be obtained.

Governors, however, have an important effect on steady-state stability as a result of their control of the division of increments of load among the various generating units. It is necessary, therefore, to give consideration to the actual distribution of the incremental load when the stability limit is being approached. Furthermore, where loads and generating equipment are distributed throughout a network, a large difference of phase is sometimes introduced between the principal generating stations on the system. Under such conditions a system fault can sometimes produce a severe oscillation and result in instability. Such a condition can be avoided by control³⁸ of the phase angle between the machines so as to limit the initial angle between principal generating stations to a safe value for the initial condition, that is, prior to the fault.

Governors may introduce a disturbing factor and tend to produce hunting and even loss of synchronism. This condition produced by governor action is identical with the other forms of pulsating disturbances applied to a system and discussed in Sec. 18, Hunting of Synchronous Machines. The adjustment of the governor is an important factor in preventing any tendency toward hunting action. The time lag of the governor and its natural period of movement, if closely related to that natural period of the system, can contribute to hunting action.

If a machine pulls out of step with the remainder of the system, the governor is called into action by the overspeeding of the machine. The slipping of poles produces a pulsating disturbance of low frequency¹⁵, which the governor can or cannot follow, depending upon its adjustment. For this reason radically different results can be obtained when two generally similar generators pull out of step. There is, therefore, some advantage in adjusting governors so as to minimize the resulting disturbance to the system in the event of the machine losing synchronism.

20. Calculation of System Oscillations

The electro-mechanical oscillations produced by a transient disturbance on a two-machine system are very complicated. The formal mathematical solution of these os-

*American Standard for Rotating Electrical Machinery, ASA, C-50, 1943, page 28.

cillations is not possible as even the simplest cases involve elliptical integrals. The solution, however, can be obtained to any desired degree of accuracy by step-by-step approximate methods discussed subsequently in Sec. 23. The relations of the principal variables can readily be visualized by curves that give the acceleration, velocity, and displacement as a function of time. For this purpose it is convenient to think of an oscillation for which the change in power and angle are linear* as shown in Fig. 29 (a). The time variation of acceleration, velocity, and

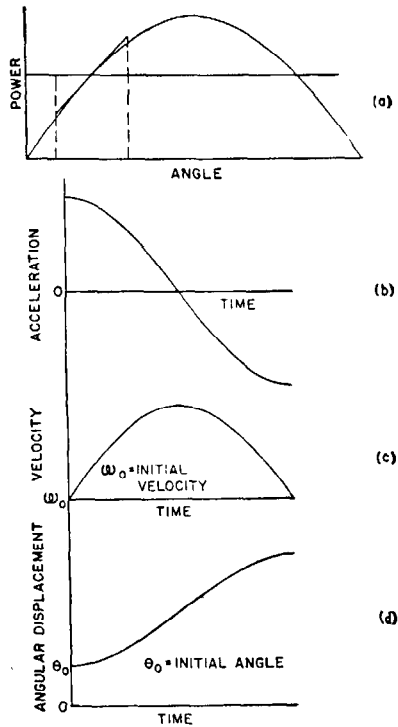


Fig. 29—Graphical solution of system oscillation

displacement are given in Fig. 29 (b) to (d). For the case chosen the quantities plotted are simple sine and cosine curves. Simple relations exist between these curves that can be derived from the basic laws of motion. Thus the change in velocity is proportional to the square root of the integral of the acceleration-angle curve, and the displacement is a function of the integral of the velocity curve.*

For the practical cases the simple trigonometric relations do not hold because the power-angle relation is not linear. However, curves similar to those of Fig. 29 (b), (c), and (d) can still be plotted, and they will help to give a picture of the variations in these quantities.

*These relations provide the basis for a graphical method proposed by Skilling and Yamakawa³⁹ for obtaining velocity-angle and time-angle curves. This method has certain advantages in comparison with a step-by-step method from the standpoint of formal mathematical presentation. It can readily be used to provide a check on the suitability of interval used in step-by-step analysis, since velocity is proportional to the square root of the integral of the acceleration-angle curve. The method is not applicable to a system with more than two machines and for this reason has not been presented in detail.

21. Use of Angle-Time or Swing Curves

Angle-time or swing curves may be calculated by means of the step-by-step procedure discussed in Sec. 23. These curves show the angular position of the rotor(s) plotted against time measured from the inception of a fault. Figure 36 is an example of an angle-time curve.

If a two-machine system is subjected to a switching transient as shown in Fig. 6, it is possible to determine by the "equal-area method" previously discussed, whether the system is stable. This answer, it will be noted, would be obtained without a knowledge of the time variation of the various electro-mechanical quantities. Similarly, if a two-machine system is subjected to a transient disturbance involving a fault with subsequent clearing, as illustrated in Fig. 7, it is also possible to determine whether the system is stable. In this case the duration of the various fault conditions must be expressed in terms of the angular swing. From a practical standpoint such information is not generally available because faults are cleared as a function of time measured from the application of the fault. Determination of this time requires solution of the electro-mechanical oscillation. Examination of the angle-time curves for a particular system subjected to a specified disturbance not only establishes whether the system is stable, but if stable it provides some basis for estimating the margin of stability as well. The angle-time or "swing curves" also provide a basis for estimating the magnitude of the voltage, current, power, and other quantities throughout the disturbance, which information is frequently of great value in circuit-breaker and relay applications.

The determination of angle-time curves is carried out by approximating methods either analytically or with the aid of the a-c network calculator. The essential parts of these methods are the same, since calculations in both cases are carried out by step-by-step methods. In this method small intervals are taken so that the accelerating forces can be assumed constant within the interval. On this basis it is a simple problem in mechanics to determine for each step the change in position of the rotor of each machine as a result of the accelerating or decelerating forces, the inertia of the machine, and the duration of the interval.

22. Inertia Constants and Acceleration

By means of the methods previously described, it is possible to reduce the electrical input or output of each machine to a simple power-angle curve or a simple trigonometric expression with the angle between internal emf's as the variable. The accelerating power depends upon the initial operating condition and upon the difference between input and output, including the effect of losses. Thus, for a generator the accelerating power, which is the variable ΔP , is

$$\Delta P = P_i - (P_o + L) \quad (35)$$

where P_i is the mechanical input, P_o is the electrical output, and L is the total loss. In the case of a synchronous motor the equation is similar in meaning, but the numerical sign of the accelerating forces is negative when the input is less than the output plus the losses. Losses are, however, often neglected.

The inertia of synchronous machines varies through a wide range depending principally upon the capacity and speed and upon whether additional inertia has been intentionally added. Fortunately, however, the constants vary through a relatively narrow range if they are expressed in terms of the stored energy per kva of capacity. The relation between the stored energy constant*, H , and WR^2 is given by the following equation:

$$H = \frac{\text{kW-sec}}{\text{kva}} = 0.231 \frac{(WR^2)(\text{rpm})^2 \times 10^{-6}}{\text{kva}} \quad (36)$$

where WR^2 is the moment of inertia in pounds-feet squared, and rpm is the speed in revolutions per minute. The inertia constants vary through a range of from less than one to about ten kilowatt-seconds per kva, depending upon the type of apparatus and the speed. Since control of the inertia is one of the possible methods of improving the stability of the system, the subject of inertia constants is discussed at some length under the first part of Sec. 47 dealing with measures for improving system stability. Reference should also be made to Chap. 6, Part XIII, for further information on inertia constants which can be used in preliminary work or in the absence of specific information applying to the machine under consideration.

Frequently it is convenient when neglecting loss to replace a system of two machines, each with finite inertia, by another system consisting of one machine with an equivalent inertia and a second machine with infinite inertia. By this means the problem is reduced to that of a single-machine system.⁵ If the stored energies of the machines are (H_a kva_a) and (H_b kva_b), then the equivalent inertia constant for one of them, $H_{eq(a)}$ is given by

$$H_{eq(a)} = \frac{H_a}{1 + \frac{H_a kva_a}{H_b kva_b}} \quad (37)$$

In this method the acceleration, velocity, and phase relation of the selected machine are obtained in relation to the other machine as reference. When losses, intermediate loads, or more than two machines are involved, it is necessary to use the more general method whereby the absolute acceleration, velocity, and phase relation for each machine are separately determined as discussed in the following section.

With the inertia constant, H , and the accelerating or decelerating power, ΔP , it is possible to compute the acceleration by means of the following important formula:

$$\alpha = \frac{(180)(f)(\Delta P)}{(H)(\text{kva})} \quad (38)$$

where α is the acceleration or deceleration in electrical degrees per second per second, f is the system frequency in cycles per second, ΔP is the kilowatts available for acceleration (or deceleration), H is the inertia constant in kilowatt-seconds per kva as obtained from Eq. (36).

23. Step-by-Step Procedure

The step-by-step procedure^{2-5,12,36} can be carried out in

*The formulas for acceleration and inertia constants are based on the forms presented in the "First Report of Power System Stability," Reference 33.

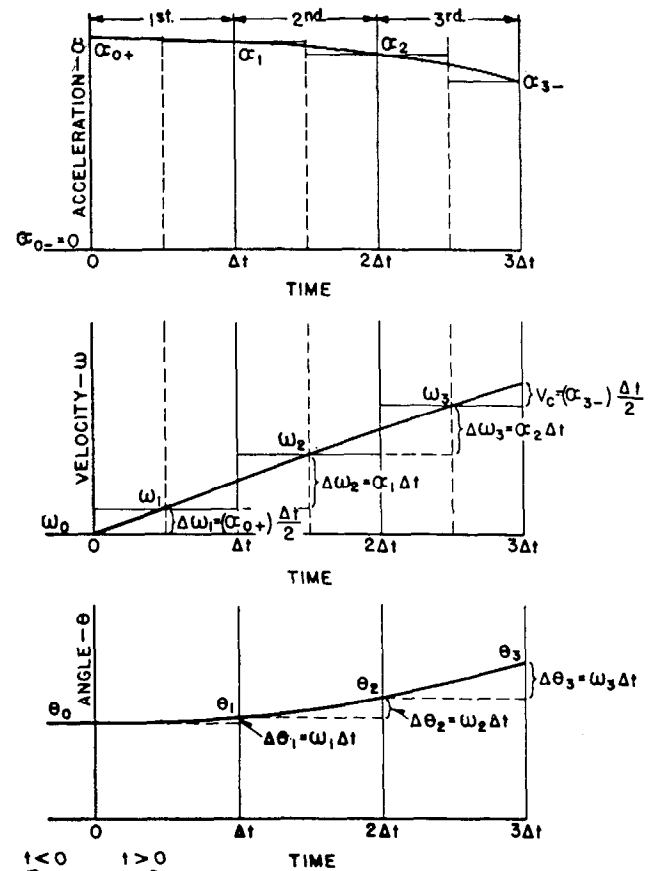


Fig. 30—Step-by-step solution—details of method for approximating acceleration, velocity, and angle changes.

NOTE: For computing velocity at the end of an interval, it is necessary to add a correction term to include change in velocity from the middle to the end of the interval as shown by V_c for the third interval.

many ways, depending upon the particular set of assumptions used to minimize the error resulting from the approximation. The following procedure is the one we have found to be the most suitable for transient-stability studies using the a-c network calculator. In studying the step-by-step method, it is suggested that consideration be given first to its application to a single-machine system, that is, a two-machine system for which one machine is of infinite inertia. Reference should be made to Fig. 30, which shows for a particular machine the variation of acceleration, velocity, and angle of rotor with respect to the other machine which is assumed to be of infinite inertia. The method upon which this figure is based can readily be modified to apply to the general case of two machines of finite inertia by making allowance for the changes in the positions of the rotor of the other machine. The calculations are arranged in tabular form as shown in Table 2. Two similar tabulations are required for a two-machine system, one for each machine. The calculation for a particular machine is tied in with that for the other machine by means of Column 11 of the tabulation, which is obtained from Column 10 of the tabulation for the other machine. If one of the machines is assumed to be of infinite inertia, the problem reduces to that of a single-machine system, and only one tabulation is

TABLE 2—SUGGESTED FORM FOR STEP-BY-STEP ANGLE-TIME CALCULATIONS

Station	Machine Nos.	Total Kva
	Machine, $WR^2 =$ lbs- ft^2	
	$H =$ stored energy, kilowatt-seconds per kva	
	Acceleration, $\alpha = \frac{180(f)(\Delta P)}{(H)(\text{kva})} = k\Delta P$, degrees per second per second	
	$k = \frac{180f}{(H)(\text{kva})} =$	
	$P_{\text{Mech.}} =$ kilowatts, mechanical input	

(1) Time Sec	(2) Angle θ Degrees	(3) Elec. Out- put plus losses* kw	(4) ΔP , kw Mechanical Input minus (Electrical Output plus losses)	(5) Accel., α Degrees per Sec per Sec	(6) Accel. Time Incre- ment	(7) Vel. change, $\Delta\omega$, Degrees per Sec	(8) Velocity ω , Degrees per Sec	(9) Angle Time Incre- ment	(10) Angular Change for Machine Under Con- sideration, $\Delta\theta$, Degrees	(11) Angular Change for Other Machine $\Delta\theta'$, Degrees	(12) Final θ , Degrees
—	—	—	$P_{\text{Mech.}} - (3)$	$(4) \times k$	—	$(5) \times (6)$	$(7) + (8)_{n-1}$	—	$(8) \times (9)$	**	$(2) + (10) + (11)$
0.0	θ_0	P_0	$P_{\text{Mech.}} - P_0$	$k\Delta P_0 = \alpha_{0+}$	$\Delta t/2$	$\Delta\omega_1$	$\omega_0 + \Delta\omega_1 = \omega_1$	Δt	$\omega_1\Delta t = \Delta\theta_1$	$\Delta\theta_1'$	$\theta_0 + \Delta\theta_1 + \Delta\theta_1' = \theta_1$
0.1	θ_1	P_1	$P_{\text{Mech.}} - P_1$	$k\Delta P_1 = \alpha_1$	Δt	$\Delta\omega_2$	$\omega_1 + \Delta\omega_2 = \omega_2$	Δt	$\omega_2\Delta t = \Delta\theta_2$	$\Delta\theta_2'$	$\theta_1 + \Delta\theta_2 + \Delta\theta_2' = \theta_2$
0.2	θ_2	P_2	$P_{\text{Mech.}} - P_2$	$k\Delta P_2 = \alpha_2$	Δt	$\Delta\omega_3$	$\omega_2 + \Delta\omega_3 = \omega_3$	Δt	$\omega_3\Delta t = \Delta\theta_3$	$\Delta\theta_3'$	$\theta_2 + \Delta\theta_3 + \Delta\theta_3' = \theta_3$
0.3	θ_3	P_3	$P_{\text{Mech.}} - P_3$	$k\Delta P_3 = \alpha_{3-}$	$\Delta t/2$	V_c	$\omega_3 + V_c$	—			
0.3+	θ_3	P_{3+}	$P_{\text{Mech.}} - P_{3+}$	$k\Delta P_{3+} = \alpha_{3+}$	$\Delta t/2$	$\Delta\omega_4$	$\omega_3 + (V_c + \Delta\omega_4) = \omega_4$	Δt	$\omega_4\Delta t = \Delta\theta_4$	$\Delta\theta_4'$	$\theta_3 + \Delta\theta_4 + \Delta\theta_4' = \theta_4$
0.4	θ_4	P_4	$P_{\text{Mech.}} - P_4$	$k\Delta P_4 = \alpha_4$	Δt	$\Delta\omega_5$	$\omega_4 + \Delta\omega_5 = \omega_5$	Δt	$\omega_5\Delta t = \Delta\theta_5$	$\Delta\theta_5'$	$\theta_4 + \Delta\theta_5 + \Delta\theta_5' = \theta_5$
0.5	θ_5										

See Fig. 30 for meaning of α , ω , $\Delta\omega$, θ and $\Delta\theta$ terms.

*Losses are often neglected where they are small compared to the machine output during the fault.

**These values obtained from similar tabulation for other machine.

required, as $\Delta\theta'$, the angular change for the other machine, can be taken as zero.

In Fig. 30 three intervals in the step-by-step method are shown, and a circuit change is assumed to take place at the end of the third interval. The velocities ω_1 , ω_2 , and ω_3 are assumed to remain constant through the corresponding three intervals. The acceleration on the other hand is assumed to remain constant from the middle of one interval to the middle of the subsequent interval. By this means acceleration is chosen to be alternately greater and less than the actual value as shown by the plotted curve. Such an arrangement is used to minimize the cumulative error.

The initial acceleration α_{0+} is computed from the power flow corresponding to the phase position at the beginning of the transient disturbance which takes place at $t=0$. This acceleration is then used for half of the first time interval Δt to determine the velocity ω_1 which is assumed throughout the interval. The angular change $\Delta\theta_1$ for the particular machine is then computed from the average velocity during the interval. Similar calculations are then made for the other machine to determine its angular change $\Delta\theta_1'$ during the same interval. The final angle, the angle θ_1 , at the end of the first interval, is the sum of the initial angle θ_0 and the angular displacements $\Delta\theta_1$ and $\Delta\theta_1'$ for the two machines.

The calculations for the second interval are made in a similar manner. The acceleration α_1 is computed with the aid of the angle θ_1 obtained at the end of the first interval. Next the increment in velocity is obtained by assuming

the acceleration α_1 through the interval Δt . This velocity is then used to compute the change in angle taking place through the second interval, which is equal to the velocity ω_2 times the increment of time Δt .

This process is repeated for each step throughout any period for which the circuit is not changed or for which the same time interval is used. If there is a change of either condition, it is necessary to compute a velocity correction term since, as pointed out previously, velocities are computed for the middle of the interval while acceleration and angular displacement are computed for the end of the interval. For the case illustrated in Fig. 30 the circuit is assumed to be changed at the end of the third interval. Consequently, it is necessary to add a correction term V_c to the velocity ω_3 to obtain the velocity at the end of the third interval as shown in the figure.

The fourth and subsequent intervals can be computed as for the first and subsequent intervals. To distinguish between the acceleration rates corresponding to the beginning of an interval or the end of the preceding interval, the practice has been followed of using plus and minus signs respectively. This procedure has been applied to the case under consideration using the terms α_{0-} and α_{0+} at zero time. In this case the acceleration α_{0-} is zero since it is assumed that the system is in equilibrium prior to the application of the transient at the time $t=0$, and the acceleration α_{0+} applies upon the application of the transient. The term α_{3-} gives acceleration at the end of the third interval prior to the circuit change, and the term α_{3+} gives

the acceleration subsequent to the circuit change. Ordinarily the plus and minus signs should be omitted, and in that case the term is understood to give the acceleration at the end of the interval indicated by the subscript.

The time interval to be used in the step-by-step analysis is a matter of judgment and convenience. In the ordinary stability problem the interval should not be longer than 0.1 second, which is a convenient interval since it gives the time in an even number of cycles. For some applications it is desirable to shorten the interval to 0.05 second, which corresponds to three cycles. The time interval can be changed from point to point throughout the transient disturbance. For example, during one part of a disturbance involving some circuit changes there can be little relative change in angular position, and relatively large intervals can be permitted. Conversely, other transient conditions can introduce large changes in angle during an interval. As a practical matter, the length of the interval should always be decreased if the change results in an angular swing of 20 degrees to 30 degrees in a single interval. The velocity-angle curve for two-machine systems can be plotted and compared with the results of calculation by the method of Skilling and Yamakawa.³⁹

The labor of making a step-by-step calculation will be reduced greatly by arranging the work in tabular form. For this reason Table 2 has been introduced. This table is based on the procedure found desirable in a-c network calculator studies and can be supplemented by additional columns if this is desirable to facilitate the calculation of the output power which in the table is assumed to have been obtained from the a-c network calculator readings or from calculated power-angle curves. The calculations have been arranged so that velocity and acceleration curves can be plotted readily; this has been found desirable in a sufficient number of cases as to justify the additional columns required.

Further details of the step-by-step procedure can be obtained from a study of the numerical examples.

V. EXAMPLES OF TRANSIENT-STABILITY PROBLEMS

In the previous sections, the concepts of calculating power-system stability are discussed in some detail. To illustrate the various salient features of stability calculations, and to make clear the exact procedure in a specific problem, two examples will be calculated in detail. All of the individual steps in the calculation are given, so that one inexperienced in this work can follow the problem readily. To facilitate understanding of the various factors involved in transient-stability calculations, references are given to the sections where the theory involved is discussed, and a considerable portion of the theory is reviewed. In addition to a thorough knowledge of the foregoing sections of this chapter, an understanding of machine characteristics, Chap. 6, is necessary in solving the problems.

The first example is a single-machine problem. This was chosen because it is the simplest case met in practice, and because in its solution the elements of a stability problem

can be illustrated with the least possibility of confusion. The single-machine problem is also useful when there are no intermediate loads, and losses can be neglected, since a two-machine problem can then be reduced to a single-machine problem, (Sec. 22). In the single-machine problem all resistances and line capacitances are neglected to simplify the calculations.

The two-machine example has been selected so that the sending end is the same for both problems. Both sending and receiving systems have finite inertia, and resistances are considered. This problem is important because it is the type most frequently calculated manually. Also, in using the general two-machine problem, all fundamental considerations affecting system stability in multi-machine systems can be illustrated.

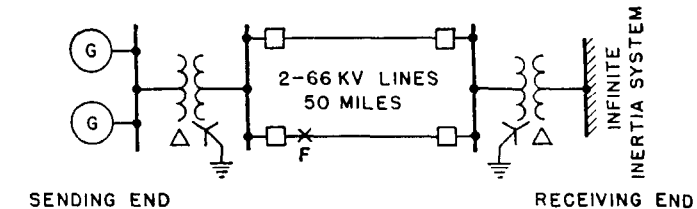


Fig. 31—Single-machine system assumed for study.

24. Description of Single-Machine System

The single-machine system selected for study, shown schematically in Fig. 31, has the following characteristics:

Transmission Lines:

Two circuits in parallel, 50 miles long, 10 foot flat spacing = 12.6 foot equivalent-delta spacing. Conductors are 250 000 circular mils, copper. Distance between line centers is 40 feet and the conductors are transposed. There are no ground wires. 50 000 kw at 100 percent power factor is delivered to the infinite receiver system. Normal voltage 66 kv.

Sending end:

Two 30 000-kva, three-phase, 60-cycle, waterwheel generators.

Unsaturated synchronous reactance	$x_d = 63.8$ percent
Rated-current transient reactance	$x_d' = 25.4$ percent

(Chap. 6, Part XIII)

Negative-sequence reactance	$x_2 = 28.9$ percent
-----------------------------	----------------------

Inertia constant (kw-sec/kva)	$H = 3$
-------------------------------	---------

Normal regulators and excitation system.	
--	--

Transformers:

One 60 000-kva, three-phase, 60-cycle bank connected as shown in Fig. 31 at each end of the transmission lines.

Reactance = 8 percent. Exciting current is neglected.

Receiving end:

Low-voltage side of receiver transformers connected to an infinite inertia system. Receiver low-voltage bus fixed at 95 percent of normal voltage.

25. Circuit Constants

This problem is calculated using the per-unit system. The values given in the illustrations are all in per unit. The base selected is the kva of the sending end, or 60 000 kva. Using the formulas in Chap. 10, Sec. 4 to 7,

$$\left. \begin{array}{l} \text{Normal Current } \bar{I}_n = \frac{60000}{\sqrt{3}(66)} = 525 \text{ amperes.} \\ \text{Normal Voltage } \bar{E}_n = \frac{66}{\sqrt{3}} = 38.1 \text{ kv line-to-neutral.} \\ \text{Normal Impedance } \bar{Z}_n = \frac{38.1 \times 10^3}{525} = 72.6 \text{ ohms.} \end{array} \right\} \quad (39)$$

These values apply to the 66-kv portion of the system. If the above normal values are desired at any other point in the system, the transformer turns ratio should be used to determine the normal voltage at that point.

The first step in the calculation is to determine the impedances of the different elements of the system in per unit. These values are then put in the network and it is reduced to its simplest form.

The percent reactance of the generators on 60 000 kva is twice the values given, but since the two machines are in parallel, the reactance in the networks is halved so the above values can be used.

Using the methods of Chap. 3, X_1 and X_2 of each line equal 39.7 ohms. X_0 equals 138.2 ohms for one line, and 108.2 ohms for the two lines in parallel. The line reactances in per unit on 60 000 kva at 66 kv are:

Single Line:

$$\begin{array}{ll} \text{Positive- and negative-sequence reactance} & X_1, X_2 = 0.547 \\ \text{Zero-sequence reactance} & X_0 = 1.90 \end{array}$$

Two lines in parallel:

$$\begin{array}{ll} \text{Positive- and negative-sequence reactance} & X_1, X_2 = 0.274 \\ \text{Zero-sequence reactance} & X_0 = 1.49 \end{array}$$

A definite voltage is usually maintained at certain cardinal points in a system, and in this case the receiver low-voltage bus is maintained at 0.95 per-unit voltage. The sending-end generator terminal voltage is desired, so it is convenient to combine the portion of the network between the two buses into a single reactance. It is:

$$\begin{aligned} X_s &= 0.434 \text{ per unit} \\ &= 31.5 \text{ ohms.} \end{aligned} \quad (40)$$

The load delivered at the receiver low-voltage bus is 50 000 kw (0.833 per unit) at unity power factor. The current in the network is:

$$\begin{aligned} \bar{I} &= \frac{0.833}{0.95} = 0.877 \text{ per unit} \\ &= 460 \text{ amperes.} \end{aligned} \quad (41)$$

With this current flowing, the terminal voltage of the sending-end generator is:

$$\begin{aligned} E_s &= 0.95 + 0.877(j0.434) \\ &= 0.95 + j0.381 \\ &= 1.023e^{j22^\circ} \text{ per unit} \\ &= 39.8e^{j22^\circ} \text{ kv line-to-neutral} \end{aligned} \quad (42)$$

With the above quantities determined, all necessary information is available to compute the sending- and receiving-end power-circle diagrams. This is often done in practical problems in order to determine the initial operating conditions, but in the problem this information is given, so circle diagrams are not necessary.

26. Transient Stability Calculation

The most critical type of transient disturbance that receives consideration in stability studies is that arising from the application of a fault and the subsequent switching necessary to isolate the fault. In this problem a zero-impedance double line-to-ground fault is assumed to take place at the sending end of one of the transmission lines as shown in Fig. 31. Both ends of the faulted line are opened simultaneously to clear the fault. The problem is to determine the maximum permissible time between the inception of the fault and the opening of the circuit breakers for which stability can be maintained. The time thus determined is not the breaker operating time that would normally be used but the maximum operating time which could be allowed and still maintain stability. The ability of a system to withstand a double line-to-ground fault is often, but not invariably, taken as the criterion of system stability.

The first step is to calculate and plot power-angle diagrams (See Chap. 10; Chap. 13, Sec. 2) for three circuit conditions: (1) the initial condition immediately prior to inception of the fault, (2) the condition during the fault, and (3) the condition after the fault is isolated. Since in this case the receiver has infinite inertia, its angular position remains fixed and it is necessary only to calculate power-angle diagrams for the sending end. The equation relating sending-end power to the known circuit quantities (See Chap. 9) reduces to the following in this problem because losses have been neglected:

$$P_s = -\frac{\bar{E}'_{d-s}\bar{E}_{\infty-R}}{X} \cos(90^\circ + \theta) \quad (43)$$

in which θ is the angle between the internal voltages \bar{E}'_{d-s} and $\bar{E}_{\infty-R}$. Since the power-angle diagrams are to be determined for transient conditions, the voltage behind transient reactance E'_{d-s} must be used, and the value of X must be determined using generator transient reactance x'_d . The generator internal voltage, or voltage behind transient reactance is the vector sum of the terminal voltage of the machine and the voltage necessary to force the load current through the transient reactance.

$$\begin{aligned} E'_{d-s} &= 0.95 + j0.381 + 0.877(j0.254) \\ &= 1.12e^{j32.2^\circ} \text{ per unit} \end{aligned} \quad (44)$$

Because of the times involved in transient disturbances, the internal voltage of the machine is generally considered constant (Sec. 30, and Chap. 6, Sec. 21), so this value of E'_{d-s} is used for the entire calculation.

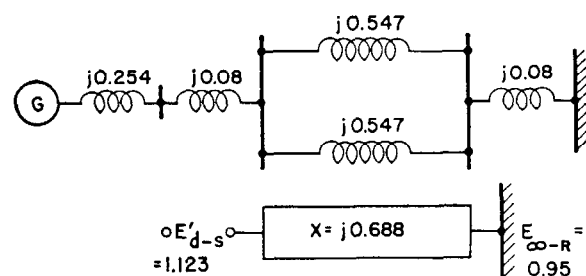


Fig. 32—Single-machine system. Network before the fault occurs.

Before the Fault—The network to be used in calculating the sending-end power before the fault is shown in Fig. 32. All necessary constants are known, so that,

$$P_s = -\frac{(1.12)(0.95)}{0.688} \cos(90 + \theta) \\ = -1.55 \cos(90 + \theta) \text{ per unit} \quad (45)$$

During the Double Line-to-Ground Fault—The first step in determining the power-angle diagram during the fault is to reduce the negative- and zero-sequence networks to single equivalent reactances to be applied at the point of fault, (Sec. 10). The constants to be used in the negative- and zero-sequence networks are known, so these networks can be drawn readily. They are shown in Fig. 33 (a)

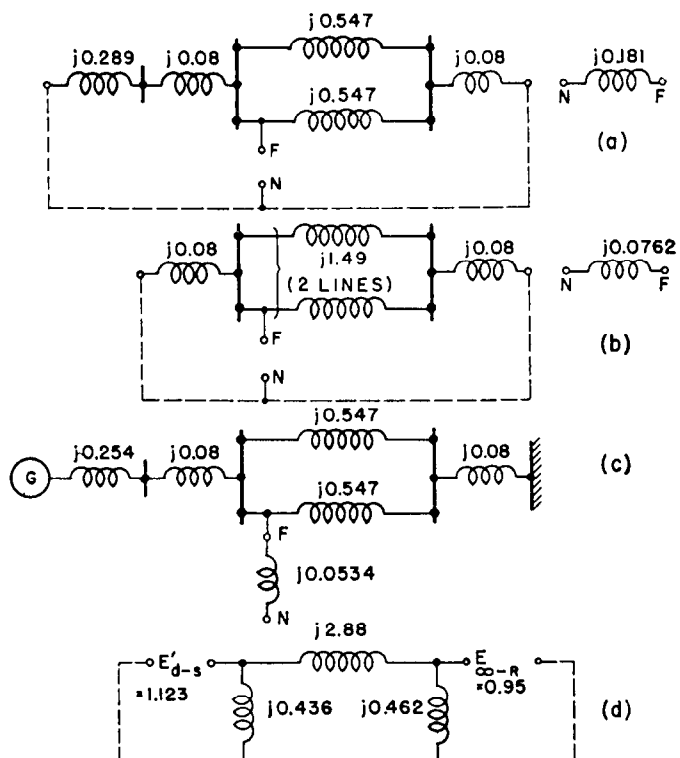


Fig. 33—Single-machine system. Networks for use during the double line-to-ground fault.

- (a)—Negative-sequence network.
- (b)—Zero-sequence network.
- (c)—Network during the fault.
- (d)—Network (c) reduced.

and (b), and to the right of each is the single equivalent reactance to which each network reduces. Since the fault is double line-to-ground, these two equivalent reactances must be paralleled (Chap. 2, Fig. 21) and connected at the point of fault. This is illustrated in Fig. 33 (c) which finally reduces to the network of Fig. 33 (d) by a simple star-delta conversion. With all losses neglected, the sending-end power is determined by Eq. (43). The shunt branches of Fig. 33 (d) need not be considered, as they only affect reactive power transfer. If maintained internal voltage had not been assumed and it was required to consider the demagnetizing effect of shunt loads, the shunt branches

would be considered. As the generator internal voltage or voltage back of transient reactance is assumed to remain constant, the same voltages calculated for the condition before the fault apply, and

$$P_s' = -\frac{(1.12)(0.95)}{2.88} \cos(90 + \theta) \\ = -0.370 \cos(90 + \theta) \text{ per unit.} \quad (46)$$

After the Fault—When the faulted line section is isolated from the system, the network to be used for calcu-

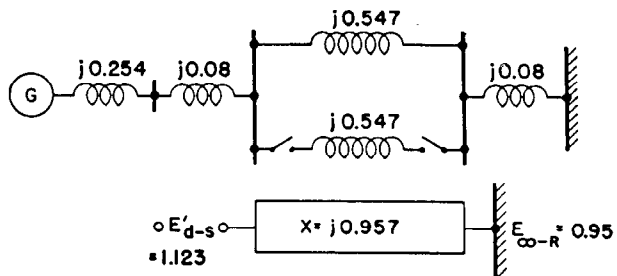


Fig. 34—Single-machine system. Network after the fault is isolated.

lating P_s'' is that shown in Fig. 34. Using the constants given, the sending-end power equation becomes:

$$P_s'' = -\frac{(1.12)(0.95)}{0.957} \cos(90 + \theta) \\ = -1.11 \cos(90 + \theta) \text{ per unit.} \quad (47)$$

Power-Angle Diagrams and Limiting Angles—

Equations (45), (46), and (47) are plotted in Fig. 35 as a function of θ , giving the power-angle diagrams of the single-machine system for the condition assumed. Inspection of the diagram or solving Eq. (45) for θ with $P_s = 0.833$ per unit shows that before the fault occurs the system is operating at an angle of 32.3 degrees. The maximum angle (critical angle of Sec. 4 and 6) to which the machine can swing, after the fault is isolated, without loss of stability is 131.6 degrees. This angle can be read from Fig. 35 or calculated by determining the value of θ between

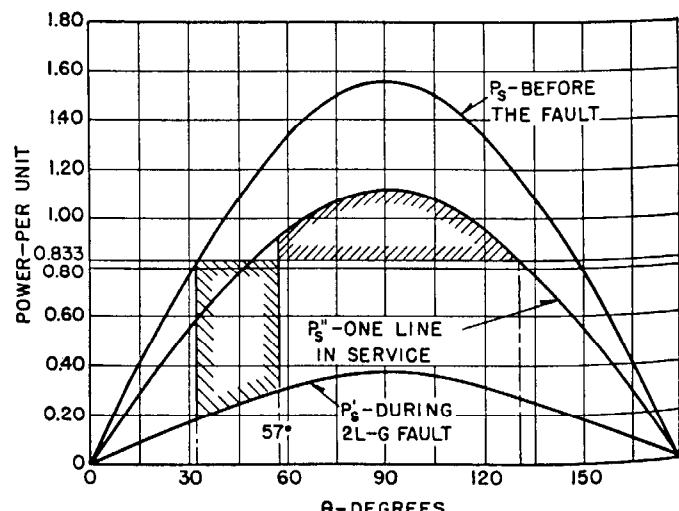


Fig. 35—Power-angle diagrams for single-machine system.

90° and 180° that will satisfy Eq. (47) with $P_s'' = 0.833$ per unit. This is the maximum value that θ can reach without the system becoming unstable. If the angle θ exceeds 131.6°, then the mechanical input to the sending-end generator exceeds its electrical output (see Fig. 35), and the generator pulls out of synchronism. By the equal-area method described in Sec. 6, an angle of approximately 57 degrees is selected as the maximum angle at which the fault can be isolated if stability is to be maintained.

Angle-Time or Swing Curves—To determine the time of fault isolation corresponding to 57 degrees, θ is determined as a function of time by a step-by-step method. The method is described in detail in Sec. 23, and a convenient means of calculating is to use the tabular form illustrated by Table 2. Such a calculation is carried out in Table 3, using this form. The first part of Table 3 assumes that the fault is not isolated, and the rapid increase in θ indicates how fast the system becomes unstable under these conditions. Note that the low inertia constant ($H = 3$ kw-sec/kva) of the generators permits them to change angular position rapidly, so that relatively small time intervals, 0.05 seconds, are chosen for the calculation.

As previously explained, the velocity is assumed constant over each period, but the acceleration is assumed constant from the middle of one period to the middle of the next. This is done to minimize cumulative errors. Column 6 shows how this is done.

The second part of the tabulation assumes that the fault is isolated in 0.15 seconds, since in this time θ has increased to 57.2 degrees which matches closely the 57 degrees chosen as the maximum switching angle to maintain stability in Fig. 35. The terms -0.15 and $+0.15$ seconds in column 1 indicate the increments of time before and after the breakers open. Note the changes in columns 6, 7, and 9 for the -0.15 second time. The calculation indicates that stability is maintained, since θ reaches a maximum value less than the critical angle of 131.6 degrees. The calculation is carried far enough to show that θ begins to return to the new operating point.

The angle-time or swing curves resulting from the step-by-step calculation are plotted in Fig. 36. Curves A and B are the graphic plot of the calculations carried out in Table 3. They show more clearly that stability will be lost quickly if the fault is not isolated and that stability is just maintained if the total fault clearing time is not greater than 0.15 seconds. Curves C and D have also been calculated by the step-by-step method, and show that stability is lost for fault clearing times slightly longer than 0.15 seconds.

27. Assumptions Made in Solving Two-Machine Problems

The two-machine problem given below is an example of the manner in which this problem can be solved by

TABLE 3—STEP-BY-STEP CALCULATION OF ANGLE-TIME CURVES FOR SINGLE-MACHINE SYSTEM

$$H=3 \quad k = \frac{180 \times 60}{3 \times 1} = 3600$$

(1)	(2)	(3)	(4)	(5)	(6)	(7)	(8)	(9)	(10)	(11)
Time in Sec at Beginning of Interval	Angle θ at Beginning of Interval	Electrical Power Output, Per Unit	ΔP , Me- chanical Input Minus Electrical Output	Accelera- tion, Degrees per Sec per Sec	Accelera- tion Time Increment, Seconds	Velocity Change, Degrees per Second	Velocity, Degrees per Second	Angle-Time Increment	Angular Change, Degrees	θ Final Angle, Degrees
—	—	—	0.833 - (3)	(4) $\times k$	—	(5) $\times (6)$	(7) + (8) _{n-1}	—	(8) $\times (9)$	(10) + (2)
0.0	32.3	0.199	0.634	2285	0.025	57.0	57.0	0.05	2.85	35.2
0.05	35.2	0.213	0.620	2230	0.05	111.5	168.5	0.05	8.43	43.6
0.10	43.6	0.255	0.578	2080	0.05	104.0	272.5	0.05	13.6	57.2
0.15	57.2	0.312	0.521	1880	0.05	94.0	366.5	0.05	18.3	75.5
0.20	75.5	0.358	0.475	1710	0.05	85.5	452.0	0.05	22.6	98.1
0.25	98.1	0.367	0.466	1680	0.05	84.0	536.0	0.05	26.8	124.9
0.30	124.9	0.303	0.530	1910	0.05	95.5	631.5	0.05	31.6	166.5
0.35	166.5

Fault Isolated in 0.15 Seconds

-0.15	57.2	0.312	0.521	1880	0.025	47.0	320
+0.15	57.2	0.936	-0.103	-372	0.025	-9.3	311	0.05	15.5	72.7
0.20	72.7	1.063	-0.230	-829	0.05	-41.5	269	0.05	13.5	86.2
0.25	86.2	1.112	-0.279	-1000	0.05	-50.0	219	0.05	11.0	97.2
0.30	97.2	1.105	-0.272	-977	0.05	-48.9	170	0.05	8.5	105.7
0.35	105.7	1.071	-0.238	-858	0.05	-42.8	127	0.05	6.4	112.1
0.40	112.1	1.032	-0.199	-714	0.05	-35.7	91	0.05	4.6	116.7
0.45	116.7	0.996	-0.163	-588	0.05	-29.4	62	0.05	3.1	119.8
0.50	119.8	0.963	-0.130	-460	0.05	-23.4	38	0.05	2.0	120.8
0.55	120.8	0.958	-0.125	-450	0.05	-22.5	16	0.05	0.8	121.6
0.60	121.6	0.950	-0.117	-420	0.05	-21.0	-5	0.05	-0.2	121.4
0.65	121.4	0.950	-0.117	-420	0.05	-21.0	-26	0.05	-1.3	120.1

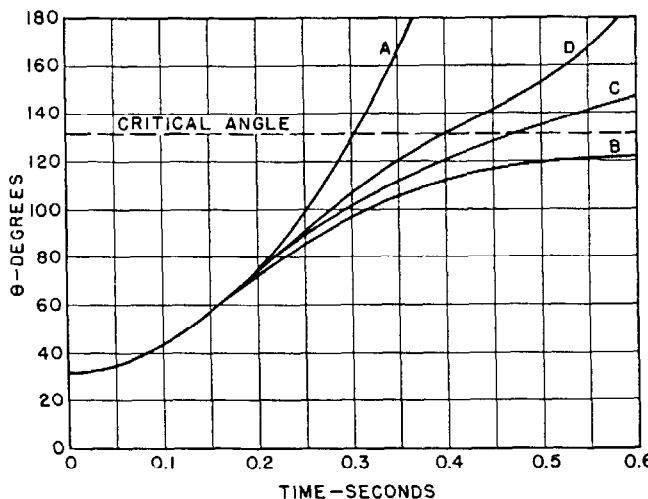


Fig. 36—Angle-time curves for single-machine system.

- A—Fault not cleared.
B—Fault isolated in 0.15 sec.
C—Fault isolated in 0.16 sec.
D—Fault isolated in 0.17 sec.

calculation. A number of simplifying assumptions are made, most of which are conservative.

The common assumptions are listed, together with references from which their effect can be determined.

1. Impedance of the load is constant (Sec. 9).
2. Effect of saliency is generally neglected (Sec. 15).
3. Negative-sequence loss varics as I_2^2 for all machines (Chap. 6, Part XIII). This assumption is inherent in the method of symmetrical components (Sec. 10).
4. Rated-current transient reactance is normally used (Chap. 6, Part XIII).
5. The losses in generators are sometimes neglected. This is permissible when the output of the machine during the fault is large compared with its losses. Typical generator resistances are given in Chap. 6. The loss due to the unidirectional component of short-circuit current is discussed in Chap. 6.
6. The internal voltage or voltage behind transient reactance is assumed to remain constant during a transient disturbance (Chap. 6, Sec. 22).
7. The effect of negative-sequence torque is generally neglected (Sec. 10).

Almost all of the above assumptions are conservative, and the net effect is conservative. More accurate calculations can be made by referring to the references given, but this is not usually done because more margin than is obtained by these assumptions is necessary for safe operation of a system from the standpoint of transient stability.

Generally, the first step in the calculation of a two-machine problem is to draw the sending-end and receiving-end circle diagrams, which would be used to determine the operating conditions of a system at the time of a fault (Chap. 10, Sec. 21). In this problem this information is given.

28. Description of Two-Machine System

The two-machine system assumed for study is illustrated in Fig. 37. The sending end is the same as in the single-

machine problem. Transformer resistance is included, but generator resistances are not. Including resistance, the transformer impedance becomes $1+j8$ percent. The line in ohms using the methods of Chap. 3 are:

Single line:

- Positive- and negative-sequence impedance
Zero-sequence impedance

$$Z_1, Z_2 = 12.9 + j39.7 \\ Z_0 = 27.2 + j138.2$$

Two lines in parallel:

- Positive- and negative-sequence impedance
Zero-sequence impedance

$$Z_1, Z_2 = 6.43 + j19.9 \\ Z_0 = 20.7 + j108.2$$

The receiving-end data are:

Generators:

- Two 62 500-kva, three-phase, 60-cycle turbine generators
Unsaturated synchronous reactance $x_d = 125$ percent
Rated-current transient reactance $x_d' = 15.6$ percent
Negative-sequence reactance $x_2 = 9.8$ percent
Inertia constant (kw-sec/kva) $H = 5$

Shunt load:

115 000 kw at 85 percent power factor located at receiving-end low-tension bus. Load is represented by a constant impedance.

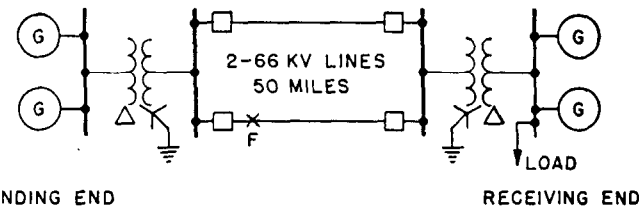


Fig. 37—Two-machine system assumed for study.

29. Circuit Constants

The two-machine problem is also calculated using the per-unit system. The kva base is optional, so for simplicity 60 000-kva base is again used.

The circuit constants in per unit on 60 000 kva are.

Transmission lines:

Single line:

- Positive- and negative-sequence impedance
Zero-sequence impedance

$$Z_1, Z_2 = 0.177 + j0.543 \\ Z_0 = 0.373 + j1.90$$

Two lines in parallel:

- Positive- and negative-sequence impedance
Zero-sequence impedance

$$Z_1, Z_2 = 0.0883 + j0.274 \\ Z_0 = 0.284 + j1.49$$

Receiving End:

Each Generator:

- Conventional synchronous reactance
Rated-current transient reactance
Negative-sequence reactance
Inertia constant (kw-sec/kva)

$$x_d = 1.20 \\ x_d' = 0.15 \\ x_2 = 0.094 \\ H = 5$$

Shunt load:

The shunt load is 1.92 per unit at 0.85 lagging power factor, or $1.92 + j1.19$ per unit.

Since the machines are in parallel, the above values must be divided by two before insertion in the sequence networks.

The capacitance of the two 50-mile transmission lines is neglected in this problem. This is justified on the basis of calculations that show the line capacitive reactance to be nearly equal in magnitude to the transformer magnetizing reactance, and the latter has also been neglected. Consideration of line capacitive reactance and transformer magnetizing reactance would add in no way to the problem's effectiveness in illustrating a typical stability calculation, nor would it add to the generality of the networks involved, since the load introduces a shunt branch. If it is necessary to include these effects, Chap. 3 gives line constants, which may be converted to general circuit (*ABCD*) constants by Table 9, Chap. 10 or by Chap. 9, Sec. 6. The equivalent π form is given in Chap. 9, Sec. 6. The appendix gives equivalent circuits for transformers, which can be introduced into the circuit.

As in the single-machine problem, voltage is considered to be maintained at the receiving low-tension bus. The receiving-end maintained bus voltage is 36.2 kv line-to-neutral (95 percent of normal). With voltage maintained at this point, it is again convenient to combine the network between the low-voltage buses into a single set of circuit constants. These quantities are tabulated in the first four columns of Table 4 in terms of the familiar *ABCD* constants (See Chap. 10), which are used in this problem to facilitate the handling of the network involving shunt branches. The *ABCD* constants for one line plus the transformers, and for two lines in parallel plus the transformers, can be written immediately without further calculation by using the quantities given above and Network Number 1 of the tabulated formulas for *ABCD* constants given in Chap. 10. These two sets of constants are listed in Table 4, Cols. (1) and (2). Since the load also forms part of the network between the points of maintained voltage, it will be combined with the constants of Cols. (1) and (2) to give those listed in Cols. (3) and (4), respectively. This is accomplished by using Network Number 10, Table 9, Chap. 10.

The load at the receiver low-tension bus is 1.92 per unit at 85 percent power factor, or $1.92+j1.19$ per unit. Part of the total kva is supplied by the sending-end generators and part by the receiving-end units. For this problem, it is assumed that the sending-end station is delivering 50 000 kw (0.833 per unit) at unity power factor to the load. This dictates that the receiving-end station is delivering $1.08+j1.19$ per unit to the load, or 1.08 per unit real power at 67.4 percent power factor. With 0.833 per unit real power coming to the load through the network, the current drawn through the network is

$$\bar{I}_s = \frac{0.833}{0.95} = 0.877 \text{ per unit at 100 percent power factor} \quad (48)$$

Note that this expression is identical to Eq. (41). With the above current flowing, the sending-end low tension bus voltage is

$$\begin{aligned} E_s &= 0.95 + 0.877 (0.108 + j0.434) \\ &= 1.045 + j0.381 \text{ per unit} \\ &= 1.11 e^{j20^\circ} \text{ per unit} \\ &= 42.5 e^{j20^\circ} \text{ kv line-to-neutral.} \end{aligned} \quad (49)$$

The current flowing to the load from the receiving-end machines, when they are delivering $1.08+j1.19$ per unit power (1.605 per unit power at 67.4 percent power factor) is

$$\begin{aligned} \bar{I}_R &= \frac{1.605}{0.95} = 1.69 \text{ per unit at 67.4 percent power factor.} \\ I_R &= 1.14 - j1.25 \text{ per unit} \\ &= 599 - j658 \text{ amperes.} \end{aligned} \quad (50)$$

30. Transient-Stability Calculation

In the single-machine problem the most severe type of transient disturbance was considered, namely, the application of a fault and its subsequent isolation. The same disturbance is considered in the present problem, and the same zero-impedance double line-to-ground fault located at the sending end of one transmission line is used. This is shown in Fig. 37. The circuit breakers are assumed to open simultaneously to isolate the faulted line, and again maximum permissible time between fault inception and breaker clearing to maintain stability is to be determined. Here again it becomes apparent that prompt switching is imperative if the assumed load is to be carried.

Before plotting power-angle diagrams for the sending and receiving ends for the three circuit conditions, (1) before, (2) during, and (3) after the fault, it is necessary to calculate the generator internal voltages using the known terminal voltages, E_s and E_R and the generator rated-current transient reactances (x_d'). The sending-end internal voltage is:

$$\begin{aligned} E'_{d-s} &= 1.045 + j0.381 + 0.877 (j0.254) \\ &= 1.045 + j0.604 \text{ per unit} \\ &= 1.21 e^{j30^\circ} \text{ per unit} \\ &= 46.2 e^{j30^\circ} \text{ kv line-to-neutral.} \end{aligned} \quad (51)$$

The receiving-end voltage behind transient reactance, remembering that E_R is 0.95 per unit volts, is

$$\begin{aligned} E'_{d-R} &= 0.95 + (1.14 - j1.25) (j0.075) \\ &= 1.044 + j0.0855 \text{ per unit} \\ &= 1.048 e^{j4.7^\circ} \text{ per unit} \\ &= 40 e^{j4.7^\circ} \text{ kv line-to-neutral.} \end{aligned} \quad (52)$$

Before the Fault—The network for use in calculating the sending- and receiving-end power is shown in Fig. 38. Since the equivalent circuits of the generators consist of a series impedance, their *ABCD* constants can be written down without calculation. These are listed in Col. (5) and (6) of Table 4. Now using Network Number 16 from the tabulation of *ABCD*-constants formulas of Chap. 10, the *ABCD* constants for the entire system can be determined. The results are given in Table 4, Col. (7). To illustrate the

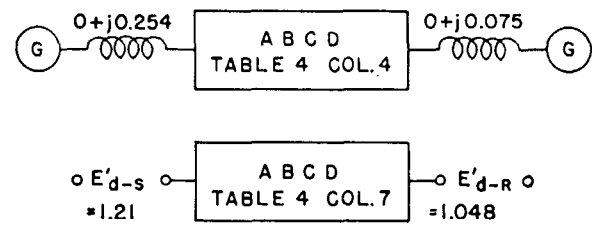


Fig. 38—Two-machine system. Network before the fault occurs.

method, the B constant is calculated below. Subscript 1 denotes the receiving-end generator; 2 denotes two parallel lines with transformers and load; and 3 the sending-end generators.

$$\begin{aligned} B &= A_3(B_1A_2 + D_1B_2) + B_3(B_1C_2 + D_1D_2) \\ &= (1+j0)[(0+j0.075)(1.799+j0.774) + (1+j0)(0.109 \\ &\quad + j0.434)] + (0+j0.254)[(0+j0.075)(2.11-j1.31) \\ &\quad + (1+j0)(1+j0)] \\ &= 0.011+j0.847 = 0.847 e^{j89.2^\circ}. \end{aligned}$$

The real parts of equations 85 and 86, Chap. 9 can be expressed in the form:

$$P_s = \frac{-\bar{E}_s^2 \bar{D}}{\bar{B}} \cos(\beta - \delta) - \frac{\bar{E}_R \bar{E}_s}{\bar{B}} \cos(\beta + \theta) \quad (53)$$

$$\text{and } P_R = -\bar{E}_R^2 \frac{\bar{A}}{\bar{B}} \cos(\beta - \alpha) + \frac{\bar{E}_R \bar{E}_s}{\bar{B}} \cos(\beta - \theta). \quad (54)$$

Where P_s and P_R are the sending- and receiving-end power, \bar{E}_s and \bar{E}_R are their respective internal voltages from equations (51) and (52), and α , β , and δ are the vector angles of the A , B , and D constants, respectively. Positive direction of power flow is out of the sending-end generators and into the receiving-end generators.

P_s and P_R for the condition before the fault can now be calculated.

$$\begin{aligned} P_s &= (1.21)^2 \frac{1.110}{0.847} \cos(89.2^\circ - 8.2^\circ) \\ &\quad - \frac{(1.21)(1.048)}{0.847} \cos(89.2^\circ + \theta) \\ &= 0.300 - 1.50 \cos(89.2^\circ + \theta) \text{ per unit.} \quad (55) \end{aligned}$$

$$\begin{aligned} P_R &= -(1.048)^2 \frac{2.50}{0.847} \cos(89.2^\circ - 31.5^\circ) \\ &\quad + \frac{(1.21)(1.048)}{0.847} \cos(89.2^\circ - \theta) \\ &= -1.73 + 1.50 \cos(89.2^\circ - \theta) \text{ per unit.} \quad (56) \end{aligned}$$

During the Fault—As in the single-machine system, the negative- and zero-sequence networks must be determined, reduced to single impedances, and applied at the point of fault. Both of these networks can be readily constructed as all of the circuit constants are given in Sec. 29. The negative- and zero-sequence networks are shown in Fig. 39 (a) and (b), and at the right of each the single equivalent impedance that represents the network is shown. Because the assumed fault is double line-to-ground, the two single impedances representing the negative- and zero-sequence networks must be paralleled before they are applied to the point of fault (Chap. 2, Fig. 21). The complete network for use during the fault is shown in Fig. 39 (c), which includes this resulting shunt impedance.

It is now necessary to reduce the network of Fig. 39 (c) to one set of circuit constants before the power equations can be solved. To do this involves a rather general usage of $ABCD$ constants and the necessary steps will be individually traced. The first step is to obtain the network of Fig. 39 (d), which is readily accomplished. The sum of the sending-end generator and transformer impedances form the left-hand branch, the receiving-end generator impedance alone forms the right-hand branch, and the shunt

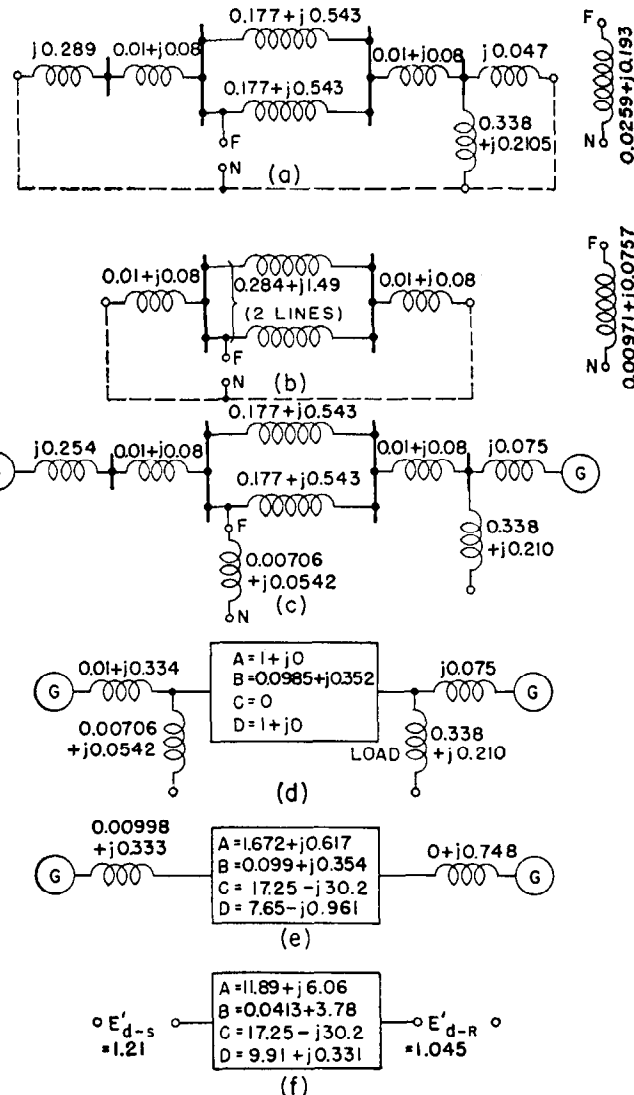


Fig. 39—Two-machine system. Networks for use during the double line-to-ground fault.

- (a)—Negative-sequence network.
- (b)—Zero-sequence network.
- (c)—Complete network during the fault.
- (d)—First reduction of complete network.
- (e)—Second reduction of complete network.
- (f)—Final reduced network during the fault.

branches consist of the impedances representing the load and the fault, both of which are taken directly from Fig. 39 (c). The center unit is found by paralleling the two transmission lines and adding the receiving-end transformer impedance. The latter renders one series impedance for which the $ABCD$ constants can be written without calculation. The network of Fig. 39 (d) is thus complete, and the next step is to simplify this network to that shown in Fig. 39 (e). This step combines the two shunt branches into the general circuit constants and can be performed by using Network Number 12 of the table of formulas for $ABCD$ constants given in Chap. 10. Before using Network Number 12, the two shunt branches must be converted to admittances by taking the reciprocal of the known

TABLE 4—CIRCUIT CONSTANTS FOR TWO-MACHINE SYSTEM

Constant	(1) One Line with Transformers	(2) Two Lines with Transformers	(3) One Line with Transformers and Load	(4) Two Lines with Transformers and Load	(5) Sending- End Gener- ators	(6) Receiving- End Gener- ators	(7) System Before The Fault	(8) System During The Fault	(9) System After The Fault
A	$1+j0$ ϵ^{j0}	$1+j0$ ϵ^{j0}	$2.34+j1.24$ $2.66\epsilon^{j27.7}$	$1.799+j0.774$ $1.955\epsilon^{j23.3}$	$1+j0$ ϵ^{j0}	$1+j0$ ϵ^{j0}	$2.13+j1.307$ $2.50\epsilon^{j31.5}$	$11.89+j6.06$ $13.34\epsilon^{j27.0}$	$2.67+j1.771$ $3.21\epsilon^{j33.5}$
B	$0.197+j0.708$ $0.735\epsilon^{j74.4}$	$0.109+j0.434$ $0.448\epsilon^{j75.9}$	$0.197+j0.708$ $0.735\epsilon^{j74.4}$	$0.109+j0.434$ $0.448\epsilon^{j75.9}$	$0+j0.254$ $0.254\epsilon^{j90}$	$0+j0.075$ $0.075\epsilon^{j90}$	$0.011+j0.847$ $0.847\epsilon^{j89.2}$	$0.0413+j3.78$ $3.79\epsilon^{j89.3}$	$0.064+j1.161$ $1.162\epsilon^{j86.8}$
C	0	0	$2.11-j1.31$ $2.48\epsilon^{-j31.8}$	$2.11-j1.31$ $2.48\epsilon^{-j31.8}$	0	0	$2.11-j1.31$ $2.48\epsilon^{-j31.8}$	$17.25-j30.2$ $34.7\epsilon^{-j60.2}$	$2.11-j1.31$ $2.48\epsilon^{-j31.8}$
D	$1+j0$ ϵ^{j0}	$1+j0$ ϵ^{j0}	$1+j0$ ϵ^{j0}	$1+j0$ ϵ^{j0}	$1+j0$ ϵ^{j0}	$1+j0$ ϵ^{j0}	$1.098+j0.1583$ $1.110\epsilon^{j8.2}$	$9.91+j0.331$ $9.91\epsilon^{j1.9}$	$1.098+j0.1583$ $1.110\epsilon^{j8.2}$

impedances. The fault and load branches expressed as admittances are, respectively:

$$Y_s = \frac{1}{0.00706+j0.0542} = 2.36-j18.14 \text{ per unit} \quad (57)$$

and

$$Y_R = \frac{1}{0.340+j0.211} = 2.11-j1.31 \text{ per unit.} \quad (58)$$

Now the network of Fig. 39 (e) is complete, and it remains only to combine the two series impedances with the central set of circuit constants, and Fig. 39 (f), the final reduction, is determined. This simplification is performed by using Network Number 16 from the table in Chap. 10 referred to above. The sample calculation of the B constant, for the network used before the fault, will illustrate the method. Col. (8) of Table 4 gives the final circuit constants for use during the fault. Using these circuit constants and the previously calculated internal voltages, which we assume to remain constant, all quantities are available for calculation of P_s' and P_R' , the sending- and receiving-end power during the fault. Substituting in Eqs. (53) and (54),

$$\begin{aligned} P_s' &= (1.21)^2 \frac{9.91}{3.79} \cos(89.3^\circ - 1.9^\circ) \\ &\quad - \frac{(1.21)(1.048)}{3.79} \cos(89.3^\circ + \theta) \\ &= 0.1753 - 0.335 \cos(89.3^\circ + \theta) \text{ per unit.} \end{aligned} \quad (59)$$

$$\begin{aligned} P_R' &= -(1.048)^2 \frac{13.34}{3.79} \cos(89.3^\circ - 27.0^\circ) \\ &\quad + \frac{(1.21)(1.048)}{3.79} \cos(89.3^\circ - \theta) \\ &= -1.797 + 0.335 \cos(89.3^\circ - \theta) \text{ per unit.} \end{aligned} \quad (60)$$

After the Fault—The network for use in calculating sending- and receiving-end power after the double line-to-ground fault has been isolated, is shown in Fig. 40. Except for the fact that one transmission line only is in service, the network is identical to that which applied before the fault occurred. Exactly the same procedure is followed in arriving at the final set of circuit constants, and these constants are listed in Col. (9) of Table 4. The power equations after the fault become;

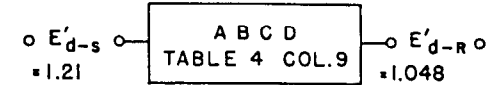
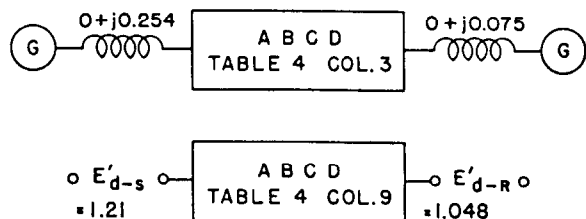


Fig. 40—Two-machine system. Network after the fault is isolated.

$$\begin{aligned} P_s'' &= (1.21)^2 \frac{1.110}{1.162} \cos(86.8^\circ - 8.2^\circ) \\ &\quad - \frac{(1.21)(1.048)}{1.162} \cos(86.8^\circ + \theta) \\ &= 0.276 - 1.09 \cos(86.8^\circ + \theta) \text{ per unit.} \end{aligned} \quad (61)$$

$$\begin{aligned} P_R'' &= -(1.048)^2 \frac{3.21}{1.162} \cos(86.8^\circ - 33.5^\circ) \\ &\quad + \frac{(1.21)(1.048)}{1.162} \cos(86.8^\circ - \theta) \\ &= -1.726 + 1.092 \cos(86.8^\circ - \theta) \text{ per unit.} \end{aligned} \quad (62)$$

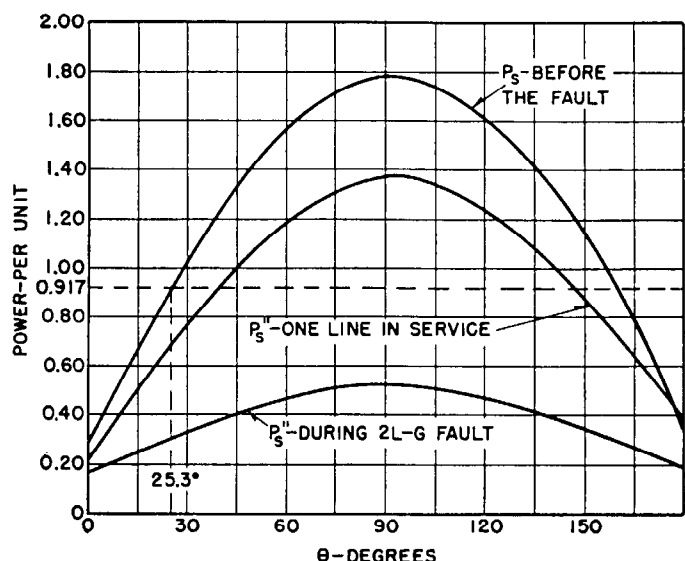


Fig. 41—Sending-end power-angle diagrams for two-machine problem.

TABLE 5—STEP-BY-STEP CALCULATION OF ANGLE-TIME CURVES FOR TWO-MACHINE SYSTEM

Fault Isolated in 0.15 Seconds

Power-Angle Diagrams—Eqs. (55), (59), and (61) are plotted in Fig. 41 as a function of θ , giving the sending-end power-angle diagrams for the conditions assumed. The receiving-end diagrams are plotted in a similar manner from Eqs. (56), (60), and (62). These are shown in Fig. 42. The solution of the receiving-end power equations to obtain Fig. 42 renders negative values, because positive direction of power flow was chosen as being into the receiving-end generators. In Fig. 42 the per-unit power scale is plotted as positive, because this is believed to be less confusing than negative values. This is permissible if the change in sign is recognized when performing the step-by-step solution for angle-time curves.

Note that in Fig. 41 the sending-end input is indicated by the horizontal line as 0.917 per-unit. This figure is the sum of the 0.833 per-unit power delivered to the load plus the line and transformer losses. Since line capacitance is neglected (Sec. 29) the total volt-ampere consumption in the system is,

$$\begin{aligned} I^2Z &= (0.877)^2(0.109 + j0.434) \\ &= 0.0838 + j0.334 \text{ per unit} \\ &= 5000 + j20\ 200 \text{ kva.} \end{aligned}$$

The in-phase portion, or loss, is 0.0838 per unit, so that the total sending-end power is $0.833 + 0.0838 = 0.917$ per unit. The receiving-end power-angle diagrams of Fig. 42 show the receiving-end input to be 1.083 per unit, which is the same figure as the power delivered to the load from the receiving bus, since there are no losses present in that end of the network.

The initial operating angle is $\theta = 25.3$ degrees as indicated in Figs. 41 and 42. This is the angular difference in

as a quick check on the calculation of the power-angle diagrams for the condition before the fault.

In the single-machine problem it was possible to estimate the maximum angle of fault clearing by simply balancing positive and negative areas on the power-angle diagram (See Sec. 26). This was possible because the movement of only one machine rotor had to be followed. In the present case, this equal-area method can not be applied because stability or instability is determined by the relative angular position of two machines. The maximum rotor-displacement angle before fault isolation is not determined from the power-angle diagrams, but will be found as a part of the calculation of angle-time curves.

Angle-Time or Swing Curves—The angle-time curves, which relate time to angular displacement, are most conveniently determined by the step-by-step integration method described in Sec. 23. The calculation is similar to that carried out for the single-machine system except that the angular swing of both sending and receiving machines must be traced during each time interval.

The best description of the actual procedure is had by referring to Table 5 in which the angle-time or swing curves are calculated. The form used is identical, for each machine, to that of Table 3, so that altogether it is similar to two single-machine system calculations. The calculations for one time interval must be made for both machines before proceeding to the next interval. This is true because the one quantity relating the angular position of the two machines, θ , is found by taking the difference in angle of the two machines at the end of each interval, and in order to find the electrical output for each machine in the succeeding interval, this value of θ is applied to each set of power-angle diagrams or calculated from the corresponding sending- and receiving-end power equations. To make this clear, refer to the first time interval in Table 5. The initial position of each rotor, with respect to the receiving-end low-tension bus voltage, is given in Cols. (2) and (12). The initial value of θ is the difference between the rotor angles, Col. (2) minus Col. (12), or 25.3 degrees as previously determined. Using this value of θ , the electrical output from each machine is determined, and the calculation proceeds to find the angle of each rotor at the end of the first interval. These figures are tabulated in Cols. (11) and (21), and subtracting (21) from (11) gives the new θ , Col. (23), to be used in the next time interval. This new θ is then used in the power-angle diagrams, or the corresponding sending- and receiving-end power equations, to obtain the electrical output from each machine in the second interval. The computation is now carried on to find θ at the end of the second interval, etc.

The first part of Table 5 assumes that the fault is not isolated, and illustrates by the continued increase of θ that the system becomes unstable under this condition. Time intervals of 0.05 second are used because of the relatively rapid swing of the sending-end machines. A comparison of Cols. (11) and (21) points out that the receiver machines swing much slower than the sending-end machines. This is caused by the relatively larger inertia constant and kva rating of the receiver generators, resulting in a much smaller acceleration [Col. (15) compared to (5)]. The second part of Table 5 assumes that the fault is isolated in

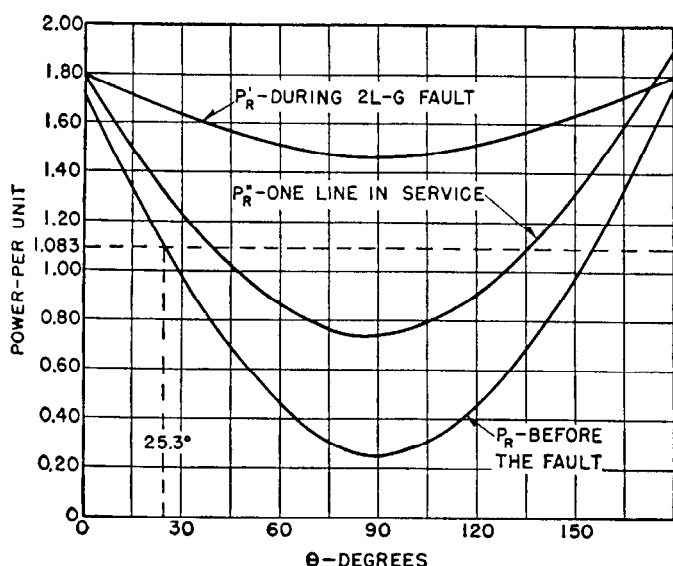


Fig. 42—Receiving-end power-angle diagrams for two-machine problem.

electrical degrees between the rotors, or internal voltages, of the sending- and receiving-end machines before the fault occurs. This figure of 25.3 degrees can be readily checked by taking the difference in angle of the internal voltages expressed in Eqs. (51) and (52). This serves

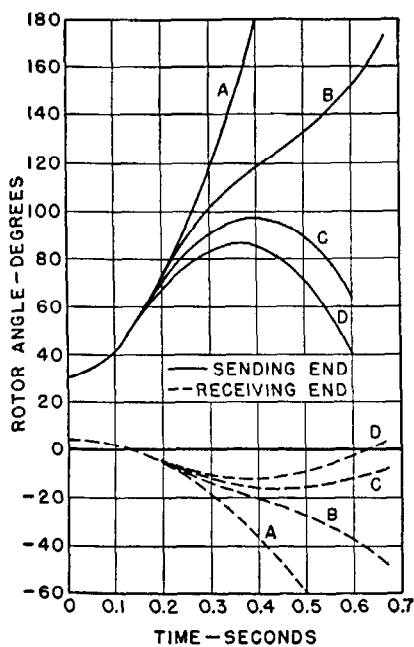


Fig. 43—Angle-time curves for each machine. Two-machine system.

- A—Fault not cleared.
- B—Fault isolated in 0.20 sec.
- C—Fault isolated in 0.17 sec.
- D—Fault isolated in 0.15 sec.

0.15 seconds. Col. (23) shows that θ reaches a maximum of 98.7 degrees and then starts to return toward a new stable operating point. Figures 41 and 42 indicate that the new operating point is at an angle $\theta = 39$ degrees.

The results of the calculations performed in Table 5 are given in Figs. 43 and 44. The swing of each rotor with respect to the fixed reference is shown in Fig. 43. Curves

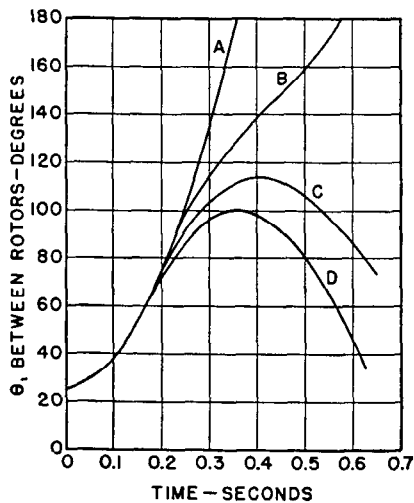


Fig. 44—Angle-time curves for two-machine system showing difference in rotor angle between sending and receiving machines.

- A—Fault not cleared.
- B—Fault isolated in 0.20 sec.
- C—Fault isolated in 0.17 sec.
- D—Fault isolated in 0.15 sec.

A and *D* of Fig. 43 represent a plot of the figures in Cols. (11) and (21) of Table 5. Curves *B* and *C* of Fig. 43 represent similar step-by-step calculations for longer times of fault isolation. By following the trend of the sending-and receiving-end angle-time curves for a given fault-clearing time, the loss or maintenance of stability can be seen. If the phase angle difference of the two machines continues to increase after fault isolation, instability results, but if the two machines tend to move back together during this time, the system is stable. It is possible for instability to occur on the second overswing, which is an exception to the above statement. This phenomenon is relatively rare but should be remembered in multi-machine problems, particularly where one or two machines are swinging very fast with respect to the other sources involved. Figure 43 indicates that for fault clearing times of 0.15 and 0.17 seconds stability is maintained, and for 0.20 seconds instability results.

In the two-machine system a more convenient way of plotting swing curves is that shown in Fig. 44, in which the difference in angular displacement, θ , is used rather than the individual position of each machine. Referring to Fig. 44, it is plain that the system is stable for fault isolation times of 0.15 and 0.17 seconds, and that stability is quickly lost if the fault duration is 0.20 seconds. Curves *A* and *D* of Fig. 44 are plotted from Col. (23) in Table 5.

VI. SHORT-CUT METHODS OF CALCULATION —TWO-MACHINE SYSTEM

Perhaps the most usual reason for making a stability calculation on this type of system is to determine how fast relays and circuit breakers must be made to operate if stability is to be maintained after a fault occurs. R. D. Evans and W. A. Lewis presented a group of curves,¹⁶ calculated for a two-machine system having the usual circuit elements, which permit the quick estimation of permissible fault durations for various types of faults.

31. Assumed System

For a complete and accurate calculation on a particular system it is necessary to consider all the various factors discussed in Part V. For determining approximate relay and circuit-breaker time, results of sufficient accuracy can be obtained, except under extreme or unusual conditions. The assumed system upon which the calculation of the general curves is based, is shown in Fig. 45, and the

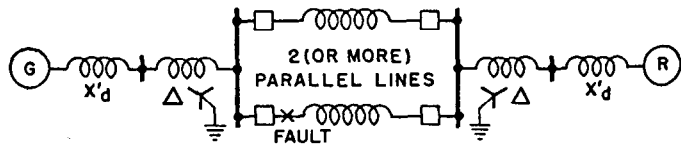


Fig. 45—System conditions assumed for study:

Symmetrical system, high tension bus at each end; line capacitance and I^2R losses neglected; transformer neutrals solidly grounded; quick response excitation (constant internal voltage); no damper windings; frequency = 60 cycles; load = 100 percent at instant of fault inception; faults located at most severe point on high-tension lines; average short-circuit losses.

simplifying assumptions made for the study are included at the bottom of the figure.

The results of the stability calculations are given in the four groups of curves, Figs. 46-49. These curves give directly the results for a system with the smallest inertia which may be expected, corresponding to water-wheel generators at both ends of the system. In the more usual case, the receiver machine will have a larger inertia constant, and correction terms to be applied to the results obtained from the curves, to adjust for this departure from assumed conditions, will be given.

32. Application of Data

The procedure for using the curves is as follows:

(1) First, it is necessary to determine the reactance between the internal voltages of the sending- and receiving-end machines. This reactance should be expressed in percent, based upon the total capacity of the generating units in operation at the time the fault occurs. If the exact

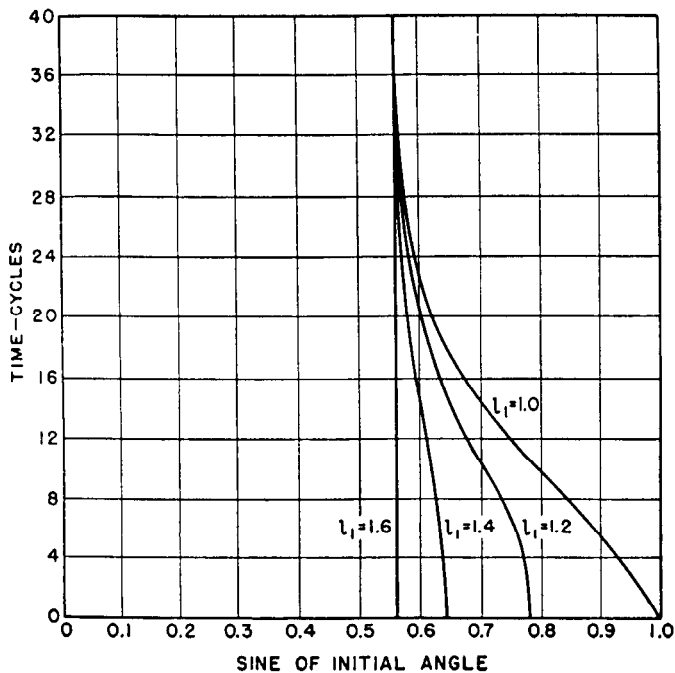


Fig. 46—Maximum permissible duration of fault to maintain stability:
SINGLE LINE-TO-GROUND FAULT

machine constants are not known, an average value can be assumed from the synchronous-machine constants given in Table 4 of Chap. 6. If other than full load is assumed, the reactance thus determined must be multiplied by the ratio of assumed load to full load.

(2) Using the value of reactance just determined, the initial angle can be found from Fig. 50.

(3) By reference to Fig. 45, the section of line that must be removed from service to clear the fault is known, so that the ratio l_1 of reactance after the fault is isolated to the initial reactance can be determined.

(4) Using the sine of the initial angle determined in (2) and the ratio l_1 determined in (3), the time in cycles should

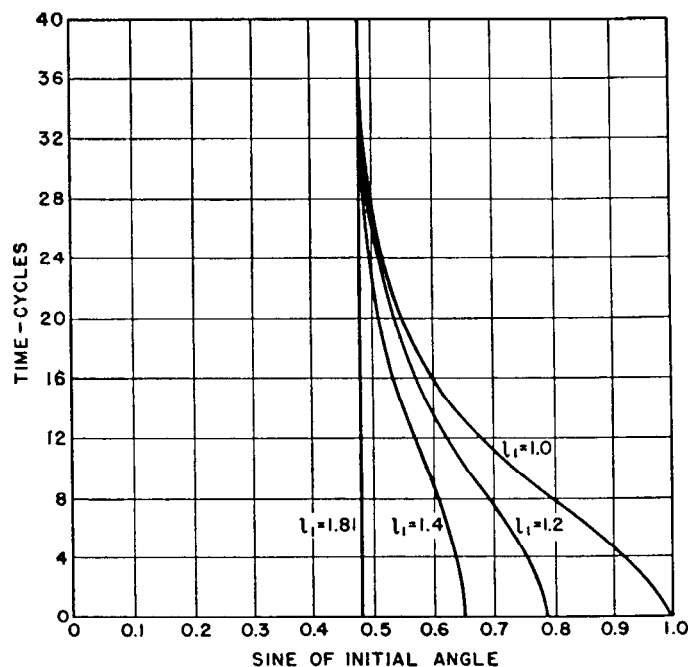


Fig. 47—Maximum permissible duration of fault to maintain stability:
LINE-TO-LINE FAULT

be read from the curve (Figs. 46-49) for the type of fault being studied.

(5) The inertia constants for the sending- and receiving-end machines should be determined. If the total mechanical inertia of the machines at one end is known, the inertia constant for that end of the system can be determined by using Eq. (37) appearing in Sec. 22. In case the inertia is not definitely known, an average value can be obtained by

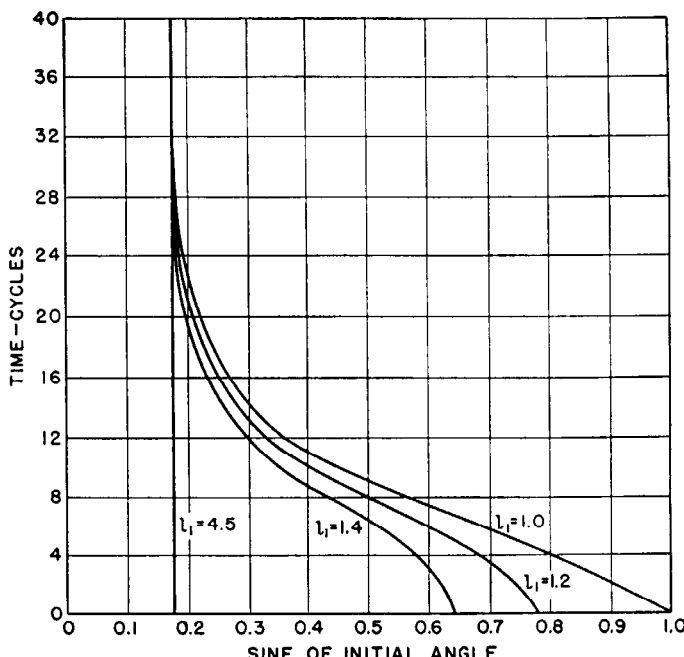


Fig. 48—Maximum permissible duration of fault to maintain stability:
DOUBLE LINE-TO-GROUND FAULT

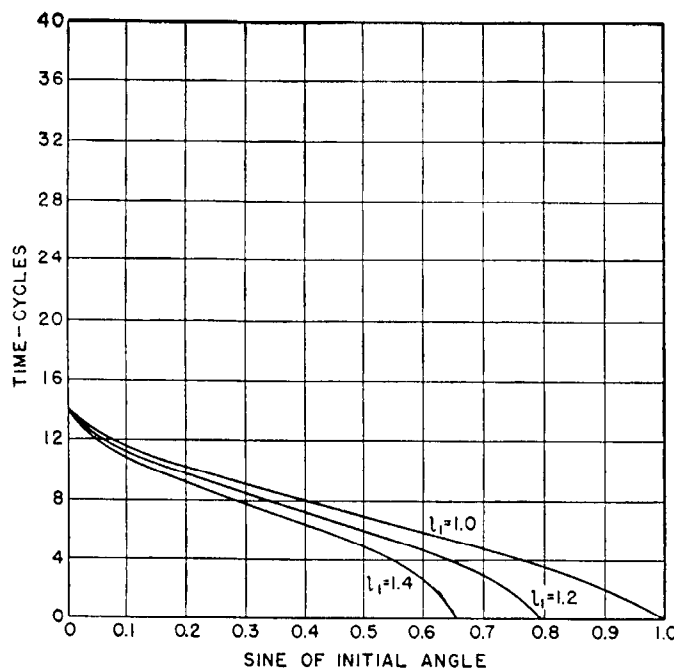


Fig. 49—Maximum permissible duration of fault to maintain stability:
THREE-PHASE FAULT

reference to Table 8. When the inertia constants, H , in kw-seconds per kva, for both ends of the system are known, the inertia correction factor by which the values of time should be multiplied can be found by reference to Table 6, or to the following equations from which Table 6 has been prepared.

$$H_{sr} = \frac{1}{\frac{1}{H_s} + \frac{1}{H_r}} = \frac{H_s H_r}{H_s + H_r} \quad (63)$$

$$k_1 = \text{Inertia correction factor} = \sqrt{\frac{H_{sr}}{1.5}}. \quad (64)$$

In these equations H_s and H_r are the inertia constants of the sending- and receiving-end machines, in kw-seconds per kva, respectively.

(6) If the frequency is other than 60 cycles, the result should be multiplied by the square root of the ratio of the new frequency to 60 cycles.

(7) If the load at the time the fault occurs is not equal to the kva rating of the generators, the result should be divided by the square root of the ratio of the actual kw load to the generator rating in kva.

Example: In order to illustrate the use of the short-cut method just described, the single-machine problem calculated in Part V of this chapter will be solved and the resulting maximum circuit-breaker clearing time will be compared to that obtained by the complete calculation. The assumed system is defined in Sec. 24, and the 50 000-kw load assumed there will still apply.

The total generator capacity is 60 000 kva and the transient reactance on this base, of the two machines in parallel, is 25.4 percent.

The assumed transformers each have eight percent reactance on a 60 000-kva base.

Each transmission line was calculated to have a positive-sequence reactance of 39.7 ohms, which can be converted to percent on this same base by conventional methods. Each line represents 54.7 percent on 60 000 kva, and the two lines in parallel equal 27.4 percent.

The receiver has no reactance since it was assumed to be an infinite inertia system of large capacity.

The total reactance between generator internal voltage and the infinite receiver is then:

Generators	25.4 percent
Transformer	8.0 percent
Two lines in parallel	27.4 percent
Transformer	8.0 percent
Total	68.8 percent on 60 000 kva.

The assumed load is 50 000 kw, so the ratio of actual load to generator rated kva is 50 000 divided by 60 000, or 0.833. Hence, at the present load, the reactance is,

$$68.8 \times 0.833 = 57.4 \text{ percent.}$$

From Fig. 50, the initial operating angle is approximately 32 degrees, the sine of which is 0.53. Note that

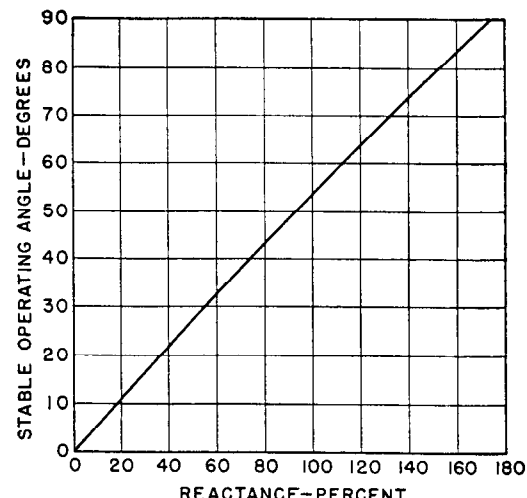


Fig. 50—Initial operating angle as a function of reactance.

the figure of 32 degrees checks closely the initial operating angle determined in the detailed calculation.

When one line is switched out to isolate the fault, which was assumed to be double line-to-ground, the reactance increases to,

$$(68.8 + 27.4) \times 0.833 = 80.1 \text{ percent.}$$

$$\text{Hence, } l_1 = \frac{80.1}{57.4} = 1.4$$

From Fig. 48, which applies for a double line-to-ground fault, corresponding to sine of initial angle = 0.53 and $l_1 = 1.4$, it is seen that $t = 5.8$ cycles, approximately.

From Table 6, corresponding to $H_s = 3$ and $H_r = \infty$, $k_1 = 1.41$.

Since the initial load is 0.833 times the generator kva rating, the corrected maximum time to fault isolation is,

$$t = 5.8 \times \frac{1.41}{\sqrt{0.833}} = 8.94 \text{ or approximately 9 cycles.}$$

TABLE 6—INERTIA CORRECTION FACTOR, k_1 .
(Computed from Eqs. (63) and (64))

H_s or H_r	H_s or H_r								
	2	3	4	8	10	11	12	50	∞
2	0.816	0.894	0.943	1.03	1.05	1.06	1.07	1.13	1.15
3	0.894	1.00	1.07	1.21	1.24	1.25	1.26	1.37	1.41
4	0.943	1.07	1.15	1.33	1.38	1.40	1.41	1.57	1.63
5	0.977	1.12	1.22	1.43	1.49	1.51	1.53	1.74	1.83
6	1.00	1.15	1.26	1.51	1.58	1.61	1.63	1.89	2.00
8	1.03	1.21	1.33	1.63	1.72	1.76	1.79	2.14	2.31
10	1.05	1.24	1.38	1.72	1.83	1.87	1.91	2.36	2.58
11	1.06	1.25	1.40	1.76	1.87	1.91	1.96	2.45	2.71
12	1.07	1.26	1.41	1.79	1.91	1.96	2.00	2.54	2.83
50	1.13	1.37	1.57	2.14	2.36	2.45	2.54	4.08	5.77
∞	1.15	1.41	1.63	2.31	2.58	2.71	2.83	5.77	∞

This figure matches the one obtained by detailed calculation to within the limits of accuracy of reading the curves, and shows that the quick-estimating curves when carefully applied give results that are dependable, as long as the actual system being considered is similar in circuit elements to the assumed system of Fig. 45.

Limitations in Using Curves—The greater the number of arbitrary assumptions and the larger the departures from the assumed conditions, the greater the resulting error. However, for systems of average characteristics the results are satisfactory. For example, if the actual system has no voltage regulators, the permissible fault duration is materially reduced. This is particularly true for cases where long fault duration is permitted. Also, if there is no high-tension bus in the actual case, more synchronizing power can be transmitted while the fault is on the system, but a greater increase in reactance occurs when the faulted line and transformers are removed as a unit from the system, so that the two effects are in the direction to compensate.

Where large steam generators are closely connected to the receiving end of the system, the effective initial angle is not determined solely by the transfer reactance from the sending-end generators, but is usually reduced considerably by the receiving-end generators. This can be taken into account approximately by reducing the reactance of the receiver machines. Where the power supplied by the receiving-end generators is greater than about three times that of the sending-end machines, it is safe to neglect the receiver reactance, and measure the total reactance to the receiver low-tension bus.

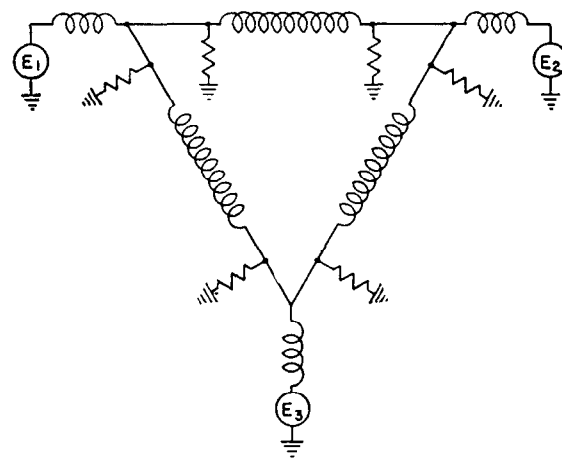
In the foregoing all breakers necessary to isolate the fault were assumed to open simultaneously. In practice, when the fault is near one breaker, a basis of discrimination for tripping the breaker does not exist until the first breaker has opened; hence the two breakers operate sequentially. In such cases the fault duration is increased to twice the time of a circuit-breaker opening. Where the distance from the fault location to each bus is short, this will require a breaker-opening time of half the permissible fault duration. If, however, the line reactance between busing points is high, the severity of the fault is greatly reduced and a longer total duration is permissible, up to probably 50 per-

cent longer than the figure obtained from the curves. The corresponding time for each breaker will thus increase to about two-thirds of the curve values. Consideration of the reactances involved will indicate a reasonable correction to be used in an individual case.

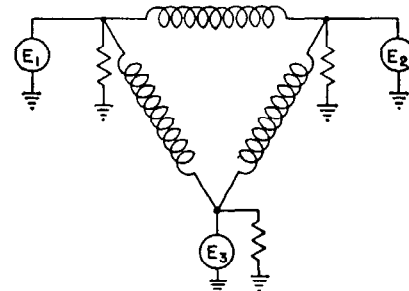
VII. METHODS OF STABILITY CALCULATION—MULTI-MACHINE SYSTEMS

33. Simplification of Networks with Multi-Machine Systems

The method of solving multi-machine stability problems follows closely the procedure just described for the general case for two-machine systems, and the same steady-state and step-by-step transient procedures should be used. The first step in the solution of multi-machine problems is to set up the equivalent network for lines, loads, and other shunt branches and for machines as previously described for the general two-machine system. Such networks involve a series impedance between each internal emf and the remainder of the system. Such a network does not lend itself to analytical calculations and should be replaced by mesh-connected systems with a single-impedance branch connecting each pair of internal emf's. For example, Fig. 51 shows a typical network for a three-machine system, characterized (1) by a hydroelectric source with voltage E_1 , and (2) by two receiver machines which have voltages E_2 and E_3 , which are connected together and to the hydro-electric machine by transmission lines represented by equivalent π method.



(a) TYPICAL NETWORK WITH THREE MACHINES



(b) EQUIVALENT MESH-CONNECTED NETWORK

Fig. 51—Method of reducing networks to the form convenient for stability studies.

Such a network should be transformed by the methods previously discussed in Chap. 2 to the form shown in Fig. 51 (b). This network involves only (1) shunt branches connected directly across the internal voltage ordinarily assumed constant and (2) mesh-connected branches connected directly between pairs of internal emf's. The power equations for such a system are readily written for each line in terms of the source emf's, in magnitude and phase position, and the series impedance of that line. Thus, it is readily possible to determine the electrical output or input for each machine if the phase position and magnitude of the various internal emf's are available.

Analytical methods of calculation can be applied to systems involving more than three machines by using the same procedure just described in connection with the three-machine system of converting the network to the simplest mesh-connected system. Such a procedure has been used for the solution of four-machine systems.¹⁰ However, the complication increases rapidly with the number of machines, and it is not practical to carry out calculations for systems with more than three or at the most more than four machines.

34. Steady-State Solution for Multi-Machine Systems

The determination of the steady-state stability limit for a multi-machine system is a problem of considerable

complexity.^{10,36} This results from the many conditions to be considered and the laboriousness of the calculations. Additional complication is introduced if, as is usually the case, automatic voltage regulators are used. Fortunately, however, the problem when considered from the practical viewpoint is greatly simplified because it becomes one of determining whether a particular system is stable for an assumed load below the actual stability limit. Under these conditions, many of the complicating factors are eliminated. It is often necessary to provide a considerable margin between the steady-state power limit with fixed excitation and the assumed operating conditions. A further factor is the action of automatic voltage regulators in increasing limits due to phenomenon of dynamic stability. For these reasons little effort is directed toward the determination of the actual stability limits of multi-machine systems. Instead, the problem takes the form of showing that the system is stable for a particular set of assumed conditions. Usually the important limit is the transient stability limit.

The practical method of solving stability problems of central-station systems is by means of the a-c network calculator.¹⁸ Analytical methods become exceedingly laborious for cases involving more than three or four machines. The average central-station utility problem usually involves more than this number of machines and solution is more easily done by a-c network calculator.

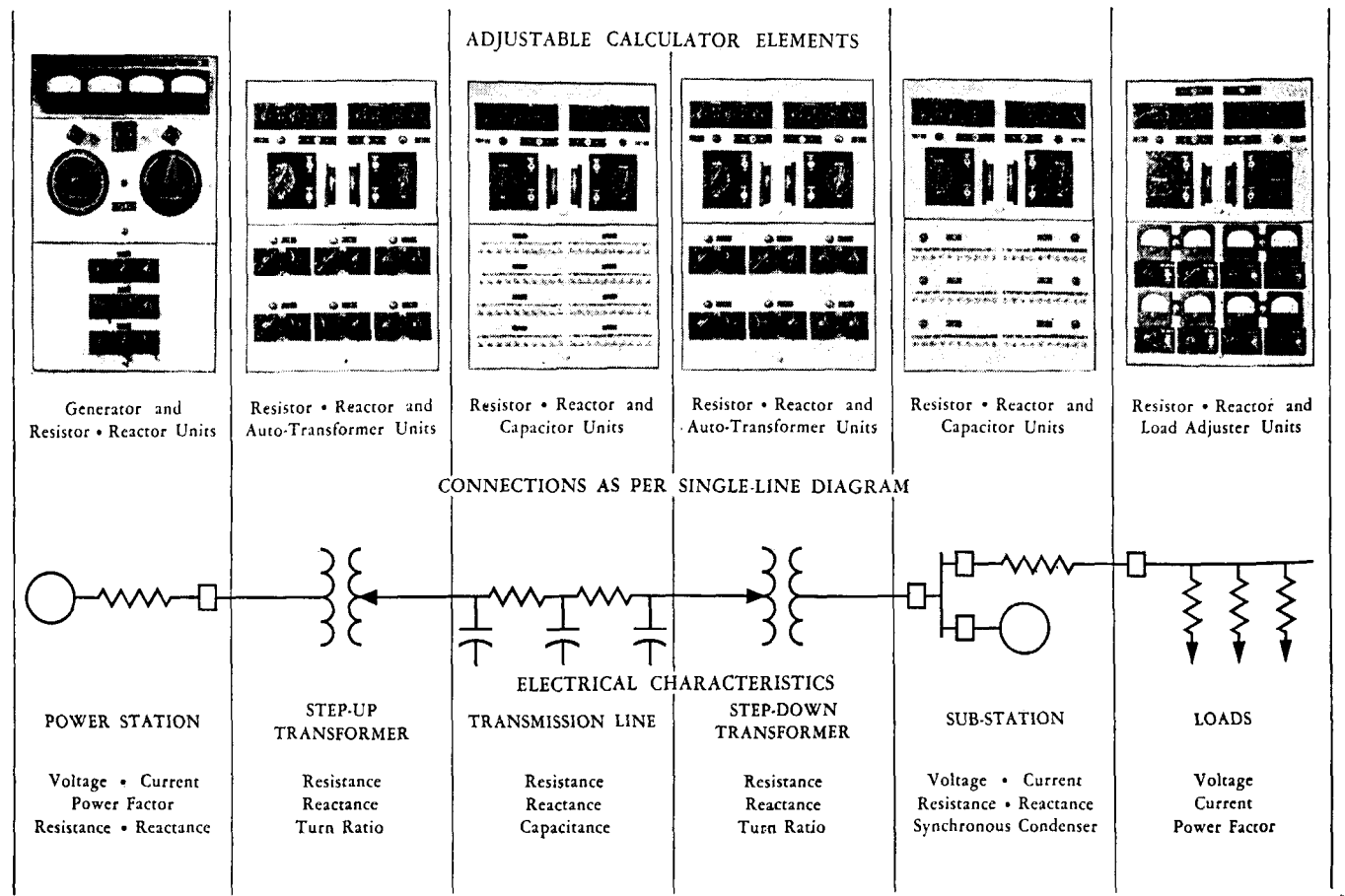


Fig. 52—Various system elements and the calculating-board elements used to represent them.

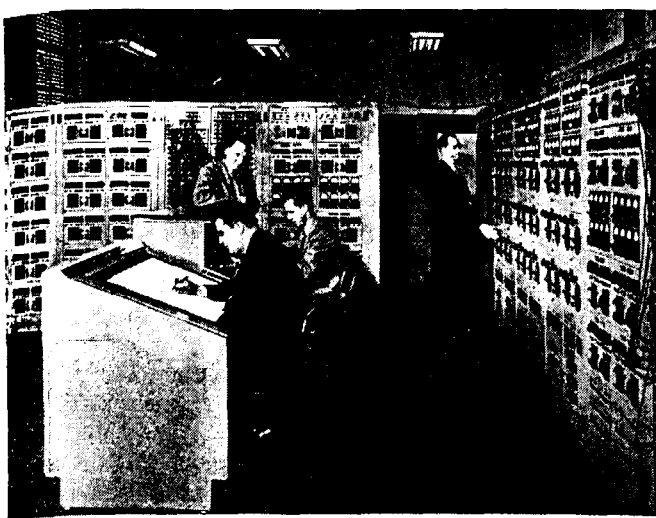


Fig. 53—The a-c network calculator at East Pittsburgh.

35. The A-C Network Calculator

The general design of the a-c network calculator is such that all of the essential elements of a modern power system can be reproduced in a miniature replica. The various parts are reproduced accurately in suitable proportion to the system values, and observations and measurements on the replica network correspond to what would obtain under like conditions on the power system. Suitable multipliers or conversion factors readily translate the calculator readings of voltage, current, watts, and vars

into the power system values. Various power-system elements and the corresponding calculator circuits are illustrated in Fig. 52, and a general view of the calculator is shown in Fig. 53.

The number and types of circuits provided in the Westinghouse a-c network calculator at East Pittsburgh are listed in Table 7.

The power supply for the calculator consists of a 440-cycle, 220-volt motor-generator set, which has its voltage controlled by an electronic voltage regulator and an electronic exciter to provide quick response and accurate regulation. The generator of this set supplies three-phase power to the calculator generator units, which are actually regulators especially designed to convert the three-phase power input to a single-phase power output having adjustable magnitude and phase angle.

Two independent sets of master instruments, circuit selector and metering controls are provided, each set being mounted on a separate metering and control desk. Direct readings of either scalar or vector values of currents and voltages, and magnitudes of watts, vars, and phase angles can be obtained. The two metering desks provide for conducting two simultaneous studies of separate systems with independent control of each system. Any calculator unit can be instantly connected to the metering equipment by a remote-control circuit selector which enables metering of system quantities at any point in the system.

The determination of the electrical conditions on the a-c network calculator gives practical solutions for the

TABLE 7—NETWORK CALCULATOR CIRCUIT ELEMENTS

Number of Circuits	Type of Circuit	Prefix	Used to Represent	Range of Adjustment	Steps
22	Generator units with voltmeter, ammeter, wattmeter, and varmeter	G	Generator, phase-shifting transformer, etc.	Voltage: 0- 400% Angle: 0- 360°	Smooth Smooth
18	Low-loss reactors	X	Generator reactance	React: 0- 499%	0.2
128	Line-impedance units	—	Lines, transformers, etc.	Resis: 0- 399% React: 0- 301%	0.2 Smooth
40	Transmission-line Pi units	—	Long, high-voltage transmission lines	Resis: 0- 399% React: 0- 301% Suscept: * 0- 41%	0.2 Smooth 0.1
48	Load-impedance units with load adjustors and voltmeters	L	Shunt loads	Resis: 0-3990% React: 0-2400% Load Adj: ±10%	2.0 Smooth 1%
48	Condenser units	C	Line-charging capacity, synchronous condensers, negative reactance	Mfd: 0- 4.1	0.1
36	Autotransformer units	T	Transformer taps, regulators	80% to 124.5%	½%
36	1 to 1 ratio transformers	M	Mutual induction, or used as 2 to 1 autotransformers for extended range studies	—	—
48	Metering jumper circuits	J	Zero-impedance metering jumper circuits	—	—

*Susceptance at each end of Pi unit.

many design and operating problems of electrical systems. The most common problems may be classified as:

- a. voltage-regulation studies for determining bus voltages, load-control studies and current-distribution studies, either as a system-design or an operating problem and for normal or emergency conditions,
- b. short-circuit studies for circuit-breaker and protective-relay application, and
- c. steady-state and transient-stability studies for determining the power limit of transmission systems.

36. Transient-Stability Solutions on the A-C Network Calculator

For stability purposes the problems need be considered merely as the solution of a set of simultaneous equations under successive steady-state conditions. The transient-stability solution, by the step-by-step procedure, is obtained by a succession of appropriately-adjusted steady-state conditions.

The system is reduced to a common base and is normally set up on the calculator on the basis of the positive-sequence network, using transient reactance in series with the generator voltage. Where large synchronous condensers are involved and the inertia of these condensers must be considered, they are represented by a voltage behind the condenser transient reactance.

The system is set up for the conditions prior to the disturbance, and the generator internal voltage, power, and angle are read at the point behind the generator reactance. The power so obtained is assumed to be the mechanical input to the generator and is maintained constant throughout the study, assuming that during the short time being considered, the governor cannot change. The internal voltage is also maintained constant throughout the study. The internal angle initially read is the normal angle, and the departure from this angle is calculated from the generator power output and machine dynamic characteristics.

The fault is then applied at the desired point in the system by connecting that point to the neutral bus in accordance with the type of fault as described in Sec. 10. The internal angles and voltages of the generators are adjusted to the values measured before the fault was applied, and the power distribution read. The difference between the power before the fault and the power after the fault is the accelerating or decelerating power available for changing the angular position of the machine rotor. From the relations between the machine inertia, the change in power, and the time interval, the change in angular position of each machine rotor is calculated, and the generator internal angles shifted to these new values. The procedure is repeated for the next time interval, and so on throughout successive intervals until the system is proven either stable or unstable for the conditions being studied.

The a-c network calculator provides a means not only for solving stability problems but also for obtaining the time variation of all the related electrical and mechanical quantities useful for circuit-breaker and relay application and for other similar purposes. The network calculator is also a device for simplifying networks and reducing them to a simpler form for more detailed study. By these meth-

ods, exceedingly complicated systems can be set up on the calculator and a practical solution obtained.

37. Two-Reaction Method Using A-C Network Calculator

The a-c network calculator also provides a means for carrying out in a practical manner calculations of complicated systems using the two-reaction method*. For this purpose each machine should be laid out so as to have two sources of voltage electrically at right angles to each other. The vector diagram for a salient-pole generator under transient conditions is shown in Fig. 25. One of these sources would represent the voltage E_d' , the magnitude and phase position of which are associated with the excitation and with the rotor position. At right angles to this vector is the voltage E_q' , which represents the reactance drop due to flux in the quadrature axis. The value of this voltage is assumed to vary instantly† so as to provide the proper quadrature-reactance drop. For each point in the stability analysis the voltage in the quadrature axis is adjusted until the vector diagram is satisfied for the particular terminal condition.

An alternative method requiring only one source of voltage for each machine is outlined in Chap. 6. This method uses the quadrature-axis reactance to relate rotor position, direct- and quadrature-axis voltages, and the terminal quantities. The method is, therefore, based on the adjustment of the network-calculator settings to allow for the variation in the direct- and quadrature-axis voltages whose transient values are separately calculated.

Both methods involve a cut-and-try proposition and are somewhat tedious. The principal merit of such a method is that it provides a basis for estimating the difference in results with the two-reaction method and the conventional round-rotor method which is generally found adequate.

VIII. SHORT-CUT METHODS OF CALCULATION—METROPOLITAN SYSTEM

The discussion in Part VI describes a useful short cut in calculating transient stability on transmission systems. Similarly, a general study has been made and general curves presented for the quick estimation of transient-stability limits on metropolitan-type systems.²³ In this discussion a metropolitan-type system is considered to be one in which the principal power sources are steam generating stations, located relatively close to their load centers, with distribution provided by a multiplicity of moderate-voltage circuits. The power supply to most metropolitan districts is of this character; there are, of course, notable exceptions.

Although most systems of this type are inherently stable as compared to systems coupled with long transmission lines, nevertheless transient stability analyses are frequently desirable. For example, other aspects of system

*This method was first used for analytical calculations by C. F. Wagner and R. D. Evans²⁴; it was adapted for use with the a-c network calculator by Dr. W. A. Lewis.

†The basis for the rapid variation of quadrature-axis flux was shown experimentally in Reference 5.

operation, such as placing of new generation, reduction of short-circuit kva, and flexibility of operation may suggest layouts differing from those at present in use, and it is desirable to be able to evaluate whether the desired changes will increase or decrease the transient limits, and whether the resulting value is satisfactory.

38. General Stability Curves

Metropolitan systems, as defined above, are similar in major characteristics making generalized studies practical. They are usually similar in the following features:

- With equal percent loadings the internal voltages of all generators are essentially in phase.

- With a multiplicity of circuits, the reactance of the connecting lines holding a generator or group of generators in step with the system does not change appreciably when a fault is cleared.

- With turbo-generators and short lines involved, the generator characteristics are no longer affected by the speed of prime mover, line charging-current requirements, etc., and they tend to become fairly uniform in their essential points, such as reactances, inertia, and short-circuit ratio.

These similarities make it possible to calculate transient stability solutions for a number of hypothetical systems and give the results in curve form, using the remaining variables as indices. The curves are then applied to specific layouts by determining these quantities for the specific case.

Space is not justified to include the derivation of the general curves, but the complete procedure is described in the paper in which these curves were originally presented, "Generalized Stability Solution for Metropolitan-Type Systems" by Griscom, Lewis, and Ellis.²³ In developing the curves some minor influences had to be eliminated from consideration with some sacrifice in accuracy of results. Such influences include resistance in the lines and the fault, variations in generator loading, and the effect of voltage regulators. The errors introduced by neglecting these influences, and possible means for compensating for them, will be discussed in a later section.

The general stability curves for metropolitan-type systems are shown in Fig. 54. These curves assume that the generators have a short-circuit ratio of 1.0. In the paper originally presenting these curves, a similar set was included using a generator short-circuit ratio of 0.8, but the resulting differences are so small that both groups of curves are not included here. Part (a) of Fig. 54 consists of a family of curves covering the range of overall reactance X , plotted in terms of short-circuit current, I_{FG} , from the faulted generator and the permissible fault duration, t . Part (b) is similar except that the power dropped by the faulted generator is used instead of I_{FG} . Part (c), as will be explained later, provides a means of correction for resistance in the fault, and for other than rated initial load. Part (a) applies directly to faults at the generator terminals. For faults occurring at other locations, a close approximation is secured by dividing I_{FG} by a factor read from Part (c) before entering Part (a). This location factor, designated as r_{FG} , is a function of the ratio of I_{FG} to I_F , the total fault current.

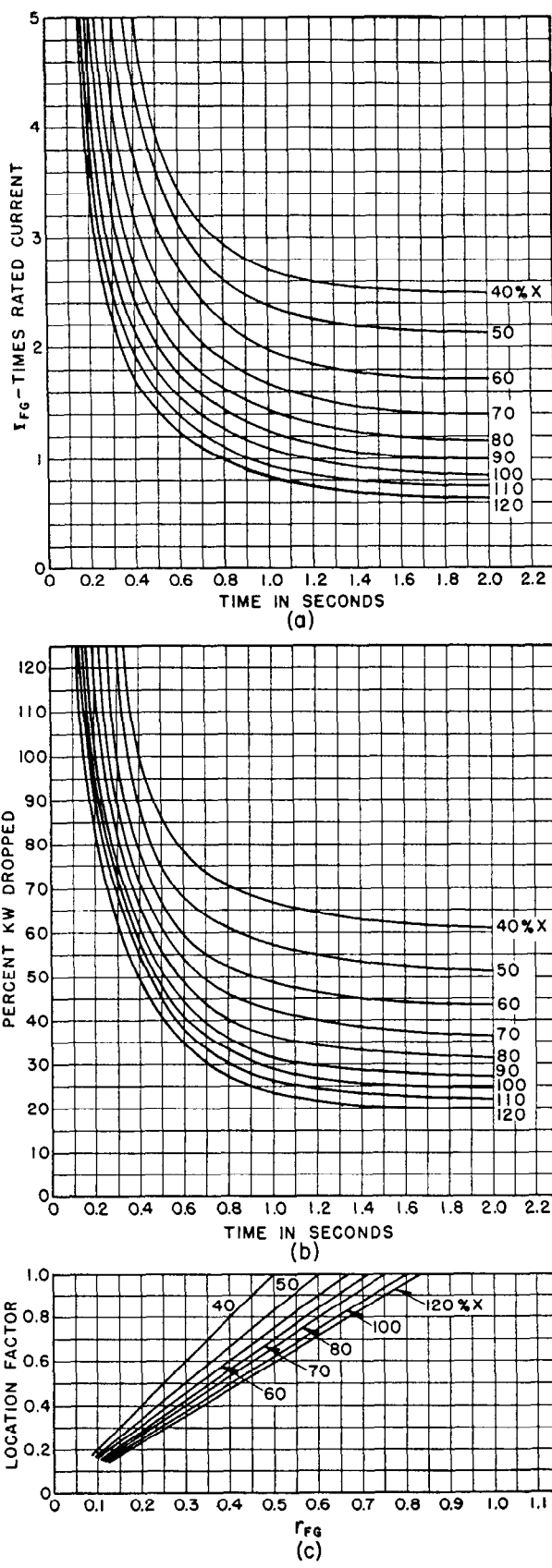


Fig. 54—General stability curves for metropolitan-type systems.

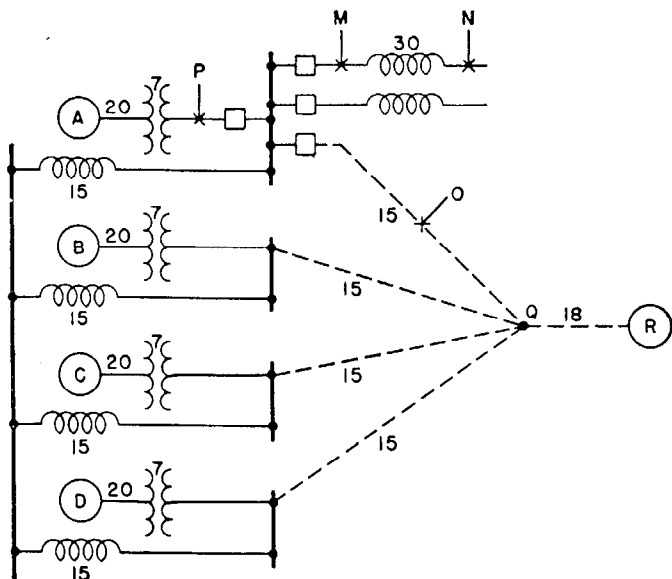


Fig. 55—Typical metropolitan-type system selected to demonstrate application of curves.

39. Application of Curves

An example is chosen to illustrate the application of this short-cut method for metropolitan systems. The typical system is shown schematically in Fig. 55, with reactances as indicated. A three-phase fault at point *M* will be considered. This fault isolates generator *A* from the remainder of the system during the fault, and this unit is then the one most likely to pull out of step first. Generator *A* therefore becomes the "faulted generator," and all other machines including those in the same group become the "remaining generators." With a fault at *M*, the network of Fig. 55 reduces to that of Fig. 56. The actual reduction can be accomplished analytically or, more easily, by using a d-c network calculator (since resistances are not included). If the network calculator is used, the actual reduction to the form shown in Fig. 56 need not be completed, as the

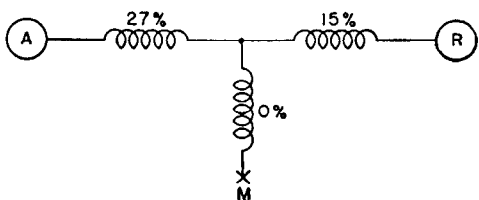


Fig. 56—Network of Fig. 55 reduced to equivalent for fault at *M*.

necessary indices can be obtained from the current readings taken to perform the reduction. From Fig. 56, the total reactance *X* between the faulted generator and the remaining generators is $27 + 15 = 42$ percent (always on the rated-kva base of the faulted generator). To determine the total fault current I_F , the branches on each side of the fault are paralleled:

$$\frac{(27 \times 15)}{42} = 9.65 \text{ percent},$$

and the total fault current is $1/0.0965 = 10.4$ times the

rating of generator *A*. The fault current supplied by the faulted generator is:

$$I_{FG} = \frac{15}{42} \times 10.4 = 3.7 \text{ times rated current.}$$

The ratio of I_{FG}/I_F gives $r_{FG} = 0.357$, so that now the indices necessary to use the curves of Fig. 54 are:

Overall reactance <i>X</i>	= 42 percent
Current from faulted generator	$= 3.7 \times \text{rating}$
Ratio $I_{FG}/I_F = r_{FG}$	= 0.357.

Using this value of r_{FG} and interpolating for a reactance of 42 percent, Fig. 54 (c) gives a location factor of 0.7. The adjusted value of I_{FG} is then 3.7 divided by 0.7 = 5.3, and the permissible fault duration can now be read from Fig. 54 (a) (by extrapolation) and is found to be 0.39 seconds.

If the fault occurs at point *N* of Fig. 55, outside of the feeder reactor, the circuit reduces to that shown in Fig. 57. The overall reactance does not change, but a high-reactance shunt branch is introduced to represent the reactor. It will be found for this case that r_{FG} remains the same because it depends only on the reactance branches adjacent to the generators. The total fault current is greatly reduced owing to the presence of the 30-percent reactance

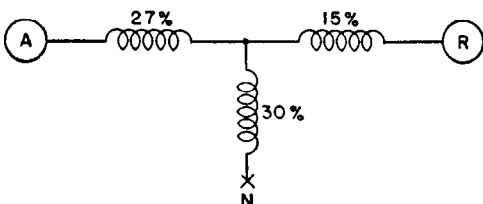


Fig. 57—Network of Fig. 55 reduced to equivalent for fault at *N*.

in series with the fault point, and becomes 2.52 times rated current of machine *A*. In this case I_{FG} calculates to be 0.9 times rated current, and when adjusted for location becomes $0.9/0.7 = 1.29$. When these indices are referred to Fig. 54 (a), it is evident that the point is beyond the range of the curves, and the permissible fault duration exceeds two seconds.

If the fault were at point *O* of Fig. 55, it would affect all four of the generators in station *A* more equally. Hence, there is a possibility that this entire group may lose synchronism with the remainder of the system. In this case, the group should be considered as the faulted generator, and all indices should be expressed in terms of the rating of the group as a base. This solution can be compared with that for generator *A* considered as the faulted unit, and the shorter of the two figures for permissible fault duration should be taken as the result.

Now, suppose that the three-phase fault occurs on the leads of generator *A*, as designated by *P* in Fig. 55. In this case generator *A* must be disconnected from the system to isolate the fault, and this must be accomplished before machines *B*, *C*, and *D* lose synchronism with the remainder of the system. Generator *A* is isolated from the system by the fault while the fault persists, and is isolated by the breaker when the fault is cleared, hence *B*, *C*, and *D* only are considered as the faulted generators, and generator *A* is eliminated from the calculation. By reduction of the

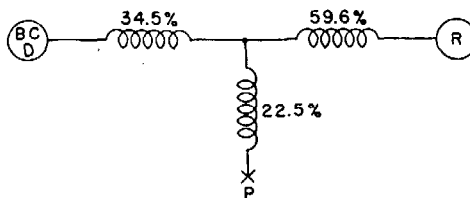


Fig. 58—Network of Fig. 55 reduced to equivalent for fault at P .

network of Fig. 55 for a fault at P , the simplified equivalent shown in Fig. 58 is obtained, the reactances now being expressed in percent on the combined kva rating of machines B , C , and D . From this point the calculations are identical to the previous examples, and the maximum fault duration is determined to be 0.53 seconds.

Unbalanced Faults—In the foregoing paragraphs three-phase faults have been assumed to demonstrate the application of the general curves. If unbalanced faults are to be considered, the method of symmetrical components can be used by adding a series impedance at the point of fault, which impedance is a function of the negative- and zero-sequence networks. This procedure is illustrated in Secs. 26 and 30 of this chapter and discussed in Sec. 10.

40. Correction Factors

As stated above, certain factors influencing stability were not considered in the preparation of the general curves. These simplifying assumptions all tend to make the permissible fault duration shorter, or to make the transient-stability solution more critical. The curves of Fig. 54 can thus be used directly for most work without applying correction factors since the error will consistently be on the safe side. It is appreciated, however, that the effect of some of these neglected considerations may be of interest in specific cases, so approximate corrections are presented, which while they are not rigorously correct, should be accurate enough for most practical work.

Effect of Resistance—The usual resistances present in power circuits have a minor effect on stability, except for the resistance in the fault circuit. Because of the very large currents in the fault circuit, a small resistance will result in a large power loss, which in a measure compensates for the drop in load on the faulted generator and lessens the tendency to pull out of step. Parts (a) and (b) of Fig. 54 are plotted for faults at the generator terminals. Applying the location factor from Fig. 54 (c) converts a fault at any other location to its equivalent fault at the generator terminals. For each point in Part (a) there is a corresponding point in Part (b), from which may be found the amount of power which would have to be dropped by the faulted generator for the equivalent fault at its terminals. If the amount of power dropped is reduced by resistance in the lines or fault, the effect would be substantially the same regardless of fault location. Hence the result may be found by reducing the equivalent amount of power dropped by the amount of resistance losses taken by the faulted generator, and reading the corrected fault duration from Fig. 54 (b). For example, with the fault at point M of Fig. 55, a clearing time of 0.39 seconds was indicated by Fig. 54 (a). The same clearing time must be indicated by Fig. 54 (b), hence, for $X = 42$ percent and $t = 0.39$, it is found that 100

percent power would have to be dropped by the machine if the fault were at its terminals. The curves show this power dropped as percent of the generator kilowatt rating, which is assumed 85 percent of the kva rating. If machine A and its transformer have a resistance of 1.5 percent, then with 3.7 times rated current flowing, the I^2R loss in the machine and transformer is $(3.7)^2 \times 1.5 = 20.5$ percent of the generator kva rating, or 20.5 divided by 0.85 = 24 percent of its kilowatt rating. So, instead of 100 percent load dropped, the equivalent load dropped is 100 minus 24, or 76 percent. The permissible fault duration, considering the effect of resistance, is then determined from Fig. 54 (b) for $X = 42$ and power = 76 to be 0.6 seconds.

If resistance in the fault itself is to be considered, the power loss in the fault must be divided between the faulted generator and the remaining generators. An approximate method of doing this is to multiply the total loss in the fault by r_{FG} , and add this figure to the loss in the generator branch of the circuit. For example, for the fault at M assume 0.25 percent resistance in addition to that of the generator and transformer. With 10.4 times normal current, $(10.4)^2 \times 0.25$ or 27 percent of generator kva is created in the fault. This is equal to 27 divided by 0.85 or 31.8 percent of generator kilowatt rating. Then multiplying by r_{FG} , $31.8 \times 0.357 = 11.3$ percent power in the fault taken by the faulted generator. As determined above, the power dropped is 100 percent when $X = 42$ percent and $t = 0.39$ seconds (from Fig. 54 (b)). When 24 percent resulting from generator and transformer resistance and 11.3 percent resulting from fault resistance are subtracted, 64.7 percent remains as the equivalent power dropped. From Fig. 54 (b) this amount of power dropped is seen to give a permissible fault duration of 2.0 seconds.

Initial Generator Load—The general curves assume that all generators are loaded to 100 percent of their kilowatt rating. For other than rated load, first find the percentage of kilowatts dropped, corresponding to X and t for rated initial load, then multiply this by the ratio of initial load to full load, and read the corrected permissible fault duration from Fig. 54 (b), for the curve corresponding to X . For example, with $X = 42$ percent, $t = 0.39$ seconds, 100 percent kilowatts is dropped, and if the initial load had been 75 percent instead of 100 percent, the fault duration can be read as $t = 0.61$ seconds for kilowatts dropped = $100 \times 0.75 = 75$ percent and $X = 42$ percent.

Voltage Regulators—Regulators with a moderate rate of response give a certain amount of improvement in stability over the amount shown by the curves of Fig. 54. The exact magnitude of this increase is difficult to determine, but a reasonable idea of the improvement can be easily obtained by multiplying the value of I_{FG} by 0.85 before entering the curves of Fig. 54 (a). This gives a relatively good estimate over most of the range of the curves.

IX. ESTIMATING PERMISSIBLE TRANSMISSION LINE LOADING

41. Surge-Impedance Loading

When a resistance equal to the surge impedance of a resistanceless transmission line is connected across the receiving end of the line, a surge introduced into the sending

end is absorbed completely without reflection. Thus a sinusoidal voltage introduced into the sending end travels along the line and is completely absorbed. The voltage at the receiving end varies sinusoidally with time, has the same magnitude as the voltage at the sending end, and is displaced by an angle equivalent to the time required for the wave to move from one end of the line to the other.

The load delivered over the line to the resistance is called "surge-impedance loading." Based on an average value of surge impedance of 400 ohms,

$$SIL = 2.5(\text{kv})^2 \quad (65)$$

where

SIL = surge-impedance loading in kw

kv = line-to-line kilovolts of transmission line

2.5 = a constant derived from the average surge impedance as shown in Chap. 9.

Thus, surge-impedance loading is a constant for lines of a particular operating voltage and can be used as a basis for comparison of lines operating at different voltages. The following analysis derives a simple method of determining the permissible loading of a straight-away transmission line based on a transient-stability criterion and expressed in terms of surge-impedance loading and the line length in miles.

42. Criterion of Stability

A rigorous determination of the power limit of a system is dependent upon many detailed considerations such as circuit-breaker clearing time, type and location of faults, type and speed of the excitation system, bussing arrangements, line-sectionalizing, station spacing, generator short-circuit ratio, generator inertia constant, etc. Even when extensive work is done along these lines, it is still necessary to apply judgment factors to calculated results. In estimating the permissible loading of long, high-voltage, straight-away transmission lines, a single overall criterion can be used rather than attempting a detailed design of the

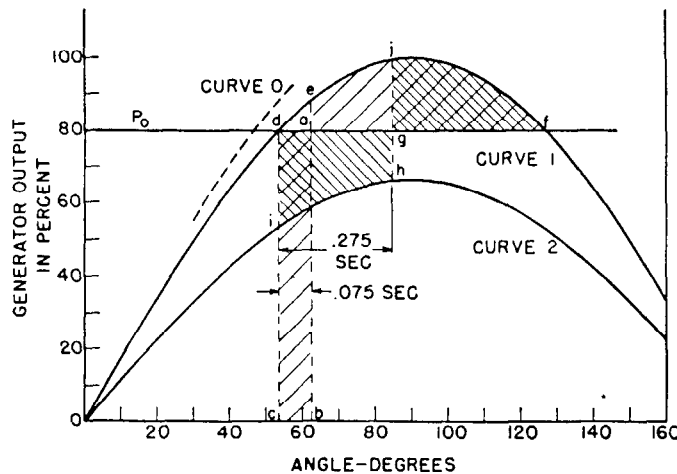


Fig. 59—Hypothetical power-angle diagrams showing switching times for maintaining stability with no margin during three-phase and single line-to-ground faults.

Curve 1—Power-angle diagram, faulty line switched.

Curve 2—Power-angle diagram, during single line-to-ground fault.

Curve 0—Power-angle diagram, system normal.

system. This criterion is that the operating load, after switching of the faulty line, be 80 percent of the crest of the transient power-angle relation.

A justification for this particular value of 80 percent is given in Fig. 59. Curve 1 is a hypothetical power-angle diagram, based on generator transient reactance, having a crest of 100 percent after switching of the faulty line section. The horizontal line P_0 represents the prime-mover input, presumed constant at 80 percent of the crest value and equal to the generator rating.

First, assume a three-phase short circuit at the generator high-voltage bus. The generator output will decrease from 80 percent to zero and remain there until the fault is relieved, after which it follows Curve 1. If the angle of swing is adjusted so that the area bounded by $abcd$ is equal to the area bounded by $aefgy$, the system will have transient stability for a three-phase fault on the high-tension bus, for the time required to increase the angle from c to b , with no margin. The time to increase the angle from c to b can be obtained if the inertia constants of the generators are known. If these are waterwheel generators, H may be about three. The acceleration for dropping full-power output is

$$\alpha = \frac{180f}{H} = \frac{(180)(60)}{3} = 3600 \text{ elec. deg./sec.}^2$$

The angle traversed in time t is

$$\theta = \frac{1}{2}\alpha t^2$$

The angular difference, $b - c$, in Fig. 59 is about 10 degrees, hence the required fault-clearing time

$$t = \sqrt{\frac{2\theta}{\alpha}} = \sqrt{\frac{(2)(10)}{3600}} = 0.075 \text{ second.}$$

Various details have been omitted for clarity in the foregoing. The power does not drop to zero because of machine losses. Curve 1 is not traced because of some decrement. Point d is not the correct starting point, but rather the intersection with P_0 of the unswitched transient power-angle diagram, Curve 0. Also, other values of inertia constant give different required fault-clearing times.

The approximate conclusions are that a three-phase fault on the generator high-voltage bus would result in instability for 8-cycle and 5-cycle circuit breakers. For 3-cycle circuit breakers, the clearing time under ideal conditions would be 0.067 second. However, a fault as severe as a three-phase fault is too rigorous a criterion.

A similar analysis is approximated for a single phase-to-ground fault on the generator high-voltage bus. On the basis of $x_0 = x_1 = x_2$, the power-angle diagram during the fault will have a crest value of about $2/3$ of Curve 1. This is shown as Curve 2. Equating area $dagh$ to area $gjif$ gives an angular change of about 32 degrees, and an approximate required clearing time of 0.275 second. This time can be obtained readily with 8-cycle breakers and carrier-current relaying and allows considerable margin.

From the preceding demonstration, it is considered quite logical to operate a system at a loading equal to 80 percent of the crest of the transient power-angle diagram. It is of interest to note that if the loading were to be increased to

85 percent of the maximum power, the area above the new P_0 line is markedly reduced; while dropping below 80 percent increases the area rapidly. While 80 percent may not be the best operating point, it is a very reasonable value.

In deriving the curves in Fig. 59, the generator power output was expressed by

$$P = 100 \sin \theta$$

where θ is the angle between sending and receiving voltages. For an actual system, the expression for generator power is

$$P = K_1 E_s^2 + K_2 E_r E_s \sin(\theta - \delta).$$

If P_0 , the maximum operating load, is taken as 80 percent of the crest of the transient power-angle diagram, the area $dejfga$ of Fig. 59, available to withstand transient disturbances is reasonably constant over a wide range of system layouts. Essentially, the above analysis was based on $K_1 E_s^2$ being small compared with $K_2 E_r E_s$. In terms of $ABCD$ constants, K_1 is the real component of D/B while K_2 is the scalar value of $1/B$. Unless the resistances of the circuits are quite high, or the lines quite long (beyond one-quarter wavelength or approximately 775 miles), $K_1 E_s^2$ remains small compared to $K_2 E_r E_s$, and close comparisons between systems can be made with the criterion.

The proposed criterion is based on holding the generating station in step with the receiving system during transient disturbances, and presumes that the receiving system inertia is infinite compared with the generating system. This is substantially true for most systems in operation today. In particular, in order for the criterion to apply at all, it is necessary that pull out, should it occur, be due primarily to overspeed of the generating station rather than underspeed of the receiving system.

43. Terminal Equipment Impedance

The transient reactance of the generators and the leakage reactance of the step-up and step-down transformers must be added to the line impedance to obtain the transient power-angle characteristic of the system. The reactance of the terminal equipment can vary through rather wide limits. The generator transient reactance may be as low as 15 percent for turbine generators and as high as 40 percent for slow-speed waterwheel generators. The majority of straight-away transmission systems are in conjunction with waterwheel generators, and generators of lower than normal reactance are used to be able to operate the lines at higher power levels. On this basis, 25 percent represents a fair approximation of the generator transient reactance.

A similar condition applies to the transformers in that the normal transformer reactance varies with voltage rating. At 138 kv, and to a lesser extent at 230 kv, the reactances of normally designed transformers are about ideal considering the opposing requirements to limit short-circuit currents and to obtain maximum stability. At higher voltages, however, it is advantageous to use transformers of reactance lower than normal. A fair average value of transformer leakage reactance is eight percent for transformers at both ends of the line.

The amount of reactance used to represent the receiving

system may vary considerably. For systems in which the transmission system supplies most of the energy used, the receiving-system impedance may represent a large percentage of the total. Where the transmission system merely augments the generating capacity already existing, and in particular where multiple terminals are used, each feeding into existing large systems, the receiver-system impedance may not be much greater than the reactance of the step-down transformer. In this analysis, the receiving-system impedance is taken as the receiver transformer reactance only for two reasons: first, it results in greater line loadings, reflecting possible future improvements in technique, and second, the stability criterion being used is probably on the conservative side.

44. Permissible-Loading Curve

With the foregoing values of reactances set, namely 25-percent generator transient reactance, and 8-percent transformer reactance, permissible line loadings as a function of distance may be obtained. The procedure is to assign a line loading, such that, when terminal equipment impedance is added, P_0 is 80 percent of the crest of the power-angle diagram. The line impedances depend upon the operating voltages, whereas the equipment impedances depend upon the kva ratings.

The first step is to obtain the power-circle diagrams of a transmission line of a given length and voltage including transformers of appropriate size. The expected loading is approximated or assumed, P_s and Q_s are available from the circle diagrams, and E_g , the internal voltage behind generator transient reactance, can be calculated. The generator reactance can then be added to the transformer and line constants, and the equations of the power-angle diagram determined, and hence the crest value of the generator output. If 80 percent of this crest does not equal the loading originally assumed, the work must be repeated, revising the generator and transformer kva ratings in accordance with the deviation noted.

When the analyses are carried through, a power-angle diagram will have been obtained for each line length studied and for each voltage rating studied, such that P_0 is 80 percent of the crest of the diagram. If the loadings of the lines are expressed in per unit of the "natural" or surge-impedance loading, there is little variation in characteristics of lines over a wide range of operating voltages. A curve of delivered power expressed in terms of per-unit surge-impedance loading and plotted as a function of transmission-line length in miles is shown in Fig. 60. The curve is closely applicable in determining transmission-line loadings based on transient stability for operating voltages between 69 and 500 kv.

As an example, the curve indicates that a 450-mile transmission line can deliver an amount of power equal to 0.69 times the surge-impedance loading. If the operating voltage were 345 kv, the line could deliver $(0.69)(2.5)(345)^2 = 205\,000$ kw. At 230 kv, the capability of the line would be 91 000 kw. In each case, the delivered power is the value of P_0 obtained in the analyses above less the line loss, and is the deliverable power for rating purposes.

Before it can be considered operable, a system must be stable under steady-state as well as transient conditions.

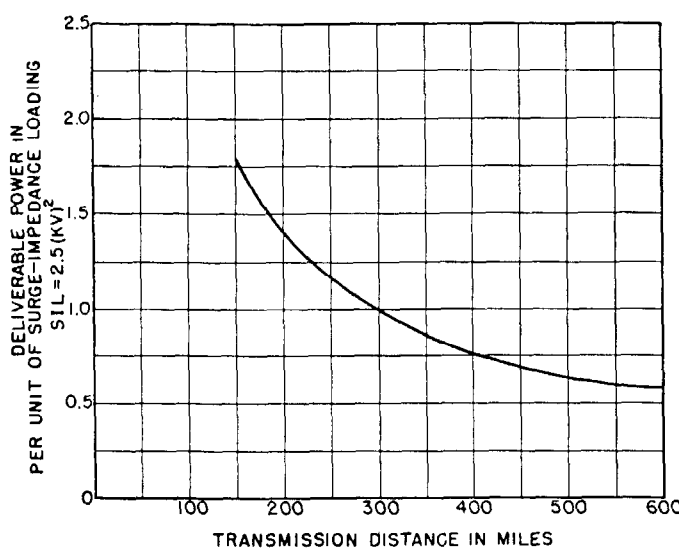


Fig. 60—Permissible loading of straight-away transmission lines as a function of line length in miles for voltages from 69 kv to 500 kv.

The curve of Fig. 60 is based on a criterion of transient stability, and it shows the permissible loading when the criterion is met. These results were examined for steady-state stability and found to be within steady-state limits with satisfactory margin. Therefore, the loadings for various line lengths may be considered acceptable under steady-state and transient criteria.

X. METHODS OF IMPROVING SYSTEM STABILITY†

The effect of various specific factors in the stability problem will be considered from the standpoint of improving system stability. For convenience these factors will be considered under the principal headings of "Power-System Layout," "Power-System Operation," and "Characteristics of Apparatus." These sections are followed by a discussion of "Other Methods of Increasing the Practical Operating Power Limits."

45. Power-System Layout

Power-system layouts should usually be analyzed from the stability point of view for the three circuit conditions associated with the transient, viz., before, during, and after the transient. Some features of layout are beneficial to stability for all three circuit conditions while other features are beneficial for one condition and detrimental for another; hence, the many features of power-system layout must be weighed individually in connection with each circuit condition.

Series Reactance—The most obvious method of increasing the stability limit of a system is to reduce the

†Part X is based largely upon the "First Report of Power System Stability," A.I.E.E. Subcommittee on Interconnection and Stability Factors, R. D. Evans, Chairman, *A.I.E.E. Transactions*, pp. 261-282, Feb. 1937. It includes some changes and additions due to progress in the art. For the practices summarized in this report see App., Table 3.

transfer reactance or "through reactance" between synchronous machines, as this directly increases the synchronizing power that can be interchanged between them. The reactance of a transmission line can be decreased by reducing the conductor spacing. Usually, however, the spacing is controlled by other features, such as lightning protection, and minimum clearance to prevent an arc from one phase involving another phase. Another method of reducing line reactance is to increase the conductor diameter by using material of low conductivity or by hollow cores. Usually, however, the characteristics of the conductors are fixed by economic conditions quite apart from stability. The use of bundle conductors (Chap. 3, Sec. 10) is an effective means of reducing series reactance.

The transformer reactance should be kept as low as practical. While some reduction from normal reactance, as shown in Chap. 5, is permissible, economic considerations usually prevent much departure from the lowest value obtainable without increasing the cost.

The series capacitor provides another means for decreasing the "series" reactance of transmission systems. However, at times of system faults the current through the capacitor raises the voltage across it to several times normal. To protect against such overvoltages, two procedures are available: (1) relatively expensive capacitors capable of withstanding the abnormal voltage can be used, (2) the capacitors can be designed for the maximum voltages produced under normal circuit conditions and provided with a device for short-circuiting it during the excess-current condition. When series capacitors are used with short-circuiting means, they are ineffective during the fault condition. However, when high-speed circuit breakers are used, the fault condition is promptly relieved and the advantage of low series reactance is obtained for the subsequent part of the oscillation. The application of series capacitors is discussed in Chap. 8.

Transmission-circuit reactance drops are commonly reduced by adding parallel lines or increasing the circuit voltage. Comparisons at times are made between several low-voltage circuits and a few high-voltage circuits. Obviously, the fewer the number of circuits the greater is the reduction in the power limit of the layout when one circuit is switched out.

Bussing Arrangements—The method of paralleling lines or apparatus, or the bussing arrangements, can have an important bearing on system stability. High-voltage busses at the ends of transmission lines or at intermediate points result in smaller change in the transfer reactance at the time of the isolation of a faulted transmission-line section than for the case with low-voltage busses, since the latter involves the loss not only of the line but also of the associated transformers. During the faulted condition the shock to the system is greater with the high-voltage bus than with the low-voltage bus. It is impossible to generalize on the relative merits of high- and low-voltage bus arrangements because the result in any particular case is dependent upon the relative reactance proportions of the system, the type and duration of the fault, and the character of system grounding. The results of calculations on a particular system with alternative bus arrangements

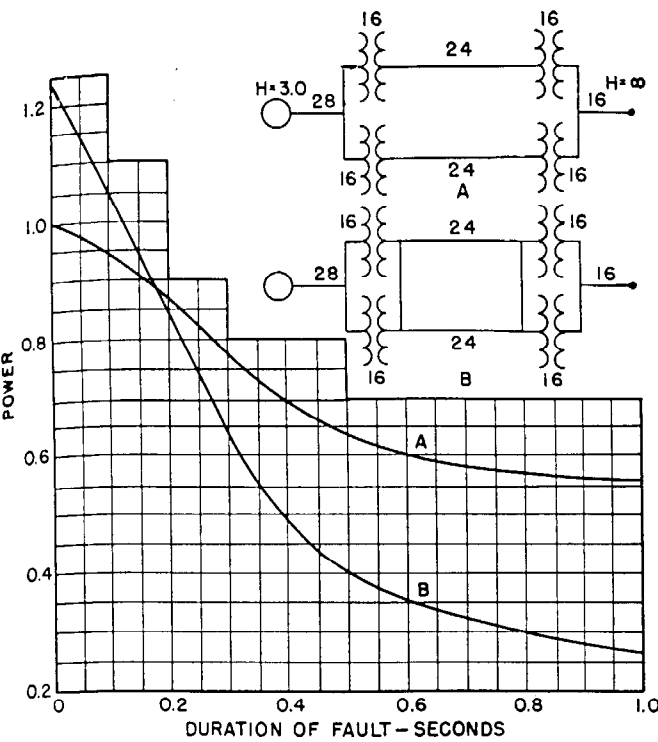


Fig. 61—Effect of bussing arrangement on stability limits; double line-to-ground fault at sending end.

A—Low voltage bussing.

B—High voltage bussing.

System reactance shown in percent; inertia constant H = kilowatt-seconds/kilovolt-ampere.

are illustrated in Fig. 61. For faults of short duration the change in the transfer reactance of the system after the fault is cleared is more important than the shock to the system during the fault, and, therefore, the high-voltage bus arrangement gives higher stability limits; for faults

of longer duration, the shock to the system is more important and the converse is true regarding layout. By using reactors between the high-voltage busses, it is possible to obtain characteristics intermediate between those for high- and low-voltage bussing, approaching either to any degree desired. The results of the study in a particular case of the effect of varying the number of intermediate switching stations on a long transmission line is shown in Fig. 62.

Another method of bussing is incorporated in the scheme known as "synchronizing at the load"¹¹ as applied to metropolitan-type power systems. By metropolitan system is meant the type of system that exists in large cities and is characterized by large turbine-generating units located close together with short transmission distances. With this scheme there are no direct ties between synchronous-machine busses but only indirect ties through a multiplicity of connections at secondary or utilization voltages. With this layout secondary faults do not have a severe effect upon the system and can be "burned clear." Faults on a particular generator bus require disconnection of that unit, but the remaining units accelerate or decelerate together. Of course, the shock to the connected load is decreased as the speed of circuit breakers and relays is increased.

While "synchronizing at the load" was developed for supplying power to metropolitan areas, the underlying general principle has been applied in connection with certain long-distance transmission projects, notably for the Conowingo-Philadelphia²⁴ and Hoover-Chino lines. The modification of the scheme for this application is characterized by the bussing of the system only on the lower-voltage side at the receiving end. On such a system transmission-line faults result in disconnection of an entire unit consisting of a generator, sending transformer, transmission line and receiving transformers. Since the plan of operation contemplates the disconnection of a unit for every fault on the transmission line or its associated apparatus, each circuit can be operated relatively close to its steady-state power limit. Faults on the lower-voltage bus at the receiving end or on the connecting lines will probably be controlling in determining the transient power limits. These connections are similar to those employed on early systems where transmission lines from separate hydroelectric plants were paralleled only at the receiver.

The same general principles of system connection have also been employed in circuits with two-winding generators and four-winding transformers.^{13,17} These schemes improve stability by limiting the severity of short circuit and by distributing the stress among the remaining units. An important advantage of the double-winding generator arises from the fact that in the event of a fault on one winding the remaining winding can carry load and thus minimize the disturbance to the system that would result from the disconnection of the faulted machine and the readjustment of load on the remaining units.

Another method of bussing is the "loose-linked" system,¹⁴ which consists of several power areas normally operated in parallel, being loosely connected for purposes of synchronizing and interchange of power. The plan of

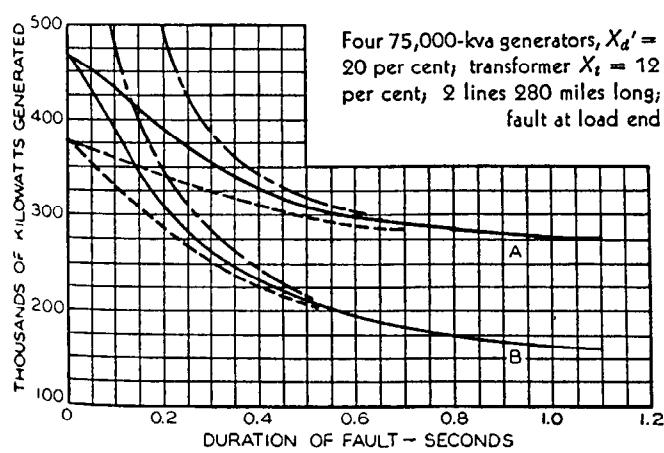


Fig. 62—Effect of number of switching stations on stability limit.

A—Single line-to-ground fault.

B—Double line-to-ground fault.

—One intermediate station.

—Two intermediate stations.

- - - Bus fault cleared with no loss of line.

operation is such that in any power area the largest generator or the interlinking ties can be lost without leaving in any area a load greater than the ability to carry it. In the event of a serious disturbance within a power area, that area including its load and sources of power is isolated from other power areas by opening of the ties at appropriate points.

Grounding—In America it is common practice on high-voltage systems to ground the neutral solidly and on moderate-voltage systems to ground the neutral solidly or through a resistance. For some types of high-voltage systems there has been recently an increased tendency to provide transformers with sufficient insulation in the neutral to permit grounding through a moderate impedance. The ground-fault neutralizer scheme in which the system is grounded through reactors tuned with the system capacitance to ground at fundamental frequency, has not been generally accepted, although it is being used successfully in an increasing number of locations. These schemes also have arc-suppression characteristics as discussed in Sec. 49. The introduction of neutral impedances, by limiting the severity of the fault, increases the stability limits. Two effects may be present: if the impedance is a pure reactance, the current is limited and the synchronizing power is increased thereby; if the impedance is a resistance, power is absorbed in it

and the generator output increases and its acceleration is correspondingly retarded. The effects of these factors are illustrated in Fig. 63, which shows the stability limit as a function of the duration of the fault and the connection of the neutral impedance for single and double line-to-ground faults on the high-voltage line at both the sending and receiving ends of a typical system. These curves show that neutral impedances, preferably resistance at the sending end and reactance at the receiving end,* help maintain stability. The importance of the method of grounding in relation to power-system stability has been minimized by the development of high-speed breakers and relays and the trend in the direction of basing system design upon the more severe types of faults. In general, however, factors such as lightning protection and relaying, and cost affected by insulation and interconnection with other systems, rather than stability, determine particular methods of grounding to be employed. For further discussion, refer to Chap. 19.

46. Power-System Operation

Power-system operation is often as great a factor to insure system stability as proper system design. The allocation of generator capacity in relation to the system-load and circuit conditions is of considerable importance, particularly under abnormal circuit conditions. The stability problem can be accentuated by interconnection and is complicated by the related problems that arise when frequency control is applied or when the location of generating capacity is determined by maximum-economy considerations rather than system-load requirements.

Most power systems are designed for adequate stability under steady-state conditions. There are, however, many systems where a stability problem is encountered as a result of a fault, and for economic reasons it is not always possible to eliminate this condition. Observance of certain basic operating principles will prevent exceeding the steady-state limits and insure prompt recovery following a fault.

Adequate spinning-reserve capacity either in the form of spare generators or reliable interconnections, must be available in each load area to insure a steady-state limit in excess of the power and reactive kva requirements in event of loss of a generating unit or loss of excitation.

The method of supplying excitation to a system has an important effect on stability. The choice of the bus voltages to be maintained or compensated for load and circuit changes, can be of great importance. Voltage regulators tend to improve stability conditions by automatically changing the excitation in accordance with loads. They are capable of sustaining system voltages within safe limits even in the event of the loss of excitation on one of the units. They also tend to keep the field strength of individual units within reasonable limits thereby preventing the cascading of trouble following the initial disturbance. Other characteristics of excitation systems and their control in relation to stability are discussed in Sec. 47.

The increasing use of automatic devices, such as refrigerators, water heaters, water pumps, etc., which are

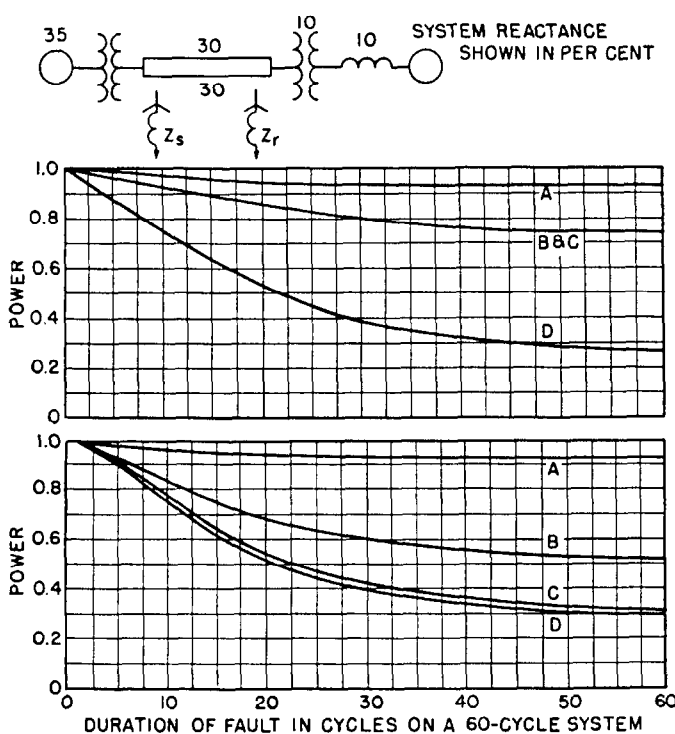


Fig. 63—Effect of grounding method upon system stability.

Curve	Z _s , Percent	Z _r , Percent
A—Single line-to-ground.....	13	+j10
B—Double line-to-ground.....	13	+j10
C—Double line-to-ground.....	13	0
D—Double line-to-ground.....	0	0

Upper set of curves for fault on high-voltage bus at sending end.
Lower set of curves for fault on high-voltage bus at receiving end.

*This particular arrangement is used on the 15-Mile Falls Development.^{20,21}

not locked out following an outage, results in extremely high power demands when service is restored. A recent outage resulted in a peak following restoration of service which was approximately 45 percent more than the load interrupted. Provision must be made for excess generator capacity for a short period when service is resumed, or the service must be restored slowly to limit the temporary load until its diversity becomes normal. The spinning-reserve capacity for best results should be distributed in the several load areas so that its availability is not restricted by tie-line limitations.

The use of automatic load control on interconnecting tie lines has increased the practical load limits of these lines by preventing the usual drift in the tie-line load, thereby holding the scheduled load well below the tie-line limits. These devices are of no value for transient conditions.

Coordination of stability studies and operating instructions for abnormal conditions is a matter of considerable importance for insuring the maintenance of stability or avoidance of service interruption.

When synchronism is lost on a system having synchronous condensers, a state of equilibrium is sometimes reached under which the system will neither accelerate nor retard until conditions are changed by switching operations, or by removal of synchronous condensers. The removal of synchronous condensers, either manually or by underspeed relays, relieves the system of superposed low-frequency currents caused by condenser excitation, and permits a more rapid restoration of service.

47. Characteristics of Apparatus

Synchronous Machines—The characteristics of synchronous machines that are important from the stand-point of stability are substantially the same in the synchronous generator, motor, or condenser. In general, the characteristics of generators are of much more importance because they constitute the largest percentage of the total connected synchronous capacity and because they have such an important bearing on the overall system angles. The following discussion will be given in terms of synchronous generators with the understanding that for synchronous condensers and motors the general features are the same but generally of relatively less importance.

The best criterion of generator performance under conditions in which system stability is determined chiefly by the transient characteristics is its transient reactance or more definitely, the direct-axis component commonly designated as x_d' , as discussed in Secs. 15 and 16. The effects of decreasing the transient reactance of generators upon increasing the stability limits for a particular study are shown in the curve of Fig. 64. The normal value of the constants of various types of synchronous machines are shown in Table 4 of Chap. 6. The effect of decreasing the transient reactance upon the cost of a machine is indicated in a general way by the curves of Fig. 65. In a considerable number of installations, beginning with Conowingo³⁴ and including Hoover Dam,³¹ it has been found desirable to employ generators of less than normal transient reactance.

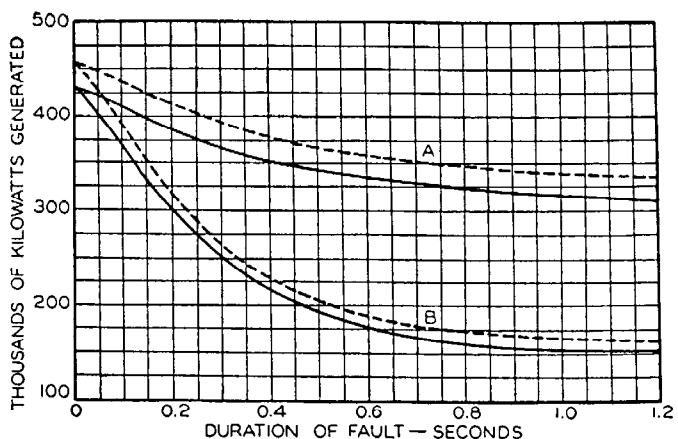


Fig. 64—Effect of generator reactance upon stability.

A—Single line-to-ground fault.

B—Double line-to-ground fault.

Solid curves for generator transient reactance $x_d' = 30$ percent; broken curves for $x_d' = 21$ percent.

Fault at load end; 2 lines, 280 miles, 3 sections; transformer $x_t = 10$ percent; 4-70 000-kva generators.

For most present-day systems, steady-state stability limits are unimportant. With increased application of faster breakers and relays and the logical attempt to increase the load carried on these circuits, the steady-state stability limitations will become increasingly important. A useful criterion of machine performance with reference to steady-state stability is the machine short-circuit ratio. The short-circuit ratio is a direct measure of the relative pull-out torques for generators with the same per-unit excitation. However, for the same current and power factor on machines of different short-circuit ratios, the relative short-circuit ratios do not give a direct measure of the relative pull-out torques, because the excitations are not equal. In general, the higher the short-circuit ratio, the higher is the pull-out torque. It is the one constant of the generator that comes closest to being a direct index of pull-out torque.

Short-circuit ratio is also of value as an approximate measure of the size of machine. Its use for this purpose depends upon the fact that to a considerable extent any reduction of reactance in a machine below its normal value is obtained by derating a larger machine and modi-

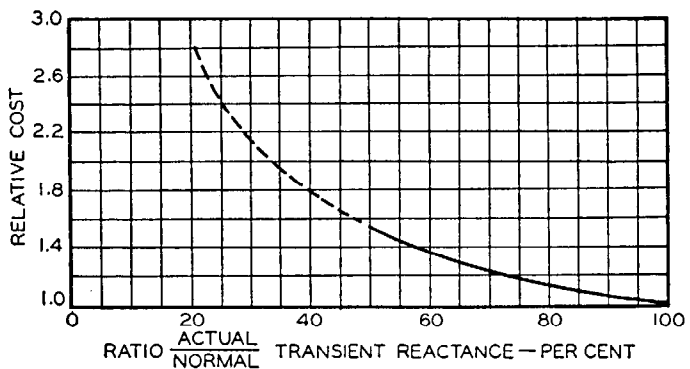


Fig. 65—Approximate cost of decreasing the transient reactance of salient-pole synchronous generators.

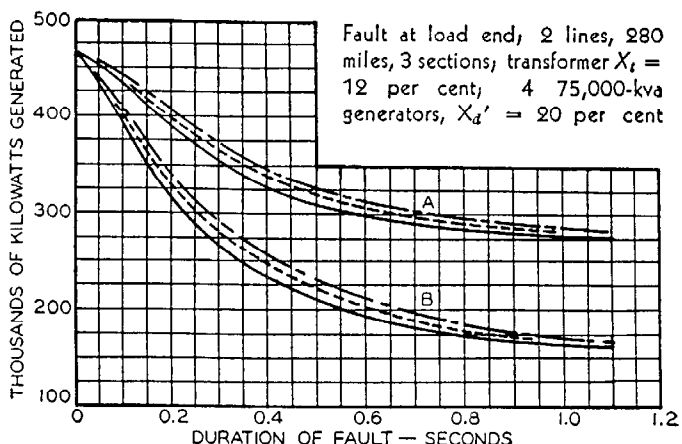


Fig. 66—Effect of generator inertia upon system stability.

A—Single line-to-ground fault.
 B—Double line-to-ground fault.
 — Minimum WR^2 (31×10^6 lbs·ft 2).
 - - - 50 percent additional WR^2 .
 - - - 100 percent additional WR^2 .

fying the current-carrying parts to meet the reduced values.

The inertia of a synchronous generator or motor is also a factor in the stability problem since it affects the natural period of system oscillation, or the time required to reach a point beyond which recovery would be impossible. Figure 66 shows the results of calculations for various values of generator inertia upon the stability limits for a particular system. The range of inertia constants for various types of synchronous machines is shown in Table 8, and more specific data based on speed and kva are given in Chap. 6, Part XIII. The cost of adding inertia to large vertical waterwheel generators increases about one-fifth as fast as the inertia. In a few cases, including Hoover Dam, where calculations have indicated that a particular system would operate relatively close to the stability limits, generators of higher than normal inertia have been installed.

TABLE 8—TYPICAL INERTIA CONSTANTS OF SYNCHRONOUS MACHINES*

Type of Machine	Inertia Constant H Stored Energy in Kw-sec per Kva**	
Turbine Generator		
Condensing	1800 rpm 3600 rpm	9-6 7-4
Non-condensing	3600 rpm	4-3
Waterwheel Generator		
Slow-speed (<200 rpm)	2-3	
High-speed (>200 rpm)	2-4	
Synchronous Condenser***		
Large	1.25	
Small	1.00	
Synchronous Motor with Load	2.00	
varies from 1.0 to 5.0 and higher for heavy flywheels		

*For more specific figures, see Fig. 75 of Chap. 6.

**Where range is given, the first figure applies to the smaller kva sizes.

***Hydrogen-cooled, 25 percent less.

The severity of unsymmetrical system faults is affected by the negative-sequence impedance of the connected machines. Amortisseurs or damper windings affect both the real and reactive components of this impedance. Machines without damper windings possess the highest negative-sequence reactance, but machines with high-resistance damper windings possess the highest negative-sequence resistance. The curves of Fig. 67 show the combined effect of the damper material upon the stability limit of a typical system for line-to-line and double line-to-ground faults on the high-voltage bus at the generator end. The improvement with high-resistance dampers is quite appreciable for long fault duration, but for the duration that can be obtained at present with high-speed breakers, the improvement is very much less. In the event of system oscillations low-resistance copper damper windings produce the greatest damping of the mechanical movement. However, this effect is unimportant during and following a system fault except in the rather rare case in which the system is so constituted that pullout takes place as a result of compound oscillations following a disturbance. To obtain the partial advantage of the high loss associated with high-resistance dampers at times of

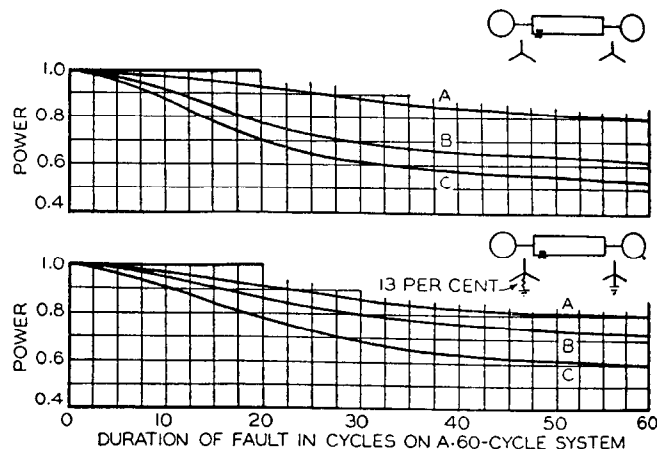


Fig. 67—Effect of damper-winding material upon stability limits.

System Same as Fig. 63-C.
 A—High resistance. B—No dampers. C—Copper.
 Upper curves for line-to-line fault.
 Lower curves for double line-to-ground fault.

unbalanced faults and the damping of oscillations associated with low-resistance dampers, the generators of one installation, i.e., 15-Mile Falls,^{19,20} were supplied with a special type of damper winding which consists of a double-cage arrangement in which the outer row of bars is made of high-resistance material and the inner row of bars is made of a low-resistance material imbedded in the iron. For the double frequency associated with negative-sequence, the copper bars possess a high reactance and, therefore, force most of the current through the high-resistance bars. For the low frequency associated with the system oscillations, the current varies inversely with the resistance of the damper bars and allows most of the current to flow through the copper winding. The benefit from high-resistance damper windings is decreased as the fault duration is de-

creased by the use of faster breakers and relays. Damper windings also have characteristics which tend to suppress spontaneous hunting and to reduce system overvoltages and recovery rates arising from short circuits; in these respects, low-resistance copper dampers are somewhat more effective than high-resistance dampers.

With the increase in size of generator units, the greater concentration of power on a single bus has increased the duty on circuit breakers and the area affected by a fault on or near the bus. These effects can be minimized by the use of the two-winding generator¹³⁻¹⁷ in which the two armature windings are connected only through their mutual coupling which can be controlled by suitable design. Generators of this character lend themselves to incorporation as units in the system layout known as "synchronizing at the load" or its variations as described previously.

Excitation Systems—Control of the excitation system on synchronous machines provides a means for improving stability limits for transient conditions and also for steady-state conditions. Excitation systems that are effective from the standpoint of stability are commonly termed quick-response excitation systems, the principal features of which are:

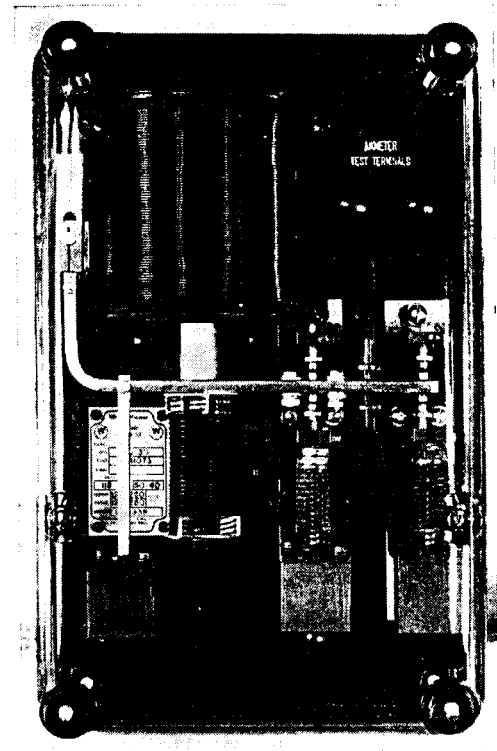
1. Exciter of quick response, i.e., of high rate of build-up and of high "ceiling" voltage.
2. A reliable source of power to the exciter.
3. Quick-responding regulator.

Exciter response is the rate of build-up or build-down of the main-exciter voltage when a change in this voltage is demanded by the action of the voltage regulator. The response of the exciter was formerly expressed in "volts per second" corresponding to the average value effective through an interval of one-half second beginning at rated-load field voltage. This rate is standardized as the numerical value obtained, called the *response ratio*, by dividing the average value of volts per second in the same time interval by the rated-load field voltage. The method of determining exciter response is illustrated and formal definitions are given in Chap. 7. Exciter response ratio of 0.5 on the per unit basis just described is now standard; faster response up to 2.0 is regularly available at a small additional cost, and still faster response can be provided.

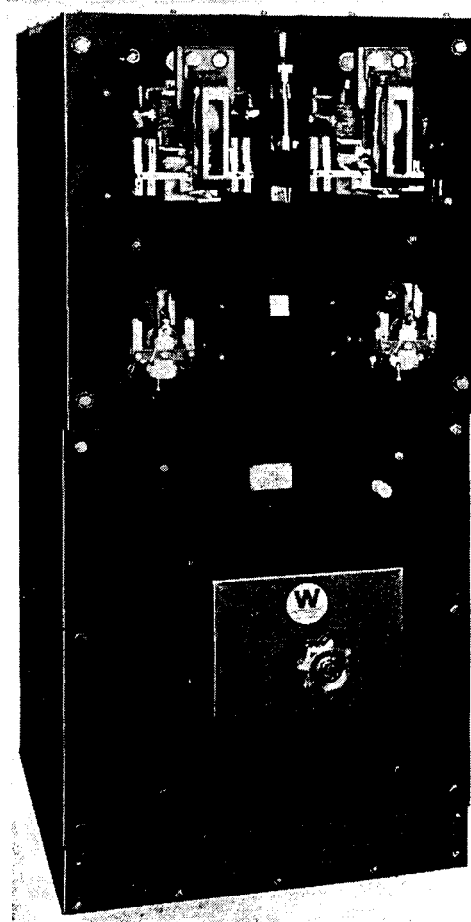
The characteristics which an excitation system must have to obtain the benefits of quick response include a high-ceiling voltage as well as a high rate of build-up. The ceiling voltage of an exciter varies through quite a wide range depending upon the particular design. The actual value in a particular case is adjusted so as to give the desired response through the half-second interval. Usually the ceiling voltage will be considerably more than 50 percent above the normal exciter voltage for the maximum rated load.

Fig. 68—Typical voltage regulator for control of the quick-response excitation system for a large waterwheel generator. Type BJ indirect-acting exciter-rheostatic voltage regulator.

- (a) Main control element in projection-type case with glass cover.
- (b) Cubicle-type assembly of regulator-contactor panel and plate-type motor-operated main-exciter field rheostat.



(a)



(b)

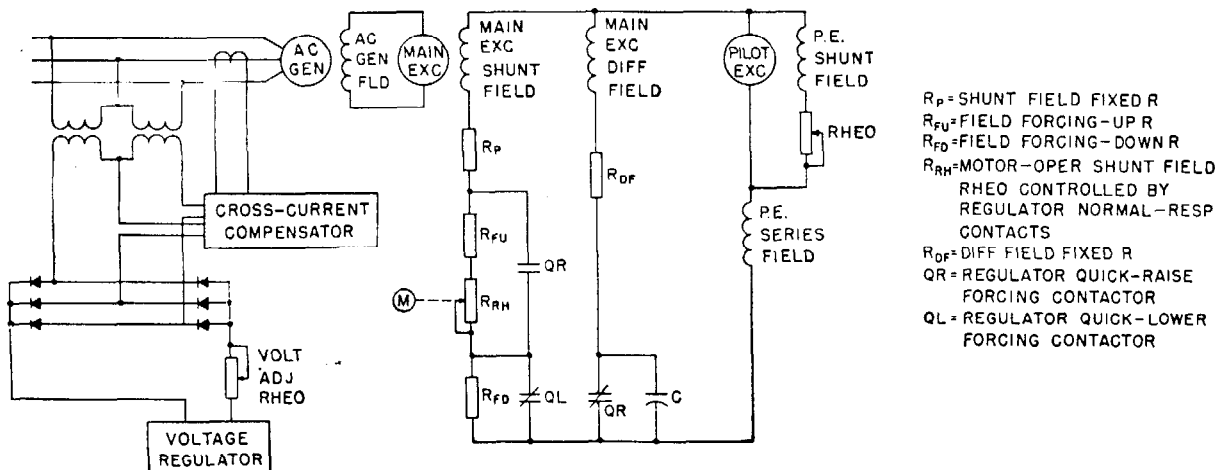


Fig. 69—Elementary schematic diagram of Type BJ regulator illustrated in Fig. 68.

The excitors, regulators, and other voltage-control equipment required for quick-response excitation are built in various forms, which are discussed in detail in Chap. 7. The most common system in recent years has been that using a separately-excited main exciter and an exciter-rheostatic regulator such as the *BJ* type illustrated in Fig. 68 and shown schematically in Fig. 69. The main exciter is of liberal design having specially designed field circuits to reduce the time constants to a minimum. Excitation for the separately-excited field is under control of the voltage regulator and is supplied by a flat-compounded, self-excited d-c generator, called the pilot exciter.

The exciter-rheostatic regulator has two sets of contacts:

1. Normal-response contacts that operate for normal load changes causing small voltage changes, and which control the motor *M* driving rheostat R_{RH} to increase or decrease the exciter field current.

2. Quick-response contacts which control the high-speed contactors *QR* and *QL*, and which operate for sudden, large changes in system voltage and excitation requirements. The normal-response contacts are sensitive to a change in a-c voltage of $\frac{1}{2}$ of one percent. These contacts control the main-exciter motor-operated field rheostat. Modern regulating equipment is designed to initiate excitation corrective action within a period of 3 cycles on a 60-cycle basis. This action is controlled by the quick-response contacts, which in combination with the high-speed contactor start to change the exciter-field current within 3 cycles after the generator voltage has departed from normal by an amount equal to approximately three times the sensitivity setting of the quick-response contacts.

Quick-response excitation systems tend to improve stability limits of power systems in three ways:

1. Maintaining or increasing machine flux against demagnetizing action of fault currents.
2. Supplying deficiency in system excitation due to loss of other sources of excitation.
3. Increasing steady-state stability limits by facilitating action in the region of dynamic stability.

The effect of quick-response on the magnitude of the

internal voltages of a waterwheel generator connected to a typical system subjected to faults is illustrated in Fig. 70. The internal voltages are calculated by the method outlined in Chap. 6 for two conditions, which give per-unit demagnetizing currents of about 1.5 and 1.0 for line-to-line and line-to-ground faults, respectively. These curves are based on constant phase displacement between the machine and the receiver. The correction for this factor would slightly reduce the voltages and alter the shapes for all curves without changing the relative effects. Quick-response excitors do not make very important gains in main-machine flux for line faults of the short durations possible with high-speed circuit breakers and relays. However, the flux conditions within the machine will continue below normal throughout the "first swing," even though the fault has been removed, particularly if a line section has been removed from the circuit for isolating the fault. This circumstance increases the scope of beneficial action possible by a quick-response excitation system. If the line faults are not cleared in the normal high-speed manner, a very substantial improvement in the stability limits is accomplished. With exciter-response ratios greater than 0.5 per unit, it is possible not only to overcome the demagnetizing action of the fault currents, but actually to increase the main-machine flux in the time normally required for the system to reach the critical point in its oscillation.

Quick-response excitation provided one of the earliest methods used for improving the transient-stability limits of systems. Its importance in this respect has, however, been minimized by the developments of high-speed circuit breakers and relays which limit the duration of fault currents and their demagnetizing effects.

Another feature of quick-response excitation systems is the ability to increase the excitation to meet the requirements of a system arising from the loss of other sources of excitation, as from the disconnection of a generator or condenser. This feature cannot, of course, be supplied by high-speed circuit breakers. In order to be effective in this respect, a quick-response excitation system must have a relatively high ratio of ceiling to normal-operating voltage and the regulating equipment must be such as to permit operation under these conditions for

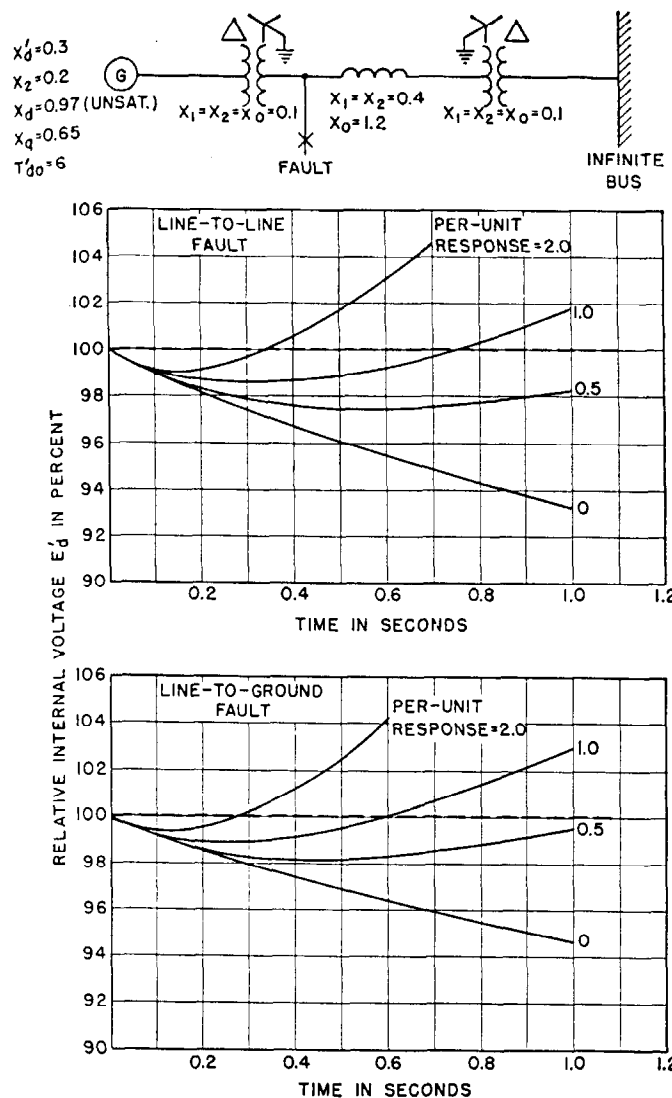


Fig. 70—The effect of different speeds of exciter response on the internal voltage of a waterwheel generator with damper windings. System shown in the insert is subjected to line-to-line and line-to-ground faults at sending end. The ratios of ceiling to normal exciter voltage are 2.2, 1.6 and 1.6 for per-unit exciter responses of 2.0, 1.0 and 0.5, respectively.

the length of time necessary for some readjustment of the system. Ordinarily the speed of exciter response is of secondary importance in comparison with the exciter range. However, quick-response excitation systems normally possess the essential exciter range and whatever advantage that resides in the quicker response.

Quick-response excitation systems also provide means for increasing the steady-state stability limits by facilitating operation in the zone of dynamic stability as discussed in Sec. 17. In a few cases it appears probable that some beneficial action from regulators in the region of dynamic stability is required to explain the absence of pullouts. In general, however, since the steady-state limits are higher than the transient limits, the favorable characteristics of a voltage regulator to increase the steady-state limits has been without real significance. There is also the question as to the desirability of having the opera-

tion of a station at its rated load being dependent upon the functioning of a regulator. Consequently, the choice of regulator has been determined from its performance under transient conditions and its maintenance under ordinary operation.

High-Speed Circuit Breakers and Relays—The duration of a fault condition has a very important effect on the stability of a system. The fault condition reduces synchronizing power, (1) directly by altering the equivalent-circuit constants and (2) indirectly by reducing the effective machine voltages through the demagnetizing action of fault currents. The stability limits as affected by the speed of breaker and relay operation vary through a wide range from (1) the limits corresponding to sustained faults to (2) a mere switching operation assuming extremely fast fault isolation. High-speed circuit breakers and relays are capable of covering most of this range and thus constitute a very important measure for increasing the stability limits, particularly for transmission systems.¹⁶

The relation between the speed of fault isolation and the transient-stability limits for a typical transmission system is indicated in Fig. 71, which also gives the impedance constants of the various system elements. The system is assumed to be subjected to a fault on one line near the high-voltage bus at the sending end and to be cleared by the opening of the two breakers simultaneously. The curves assume waterwheel-type generators, and receiving-end machines of relatively high inertia. The calculations were made for the four different types of faults shown on the curves, which are plotted in terms of the time required for the isolation of the fault and the ratio of the power that can be transmitted to the power limit corresponding to the

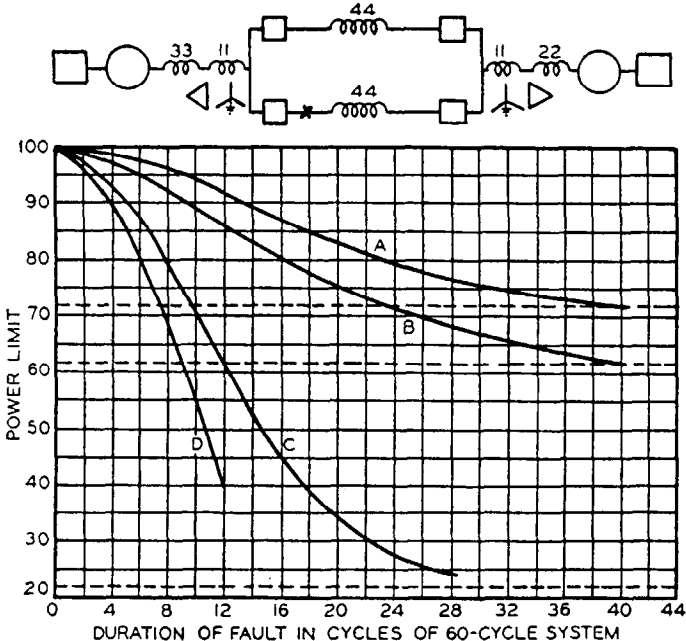


Fig. 71—Effect of duration of fault on power limits for different kinds of faults.

A—Single line-to-ground fault. C—Double line-to-ground fault.
 B—Line-to-line fault. D—Three-phase fault.
 System reactance shown in percent.

switching out of one section of the transmission line. The dotted lines show the loads which can be carried with sustained short circuits of the various types assuming quick-response excitation systems capable of preventing demagnetization of the machines.

The curves in Fig. 71 apply to a system subjected to a fault at the sending end. The relative stability conditions for the fault at sending and receiving ends of a somewhat different system were given in Fig. 63 which has been discussed previously in connection with the use of neutral impedances. A moderate value of neutral resistance at the sending end can make a fault at that end on a grounded-neutral system relatively less severe than a fault at the receiver. However, the gains in stability due to the use of high-speed circuit breakers are of the same order for faults at the sending or receiving ends of the transmission system.

On metropolitan-type systems the permissible time for isolating the fault will be relatively longer than for transmission systems since the latter are usually operated closer to the stability limits. Thus in the metropolitan systems it is possible to introduce reactance in the system in such a way as to limit the duty on circuit breakers. This problem can conveniently be studied by the short-cut method²³ discussed in detail in Part VIII.

The curves used in this method indicate that by taking advantage of the faster speeds made possible by the recent developments of circuit breakers, increased amounts of reactance can be introduced in the system either to reduce the duty on circuit breakers or to increase the continuity of power supply or reliability of the service to the customer.

The speed of circuit breakers and relays in relation to power-system stability can conveniently be analyzed under three headings as follows:

1. Conventional or slow-speed breakers and relays for fault isolation.
2. High-speed breakers and relays capable of isolating fault in time to improve stability limit.
3. High-speed breakers and relays with reclosure in time to improve stability limit.

The curves of Fig. 71 show that conventional slow-speed circuit breakers and relays of the type commonly in use prior to 1929 were so slow from the stability point of view that the limits corresponded to sustained faults. The power limit for the three-phase fault is almost negligible with the conventional slow-speed breakers formerly in use. The benefits which arise from the use of high-speed circuit breakers and relays in maintaining stability depend upon isolating the fault in an interval of time which is short in respect to the period of system oscillation. The preceding discussion has been based on the isolation of the fault in a single step. For sequential operation the time permissible for each breaker will be less than that shown but need not be reduced to half value. This is, of course, due to the fact that the stability conditions are generally much improved upon the operation of the first circuit breaker.

The need for high-speed circuit breakers has brought about the development and general use of circuit breakers with shorter operating times. At present, standard breakers 115 kv and above have an operating time of 5 cycles, except 230-kv standard breakers, which have an operating time of 3 cycles. Three-cycle breakers cost about five

percent more than the standard five-cycle breakers for the same rating. The standard operating time for 69 kv and below is 8 cycles. It is interesting to note that at the time this book was originally published (1942) 8-cycle breakers were standard up to 230 kv.

For composite systems with long-transmission lines from a source of power and for interconnecting lines between various parts of the receiver, system studies will frequently show the desirability of using high-speed circuit breakers and relays in order to increase the stability limits. In a number of such cases it will be important to extend the application of the high-speed breakers to interconnecting lines of the receiver system. Otherwise, the stability limits are determined not by faults on the main transmission line but by faults on the receiving system, even though it is operating at lower voltage with transformers between it and the transmission line.

This development in the speed of circuit breakers has brought about important changes in the relaying of transmission lines. With fast circuit breakers it is no longer feasible to contemplate relay-operating times of one-quarter second to three seconds or the use of time intervals as the basis of discrimination. This has led to the use of distance or current-balance types of relays which are capable of simultaneous action for the middle section of a transmission line with high-speed sequential tripping for the end sections.

In cases where the transmission system is operated relatively close to the stability limits there is considerable advantage in providing simultaneous breaker operation. In general, such relay operation can be obtained by fundamental-frequency relays operating in conjunction with a signal transmitted by pilot wires or carrier current between the ends of the line section. This has brought about an important development in the application of high-speed relaying with superposed carrier-frequency. The relaying quantity to be transmitted by carrier frequency was selected initially as some electrical indication, such as direction of the power flow, but more recently as the position of various fundamental-frequency relays which indicate the existence of a fault on the system within predetermined zones. The carrier-current and pilot-wire relay systems also provide opportunity for including relay measures for the prevention of undesired breaker operation in the event that the system does pull out of step. Reference should be made to Chap. 11 for further information on circuit-breaker and relay applications.

Reclosing Circuit Breaker—Reclosing circuit breakers provide a means for carrying one step further the advantages possible from high-speed fault clearing. For lower-voltage systems and feeder circuits, automatic reclosing breakers make it possible to maintain the stability of a system with induction-motor load. Disconnection of the source is required for the suppression of the arc in the fault, but the total time required for disconnection and for reclosure should be made sufficiently short as to prevent pullout of induction motors. Where synchronous machines can maintain the arc, it is necessary to isolate the affected line and to reconnect it in a period of time that is relatively short with respect to the period of system oscillation if stability is to be maintained.^{28,34} Hence, if automatic re-

closing breakers are considered for maintaining the stability on a transmission system, it becomes a practical necessity to use carrier-current or pilot-wire relaying. The existence of multiple or repetitive lightning discharges may constitute an important factor in limiting the application of reclosing breakers for maintaining stability.

The selection of the operating speed required of high-speed reclosing breakers is dependent upon a compromise between two conflicting factors. One of these is the maximum permissible time between the inception of the fault and the final reclosure as determined by the power-system load and synchronizing-power conditions. The other is the de-ionization time, the minimum time that must be allowed in order to be reasonably sure that the arc will not reignite and thus create a second fault condition. In many cases where high-speed reclosing is desired, there is sufficient time to permit successful application.

The de-ionization time depends upon the circuit voltage, the conductor spacing, the fault current, and weather conditions. Furthermore, the reestablishment of the arc after an interval is a matter of probability and perhaps twenty tests may be required to establish a single point on a 95-percent probability curve for a single combination of circuit voltage, fault current, conductor spacing, and weather conditions. For these conditions the available test data on de-ionization time, although covering several hundred individual tests, is not considered to cover the field adequately for the purpose of establishing limits. From the available information²⁶ the estimated de-ionization time for successful reclosure is given in Table 9.

TABLE 9—MINIMUM DE-IONIZATION TIME FOR RECLOSED BREAKERS

System Voltage Line-to-Line Kv	Cycles on 60-Cycle Basis	
	95% Probability	75% Probability
23	4	
46	5	3.5
69	6	4
115	8.5	6
138	10	7.5
161	13	10
230	18	14

From the standpoint of maintaining stability, the maximum permissible total time from the inception of the fault to the final reclosure varies over a wide range, depending upon the system, location and severity of the fault, and the type of circuit breaker, that is, whether three-phase as discussed in this paragraph or single-phase as discussed in the next. The permissible reclosure time can be calculated with satisfactory accuracy by methods previously discussed in this chapter, or by reference to the curves²⁶ of Fig. 72. These curves apply to two systems of relatively high inertia connected through a tie line of relatively high reactance. In order to use these curves it is necessary to determine, first, the synchronizing-power limit as determined by the quantity $3\frac{E^2}{X}$ where E is the nominal system voltage line-to-neutral and X is the transfer reactance per phase. The load to be transferred

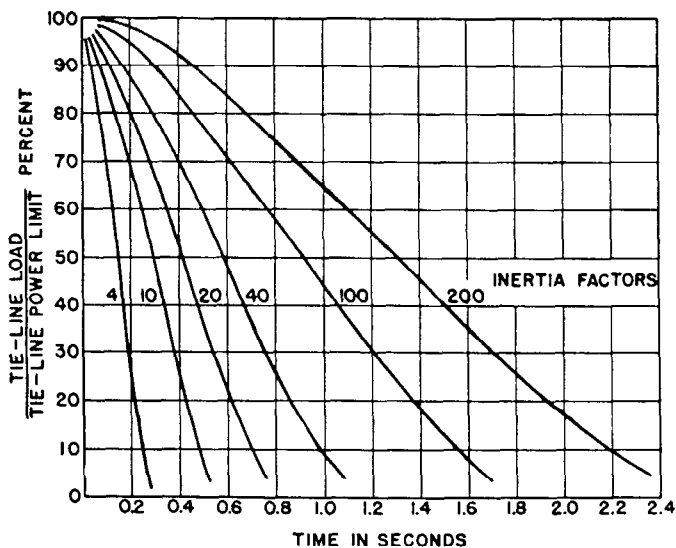


Fig. 72—Permissible time for breaker tripping and reclosure without causing loss of synchronism with gang operated breakers.

over the tie line is then expressed as a percentage of the maximum synchronizing power over the tie line and used as the ordinate of the curve of Fig. 72. If the capacity and inertia constants of the two systems are kva_a , kva_b , and H_a , H_b , then the equivalent inertia constant $H_{eq(a)}$ can be determined from Eq. (37), Sec. 22. The inertia factor to be used in the curves of Fig. 72 is obtained from

$$\text{Inertia Factor} = \frac{H_{eq(a)} kva_a}{TL_{kw}} \quad (66)$$

where TL_{kw} is the tie-line load in kw. Reclosing breakers have been used to improve the stability conditions on a number of 132-kv systems, notably of the American Gas and Electric Company³⁴ and of the West Penn Power Company. The important advantage of reclosing breakers arises from the fact that their use can frequently convert an unstable tie line to one which can be considered as a firm-power source and thus justify a reduction in the connected generating capacity.

Single-Pole Reclosing Breakers—During World War II it became necessary due to increasing demand for power to use single-circuit tie lines between systems to transfer firm blocks of power. Single-pole reclosing breakers have been used successfully in this application. Ground-fault neutralizers are useful in this application, but provide improvement only in the case of single line-to-ground faults, whereas single-pole reclosing breakers improve the stability limits of a single tie line for all types of faults, except three-phase. In this case the operation is that of a gang-operated reclosing breaker.

The advantage of single-pole operation lies in the fact that power can be transferred over the unfaultered phase(s) during the period when the breakers are open to clear the fault. Since most line interruptions do not permanently ground a phase conductor, successful reclosure is obtained in the majority of cases and thus restores the system to its original condition without at any time reducing the power limits to as low a value as would be the case if all three conductors were disconnected.

If single-pole reclosing is to be used, the transformer banks at both ends of the tie line should be grounded solidly or through low values of impedance in order that power may be transferred during the breaker operating period.

A comparison of three-pole and single-pole reclosure has been made for the system shown in the insert of Fig. 73. The result of stability calculations for the two types of reclosure are plotted in Fig. 73 in terms of the per-

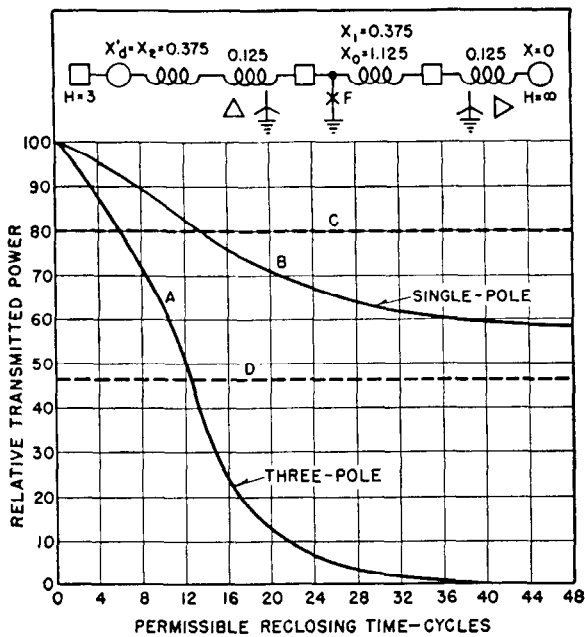


Fig. 73—Comparison of three-pole and single-pole reclosing breakers from standpoint of permissible transmitted power and reclosing time for clearing one line-to-ground fault and maintaining stability for the system shown in the insert.

- A—Three-pole reclosing breaker, 4-cycle opening time.
- B—Single-pole reclosing breaker, 4 to 10-cycle opening time.
- C—Stability limit for system, one phase switched open—system same as insert except for theoretical condition of zero-sequence impedance equal zero—10-cycle opening time.
- D—Stability limit for system, one phase switched open—system same as insert but grounded at fault end only.

missible transmitted loads and reclosure times. The curves show the advantages of single-pole reclosure which can be used (1) to transmit greater power, (2) to provide greater deionizing time, (3) to permit the use of slower-speed breakers for fault clearing or reclosure, or a combination of these three. The power-transferring ability of a system for a sustained one-phase open condition varies with the zero-sequence impedance of the circuit between the limits of (1) infinite impedance which obtains with the ungrounded system, and (2) zero impedance, a theoretical condition which is rarely approached even for solidly-grounded systems. The practical case for grounded systems lies between these two extremes.

The single-pole reclosing breaker is somewhat more expensive than the three-pole breaker because of the three separate mechanisms and the more complicated relay system required.

48. Double Line-to-Ground Fault on Single Tie Line

The transient-stability performance of a single tie line between two systems can be calculated using the step-by-step procedure discussed previously. The only difference between this calculation and the previous examples lies in the fact that the sequence networks must be set up so that the power transferred during the period the breakers are open can be determined.

In calculating a transient-stability problem involving single-pole reclosing, it is convenient to divide the sequence of operations into four steps as follows:

1. Condition before the fault.
2. Condition during the fault.
3. Condition with faulted phase(s) open.
4. Condition after fault (line re-energized).

In setting up the sequence networks for condition 3 it is generally sufficiently accurate to use connections n to r inclusive of Fig. 21, Chap. 2, which assumes equal shunt capacitance on all phases. A more accurate calculation can be made using the method presented in Fig. 22, Chap. 2. Reference 41 gives the sequence-network connections.

Figure 74 presents the results of investigations of over 100 practical solutions.⁴² These curves apply only to double line-to-ground faults and can be used to estimate breaker requirements under proposed operating conditions and also to estimate the transient performance of existing lines.

In the study upon which these curves are based, the sending and receiving systems were assumed to be made up of 1800-rpm, 80-percent power-factor machines operating at full load with necessary excitation. Typical system constants were used. The shunt loads were assumed to be 85-percent power factor. In each case the line regulation was adjusted to ten percent. In certain cases this required synchronous condensers at the receiving end to furnish the necessary reactive kva in excess of the capacity of the receiver generators. The inertia of the condensers is not included in the swing calculations because it is usually found to be negligible.

Conventional a-c network calculator studies were carried through for each principle system chosen until the maximum length of line was determined for which transient stability would be maintained keeping all system elements constant except the line length. These curves give only the minimum reclosing equipment that can be safely applied. Allowance should be made for system growth.

These curves give transient-stability solutions using different types of reclosing equipment. Double line-to-ground faults were used in each case.

To determine the maximum power which could be safely transferred over a tie line, plot the ratio, PS/PR, on the proper "(miles/kv²)PR" curve for the reclosing equipment under consideration. The ordinate of the plotted point is the maximum power which could be safely transferred in per unit, based on receiving-end generation. These curves are not intended as a solution of all problems concerning high-speed reclosing, but are presented merely as a guide. These general curves are calculated to apply specifically to tie lines between systems on which steam turbines predominate. Detailed calculations should be made where

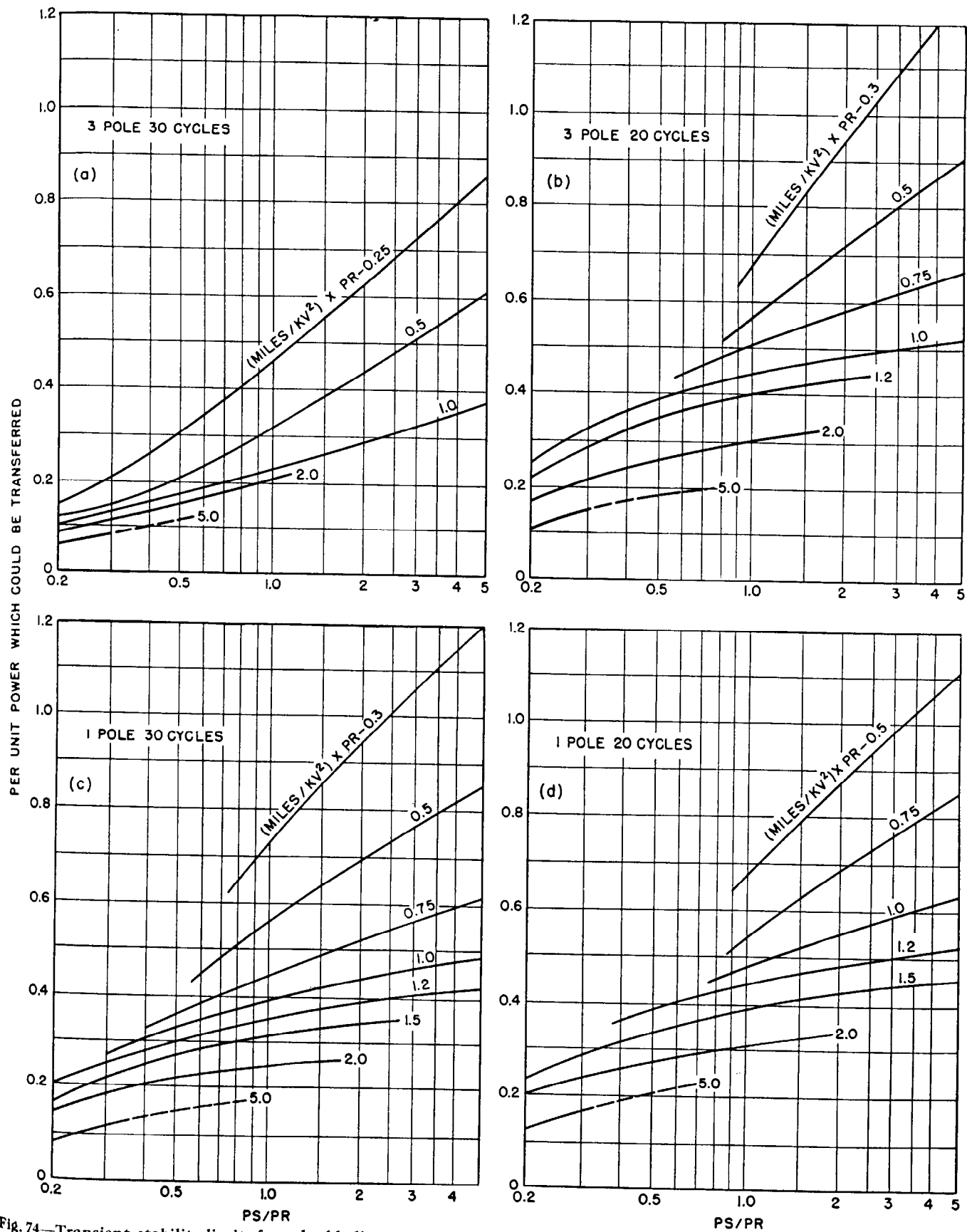


Fig. 74—Transient-stability limits for a double line-to-ground fault on a single tie-line between two systems on which steam turbines predominate.

PS and PR = sending and receiving-end generation, in mw, respectively; KV = Line-to-line kilovolts.

marginal or unstable conditions are indicated by these curves.

49. Other Methods of Increasing the Practical Operating Power Limits

Flashover-Prevention and Arc-Suppression—A different approach to the problem of improving the practical operating power limit of a system is obtained by the use of flashover-prevention and arc-suppression measures. It is obvious, of course, that a system rarely subjected to faults can be operated relatively close to the stability limits. Consequently, under some conditions it is more advantageous to spend money for minimizing the likelihood of faults than for increasing the capacity of the system to withstand the system disturbances resulting from faults.

The principal cause of flashover on high-voltage lines is lightning. Much has been accomplished during the past fifteen years to minimize flashovers resulting not only from induced strokes but particularly from direct strokes.* Increased transmission-line spacing and increased insulation in the form of insulator strings and wood have generally been adopted. On the higher-voltage lines the use of ground wires is of great value when suitably located with respect to the conductors to be protected. Special efforts have been made to reduce the tower-footing resistance to a relatively low value in order to prevent a flashover of the insulator string as a result of the building up of high potential due to the flow of lightning current through the tower to ground.

The use of the ground wires reduces the zero-sequence impedance of the system and thus increases the severity of the shock resulting from a single or double line-to-ground fault. With the development of high-speed circuit breakers and relays these faults can be cleared promptly; consequently, the use of ground wires results in a gain from the stability point of view by reducing the number of flashovers which overbalances any disadvantage from the standpoint of the shock to the system in case the fault occurs.

The fault-suppression measures have as their object the interruption of the power-arc following a flashover without the necessity for isolating the affected circuit. The use of fused arcing rings or special tube-type protectors in parallel with the insulators permits flashover to take place through a path that insures the subsequent interruption of the power arc. Lightning arresters distributed along the line will accomplish this same general objective. See also Chap. 17.

Arc-suppression devices of the ground-fault neutralizer or Petersen-coil type have received consideration for minimizing circuit outages in connection with multiple-circuit systems of the type in common use and have been used in the single-circuit Hoover-Chino transmission line

*Reference should be made to Chaps. 16 and, particularly, 17.

system. In America, however, little use is made of this type of arc-suppression device as dependence is placed on circuit breakers and relays for automatically isolating a faulty section of line. Circuit-breaker schemes have the merit of suppressing all types of faults that occur on systems regardless of whether they are of the single line-to-ground or more severe types. In addition they permit grounding the system so that the tendency for a single-phase fault to develop into a multi-phase fault is minimized. See also Chap. 19.

High-Voltage D-C, and Low-Frequency A-C Transmission—Low-frequency a-c systems have been proposed frequently for increasing the practical operating stability limits of long-distance transmission systems. More recently d-c transmission has been proposed as a means for avoiding the stability limits since such a system inherently provides a non-synchronous tie. In America, 60-cycle a-c is very generally established for utilization. Consequently, the proposals to use low-frequency a-c and high-voltage d-c transmission schemes have included conversion means at the receiving end. In general, the use of the low-frequency a-c system involves no new problem in apparatus or application so that its use is not hindered on this account, although static apparatus might find application in the field of frequency conversion. In the case of d-c transmission, however, the conversion from a-c generation to the d-c high voltage required for the transmission line involves rectifiers for which there is no comparable operating experience; in the case of the inverters at the receiving end still less work has been done. Considerable interest has been displayed in d-c transmission, but it is still generally considered impractical especially in this country. During the recent war the Germans considered d-c transmission particularly as a means of getting power from Scandinavian peninsula to Germany. D-c transmission can show economic gains over high-voltage a-c transmission only where large blocks of power are to be transferred⁴⁰ for extremely long distances. Even then d-c transmission may not be economical if it is desired to tap off intermediate loads because of the high cost of the terminal equipment. Much work remains to be done before d-c transmission can seriously compete with a-c transmission.

At the present time the limitations in 60-cycle systems, from the standpoint of system stability, are not of sufficient importance as to justify the adoption of either low-frequency a-c or high-voltage d-c transmission^{29,37}. The possible field for d-c transmission depends largely on the practical necessity for transmitting power to considerably greater distances than those used heretofore, on the usefulness of its operating characteristics aside from stability, and on the future development of conversion apparatus. In this connection it should be noted that the series capacitor offers tremendous improvement in a-c transmission at normal frequencies.

STABILITY REFERENCES IN THE ENGLISH LANGUAGE

The "First Report of Power System Stability," item 33, includes a list of 180 articles, which are arranged in chronological order and bear symbols indicating their character.

1. Experimental Analysis of Stability and Power Limitations, by R. D. Evans and R. C. Bergvall, *A.I.E.E. Transactions*, 1924, pp. 39-58. Disc., pp. 71-103.
2. Power System Transients, by V. Bush and R. D. Booth, *A.I.E.E. Transactions*, Feb. 1925, pp. 80-97. Disc., pp. 97-103.
3. Transmission Stability, Analytical Discussion of Some Factors Entering into the Problem, by C. L. Fortescue, *A.I.E.E. Transactions*, Sept. 1925, pp. 984-994. Disc., pp. 994-1003.
4. Practical Aspects of System Stability, by Roy Wilkins, *A.I.E.E. Transactions*, 1926, pp. 41-50. Disc., pp. 80-94.
5. Further Studies of Transmission System Stability, by R. D. Evans and C. F. Wagner, *A.I.E.E. Transactions*, 1926, pp. 51-80. Disc., pp. 80-94.
6. A Mechanical Analogy of the Problem of Transmission Stability, by S. B. Griscom, *The Electric Journal*, May 1926, pp. 230-235.
7. Excitation Systems: Their Influence on Short Circuits and Maximum Power, by R. E. Doherty, *A.I.E.E. Transactions*, July 1928, pp. 944-956. Disc., pp. 969-979.
8. System Stability with Quick-Response Excitation and Voltage Regulators, by J. H. Ashbaugh and H. C. Nycum, *The Electric Journal*, Oct. 1928, pp. 504-509.
9. Transients Due to Short Circuits—A Study of Tests Made on the Southern California Edison 220-Kv System, by R. J. C. Wood, L. F. Hunt, and S. B. Griscom, *A.I.E.E. Transactions*, Jan. 1928, pp. 68-86. Disc., pp. 86-89.
10. Static Stability Limits and the Intermediate Condenser Station, by C. F. Wagner and R. D. Evans, *A.I.E.E. Transactions*, 1928, pp. 94-121. Disc., pp. 121-123.
11. Synchronized at the Load—A Symposium on New York City 60-Cycle Power System Connection, by A. H. Kehoe, S. B. Griscom, H. R. Searing, and G. R. Milne, *A.I.E.E. Transactions*, Oct. 1929, pp. 1079-1100. Disc., pp. 1100-1107.
12. Progress in the Study of System Stability, by I. H. Summers and J. B. McClure, *A.I.E.E. Transactions*, 1930, pp. 132-158. Disc., pp. 159-161.
13. Double Windings for Turbine Alternators, by P. L. Alger, E. H. Freiburghouse, and D. D. Chase, *A.I.E.E. Transactions*, Jan. 1930, pp. 226-238. Disc., pp. 238-244.
14. Fundamental Plan of Power Supply of the Detroit Edison Company, by S. M. Dean, *A.I.E.E. Transactions*, 1930, pp. 597-604. Disc., pp. 612-620.
15. Operating Characteristics of Turbine Governors, by T. E. Purcell and A. P. Hayward, *A.I.E.E. Transactions*, April 1930, pp. 715-719. Disc., pp. 719-722.
16. Selecting Breaker Speeds for Stable Operation, by R. D. Evans and W. A. Lewis, *Electrical World*, Feb. 15, 1930, pp. 336-340.
17. Double-Winding Generators, by R. E. Powers and L. A. Kilgore, *The Electric Journal*, Feb. 1930, pp. 107-111.
18. An Alternating-Current Calculating Board, by H. A. Travers and W. W. Parker, *The Electric Journal*, May 1930, pp. 266-270.
19. Effect of Armature Resistance Upon Hunting of Synchronous Machines, by C. F. Wagner, *A.I.E.E. Transactions*, July 1930, pp. 1011-1024. Disc., pp. 1024-1026.
20. Generator Stability Features—Fifteen Mile Falls Development, by R. Coe and H. R. Stewart, *The Electric Journal*, March 1931, pp. 139-143.
21. Stability Precautions on a 220-Kv System, by H. H. Spencer, *Electrical World*, Aug. 15, 1931, pp. 276-280.
22. Proposed Definitions of Terms Used in Power System Studies—Report of Subject Committee on Definitions, by H. K. Sels, *A.I.E.E. paper 32M-2, Abstract Electrical Engineering*, 1932, p. 106.
23. Generalized Stability Solution for Metropolitan-Type Systems, by S. B. Griscom, W. A. Lewis, and W. R. Ellis, *A.I.E.E. Transactions*, June 1932, pp. 363-372. Disc., pp. 373-374.
24. Stability Experiences with Conowingo Hydro-Electric Plant, by R. A. Hentz and J. W. Jones, *A.I.E.E. Transactions*, June 1932, pp. 375-384. Disc., p. 384.
25. Adjusted Synchronous Reactance and Its Relation to Stability, by H. B. Dwight, *General Electric Review*, Dec. 1932, pp. 609-614.
26. Keeping the Line in Service by Rapid Reclosure, by S. B. Griscom and J. J. Torok, *The Electric Journal*, May 1933, p. 201.
27. *Symmetrical Components*, by C. F. Wagner and R. D. Evans (a book), McGraw-Hill Book Company, New York, 1933.
28. Quick-Response Excitation, by W. A. Lewis, *The Electric Journal*, Aug. 1934, pp. 308-312.
29. Constant Current D-C Transmission, by C. H. Willis, B. D. Bedford, and F. R. Elder, *A.I.E.E. Transactions*, Jan. 1935, pp. 102-108. Disc., Mar. 1935, pp. 327-329, and Apr. 1935, pp. 447-449. Aug. 1935, pp. 882-883.
30. Steady-State Solution of Saturated Circuits, by Sterling Beckwith, *A.I.E.E. Transactions*, July 1935, pp. 728-734.
31. Engineering Features of the Boulder Dam-Los Angeles Line, by E. F. Scattergood, *A.I.E.E. Transactions*, May 1935, pp. 494-512. Disc., 1936, pp. 200-204 and 208.
32. *The Scientific Basis of Illuminating Engineering*, by Parry Moon (a book), McGraw-Hill Book Company, New York, 1936.
33. First Report of Power System Stability: Report of Subcommittee on Interconnection and Stability Factors, by R. D. Evans, Chairman, *A.I.E.E. Transactions*, 1937, pp. 261-282. Disc., May, pp. 632-634 and Sept., p. 1204.
34. Ultra High-Speed Reclosing of High-Voltage Transmission Lines, by Philip Sporn and D. C. Prince, *A.I.E.E. Transactions*, 1937, pp. 81-90 and 100. Disc., p. 1036.
35. Unsymmetrical Short Circuits on Waterwheel Generators Under Capacitive Loading, by C. F. Wagner, *A.I.E.E. Transactions*, 1937, pp. 1385-1395. Disc., 1938, p. 406.
36. *Electric Power Circuits—Theory and Operation—System Stability*, by O. G. C. Dahl (a book), vol. 2, McGraw-Hill Book Company, New York, 1938.
37. D-C Transmission Evolving Slowly, by D. M. Jones, C. H. Willis, M. M. Morrack, and B. D. Bedford, *Electrical World*, Feb. 25, 1939, pp. 41-42.
38. Phase-Angle Control of System Interconnection, by R. E. Pierce and G. W. Hamilton, *A.I.E.E. Transactions*, 1939, pp. 83-91. Disc., p. 92.
39. A Graphical Solution of Transient Stability, by H. H. Skilling and M. H. Yamakawa, *Electrical Engineering*, Nov. 1940, pp. 462-465.
40. Brown Boveri Review, Issue on D.C. Transmission, Vol. XXXII, No. 9.
41. Reclosing of Single Tie Lines Between Systems, by W. W. Parker and H. A. Travers, *A.I.E.E. Transactions*, 1944, pp. 119-122. Disc., p. 472.
42. Reclosing Single-Circuit Tie Lines, by H. N. Muller, Jr. and W. W. Parker, *WESTINGHOUSE ENGINEER*, March 1945, pp. 60-63.

CHAPTER 14

POWER SYSTEM VOLTAGES AND CURRENTS DURING ABNORMAL CONDITIONS

Original Author:

R. L. Witzke

Revised by:

R. L. Witzke

FOR many years it was common practice to base the requirements of system apparatus on normal load conditions and on three-phase short circuits. More or less empirical multiplying factors were sometimes used to predict the probable ground-fault currents from the three-phase fault currents. However, this procedure is unsatisfactory because the relations between three-phase and ground-fault currents vary greatly between systems. In some systems the current for a single line-to-ground fault is less than normal load current, whereas, in other systems, or at other locations in the same systems, the current for a single line-to-ground fault is larger than the three-phase fault current. The analysis of power systems by symmetrical components¹ (see Chap. 2) has made possible the accurate calculation of fault currents and voltages for unsymmetrical faults directly from system constants.

Under many conditions the voltages present on a power system may be higher than those calculated for steady-state conditions. These higher voltages are usually of a transient nature and exist during the transition from one steady-state condition to another. Transient voltages can be produced by simple circuit changes such as the opening of a circuit breaker or the grounding of a conductor; or they can be produced by an intermittent arc in a circuit breaker or in a fault. Usually the higher voltages are associated with intermittent arcs rather than with simple circuit changes without arcing. Most transient voltages are not of large magnitude but may still be important because of their effect on the performance of circuit-interrupting equipment and protective devices. An appreciable number of these transient voltages are of sufficient magnitude to cause insulation breakdown.

The various factors that determine the magnitudes of currents and voltages in power systems during abnormal conditions will be discussed in this chapter.

I. STEADY-STATE VOLTAGES AND CURRENTS DURING FAULT CONDITIONS

1. Assumptions

Voltages and currents produced under fault conditions are a function of the type of fault and the ratios of the sequence impedances. The effect of these factors on the voltages and currents produced can be shown by sets of curves as will be done here. The four types of faults illustrated in Fig. 1 will be considered. It is assumed that the network is symmetrical to the point of fault, F , and can be reduced to series impedances, Z_1 , Z_2 , and Z_0 for

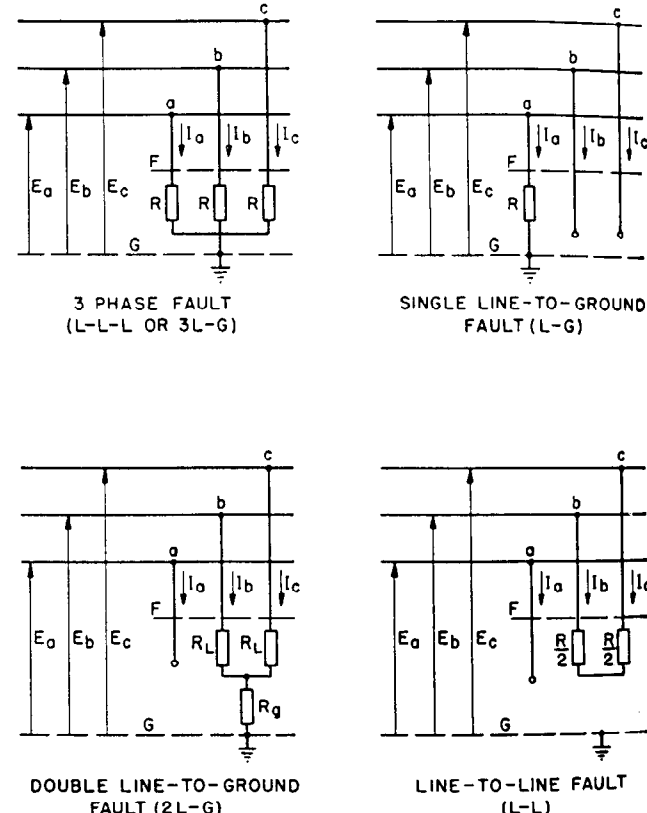


Fig. 1—Types of faults on three-phase systems.

the positive-, negative-, and zero-sequence networks, respectively. In the present analysis the fault resistance is represented by R and is not included in Z_0 . Z_0 includes all zero-sequence resistance to the point of fault but does not include the fault resistance. It is further assumed that all the generated emfs can be reduced to a single positive-sequence emf, E_g .

2. Formulas

In Tables 1 and 2 are given the formulas* for calculating the line currents and line-to-ground voltages for the faults illustrated in Fig. 1. These formulas are complicated to such an extent that it is difficult to visualize readily the currents and voltages that can be produced under fault conditions for ranges of system constants. For this reason the currents and voltages have been calculated for various

*Formulas taken from pages 224 and 226 of reference 1.

ratios of system constants and the results are presented as a series of curves.

3. Range of Sequence Impedances Considered

The principal impedances that usually apply to transient conditions are the positive-sequence impedance Z_1 , the negative-sequence impedance Z_2 , and the zero-sequence impedance Z_0 , each consisting of a resistance and a reactance component. In general, the positive-sequence resistance R_1 and the negative-sequence resistance R_2 are small in comparison to the positive- and negative-sequence reactances. Consequently, the effect of these two resistances on the magnitude of the voltages and currents during fault conditions is small. For this reason and because of complications introduced by considering positive- and negative-sequence resistances, these factors will be neglected. Zero-sequence resistance R_0 and zero-sequence reactance X_0 can vary through wide ranges depending on the type of system grounding used, hence the curves are arranged to cover a wide range of zero-sequence resistance and zero-sequence reactance.

The positive-sequence reactance that applies to transient conditions may be either the sub-transient or the transient reactance depending on whether or not the initial high decrement component of the current is to be considered or neglected. The ratio of X_2 to X_1 for commercial machines usually lies between 0.5 and 1.5, although with special machines it is possible to exceed this range. The higher ratios of X_2 to X_1 are in machines without dampers whereas the lower ratios are in machines with dampers or their equivalent. In general calculations it is usually permissible to assume a ratio of X_2/X_1 of unity especially if an appreciable percentage of the negative-sequence reactance to the point of fault is in static apparatus or transmission lines. The general curves are limited to ratios of X_2 to X_1 within the range of 0.5 to 1.5; the formulas in Tables 1 and 2 can be used for ratios outside of this range.

4. Fault Current and Voltage Curves

Curves prepared in accordance with the preceding discussion are plotted in Figs. 2 to 6 inclusive. In these figures the fault current is plotted as a ratio of the three-phase short-circuit, and the line-to-ground and line-to-line voltages are plotted as a ratio to their respective normal values.

In Figs. 2, 3, and 4 all resistances are equal to zero. Figs. 2 and 3 show the ranges of line currents and line-to-

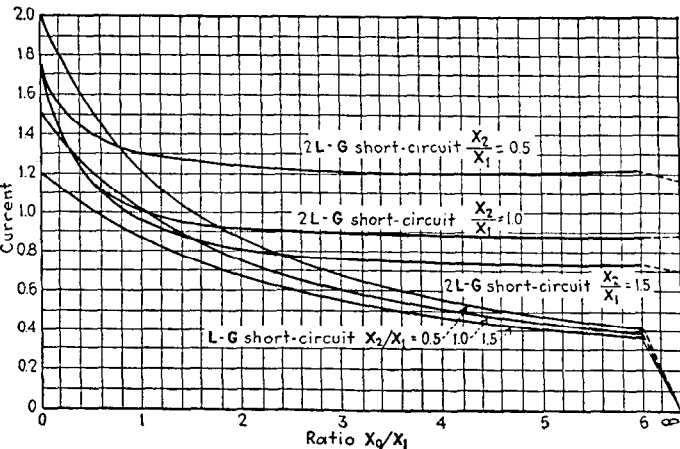


Fig. 2—Curves of fault currents vs. system reactances for single and double line-to-ground faults. Each curve is labeled to indicate the type of fault and the ratio of X_2/X_1 . All currents are expressed as a ratio to the three-phase short-circuit current. For these curves, all resistances are assumed equal to zero¹.

ground voltages respectively for single and double line-to-ground faults for ratios of X_0/X_1 from zero to six. The ranges of fault current and fault voltages for ratios of X_2/X_1 between 0.5 and 1.5 are shown in Fig. 4.

The ranges of fault current for ratios of $\frac{R_0}{X_1}$ between zero and six are given in Fig. 5. In this figure the ratio X_2/X_1

TABLE 1—FAULT CURRENTS

Type of fault	Vector expression, effect of fault resistance included	Magnitude of currents when $R_0 = R_1 = R_2 = R = R_g = 0$
Three-phase.....	$I_a = \frac{E_g}{Z_1 + R}$	$I_a = I_b = I_c = \frac{E_g}{X_1}$
Line-to-line.....	$I_b = \frac{-j\sqrt{3}E_g}{Z_1 + Z_2 + R}$ $I_c = -I_b$	$I_b = I_c = \frac{\sqrt{3}E_g}{X_1 + X_2}$
Single line-to-ground.....	$I_a = \frac{3E_g}{Z_0 + Z_1 + Z_2 + 3R}$	$I_a = \frac{3E_g}{X_0 + X_1 + X_2}$
Double line-to-ground.....	$I_b = \frac{-\sqrt{3}E_g}{2\Delta v} [\sqrt{3}(Z_2 + R_L) + j(2Z_0 + Z_1 + 3R_L + 6R_g)]$ $I_c = \frac{-\sqrt{3}E_g}{2\Delta v} [\sqrt{3}(Z_2 + R_L) - j(2Z_0 + Z_1 + 3R_L + 6R_g)]$ $I_g = I_b + I_c = 3I_b$ $= \frac{-3E_g}{\Delta v} (Z_2 + R_L)$ $\Delta v = (Z_1 + R_L)(Z_2 + R_L) + (Z_1 + Z_2 + 2R_L)(Z_0 + R_L + 3R_g)$	$I_b = I_c = \frac{\sqrt{3}E_g}{\Delta_M} \sqrt{X_0^2 + X_0X_2 + X_2^2}$ $I_g = \frac{3E_g}{\Delta_M} X_2$ $\Delta_M = X_1X_2 + X_0(X_1 + X_2)$

Z_1 =positive-sequence impedance to the point of fault
 Z_2 =negative-sequence impedance to the point of fault

Z_0 =zero-sequence impedance to the point of fault and does not include any fault resistance
See Fig. 1 for definitions of R , R_L and R_g

covers the range of 0.5 to 1.5 and the ratio X_0/X_1 covers the range of zero to five. As pointed out previously, fault

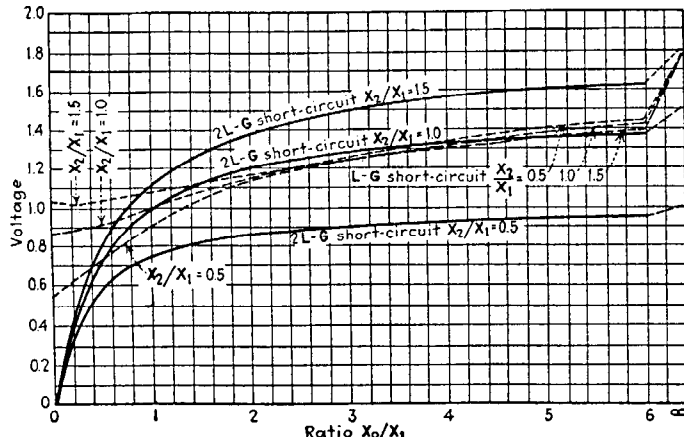


Fig. 3—Curves of fault voltages vs. system reactances for single and double line-to-ground faults. Each curve is labeled to indicate the type of fault and the ratio of X_2/X_1 . The voltages are from line-to-ground and are expressed as a ratio to the normal line-to-neutral voltages. For these curves, all resistances are assumed equal to zero¹.

resistance has been neglected in these curves; R_0 is the zero-sequence resistance to the point of fault F and does not include R , R_L , or R_g (see Fig. 1). It is, however, possible to include the effect of R and R_g in Fig. 1 by including them in R_0 .

The ranges of fault voltages for ratios of R_0/X_1 between zero and six are shown in Fig. 6. The ratios X_0/X_1 and

X_2/X_1 cover the same ranges as in Fig. 5. In the preparation of these curves fault resistance has been neglected. All voltages are measured to true ground at the point of fault.

In special cases, for example in the application of lightning arresters, it is necessary to consider the effect of fault resistance on the voltages produced during single line-to-

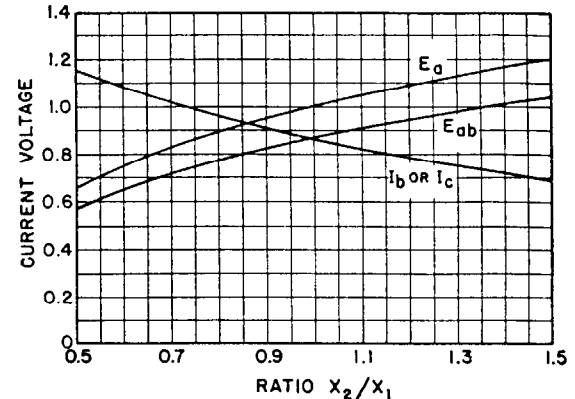


Fig. 4—Curves of fault voltages and currents vs. system reactances for line-to-line faults. Line-to-ground and line-to-line voltages are expressed as ratios to their respective normal values. Current is expressed as a ratio to the three-phase short-circuit current. All resistances are assumed equal to zero.

ground faults. The curves in Figs. 7 and 8 include this factor. The curves in Fig. 7 give the highest voltages from line to true ground for a fault through a fault resistance R_{ft} .

TABLE 2—FAULT VOLTAGES

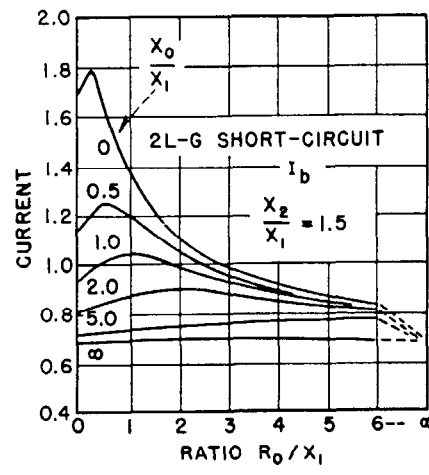
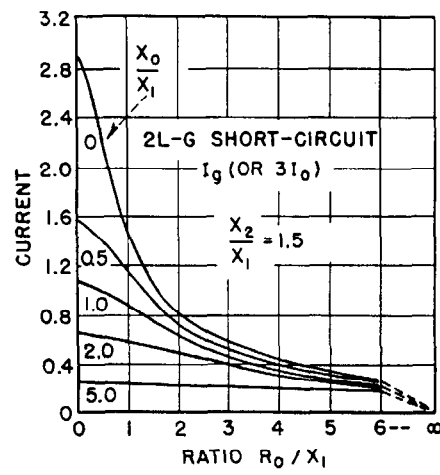
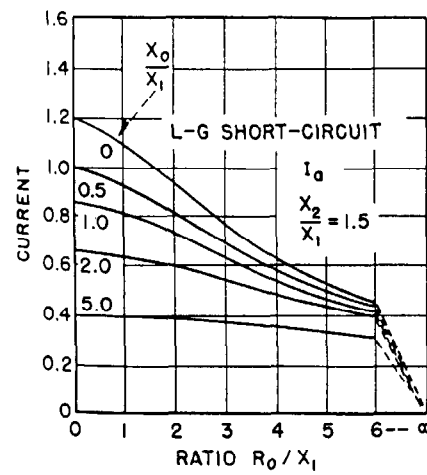
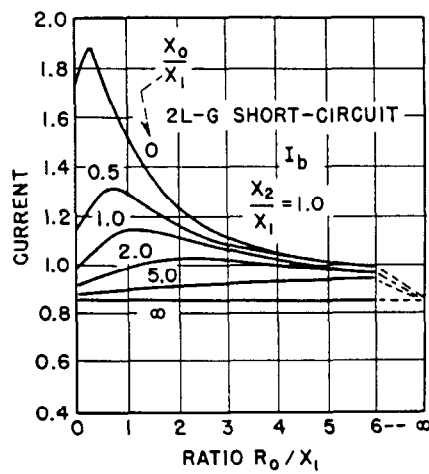
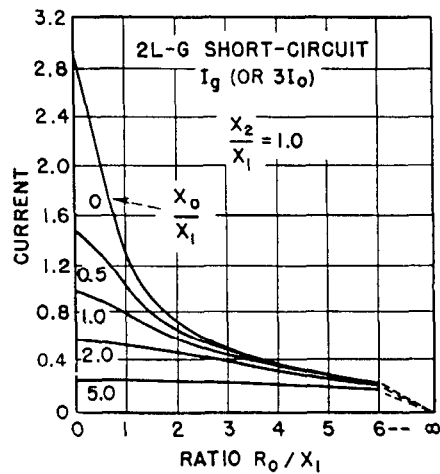
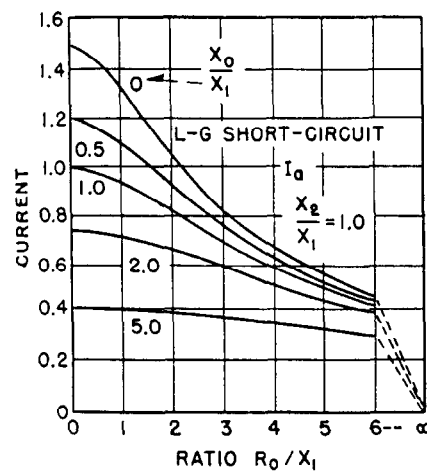
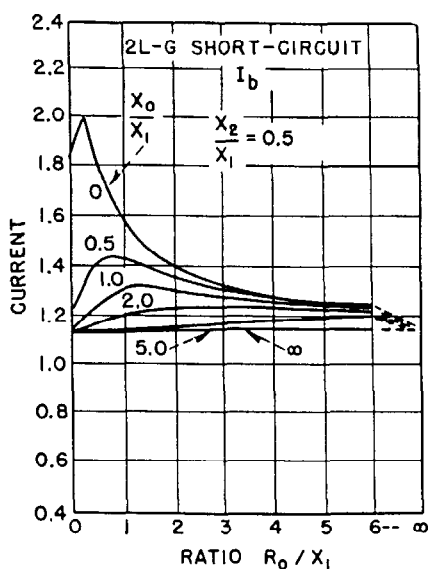
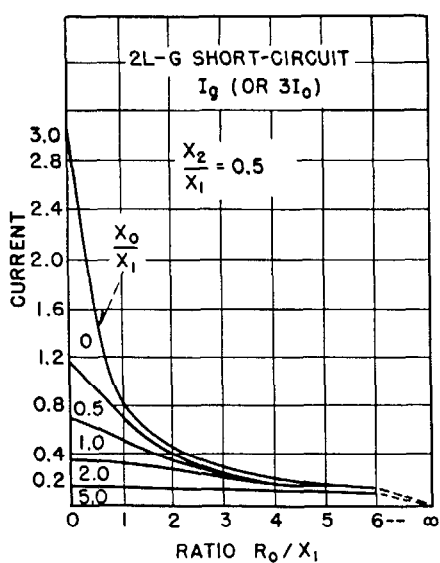
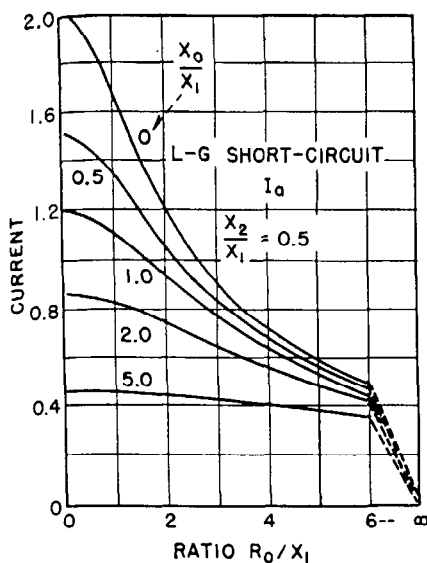
Type of Fault	Vector Expression, Effect of Fault Resistance Included	Magnitude of Voltages When $R_0 = R_1 = R_2 = 0$
Three-phase.....	$E_a = E_g \frac{R}{Z + R}$	$E_a = 0$
Line-to-line.....	$E_a = E_g \frac{2Z_2 + R}{Z_1 + Z_2 + R}$ $E_b = -E_g \frac{\frac{R}{2} + j\frac{\sqrt{3}R}{2}}{Z_1 + Z_2 + R}$ $E_c = -E_g \frac{\frac{R}{2} - j\frac{\sqrt{3}R}{2}}{Z_1 + Z_2 + R}$	$E_a = E_g \frac{2X_2}{X_1 + X_2}$ $E_b = E_c = E_g \frac{X_2}{X_1 + X_2}$ $E_{ab} = E_{ac} = E_g \frac{3X_2}{X_1 + X_2}$
Single line-to-ground.....	$E_a = E_g \frac{3R}{Z_0 + Z_1 + Z_2 + 3R}$ $E_b = -\frac{\sqrt{3}E_g}{2} \left[\frac{\sqrt{3}(Z_0 + R) + j(Z_0 + 2Z_2 + 3R)}{Z_0 + Z_1 + Z_2 + 3R} \right]$ $E_c = -\frac{\sqrt{3}E_g}{2} \left[\frac{\sqrt{3}(Z_0 + R) - j(Z_0 + 2Z_2 + 3R)}{Z_0 + Z_1 + Z_2 + 3R} \right]$	$E_a = 0$ $E_b = E_c = \sqrt{3}E_g \frac{\sqrt{X_0^2 + X_0X_2 + X_2^2}}{X_0 + X_1 + X_2}$ $E_{bc} = \sqrt{3}E_g \frac{X_0 + 2X_2}{X_0 + X_1 + X_2}$
Double line-to-ground.....	$E_a = \frac{3E_g}{\Delta v} (Z_2 + R_L)(Z_0 + R_L + 2R_g)$ $E_b = \frac{-\sqrt{3}E_g}{2\Delta v} \left[\sqrt{3}(Z_2 + R_L)(R_L + 2R_g) + jR_L(2Z_0 + Z_2 + 3R_L + 6R_g) \right]$ $E_c = \frac{-\sqrt{3}E_g}{2\Delta v} \left[\sqrt{3}(Z_2 + R_L)(R_L + 2R_g) - jR_L(2Z_0 + Z_2 + 3R_L + 6R_g) \right]$ $\Delta v = (Z_1 + R_L)(Z_2 + R_L) + (Z_1 + Z_2 + 2R_L)(Z_0 + R_L + 3R_g)$	$E_a = \frac{3E_g X_0 X_2}{\Delta v}$ $E_b = E_c = 0$ $E_{ab} = E_{ac} = E_a$ $\Delta v = X_1 X_2 + X_0(X_1 + X_2)$

Z_1 =positive-sequence impedance to the point of fault

Z_2 =negative-sequence impedance to the point of fault

Z_0 =zero-sequence impedance to the point of fault and does not include any fault resistance

See Fig. 1 for definitions of R , R_L and R_g



(a) LINE CURRENT
SINGLE LINE-TO-GROUND FAULT

(b) GROUND CURRENT
DOUBLE LINE-TO-GROUND FAULT

(c) LINE CURRENT
DOUBLE LINE-TO-GROUND FAULT

Fig. 5—Curves of fault currents vs. system impedances. The legend with each group of curves indicates the type of fault, the current plotted, and the ratio X_0/X_1 . The individual curves in each group are for various values of the ratio of X_0/X_1 . All currents are expressed as a ratio to the three-phase short-circuit current. R_0 is the zero-sequence resistance to the point of fault and does not include any fault resistance; the fault resistance is assumed equal to zero¹.

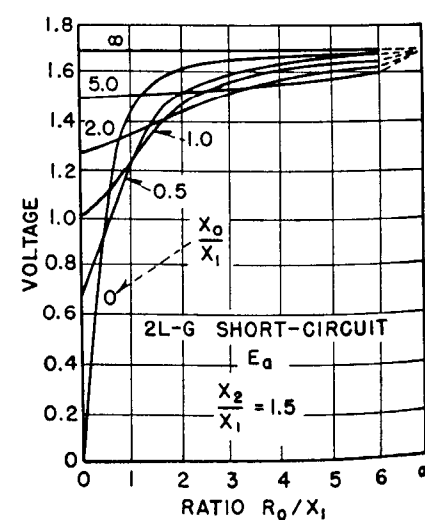
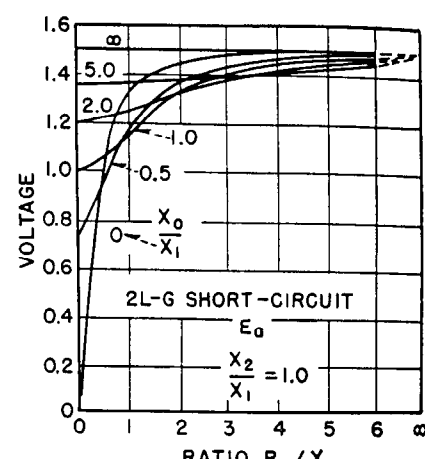
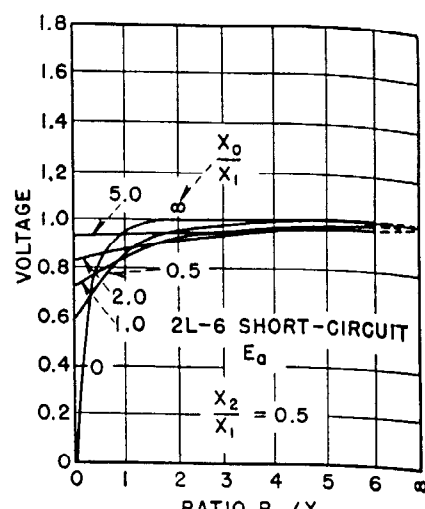
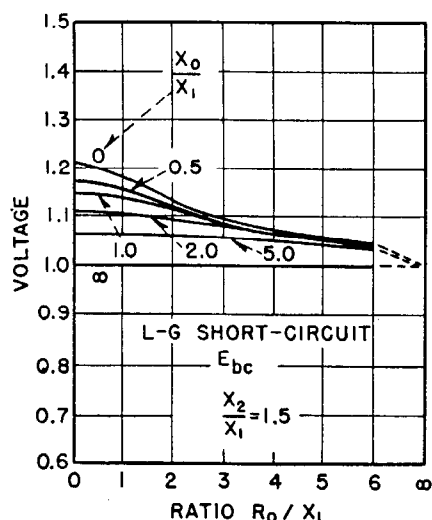
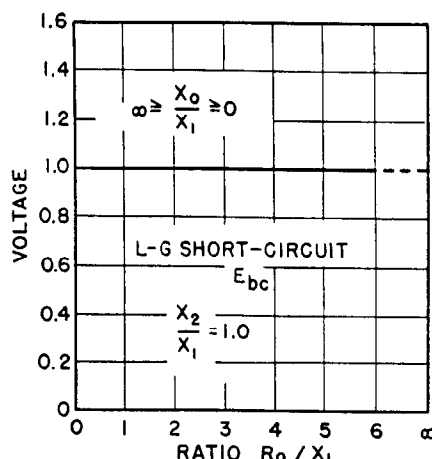
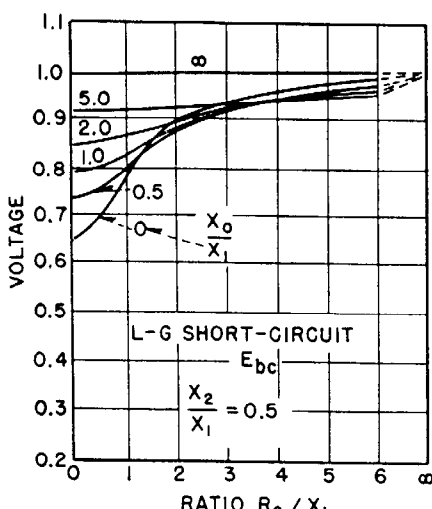
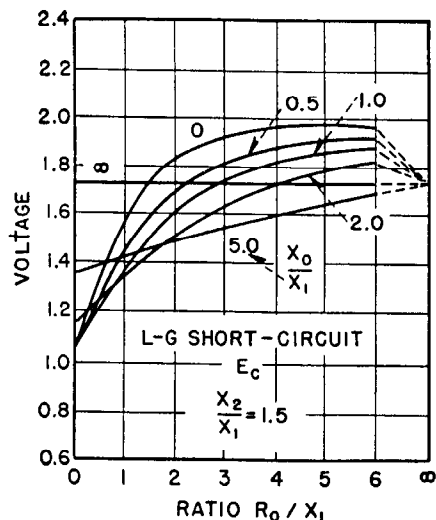
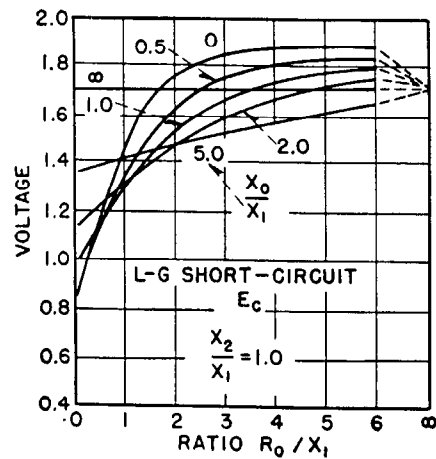
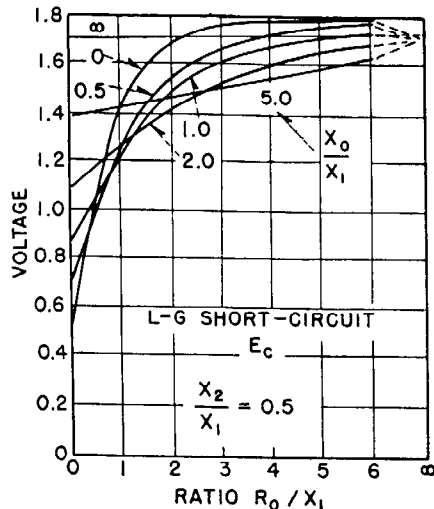


Fig. 6—Curves of fault voltages vs. system impedances. The legend with each group of curves indicates the type of fault, the voltage plotted, and the ratio of X_2/X_1 . The individual curves in each group are for the various values of the ratio of X_0/X_1 . Line-to-ground and line-to-line voltages are expressed as ratios to their respective normal values. R_0 is the zero-sequence resistance to the point of fault and does not include any fault resistance; the fault resistance is assumed equal to zero¹.

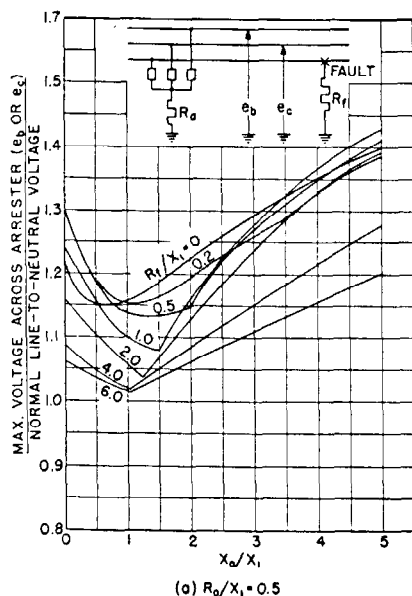
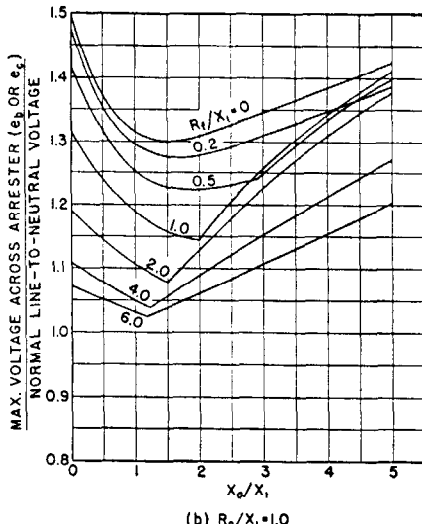
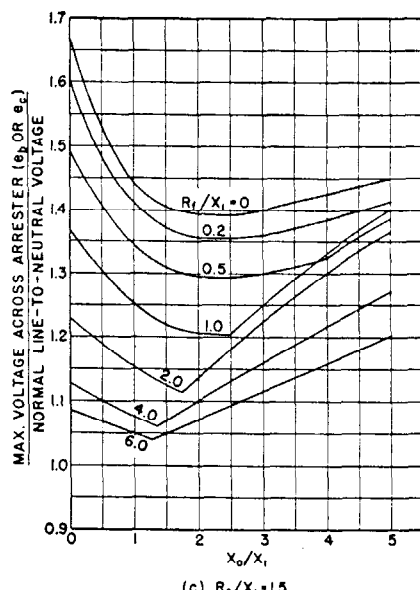
(a) $R_o/X_1 = 0.5$ (b) $R_o/X_1 = 1.0$ (c) $R_o/X_1 = 1.5$

Fig. 7—Curves of line-to-ground voltages vs. system impedances for a single-line-to-ground fault through a fault resistance R_f . R_o is the zero-sequence resistance to the point of fault and does not include R_a or R_f . X_2/X_1 is assumed equal to 1.0.

These curves cover a range of R_f/X_1 of zero to 6 and a range of R_o/X_1 of from 0.5 to 1.5. R_o is the zero-sequence resistance to the point of fault and does not include R_f .

The curves in Fig. 8 show the voltages across an arrester for a fault to the arrester neutral. As in Fig. 7, R_o is the zero-sequence resistance to the point of fault and does not include R_a .

Reference should also be made to Figs. 28 and 29 of Chap. 18, particularly in lightning arrester application

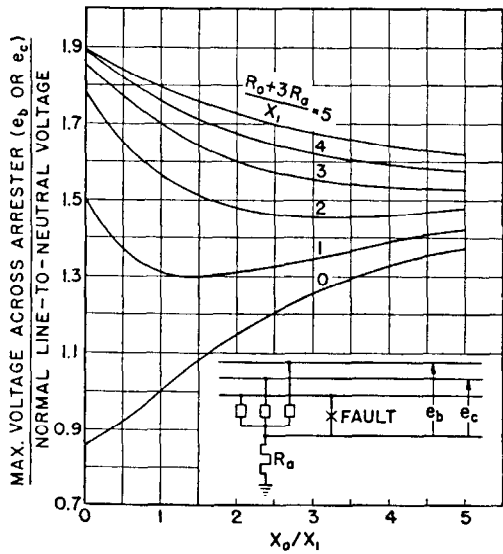


Fig. 8—Curves of the maximum voltages across a lightning arrester for a fault to the lightning arrester neutral point. R_o is the zero-sequence resistance to the point of fault and does not include R_a , the resistance of the arrester ground. The fault resistance is assumed equal to zero and X_1/X_2 is assumed equal to 1.0.

problems. These figures give the maximum line-to-ground voltages during single- or double-line-to-ground faults on ungrounded and grounded-neutral systems.

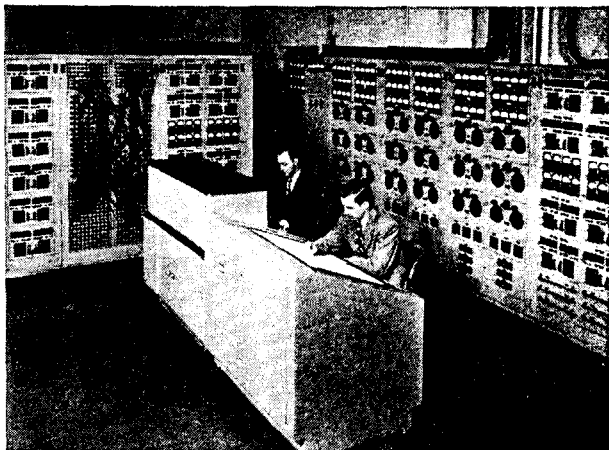


Fig. 9—A-c network calculator.

II. TRANSIENT VOLTAGES

A transient voltage of some magnitude is present on a power system each time a circuit change is made. This circuit change may be a normal switching operation such as the opening of a circuit breaker, or it may be a fault condition such as the grounding of a line conductor. The existence of transient voltages on power systems as a result of circuit changes caused by switching operations or faults was recognized at an early date². The phenomena, however, were not thoroughly investigated at the time because suitable measuring and recording devices were not available and because the immediate difficulties were largely overcome by the adoption of the practice of grounding power systems. The invention by J. F. Peters³ of the "klydonograph" made possible the collection of a mass of field data on transient voltages. However, the time and expense involved in making extensive field studies limited the scope of these investigations. Furthermore many investigators were concentrating their efforts on lightning, a

much more important problem at that time. The introduction of the protector tube for the protection of transmission lines, however, showed the need for a better understanding of power system transients because its performance is greatly affected by them. The first attempts to calculate transient voltages were made by conventional methods using differential equations. The limitations of conventional mathematical methods were soon apparent, however, because of the tremendous amount of time required. The introduction of the A-C Network Calculator Method of Studying Power System Transients⁴ gave a practical tool for studying the behavior of power systems under transient conditions and made possible general investigations of power-system transients. The later development of the Anacom, or analog computer,⁵ further increased the possible scope of power system investigations. It is the purpose of the following sections to describe these computing devices, and to present the results of general studies made with them.

5. The A-C Network Calculator Method of Studying Transient Voltages

To study transients on power systems by the A-C Network Calculator Method, the system in question is set up in miniature on the A-C Network Calculator. In Fig. 10 is shown the equivalent circuit for a relatively simple system consisting of a generator, a transformer, and a transmission line. The generator is represented by a low-impedance three-phase supply with additional impedance in series to give the miniature system the same impedance as the impedance of the actual system. The zero-sequence impedance of the source is represented by a grounding transformer of low impedance grounded through reactance or

depends upon several factors, such as line length, supply impedance, etc.

After the miniature system has been set up as shown in Fig. 10, the equipment shown diagrammatically in Fig. 11 is used for performing switching operations or for applying faults. Each of the synchronous switches shown at the

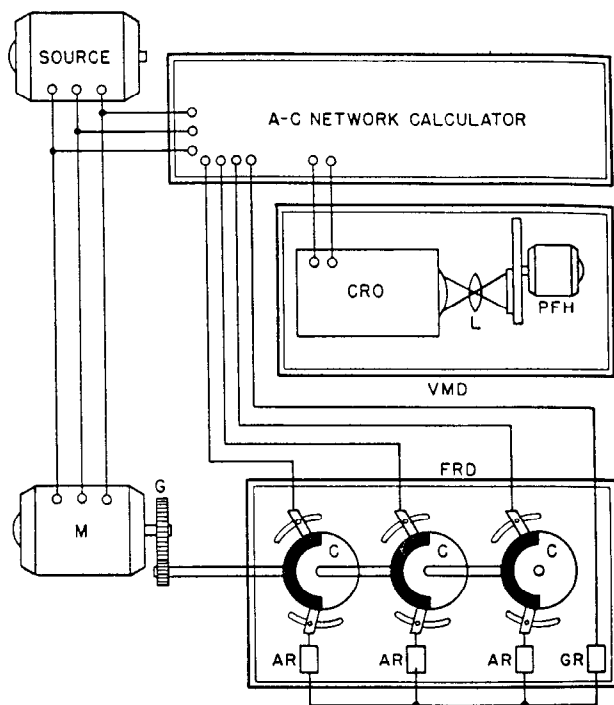


Fig. 11—Schematic diagram showing equipment used in a-c network calculator method of studying transients.

- M—Synchronous motor
- G—Gear
- FRD—Fault representation device
- C—Synchronous switches
- AR—Arc resistance representation
- GR—Ground resistance representation
- VMD—Voltage measuring device
- CRO—Cathode-ray oscilloscope
- L—Lens system
- PFH—Polar film holder

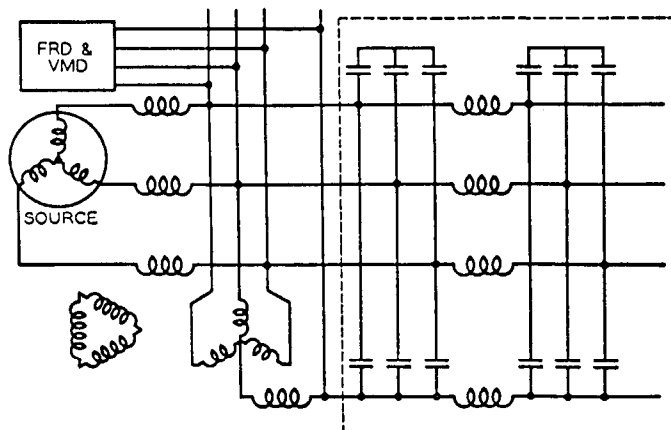


Fig. 10—Schematic diagram illustrating method of system representation used on the a-c network calculator.

- FRD—Fault representation device
- VMD—Voltage measuring device

resistance depending upon the type of grounding used. In the equivalent circuit in Fig. 10 the transmission line is represented by an equivalent π section. This type of line representation is used in some studies but often it is necessary to employ more complicated networks. The choice of the network to use for representing a section of line

bottom of Fig. 11 consists essentially of a conducting and an insulating segment on a drum and two movable brushes, one for controlling the closing and the other the opening of the switch. Each brush is located on a gear that can be rotated by a worm, making the brush adjustable through 360 degrees.

For representing faults on power systems the switches are connected between line and ground or between lines depending upon the type of fault being studied. Where circuit breaker operations are to be simulated the switches are inserted in series with the line. The switching operations are repeated once per revolution of the drum and, as the drums are rotated by a synchronous motor, the switching operations always take place in synchronism with the system voltage. The transient voltage produced by the switching operation is therefore repeated once per revolution of the drum. All transient voltages are measured by a

cathode-ray oscilloscope connected to the miniature network. By repeating the transient a number of times per second, the equivalent of a steady-state voltage is produced on the screen of the cathode ray oscilloscope. This makes it possible to study a transient that lasts for a fraction of a cycle without taking oscillograms. The effect of initiating

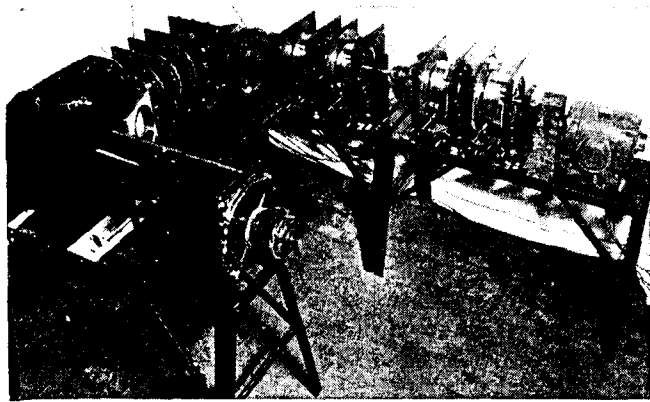


Fig. 12—Switching and recording equipment used with a-c network calculator.

the transient at different points on the normal dynamic voltage wave can be studied by simply changing the positions of the brushes on the synchronous switch. The time interval between successive transients is so chosen as to bring the system back to normal between switching operations.

6. The Analog Computer

The analog for many systems (electrical, mechanical, thermal, etc.) requires low-loss inductance coils, amplifiers, multipliers, and other special circuit elements. The analog computer,⁵ or Anacom, was developed primarily for the solution of these systems. Its characteristics, however, make it ideally suited to the solution of all power-system transient problems formerly studied on the a-c network calculator. The Westinghouse Electric Corporation now makes all electric transient studies on the Anacom, reserving the a-c network calculator for power system problems such as voltage regulation, load flow, stability, etc.

In most cases the procedure for setting up a problem and obtaining a solution is the same with the Anacom as with

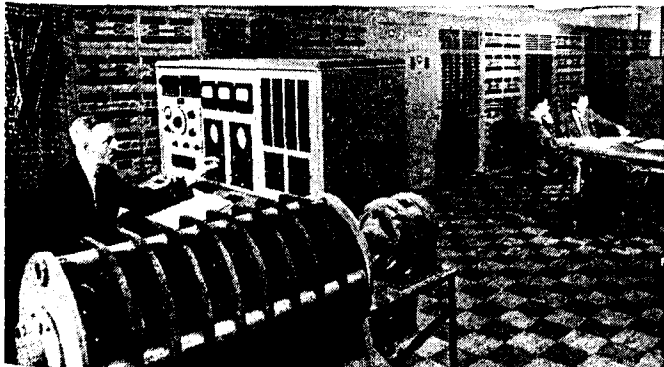


Fig. 13—General view of the large-scale, general-purpose electric analog computer.



Fig. 14—Close-up view of the Anacom control desk and synchronous switch.

the a-c network calculator. An analog is formed by connecting circuit elements, R , L , and C , into a circuit that has the same differential equation as the system under consideration. Synchronous switches are usually used to repeat the desired transient solution a number of times per second, which permits visual and photographic measurements on a cathode-ray oscilloscope. In power system studies the switches normally represent circuit breaker operation or faults.

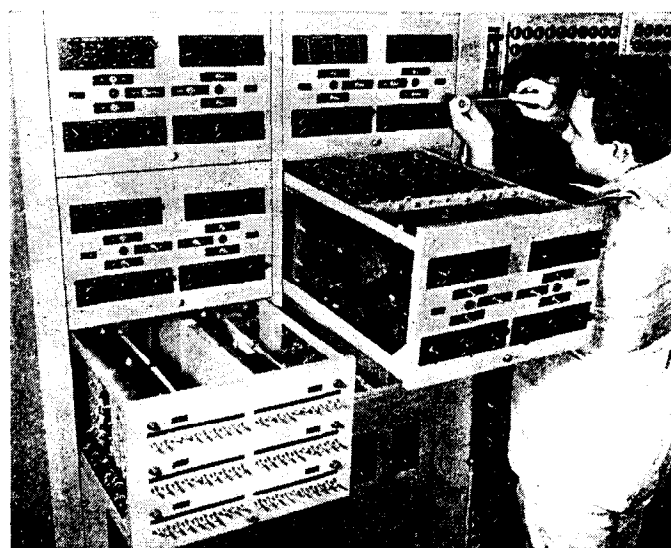


Fig. 15—Details of an Anacom inductance-resistance drawer.

The computer elements include inductance coils having a Q of 100 or higher over the frequency range from 100 to 1000 cycles; precision capacitors and resistors; special transformers having minimum exciting current, leakage impedance, and distributed capacitance; amplifiers, and multipliers. Special analogs have been developed to represent lightning arresters, corona, and other non-linear char-

acteristics. The use of the synchronous switches in combination with R , L , and C circuit elements, amplifiers and multipliers permit the formation of special forcing functions such as lightning surges, air-gap torques in turbine generators during short circuits, etc. The measuring equipment includes cathode ray oscilloscopes with suitable photographic means, harmonic analyzers, wire and tape recorders, and all types of conventional ammeters, voltmeters and wattmeters.

The Anacom is arranged with d-c, 440-cycle, and 60-cycle power supplies to solve problems normally assigned to the a-c and d-c network calculators; however it is normally used in the transient field. It is suited to the solution of many problems of concern to power company engineers, including recovery voltage, switching-surge and arcing-ground investigations, surge-protection applications, turbine generator short-circuit torques, analysis of generator voltage regulating systems and motor-starting problems. It can be used in solving many equipment design problems such as surge-voltage distribution in transformers and rotating machines, dielectric field mapping, and heat-flow. Its possible application in the fields of applied mechanics, hydraulics, thermodynamics and servomechanisms is almost unlimited.

7. Recovery Voltage

Theory—One transient phenomenon studied by the A-C Network Calculator Method is system recovery voltage, which is important because of its effect upon the operation of circuit interrupting and protective devices, such as circuit-breakers, protector tubes, etc. The simple circuit in Fig. 16 can be used for defining system recovery volt-

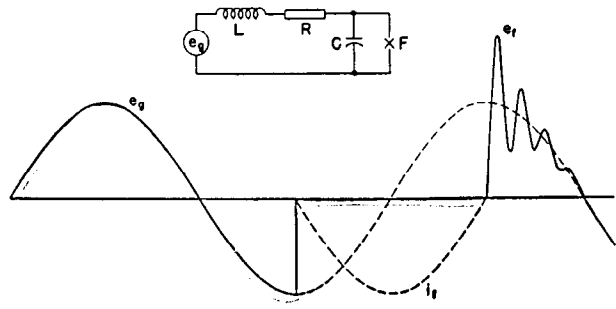


Fig. 16—Simple system for illustrating recovery voltage for a fault (F).

e_f —Voltage across fault
 i_f —Fault current

ages. In this circuit a condenser C is used to represent a transmission line, and a voltage and an impedance, the source. Applying a short-circuit across the condenser in this circuit is equivalent to applying a line-to-ground fault on a single-phase power system. During the time the condenser is short-circuited, a fault current i_f will flow. If the resistance in the source is small in comparison to the reactance, this fault current will lag the generated voltage e_g by approximately 90 degrees. If the short-circuit is removed at the instant the fault current passes through zero, the voltage across the condenser will not immediately return to normal but will reach normal only after a series of oscilla-

tions. No voltage can appear across the condenser until it is charged up and the charging rate is fixed by the source inductance and the capacitance. When the short-circuit is removed, the condenser voltage will be accelerated toward normal but will overshoot because of the circuit inductance. If no losses were present in the circuit the transient voltage across the condenser would reach a crest equal to twice normal crest voltage. In a practical circuit with some loss, the oscillation will not quite reach twice normal; it will eventually be damped out, leaving only the normal-frequency voltage across the condenser.

This transient voltage across the condenser, following the removal of the fault, is commonly referred to as the system recovery voltage as it defines the manner in which the system voltage "recovers" following the removal of the fault. Changing the source reactance in the circuit in Fig. 16 is equivalent to changing the amount of generation connected in a power system, and changing the value of capacitance is equivalent to varying the length of line connected. The natural frequency of the oscillation in the circuit in Fig. 16 depends upon both the inductance and the capacitance and varies inversely as the square root of the product of these two quantities. The recovery voltage of a power system therefore depends upon the connected generator capacity and the length of line.

The De-ion Protector Tube—As previously stated, recovery voltage is important because of its effect on the performance of circuit interrupting and protective devices. This can be shown by a detailed study of the operation of a De-ion protector tube. A typical installation of protector tubes is shown in Fig. 17. In this case the protector tube is mounted vertically just below the line conductors. The lower electrode of the tube is connected to ground and the upper electrode is connected to an arcing horn used to maintain a constant external gap between the upper elec-

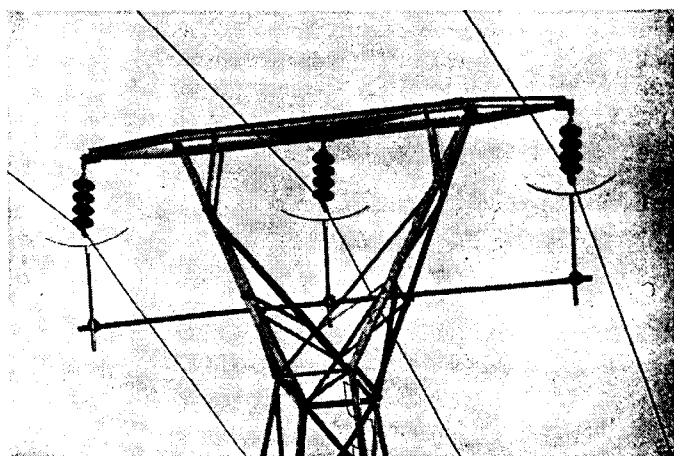


Fig. 17—Typical installation of De-ion protector tubes.

trode and the line conductor. The cross-section of a protector tube in Fig. 18 shows the two electrodes and the internal gap. In operation, lightning striking the line breaks down the series gap instead of flashing over the insulator string because the tube has the lower breakdown voltage. After breakdown of the gap, power-follow current volatilizes a small layer of the fiber wall and the gas given

off mixes in the arc to help de-ionize the space between the electrodes. A pressure is built up in the tube and the hot gases are discharged through the lower electrode, which is hollow. If the de-ionizing action is sufficiently strong and if the voltage does not build up too rapidly across the tube, the arc will go out at a current zero and will not be re-established.

While the tube is discharging, it is a good conductor and after the arc has been extinguished it is a good insulator.

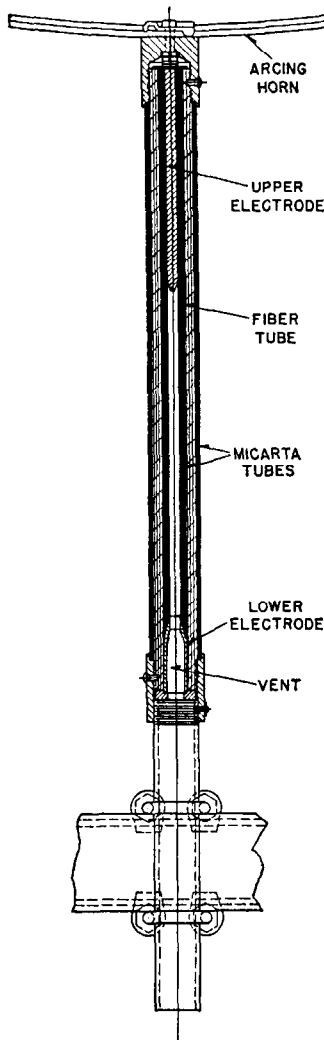


Fig. 18—Cross-section of a typical De-ion protector tube.

This change from a good conductor to a good insulator does not take place instantaneously because time is required to discharge the hot gases from the tube. It is therefore important that the voltage across the tube does not build up more rapidly than the change in the protector tube dielectric strength. This is where recovery voltage enters the picture because recovery voltage determines the rate of build-up of the voltage across the tube.

In Fig. 19 the recovery voltage for the circuit in Fig. 16 is replotted to a larger scale. Curves A and B in this figure are typical of the shape of insulation recovery curves for two different protector tubes. It is of utmost importance that the protector tube insulation recovery curves always

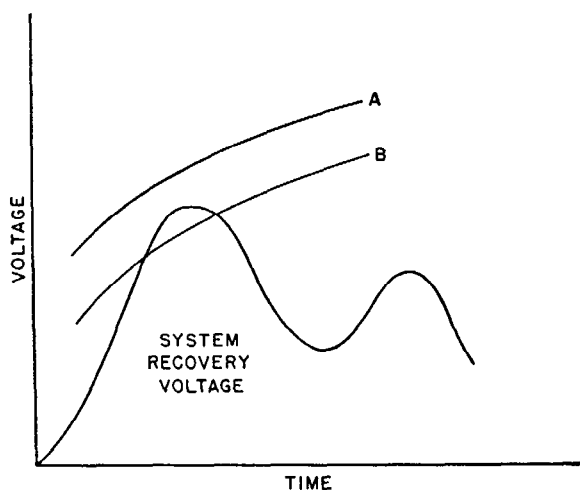


Fig. 19—Comparison of system recovery voltage and insulation recovery curves.

A—Insulation Recovery Curve for Tube A
B—Insulation Recovery Curve for Tube B

lie above the system recovery voltage curve, otherwise the arc will be re-established in the tube. Protector tube B would not operate satisfactorily on a system having recovery voltage characteristics similar to the recovery voltage in Fig. 19. A tube similar to tube A would have to be used.

The recovery voltage for the simple circuit in Fig. 16 is made up of a single-frequency oscillation. In a practical power system, the recovery voltage does not usually consist of a single-frequency oscillation but is usually made up of two or more high-frequency components. In Fig. 20 is shown the recovery voltage following a single line-to-ground fault on a 138-kv, three-phase system having a symmetrical three-phase short-circuit current of 1000 amperes and 90 miles of overhead transmission line. The recovery voltage in this case consists of two high-frequency components and is typical of the shape of the recovery voltage on many three-phase power systems.

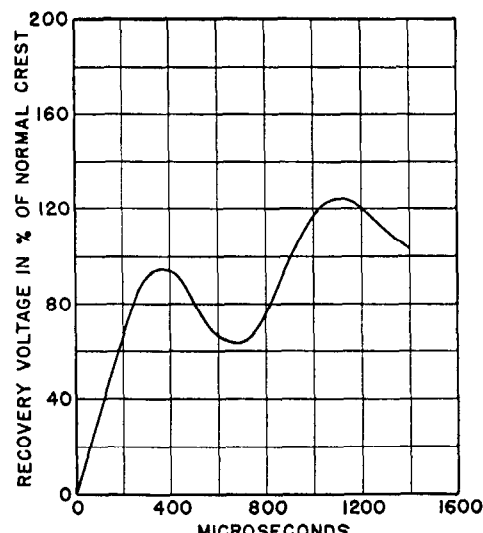


Fig. 20—Recovery voltage curve for a typical power system.

General Recovery Voltage Study—A broad perspective of the recovery-voltage problem can be obtained from the study of a representative set of systems. For this purpose three-phase, 60-cycle systems with transmission lines of three voltage classes, namely, 34.5, 69, and 138-kv were selected. Since the recovery voltage of a system is materially affected by the length of connected line, the lengths were selected to represent the shortest that would be encountered at that particular voltage for the large majority of systems. These selections were as follows: 22.5 miles for 34.5 kv, 45 miles for 69 kv, and 90 miles for 138 kv. Although it was recognized that more than one circuit would be required to transmit the maximum amount of power a single-circuit line was used because this gives the more severe recovery-voltage conditions.

The general features of these systems are shown schematically in Fig. 21. For each voltage class three different

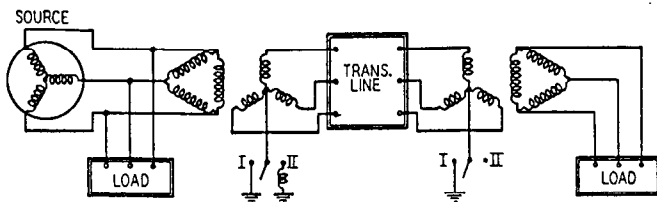


Fig. 21—Schematic diagram of system selected for study.

Group I. Solidly grounded at both ends. Used for curves of Fig. 22.

Group II. Reactance grounded at sending end; ungrounded at receiving end. Used for curves of Fig. 23.

conditions were assumed, each having different amounts of generating capacity and load. Table 3 gives the symmetrical three-phase short-circuit current that would be encountered for a "bolted fault" at the sending end. Systems capable of supplying the higher short-circuit currents have in general larger connected loads. Table 3 gives the ratio of short circuit kilovolt-amperes to load kilovolt-amperes

TABLE 3—CHARACTERISTICS OF SYSTEMS SELECTED FOR STUDY

Voltage	34.5 Kv	69 Kv	138 Kv
Short-Circuit Amperes			
(a)	500	500	500
(b)	2 000	2 000	1 000
(c)	6 000	6 000	4 000
Short-Circuit KVA			
Load KVA	5.0	4.0	3.0
Line Length (miles)	22.5	45	90

that was used in this study. Both no-load and loaded conditions were considered. An 80 percent power factor load was divided equally between the generator bus and the receiver bus as shown in Fig. 21.

The generating and transformer capacities were proportioned to the load for the particular system and short-circuit current, and typical constants were assumed for all of the system elements. Transmission lines without ground wires were chosen. The additional complication to take care of the cases with ground wires is not warranted be-

cause the problems are similar and also the recovery voltages are less severe when ground wires are used.

In making the general analysis the factors varied were: method of grounding, load, type of fault, fault resistance, arc resistance, and location of fault. The studies can conveniently be divided into two groups with respect to the method of grounding, namely: group I with system solidly grounded both at sending- and receiving-end transformers, and group II with the system grounded through a reactance at the sending end only. The solidly grounded systems, of group I, were studied for both single line-to-ground and double line-to-ground faults and for fault or tower-footing resistance of 0, 25, and 100 ohms, and with and without resistance for arc representation. The effect of load was investigated by comparing the results of the above tests with results of a few tests made without load and without fault or arc resistance. The second set of tests for the reactance-grounded system, group II, was made with the addition of a neutral reactor of such magnitude as to make the zero-sequence reactance at the sending end equal to 8.5 or 34 times the zero-sequence reactance of the supply transformer.

Results of General Study—In an investigation of this type it is not practical to consider the application of the fault at several points of the system. A preliminary study was, therefore, made to determine the effect of moving the fault along the line. Considering the shape of insulation-recovery voltage curves for specific pieces of apparatus, it was concluded that the recovery-voltage conditions were about as severe for faults at the sending end as at any location along the line. Therefore, the fault at the sending end was considered to be representative and was used in the general studies.

Based on the selected systems, a series of studies was made on the a-c network calculator to determine the effect of the different factors entering into the recovery-voltage problem. These studies may be divided into two groups; group I for systems with solidly-grounded neutral, and group II for the reactance-grounded systems, described in connection with Fig. 21. The results of these studies are presented in Figs. 22 and 23 respectively. The manner in which these data are plotted can more readily be understood by referring to Fig. 20. The recovery voltage curve in this illustration has two predominate crests. If the insulation recovery curve for a protector tube lies above these crests, the tube will perform satisfactorily. In the general application of protector tubes it is not necessary to have the complete recovery-voltage curve if the data corresponding to these predominate crests are available. Therefore, in summarizing the results of the general study only the data pertaining to these predominate crests were plotted in Figs. 22 and 23.

Referring to Fig. 22, it will be seen that for each voltage class studied the time to the first crest and to the maximum overshoot, as well as the magnitude of the first crest and the maximum overshoot are presented for the single line-to-ground and double line-to-ground fault cases. For these curves the abscissa is the current magnitude for a symmetrical three-phase short-circuit at the sending end. The results for a system under load are plotted for each current condition, with and without the arc representation device

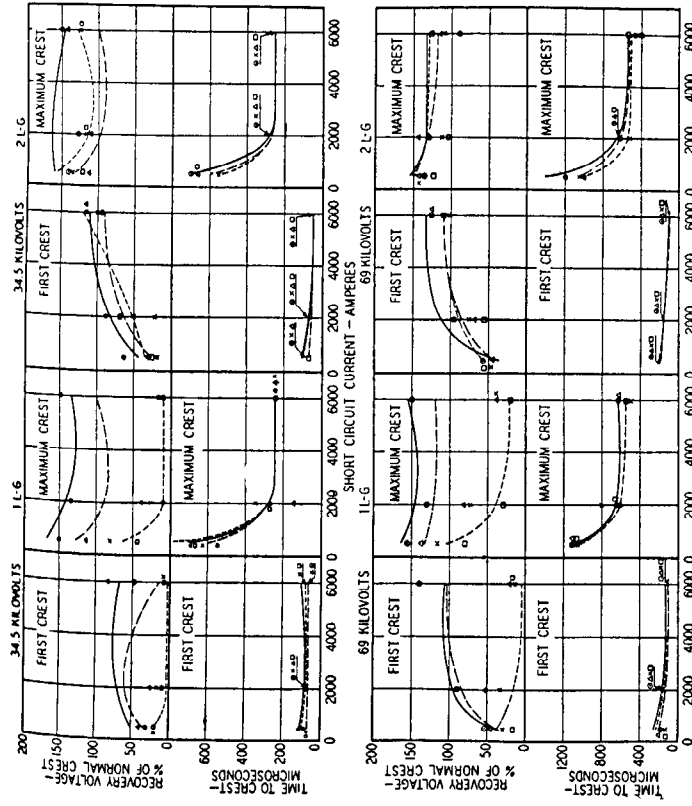
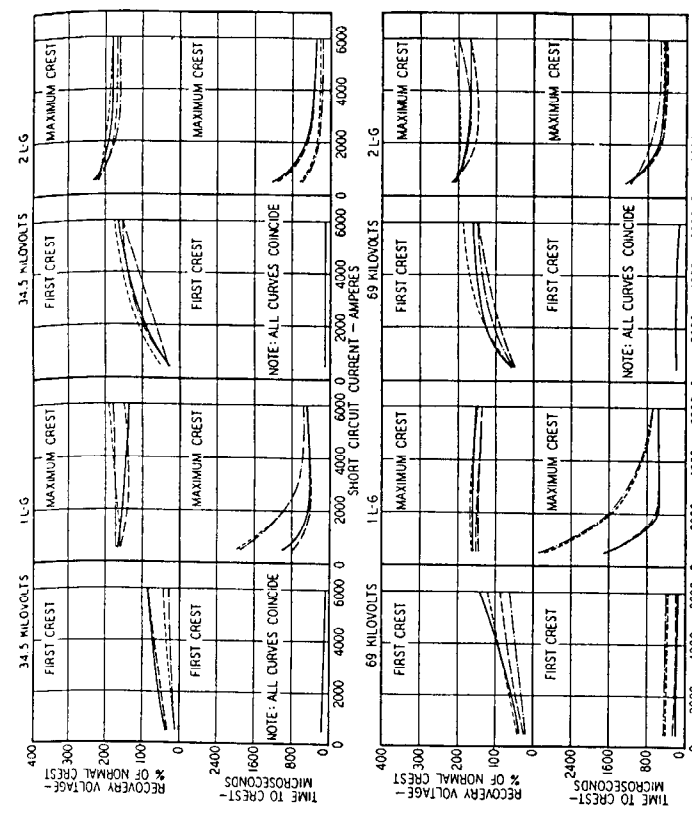


Fig. 22—Recovery voltage curves and plotted points for the nine selected systems.

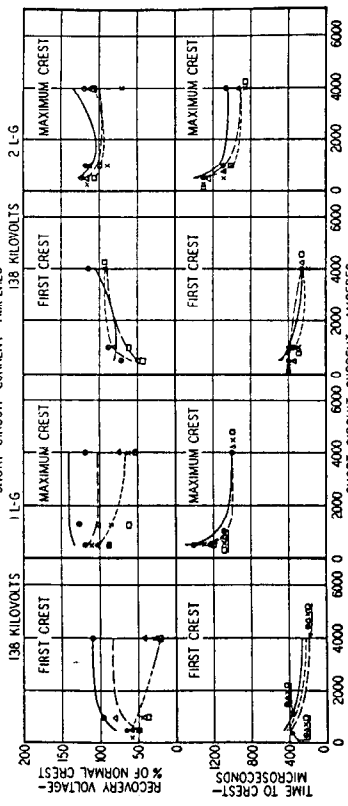
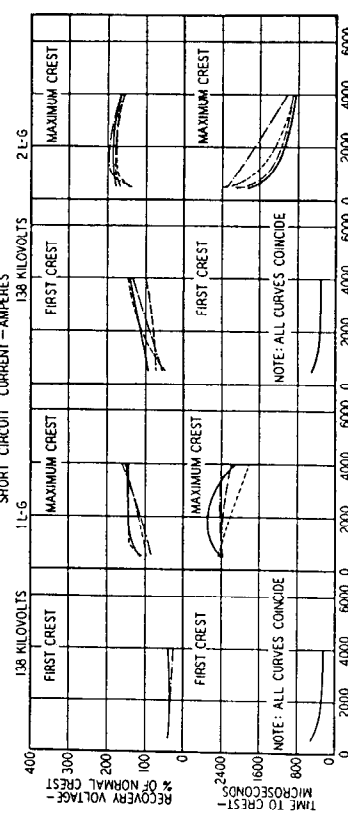


Fig. 22—Recovery-voltage curves.

Group I. Solid grounding.	Voltage magnitude and time to crest plotted as a function of three-phase symmetrical short-circuit current at the sending end.	Arc Resistance	Tower-Footing or Ground Resistance (Ohms)
No	No	No	0
Yes	Yes	Yes	0
Yes	No	No	100
Yes	Yes	No	0
Yes	Yes	Yes	25
Yes	X Yes	Yes	25
□ Yes	□ Yes	Yes	100

1-L-G—single line-to-ground fault.
2-L-G—double line-to-ground fault.

Group II. Reactance grounding.	Voltage magnitude and time to crest plotted as a function of the three-phase symmetrical short-circuit current at the sending end.	Reactance Value	Arc Resistance
No	No	Low	No
Yes	Yes	Low	Yes
No	No	High	No
Yes	Yes	High	Yes

1-L-G—single line-to-ground fault.
2-L-G—double line-to-ground fault.

for 0-, 25-, and 100-ohms tower-footing resistance. For comparison, one study with no load and with zero arc and tower-footing resistance is plotted. The arc representation device makes use of Rectox resistors to simulate the arc characteristics of a protector tube. The Rectox resistor was adjusted to give approximately 20 percent of line-to-neutral voltage at the peak of the symmetrical short-circuit current wave.

Fig. 23 presents the results of similar studies made on the same systems except with reactance grounding. The system arrangement with respect to grounding is shown in Fig. 21.

Application of Data—Although the recovery-voltage data presented are useful in a number of applications, the particular application of the protector tube will be taken as an illustration. The case of a 34.5 kv solidly-grounded system with 22.5 miles of transmission line with a symmetrical three-phase short-circuit current of 4,000 amperes at the sending end has been selected. No-load and zero-arc and tower-footing resistance give the highest recovery voltage for both single-line-to-ground and double-line-to-ground faults as shown in Fig. 22. The data for these two cases have been plotted in Fig. 24. The insulation recovery curves for two protector tubes are also included in this figure. Curve T_1 extends below the system recovery voltage curve for the case of a single-line-to-ground fault but is always above the corresponding curve for the case of a double-line-to-ground fault. As both types of faults must be considered in the application of protector tubes, a tube

having characteristics similar to curve T_2 should be used for this system.

Using the data in Figs. 22 and 23 it is possible to predict the performance of any protector tube on any of the typical systems studied in this general investigation. A more detailed discussion of the application of these data is included in Chap. 17.

8. Distribution-System Recovery Voltage Characteristics

The data in Sec. 7 are not generally applicable to the lower-voltage circuits because of the differences in source reactances, circuit arrangements, line lengths, conductor spacings, etc. For this reason, a study⁷ was made on the analog computer to obtain fundamental data on the re-

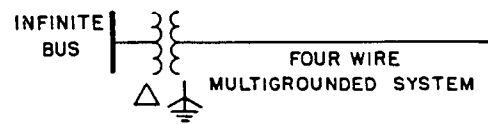


Fig. 25—Distribution system selected for study on Anacom.

covery voltage characteristics of circuits in the 2400-to 13 800-volt range. The general study was limited to the case of a four-wire, multi-grounded system supplied from a delta-star power transformer, connected to an infinite bus on the primary side and solidly grounded on the secondary side.

Geometric-mean distances of 2.66 feet between phase conductors, and 4.1 feet between the phase and the neutral conductors were assumed. These spacings give reactances that are an average of the values obtained over the range of spacings normally used between 2400 and 13 800 volts. The small variations introduced by changes in spacing are not considered significant in the general problem. A conductor height of 30 feet and a ground resistivity of 100 meter ohms were used in all studies. The phase- and neutral-conductor sizes were assumed to be the same, and were varied between 4/0 and No. 6 copper. The line constants for these two extreme conductor sizes are included in Table 4.

TABLE 4—CONSTANTS OF TYPICAL DISTRIBUTION CIRCUITS

System	Copper Size	Z_1	Z_0	C_1	C_0
4-wire	4/0	$0.278+j0.615$	$0.564+j1.89$	0.0187	0.0078
	No. 6	$2.18+j0.756$	$2.93+j2.77$	0.0149	0.0069
3-wire	4/0	$0.278+j0.615$	$0.564+j3.15$	0.0187	0.0063
	No. 6	$2.18+j0.756$	$2.47+j3.29$	0.0149	0.0059
Single-phase	4/0	$Z = 0.373+j1.04$			

Note: All impedances in ohms per mile at 60-cycles. All capacitances in microfarads per mile.

Fault location was found to have a significant effect so faults were applied on the sending-end bus and at the $\frac{1}{4}$, $\frac{1}{2}$, and 1.0 points, the latter being the open end of the line.

The studies were made by applying single- and double-line-to-ground faults at four locations, and recording the

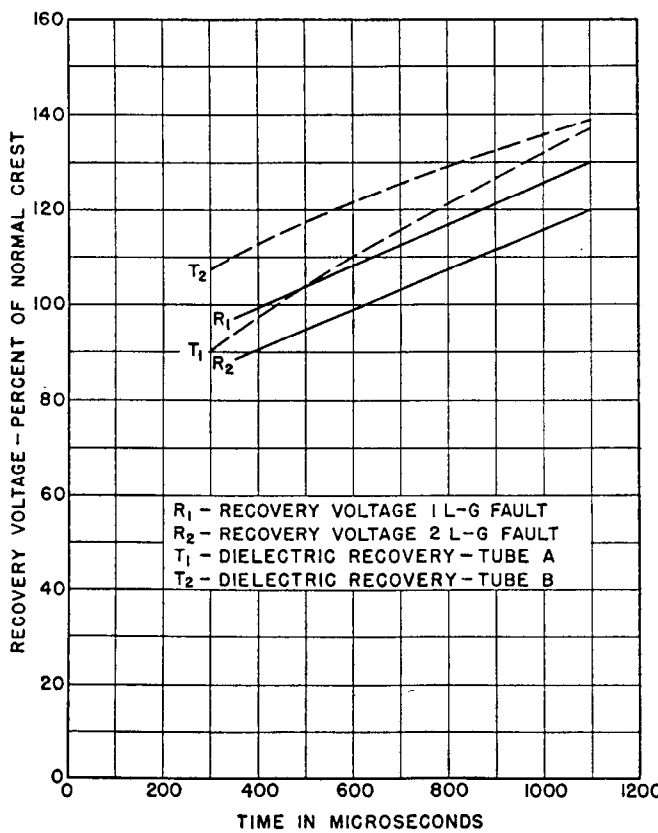


Fig. 24—Comparison of system recovery voltage and dielectric recovery curves for De-ion protector tubes. Recovery voltage data re-plotted from Fig. 22.

times to 90-percent voltage, and the times and magnitudes associated with the maximum recovery-voltage transient. These data are illustrated in Fig. 26 for the case of a single-line-to-ground fault on an eight-mile system. Time is expressed in microseconds and voltage in percent of normal line-to-ground crest voltage. It is evident that fault location has considerable influence on the pertinent data. With

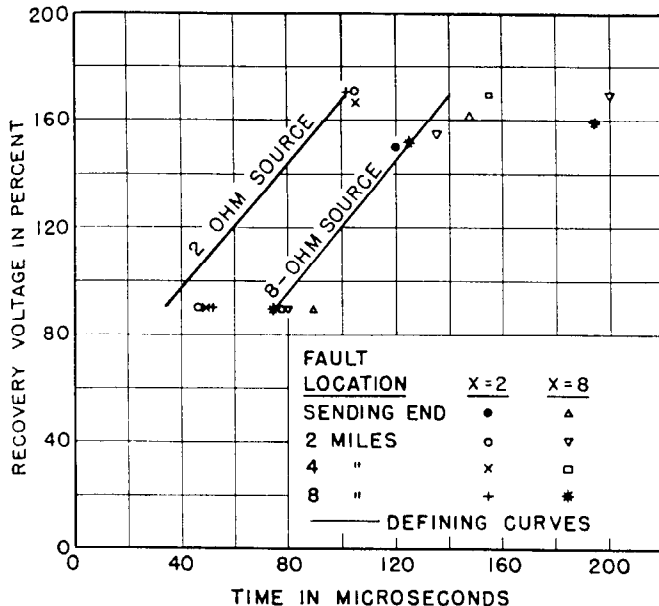


Fig. 26—Method of recording and interpreting data illustrated for one line-to-ground fault on eight-mile, four-wire system.

a two-ohm source, the time to 90-percent voltage is a minimum for a sending-end fault, whereas a receiving-end fault dictates this time with an eight-ohm source. Maximum voltages are obtained for faults away from the sending-end bus. However, many cases were noted where the maximum voltage did occur for sending-end faults, especially where small line conductors were represented. This illustrates the complexity of the problem, and the need for considerable data before formulating conclusions.

As it would be impractical to summarize, in the form of useful curves, all of the data obtained, a simple uniform method of interpretation was adopted. As a protective device must function at any location on a circuit, it is necessary to know only the most severe circuit conditions, regardless of fault location. With this in mind, a straight line was drawn to connect the points giving the minimum times to 90-percent and maximum recovery voltage. This line then defines the voltage-recovery characteristics of the particular system. In certain cases, such as the eight-ohm system in Fig. 26, the defining straight line was extended through one maximum voltage point to a horizontal line that intercepts the highest voltage recorded. This results in a simple method of plotting data without being ultra-conservative. In the case illustrated, the maximum recovery voltage would be recorded as 170 percent at 140 microseconds.

The times to 90 percent and to maximum recovery voltage were obtained by plots similar to Fig. 26. These times

were then reduced to a one-mile basis by dividing by the line length in miles; then plotted as a function of the X/M ratio (ratio of source ohms to line length in miles). These data are summarized in Fig. 27 for single- and double-line-to-ground faults, and 4/0 and No. 6 copper conductors. The times, for a given X/M ratio, do not vary greatly with the type of fault or the conductor size, even though consideration was given to various fault locations. For this reason, it was decided that practical answers could be obtained by drawing a single curve under each set of data. The differences between the actual times and those defined by the lower-limit curves were not considered important in view of the complexity of the overall problem, and the complicated circuits encountered in practice. The actual times for any given line length can be obtained by multiplying the values in Fig. 27 by the line length in miles.

The maximum voltages measured are plotted in Fig. 28 as a function of the X/M ratio. Values are included for four conductor sizes, which allows an evaluation of this

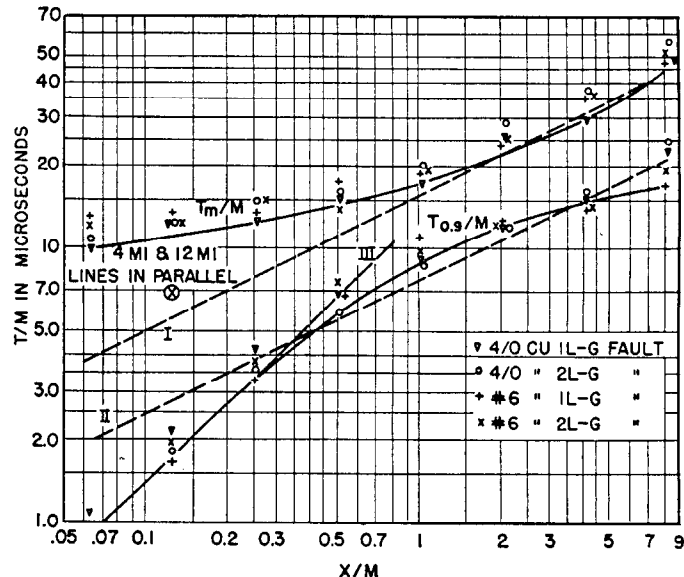


Fig. 27—Times to 90 percent and maximum recovery voltage referred to a one-mile line basis. $T_{0.9}/M$, T_m/M —times to 90 percent and maximum voltage divided by line length in miles.

X—60-cycle source reactance in ohms

I— T_m/M neglecting line inductance

II— $T_{0.9}/M$ neglecting line inductance

III— $T_{0.9}/M$ neglecting line reflections

variable on the voltages obtained. Conductor size has the most influence on the maximum voltages when the X/M ratio is small. With 4/0 conductors the voltages do not vary appreciably with the X/M ratio, and can be represented by a straight horizontal line equal to 175 percent for single-line-to-ground faults and 205 percent for double-line-to-ground faults. If protective devices are to be applied independent of conductor size, these maximum values should be considered as a basis for standardization. The voltages are expressed in percent of normal line-to-ground crest voltage and apply to systems in the 2400- to 13 800-volt range.

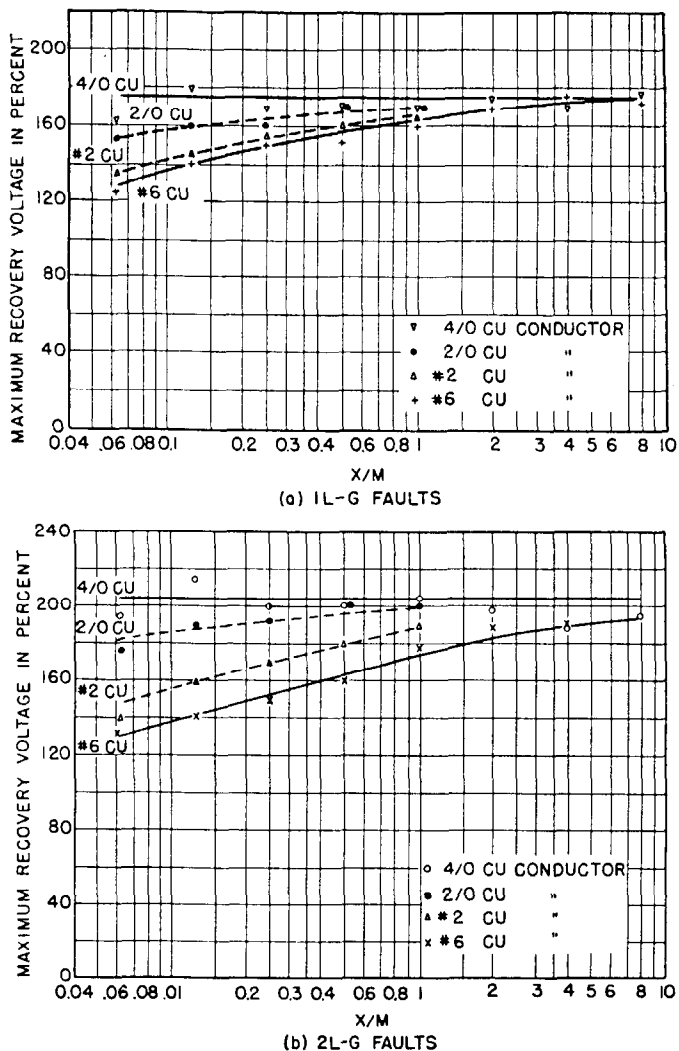


Fig. 28—Maximum recovery voltages as a function of X/M ratio.

X —Source reactance in ohms
 M —Line length in miles

General Circuit Arrangements—The data in Figs. 27 and 28 are obtained for a source and a single line, which would be an exceptional condition in practice. It is therefore necessary to have available a definite procedure for estimating the voltage-recovery characteristics of the more practical systems, consisting of a multiplicity of trunk feeders and laterals. Guided by the results of analog computer studies of a few special cases, theoretical equations have been derived for estimating the voltage-recovery characteristics of practical systems, and are included in this section.

Studies⁷ were made of a system with 16 miles of line connected as (1) one 16 mile line, (2) two eight-mile lines in parallel, and (3) one four-mile line in parallel with one 12-mile line. The following conclusions were drawn from the data obtained:

1. The time to 90-percent voltage is a minimum with a single line.
2. The time to maximum recovery voltage is a minimum with more than one line in parallel.

Because of conclusion 2, calculations were made for the case of an infinite number of lines in parallel, by neglecting all line inductance and representing the lines by lumped capacitances. These data, for a single-line-to-ground fault on a two-ohm, 16-mile system are given in Table 5. The maximum voltages vary between 168 and

TABLE 5—CALCULATED RECOVERY-VOLTAGE DATA FOR A SOLIDLY-GROUNDED SYSTEM CONSISTING OF A TWO-OHM SOURCE AND 16-MILES OF LINE

Conductor Size	System	$T_{0.9}$	T_m	E_m
No. 6	3-wire	43.5	90	175
	4-wire	45.3	94	183
4/0	3-wire	47.3	95	168
	4-wire	49.6	103	180

Note: The above data were calculated for a single-line-to-ground fault, neglecting loss and line inductance.

183 percent, and compare favorably with the 175 percent obtained in the general study for single-line-to-ground faults. The times to maximum voltage range between 90 and 103 microseconds, the shorter time being obtained with the smaller conductor on a three-wire system. The time to 90-percent voltage is also a minimum for this same system.

Whenever line inductance can be neglected, the significant recovery voltage times vary as \sqrt{XM} , where X is the 60-cycle source reactance and M is the total miles of connected line, assumed to be equal on the three-phases. Curve I, Fig. 27, is the calculated curve for times to maximum voltage for a single-line-to-ground fault on a No. 6-conductor, three-wire system. This straight-line curve approaches the analog computer data for X/M ratios above 1.0, even though the computer data were obtained for a single line, and the calculated curve applies for an infinite number of lines in parallel. This shows that line inductance has little effect on the times to maximum voltage for large X/M ratios. The significant time to maximum voltage for the case of a 4-mile line and a 12-mile line in parallel is plotted in Fig. 27. This point falls closer to Curve I than to the single-line curve. As most systems have a multiplicity of circuits, it is suggested that curve I be used for estimating times to maximum voltage, regardless of circuit arrangement. Curve II, Fig. 27, represents the times to 90-percent voltage for the case of an infinite number of parallel circuits. The times to 90-percent and maximum voltage, for the limiting case of an infinite number of feeders in parallel, can be estimated as follows:

$$(1) T_{0.9} = 7.7 \sqrt{XM} \text{ microseconds.}$$

$$(2) T_m = 15.9 \sqrt{XM} \text{ microseconds.}$$

Note: X is the 60-cycle source reactance in ohms, and M is the connected overhead line in miles per phase, including trunk feeders and laterals.

The constants in the equations were derived from the calculated times in Table 5 for a No. 6 conductor, three-wire system.

The computer data in Fig. 27 fall close to Curve II for X/M ratios larger than approximately $1/3$. Below this

ratio, the times for a single line are not a function of line length, but only of source reactance. The minimum times were obtained for single-line-to-ground faults on the sending-end bus, and the recovery voltage reached the 90-percent values before reflections returned from the open end of the line. These times therefore vary directly with the 60-cycle source reactance, and follow Curve III.

With several long feeders in parallel, and a low source reactance, the times to 90-percent voltage are independent of line length, and vary directly with source reactance and with the number of feeders connected to the source bus. These cases can be represented in Fig. 27 by additional curves in parallel with Curve III, and with the times for a given X/M ratio increased directly with the number of parallel feeders. The times to 90-percent voltage for these long-line cases, where line reflections can be neglected, can be estimated from the following relation:

(3) $T_{0.9} = 13.8 NX$, where X is the 60-cycle source reactance in ohms and N is the number of long feeders in parallel. The constant in the equation is the calculated time to 90-percent voltage for a system consisting of a one-ohm source and a single No. 6 copper overhead circuit.

In any particular case being studied, the time to 90-percent voltage should be calculated by Eqs. (1) and (3), and the minimum time thus obtained should be used. This procedure will give conservative results for systems normally encountered in practice.

9. Switching Surges and Arcing Grounds

The transient voltages discussed in the previous section were based on the opening of a circuit without restriking. Under some conditions restriking of the arc can occur, resulting in transient voltages of higher magnitude than produced with no restriking. Circuit changes that produce the highest transient voltages involve arc paths. The arc path may be in the fault or it may be in a circuit-interrupting device such as a circuit breaker. If the intermittent arcing takes place in a fault to ground, the phenomenon is called an arcing ground. However, if the arcing occurs in a circuit-interrupting device the voltages produced are called switching surges.

The mechanism by which intermittent arcs produce high transient voltages can best be explained by using simple circuits that are basically equivalent to actual power systems. Also it is convenient to represent the intermittent arc by a switch, the opening and closing of which is equivalent to the extinction and restriking of the arc, respectively. Using simple circuits, the mechanism of producing transient voltages will be explained for both arcing grounds and switching surges.

Arcing Grounds—Theory—The circuit in Fig. 29 illustrates the phenomenon during an arcing ground on a system. The windings of a three-phase generator are represented by simple T networks. The generator is assumed to be grounded through a neutral reactor, the reactance of which is large in comparison with the generator winding reactance. It is further assumed that an arcing fault occurs at the terminals of the generator. If, for the purpose of discussion, the unfaulted phases are

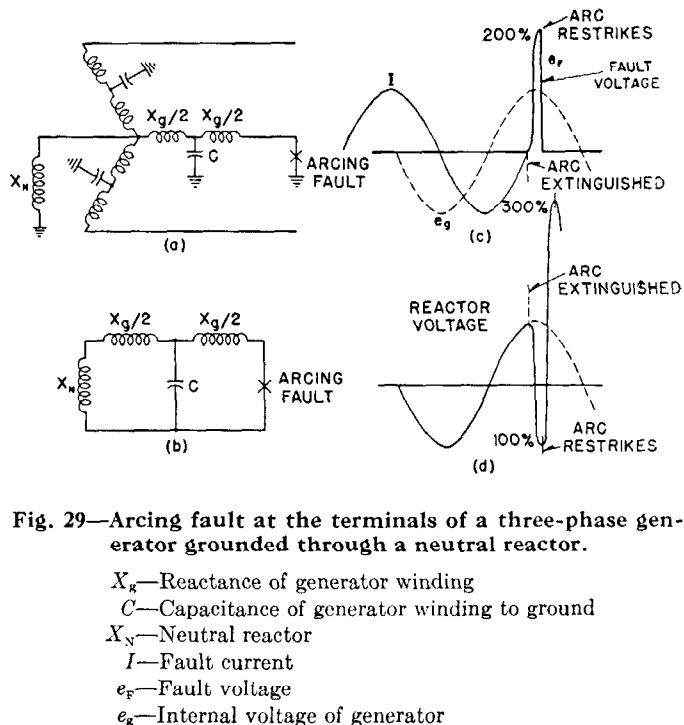


Fig. 29—Arcing fault at the terminals of a three-phase generator grounded through a neutral reactor.

X_g —Reactance of generator winding
 C —Capacitance of generator winding to ground
 X_N —Neutral reactor
 I —Fault current
 e_f —Fault voltage
 e_g —Internal voltage of generator

neglected, the circuit in Fig. 29 (a) can be reduced to the simple circuit in Fig. 29 (b).

In the assumed circuit the fault current will lag the generated voltage by 90 electrical degrees as loss has been neglected. If the arc in the fault is extinguished at the instant the fault current passes through zero, as shown in Fig. 29 (c), the voltage across the fault will not immediately return to normal but will oscillate around normal. It will reach a crest of twice normal voltage, $\frac{1}{2}$ cycle of the high frequency oscillation after the arc is extinguished. This oscillation is the same as the simple oscillation discussed in connection with Fig. 16. During the fault, approximately full generated voltage appears across the neutral reactor as it has been assumed that the reactance of the neutral reactor is large in comparison to the machine reactance. Therefore at the instant the arc is extinguished in the fault, the voltage across the reactor is approximately equal to the crest value of the generated voltage. After the arc is extinguished the steady-state voltage across the neutral reactor is zero. The reactor voltage will therefore oscillate from a plus 100 percent voltage to a negative 100 percent voltage following arc extinction.

Now, if the voltage across the arc rises faster than the dielectric strength of the arc space recovers, the arc will restrike. This restriking of the arc can occur at any point on the wave of high frequency voltage across the arc. Suppose the arc restrikes when the voltage across the dielectric reaches its maximum value of twice normal. After the restrike occurs the fault voltage will drop to zero as shown in Fig. 29 (c). After the arc restrikes the steady-state voltage across the neutral reactor will be approximately equal to the crest value of the generated voltage. The reactor voltage will therefore start at a negative 100 percent voltage at the instant the arc is

reestablished and will oscillate around normal voltage, reaching a crest of three times normal.

In the above analysis it was shown that the voltage across the neutral reactor can reach three times normal line-to-ground voltage even when the arc is reestablished only once. This process can be repeated several times resulting in still higher voltages. In this analysis it was assumed that arcs were extinguished at zero points of the high-frequency current wave (except for the first extinction) and arcs were established at the crest of voltage waves. Other theories^{2,8} of arcing are based upon fundamental frequency arc extinction and restriking.

Switching Surges—Theory—The transient voltages produced during the de-energizing of an unfaultered line section are shown in Fig. 30 for a single-phase system in which the line is represented by a condenser. The successive steps of building up the capacitor voltage are shown in Fig. 30 (b). Normal capacitor voltage has been added as a dotted curve. The capacitor voltage is normal and at point A the switch is opened and a charge is left on the capacitor. The switch voltage is now the algebraic sum of the generated voltage and the voltage resulting from the charge on the capacitor. It will reach a maximum of twice normal generated voltage at one-half cycle of fundamental frequency after the switch is opened. At point B the capacitor voltage has a value of +1 in per unit values, whereas the normal capacitor voltage, with the switch closed, is -1. If the switch is

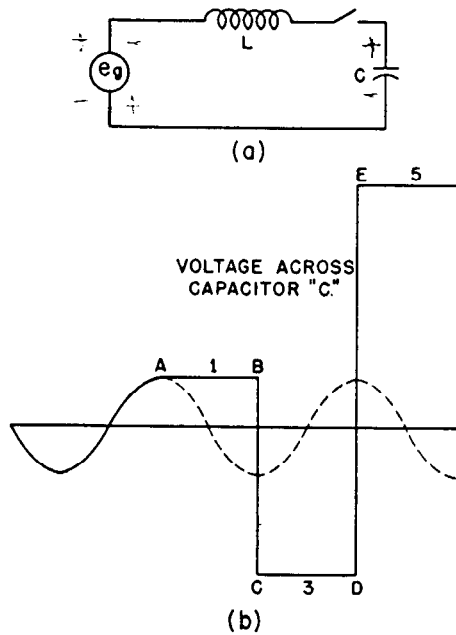


Fig. 30—De-energizing an unfaultered line section.

Note: Switch opened at A, C, E
Switch closed at B, D

closed at this time the capacitor voltage will tend to reach a value of -1 but because of the circuit inductance or inertia the voltage will overshoot and, without damping, will reach -3. If now the switch is opened, the capacitor will have a charge corresponding to a voltage of -3. If the switch is again reclosed one-half cycle after

opening, the capacitor voltage will tend to reach a value of +1 but will overshoot to +5. Thus the voltage builds up according to the series, 1, 3, 5, 7, . . . and will have no limit if damping is neglected. In this analysis it has been assumed that the inductance is small and that the natural frequency of the circuit is high in comparison to the fundamental frequency.

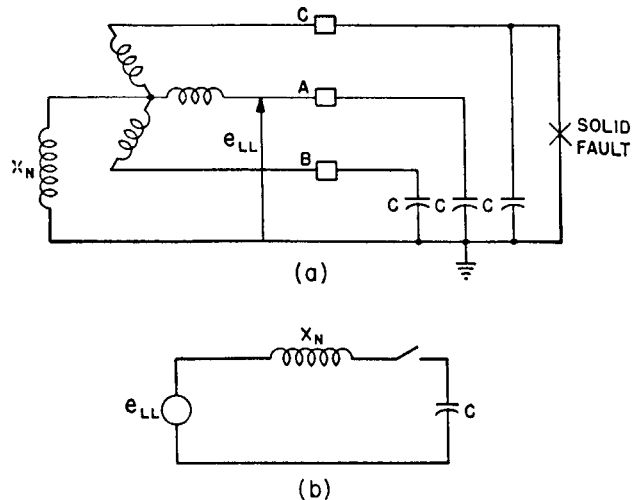


Fig. 31—De-energizing a line section subjected to a single line-to-ground fault.

A third important case is de-energizing a line section subjected to a single line-to-ground fault. Consider a solid single line-to-ground fault on phase C of the three-phase system in Fig. 31. Assume the fault is cleared by the opening of the circuit breaker with arcing in pole A. First, if X_N is large in comparison to the reactance of the generator, full line-to-line voltage will appear between phase A and ground, independent of whether pole A of the breaker is closed or open. For simplicity the three-phase system can be reduced to the circuit in Fig. 31 (b) in which the breaker is represented by a switch. Normal line-to-line voltage has been inserted back of X_N . The only difference between this circuit and the one in Fig. 30 is in the voltage back of the circuit reactance; the voltage in Fig. 30 (a) is normal line-to-neutral voltage and the voltage in 31 (b) is normal line-to-line voltage. The transient voltages produced in the circuit in Fig. 31 (b) will therefore be equal to $\sqrt{3}$ times the voltages produced in Fig. 30 (b). The voltage across the capacitor will then increase according to the series $\sqrt{3} (1, 3, 5, 7, \dots)$.

Characteristics of Arc Path—In Fig. 32 is shown the voltage across the switch for the transient conditions in Fig. 30. The switch voltage is found by subtracting the condenser voltage from normal generated voltage. The first arc reestablishment occurs at A at twice normal voltage. This requires that the dielectric strength of the arc path recovers along some curve such as I, that is, along a curve above the curve of recovery voltage until at point A where they intersect. While the arc path is conducting, the dielectric strength of the switch is practically zero. When the arc is again extinguished, the dielectric strength curve again starts from zero but recovers much more rapidly and intersects the curve of

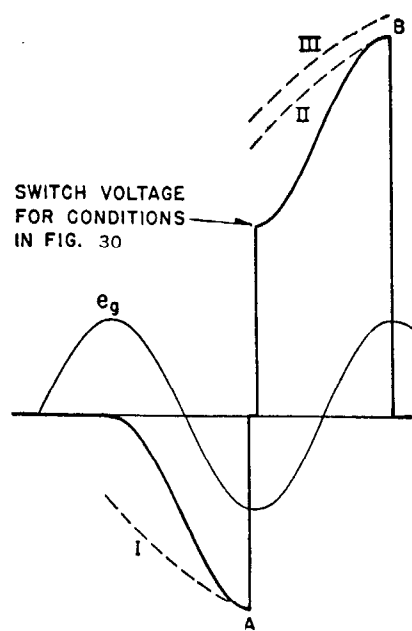


Fig. 32—Dielectric recovery characteristics assumed in Fig. 30.

recovery voltage at the point *B* causing a second restrike. If the dielectric strength of the arc path recovered along some curve III the arc would not reestablish at *B*. These curves show the requirement for the dielectric strength of the arc path to obtain high overvoltages. If curve I were not as high as shown, the restrike would have occurred at a lower voltage, and the capacitor voltage would not have been as large as shown in Fig. 30 (b). If the dielectric strength had built up at a more rapid rate, no restrike would have taken place. Thus, the dielectric strength must build up at a higher rate after any extinction than it did after the preceding extinction to develop cumulatively higher voltages. This phenomenon is unlikely to take place in open air between stationary contacts because such an arc path is unlikely to develop the required dielectric recovery strength. In confined arcs, where the pressure may increase after each conduction period, this phenomenon may take place. Separation of breaker contacts has a tendency to cause higher dielectric strength recovery rates after each conducting period because of the increasingly larger contact separation. These requirements of the arc path probably provide an explanation for the difficulties experienced in attempts to produce high voltages by arcing in air over insulator strings. The conditions for producing high voltages by intermittent arcing are somewhat more favorable for apparatus failure under oil than for flashover of an insulator string. Perhaps apparatus failure under oil causes line flashover instead of a line flashover causing apparatus failure.

General Study—The foregoing discussion has been based on simple circuits for the purpose of illustrating the essential elements of the theories of intermittent arcing. All actual systems are relatively quite complicated and cannot be reduced to the simple circuits used. Because of this complexity, the maximum voltages with intermittent arcing are not quite in accord with the pre-

ceding theories. More specifically, the maximum voltages are obtained for simple circuits with the arcs recurring at either the high-frequency voltage crest or at the fundamental-frequency voltage crest. With complicated circuits higher voltages may be obtained if the arc is established before or after these points. This is because the oscillating circuits have several natural frequencies. The determination of the exact manner of restriking is difficult to define analytically. Because of this fact and because of the importance of damping it is impractical to

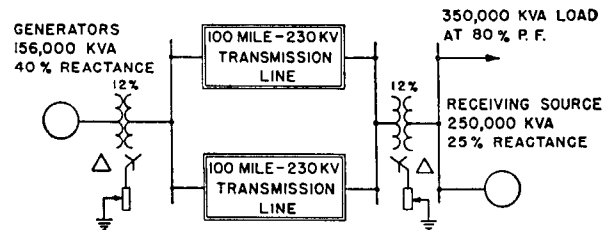


Fig. 33—Schematic diagram of system selected for study.

study arcing grounds and switching transients by the usual mathematical methods. It is more convenient to represent actual systems in miniature on the a-c network calculator and perform the switching operations with the special switches described previously.

To study the magnitude and other characteristics of transient voltages produced by switching operations and faults with intermittent arcing, a typical transmission system (Fig. 33) was selected for a study³ on the a-c network calculator. Since these transient voltages are greatly influenced by the method of grounding, the neutral impedances of the system were varied through a wide range of resistances and reactances, between the limits of the solidly grounded system and the ungrounded system.

The system consists of a hydroelectric generating station, the output of which is transmitted 100 miles over 230-kv lines to a load, which is also supplied by local steam generators. The sending and receiving-end transformers are star-connected on the 230-kv side to permit grounding, as discussed subsequently. The reactance characteristics of the different parts of the system are shown in Fig. 33 and the wire sizes and configuration of

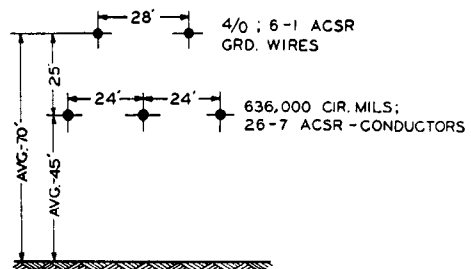


Fig. 34—Configuration of transmission line.

the transmission lines are shown in Fig. 34. The transmission lines are separated so there is no mutual effect between them. Also, the generators at both ends of the line are assumed to be in phase and to have the same internal voltage.

The general method of setting up the network calculator makes use of equivalent three-phase networks for each circuit element such as machines, transformers, and transmission lines. The character of these equivalent circuits is obvious and requires no comment except for the transmission lines, and these are represented by the circuit shown schematically in Fig. 35.

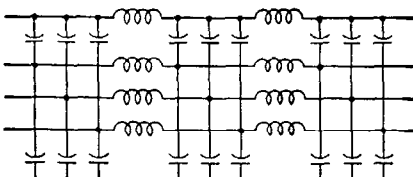


Fig. 35—Equivalent network used for representing each 230 kv transmission line of Fig. 33.

The highest voltages for a particular condition are sought throughout the investigation. In the arcing ground the fault is applied at the crest of the normal line-to-ground voltage and is then removed at the first current zero. The point of restriking is adjusted to give the maximum voltage for the number of restrikes considered. The fault is always removed at the first current zero following each arc recurrence. In the case of switching operations the circuit is initially opened at a fundamental current zero. The point of restriking is adjusted so as to give the maximum voltage for a given number of restrikes. The subsequent circuit openings are always assumed to take place at the first current zero following the arc reestablishment.

The highest voltages at the point of circuit change are always recorded. For example, for arcing-gounds the voltages are measured at the receiver end. On the other hand, in the case of de-energizing an unfaulted or faulted line, the voltages are measured at the sending end where the switching is done. When arcing grounds are considered on the system, several phase voltages as well as the neutral voltage are recorded. In the case of switching operations the voltages are recorded on the phase being switched, both on the line and supply sides as well as across the switch that is opening the circuit.

The voltages recorded are those occurring within $1\frac{1}{2}$ cycles of the first interruption considered. In some cases, either because of system loss or because of the relation of the natural frequency to the fundamental frequency, higher voltages may be experienced with one or no restrikes than with two or one restrikes, respectively. In some cases, particularly in the ground-fault neutralizer case, the voltages after the $1\frac{1}{2}$ -cycle period may continue to increase to a much higher steady-state voltage. With a ground-fault neutralizer quite high voltages are obtained if the circuit is in tune at fundamental frequency and a residual voltage is produced as by some unbalance. For example, the opening of one phase of a system subjected to a three-phase or a line-to-line fault on the phase being opened will produce a steady-state voltage of many times normal.

In this investigation of transient overvoltages produced by switching operations and faults, four principal cases have been selected for study as follows:

1. Arcing-ground conditions on one phase to ground.
2. De-energizing an unfaulted line, one pole unit opening and two remaining closed.
3. De-energizing an unfaulted phase with a ground fault on one of the other phases, one pole opening and the other two remaining closed.
4. De-energizing an unfaulted phase with a ground fault on the two other phases, one pole opening and the other two remaining closed.

In general, arcing-ground conditions are for a fault on one phase. De-energizing a line section is considered more important than energizing because for the latter the intermittent arcing is limited in duration by the closing of the switch. In the case of opening the faulted lines it is assumed that the unfaulted phase opens before the pole units of the faulted phase or phases. Such an assumption is based on the ability of the switch to recover dielectric strength at a high rate. This assumption tends to give higher magnitudes of transient voltage. If the pole unit in the sound phase tends to open after the fault is cleared, then the voltages will be similar to those produced when an unfaulted line is de-energized. The voltages will range between these limits as the time of relative opening is varied. The conditions selected for study illustrate possible circuit-breaker operations on an actual system.

In this study the transient voltages are obtained for the conditions corresponding to both one and two restrikes. This number of restrikes may be taken as the equivalent of a larger number with the earlier restrikes taking place so quickly that they do not contribute much to the voltage magnitude.

One of the variable factors considered is the method of system grounding that includes both resistances and reactances between the limits of a solidly grounded system and an ungrounded system. When the system is solidly grounded, the transformer at the sending end is solidly grounded when one line is in operation, and the transformers are solidly grounded at both ends when two lines are in operation. In the case of impedance grounding a reactor or resistor of varying ohmic value is considered in the neutral-to-ground circuit at the sending end when one line is in operation, and a reactor or resistor of equal magnitude is considered in the circuit in the sending and receiving ends when two lines are in operation. The ohmic values plotted on the figures to be discussed later are the actual ohms considered in the ground connection at one point. For example, 50 ohms on a system with one ground point is the resistance or reactance considered in the sending end ground. When two lines are considered in operation, 50 ohms corresponds to the ohms in the sending-end neutral connection and a like value in the receiving-end neutral connection.

Results of General Study—The results of the a-c network calculator study are presented in graphical form in Figs. 36 to 39 inclusive. They give the transient voltages expressed in percent of the normal line-to-ground voltage crest and are plotted as a function of the reactance or resistance in the neutral connection. The solid-line curves are for reactance grounding and the dotted-line curves are for resistance grounding. The neutral

reactance corresponding to a ground-fault neutralizer is indicated. In each of these figures the data is plotted for one and two lines and one and two restrikes.

As shown in Fig. 36 transient voltages can be avoided by the use of the solidly-grounded system or the system grounded through a ground-fault neutralizer, both of

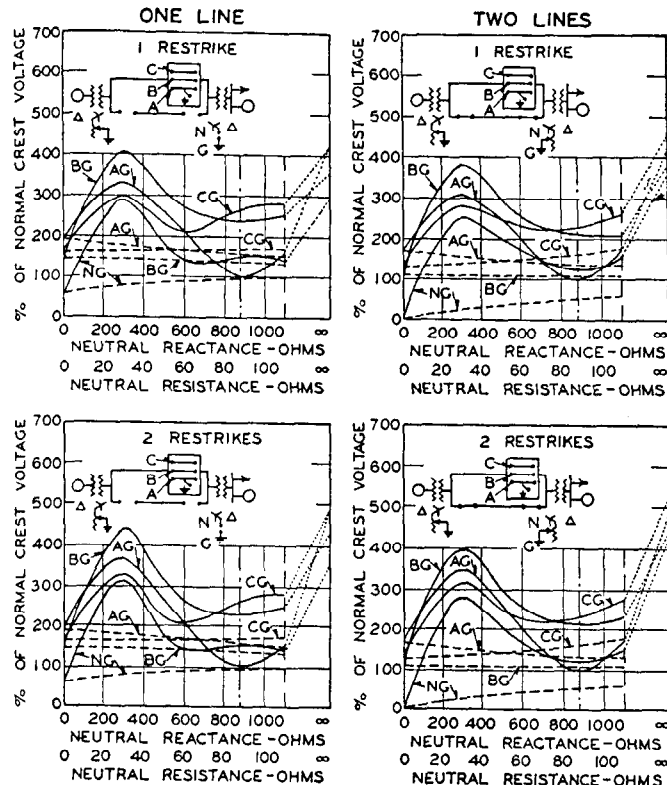


Fig. 36—Effect of grounding impedance on transient voltages caused by arcing grounds.

Solid curve: Reactance grounding

Dotted curve: Resistance grounding

Note: Letters on curves refer to lettered points on inset circuit.
Ground-fault neutralizer reactance: 875 ohms

which have been employed for many years to avoid the abnormal voltages encountered on ungrounded systems. The voltages corresponding to resistance grounding are fairly uniform and relatively low for the range of resistance studied. However, for neutral resistances approaching infinity, the transient voltages will approach those of the ungrounded system. The study shows that there is a value of reactance intermediate between the solidly grounded system and the system grounded through a ground-fault neutralizer almost as high as for the ungrounded system.

The transient voltages resulting from the de-energizing of an unfaulted line are shown in Fig. 37. The lowest transient voltages, with the exception of those across the neutral impedances, are obtained for a system grounded through a ground-fault neutralizer. In all cases the neutral-point voltage increases as the neutral impedance increases. For the range of practical neutral impedances, there is no appreciable difference between the voltages obtained for the case of one and of two lines. However,

for a free-neutral system the voltages are appreciably lower for the larger lengths of connected line.

The transient voltages for the condition of de-energizing a line section with a fault on a phase other than that which is being switched are shown in Fig. 38. The voltages in all cases of reactance grounding increase as the neutral reactance increases. The voltages between neutral point and ground also increase for resistance grounding as the magnitude of the resistance is increased. The voltages with a ground-fault neutralizer are definitely higher than for any of the lower values of reactance grounding. This is to be contrasted with the dip in the voltage curves of Figs. 36 and 37. In Fig. 38 the voltages with two restrikes increase as compared to the case with one restrike. As would be expected, the longer the connected line, the lower the magnitude of the transient voltages.

Figure 39 shows the results of a study similar to that of Fig. 38 except that a double instead of a single line-to-ground fault is applied to the line section being de-energized. In general, the comments are the same as for

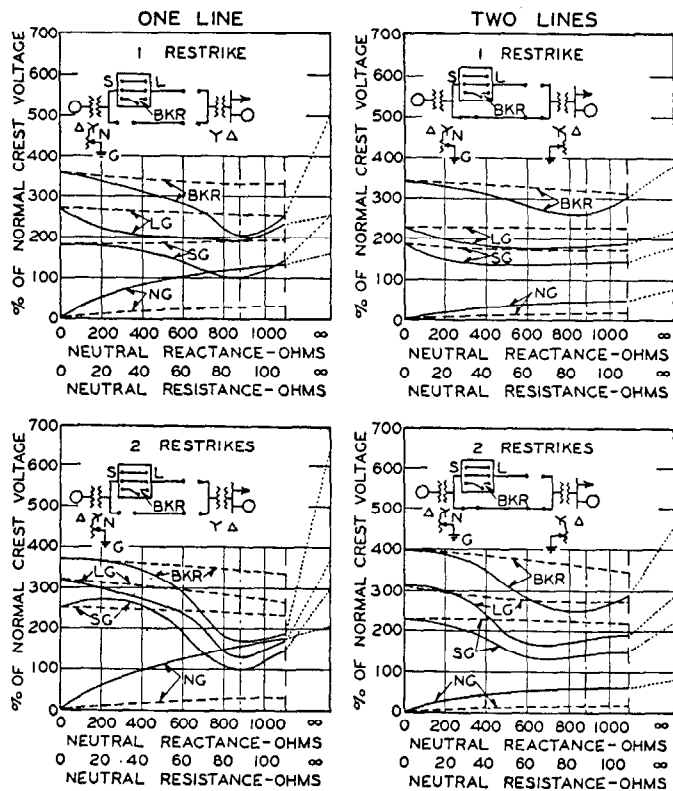


Fig. 37—Effect of grounding impedance on transient voltages caused by de-energizing an unfaulted line
See subcaption of Fig. 36.

the case of Fig. 38. For reactance grounding the transient voltages increase rapidly for a relatively small addition of neutral reactance, so that for low neutral reactances the transient voltages closely approach those of the free-neutral system.

The results obtained in the a-c network calculator studies are based on a definite number of restrikes which are spaced at such intervals as to give the maximum volt-

age for this number of restrikes. Thus, in the average case, since the restrikes may not occur at the optimum point, the voltages will be of lower magnitude giving a probability curve for the voltage. Of course, only a minority of the cases of system faults and switching produce abnormal voltages.

The a-c network calculator studies have also been based on the assumption that transient voltages of increasing magnitude can be impressed on the system without altering the characteristics of the system. Actually, the transient voltages will be limited by other factors that become of increasing importance as the transient voltage increases. On some systems corona will limit the magnitude of transient voltage by introducing losses in the oscillating circuits. Under some conditions excess

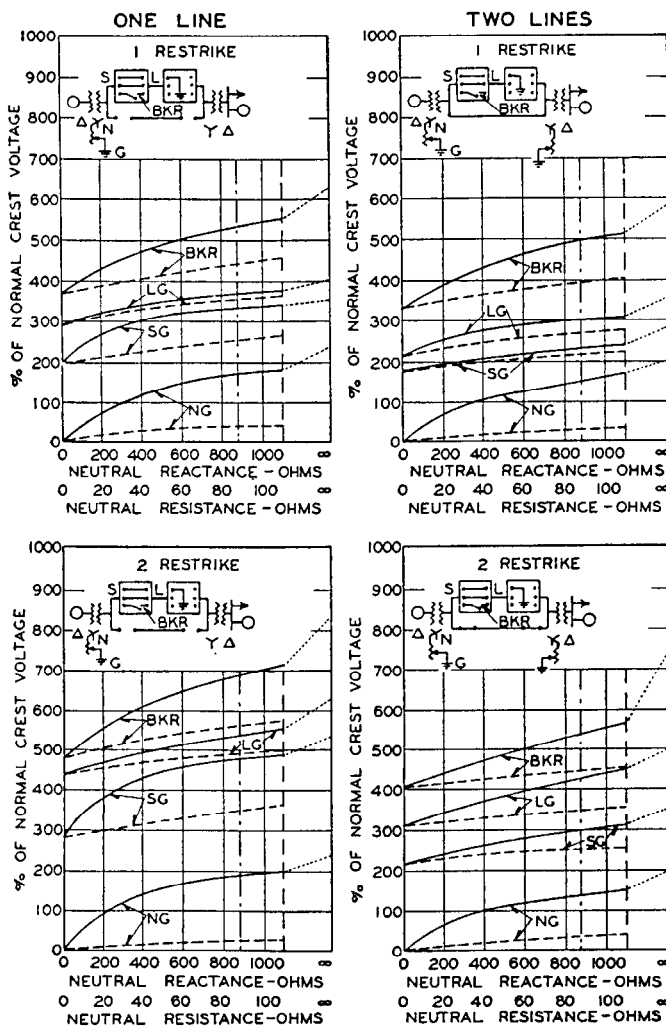


Fig. 38—Effect of grounding impedance on transient voltages caused by de-energizing line with single line-to-ground fault
See subcaption of Fig. 36.

voltages will produce increases in exciting current particularly at the lower frequencies, but usually this factor is unimportant. Transient voltages can also be limited by the operation of lightning arresters or protective gaps adjusted to operate below the flashover level of line or apparatus insulation. These devices may limit the magni-

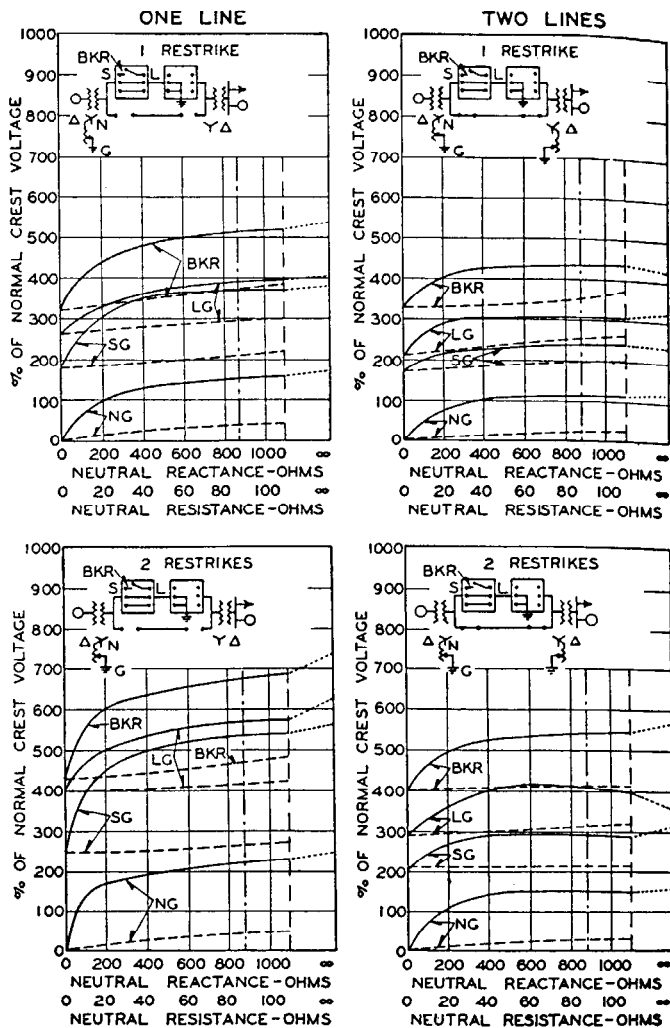


Fig. 39—Effect of grounding impedance on transient voltages caused by de-energizing line with double line-to-ground fault
See subcaption of Fig. 36

tude of transient voltages on a particular system. Finally, the transient voltage is limited by the flashover characteristics of line and apparatus insulation. Operating experience confirms the results of this study in that some switching operations do result in flashover of line or neutral-point insulation.

Many klydonograph investigations have been reported in the literature, and frequently overvoltages resulting from switching operations are segregated from those due to lightning. Extensive investigations were reported by Cox, McAuley, and Huggins,⁹ Gross and Cox,¹⁰ Lewis and Foust,¹¹ and by some European investigators. The Joint Subcommittee on Development and Research of the Edison Electric Institute and Bell Telephone System, has also carried on investigations and has made an excellent summary¹² of the more important published data.

The principal results of the switching-surge studies using the klydonograph have been summarized in Fig. 40. Curves A and B, obtained from the original investigation by Cox, McAuley, and Huggins, give the voltages caused by energizing or de-energizing operations and the voltages resulting from faults with subsequent switching,

respectively. Curve C gives a summary derived from the work of Lewis and Foust. In order to give a more suitable scale for plotting the results of the surge studies all the surges of a magnitude less than twice normal have been disregarded. The Lewis and Foust paper, however,

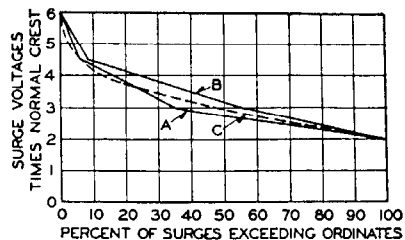


Fig. 40—Distribution of surge voltages caused by switching and faults.

- A—Switching surges—Cox, McAuley, and Huggins
- B—Surges from faults—Cox, McAuley, and Huggins
- C—Switching surges—Lewis and Foust
- A and B—Eighteen systems—1925 to 1926
- C—Fourteen systems—1926 to 1930

shows that of all the reported surges above normal voltage, 45 percent were above twice normal. Fig. 40 shows that the limiting value of the surges is about six times normal crest voltage, 5 percent exceed five times normal, and 20 percent exceed four times normal. These results show that there is an upper limit to the voltage recorded, indicating the possibility of some limiting factor. Fig. 41 shows the ratio of flashover voltage to the normal crest voltage, for transmission lines of different voltages. The shape of the curve of Fig. 40 compared with the data given in Fig. 41 indicates that the magnitude of switching

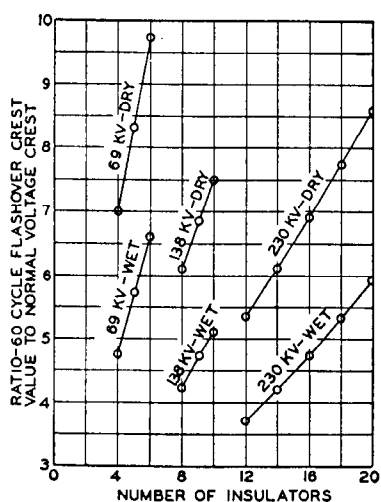


Fig. 41—60-cycle flashover voltage ratios for 10-inch suspension insulators.

surges recorded could be limited by line flashover. While it is undoubtedly true that a considerable portion of these switching operations occur with relatively little energy in the oscillation and at relatively high frequency, it is also true that as systems expand the natural frequency of systems for switching operations decreases

and the amount of energy in these oscillations increases. Thus, these factors tend to increase the importance of switching surges.

The maximum voltages of Figs. 36 to 39 correspond closely with the limiting voltage of six times normal indicated in Fig. 40. The shape of the curves of Fig. 40 should probably not be accepted too freely as these are no doubt influenced by the flashover of lines or apparatus, or the operation of lightning arresters.

10. Effect of Generator Grounding on Transient Voltages

The results of the general study of transient overvoltages produced by switching and faults in the preceding section were based on the assumption that there was no appreciable arc drop and that the arc was always extinguished at a current zero, either fundamental or high-frequency. In some cases, especially in low-voltage circuits, additional characteristics of an arc must be considered because of their influence on transient voltages.

Arc Characteristics—Prior to the actual interruption of the arc in a circuit breaker there is a voltage drop between the breaker terminals. The magnitude of this drop varies for different types of breakers, being lower for the higher voltage circuit breakers when expressed in percent of system voltage. This drop is of two parts, first an arc drop that is fairly uniform in magnitude and lasts during the entire arcing period, and second, a drop that is a function of the efficiency of arc interruption and the current being handled. Fig. 43 shows a fairly uniform breaker voltage until the arc is ruptured at which time the voltage increases quite rapidly to a negative crest of approximately normal line-to-ground crest voltage. This negative crest voltage is commonly referred to as the breaker "extinction voltage." An analysis made of oscillograms of many breaker operations indicates that for a circuit breaker opening 12 000 and 13 200-volt circuits this "extinction voltage" may be as large as 125 percent of the normal line-to-ground crest voltage but is usually much lower. This extinction voltage is produced by extinction of the arc before a normal current zero, that is, before the current in the arc would normally pass through zero.

In general, the same characteristics as mentioned above are found in all arcs under oil or in confined spaces, such as arcs caused by flashover of apparatus under oil, in cables, etc. Arcs between stationary contacts in air will usually have entirely different characteristics because no large de-ionizing agent is present.

Effect of Extinction Voltage on Transient Voltages—The system in Fig. 42 will be used in presenting the theory involved in the production of transient voltages by switching or arcing grounds. In this circuit the generator windings are represented by simple T networks and additional capacitance is added at the machine terminals to represent the capacitance of connected feeders. The positive, negative, and zero-sequence reactances of the generator and feeders are assumed to be equal. The generator is grounded through a neutral reactor, and a single line-to-ground fault is assumed on a feeder outside of a breaker. The effect of the unfaulted phases on the

transient voltages can be neglected, reducing the circuit to the one shown in Fig. 42 (b).

Consider the case of a single line-to-ground fault occurring on a feeder and the fault removed by operation of the breaker. The fault is assumed to last long enough to allow damping out of all initiating transients and the

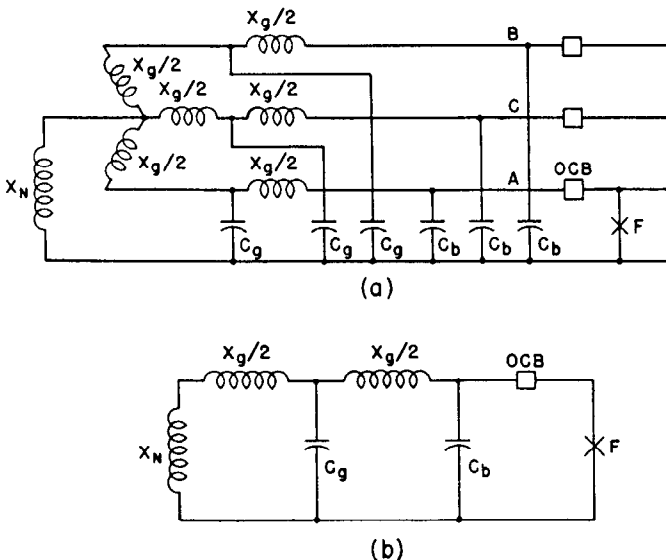


Fig. 42—Generator grounded through neutral reactor.

- (a) Simple three-phase system
- (b) Simplified single-phase system
- X_g —Generator subtransient reactance
- C_g —Generator winding capacitance to ground
- C_b —Capacitance of bus, cables, etc.
- OCB—Oil circuit breaker
- F—Fault
- X_N —Neutral reactor

arc in the breaker is ruptured far enough ahead of a normal current zero to give an extinction voltage equal to normal line-to-ground crest voltage. The generated voltage and fault current are shown in Fig. 43 for this condition. A small arc drop in phase with the current appears across the breaker terminals during the entire arcing period.

If the neutral reactance is large in comparison to the machine reactance, practically all of the generated voltage will appear as a drop across the neutral reactor while the fault is present. The reactor voltage will then be approximately equal to the generated voltage until the breaker terminal voltage starts to increase as a result of the de-ionizing action of the breaker. As the neutral reactor was assumed to be large in comparison to the machine reactance, the reactor voltage is approximately equal to the difference between the generated voltage and the breaker voltage. It therefore reaches a crest of twice normal at A' . If the arc is ruptured* at A, normal generated voltage is removed from the reactor as with no fault on the system no voltage appears across the neutral reactor. The reactor voltage therefore oscillates around

*In this analysis the arc is assumed to be ruptured at the instant of crest negative voltage between breaker terminals. It is realized that the arc may be ruptured before this time.

zero; and without damping it would reach a negative crest of twice normal. With damping it reaches a negative crest somewhat less as shown in Fig. 43.

With the breaker open and with the fault on the system, the normal steady-state voltage across the breaker is approximately equal to the generated voltage. When the arc is ruptured at A the breaker voltage will start at a negative crest of 100 percent and oscillate around the generated voltage. It will reach a positive crest of three times normal with no damping or some less with damping.

The maximum reactor voltage is equal to the breaker extinction voltage plus the generated voltage at the time this extinction voltage appears across the breaker terminals. In the case of a reactance grounded generator the arc is ruptured at near crest generated voltage so the reactor voltage is equal to the extinction voltage plus normal crest generated voltage. The breaker voltage approaches a crest equal to twice the generated voltage plus the extinction voltage.

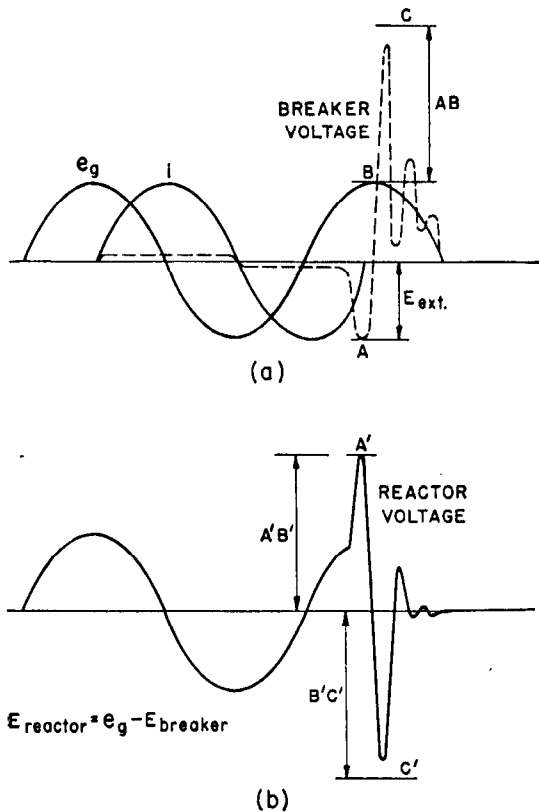


Fig. 43—Transient voltages with no restriking.

- (a) Breaker voltage.
- (b) Reactor voltage
- e_g —Normal line-to-ground voltage
- E_{ext} —Extinction voltage
- i—Fault current

As shown in Fig. 43, the breaker voltage may build up fairly high. If at any time this voltage exceeds the dielectric strength of the arc space between the breaker contacts, the arc will restrike. In Fig. 44 the restriking is assumed to occur at the instant the breaker voltage reaches its maximum value at C. Assuming that 100

percent extinction voltage appeared across the breaker terminals at the instant of arc rupture and further assuming no damping, this maximum breaker voltage will be three times normal. When the breaker voltage is at C the reactor voltage will be at a negative 200 percent voltage. When the arc is reestablished the breaker voltage will decrease to a very small arc drop as shown in Fig. 44. After the restrike occurs the steady state voltage across the reactor is approximately equal to the normal generated voltage. The reactor voltage will therefore start at C' and oscillate around normal generated voltage. It will overshoot to a crest voltage of four times normal if losses are neglected.

With one restrike and without damping the reactor voltage will reach three times normal crest generated voltage plus the breaker extinction voltage. With additional restrikes the voltage can increase further if the restrikes occur at the right time. It is of course rather

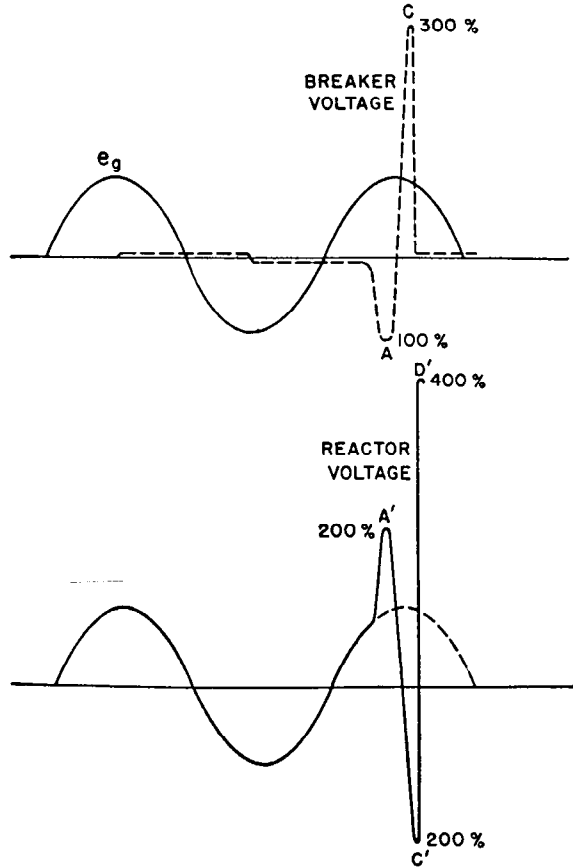


Fig. 44—Transient voltages produced with restriking.

improbable that more than one or two restrikes will occur at just the right time to give these high overvoltages.

Resistance Grounding—If the neutral reactor is replaced with a resistor having the same impedance, the power factor of the fault circuit will be approximately unity. The breaker and resistor voltages for this condition are shown in Fig. 45. Normal current zero will coincide with normal voltage zero. As the arc drop is still in phase with the current, the breaker extinction voltage and normal generated voltage are on the same side of the

axis. As the resulting breaker voltage oscillation after the arc is ruptured at A depends upon the generated voltage, the oscillations will be quite small. No voltage appears across the resistor at the time the arc is ruptured because no current is flowing at that time. The oscillation in the resistor voltage will be small and will be

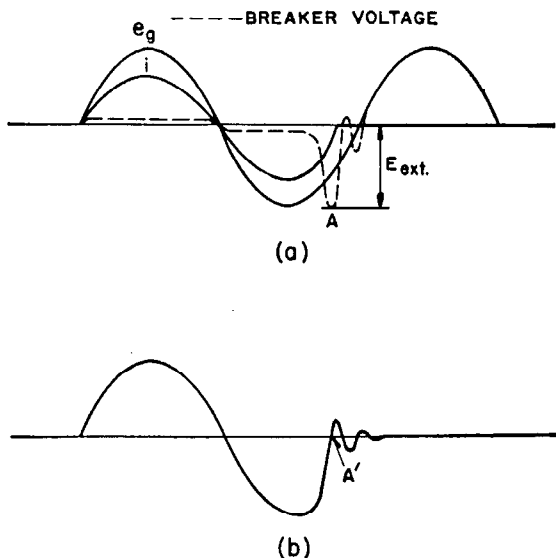


Fig. 45—Transient voltages produced with resistance grounding.

- (a) Breaker voltage
- (b) Voltage across neutral resistor

damped out rapidly because of the high loss present in the system.

Parallel Resistance and Reactance—Since fairly high voltages can be produced when a neutral reactor is used and since these voltages are greatly reduced when a neutral resistor is used, the question naturally arises as to whether it would be possible to compromise and use a combination of both. With resistance and reactance in parallel the phenomenon will follow closely one of the cases above depending upon which predominates. Resistance in parallel with a reactor will usually prevent cumulative building up of the reactor voltage on successive restrikes but a low parallel resistance is necessary in order to prevent the breaker extinction voltage from appearing across the neutral reactor. As shown in Fig. 43 the reactor voltage is the sum of the generated voltage and the extinction voltage. Because the resistance required to keep most of the extinction voltage from appearing across the neutral reactor is small, it is usually preferable to omit the reactor entirely and use resistance grounding.

Analog Computer Studies—In the theoretical discussion given above the neutral reactance was assumed to be much larger than the machine reactance. To show the effect of variations in transient voltages with neutral reactance, studies were made on the analog computer. The circuit employed was similar to the one in Fig. 42(a) excepting that the oil circuit breaker was omitted, and an arcing fault was applied between phase A and ground

TABLE 6—SURGE VOLTAGES PRODUCED WITH REACTANCE GROUNDING

X_0/X_1 Ratio	Surge Voltages*					
	Faulted Phase		Unfaulted Phases		Across Neutral Reactor	
	One Restrike	Two Restrikes	One Restrike	Two Restrikes	One Restrike	Two Restrikes
1	170	170	160	100	0	0
2	165	168	140	142	45	45
3	165	165	180	193	100	100
4	165	165	190	215	115	130
6	185	185	200	230	150	155
8	190	190	260	260	180	180
10	280	430	285	400	175	270
12	...	460	...	450	...	300
14	400	440	390	490	250	350
20	390	400	410	450	250	270
30	370	400	390	500	250	300
50	330	370	400	430	230	300
100	280	260	400	410	230	280

*Expressed in percent of normal line-to-ground crest voltage.

at the generator terminals. The following constants were used:

$$\begin{aligned} X_g &= 1.28 \text{ ohms at 60 cycles.} \\ C_g &= 0.35 \text{ microfarad.} \\ C_b &= 0.20 \text{ microfarad.} \end{aligned}$$

The fault was applied at the instant the 60-cycle voltage between phase A and ground was equal to its crest value, and removed at the first current zero, either 60-cycle or high frequency. The fault was re-applied at crest recovery voltage across the fault and then removed at the first current zero following the restrike, or fault re-application. In the case of two restrikes the latter procedure was repeated. Table 6 is a summary of the results obtained with one and two restrikes for X_0/X_1 ratios between one and 100. In this table X_1 is equal to X_g in Fig. 42, and X_0 is equal to X_g plus $3X_n$, the positive- and zero-sequence machine reactances being equal in the equivalent circuit employed. The faulted phase, maximum unfaulted phase and neutral reactor voltages are included in the summary.

In making these studies it was noted that the magnitude of the transient voltages was influenced to a large extent by the presence or absence of high-frequency current zeros following the fault application or a restrike. With an X_0/X_1 ratio of eight, there was no high-frequency current zero, even following a restrike, and the circuit-opening operation was delayed until the 60-cycle current went through zero. As considerable time was available for dissipation of transient energy between circuit-closing and circuit-opening operations, the transient voltages did not exceed 260 percent with two restrikes. Increasing the X_0/X_1 ratio to ten gave a high-frequency current zero following the first restrike, permitting a circuit-opening operation without waiting for a 60-cycle current zero. In

this case the maximum voltage was recorded as 430 percent. These results show that it would be desirable to limit the X_0/X_1 ratio to some value less than ten, in order to rule out the possibility of obtaining the excessive transient voltages associated with the larger X_0/X_1 ratios. More fundamentally an X_0/X_1 ratio should be selected that does not produce a high-frequency current zero following a restrike. If this condition is met, the voltages is not appreciably higher with two restrikes than with one, and no cumulative build-up of voltages is possible with successive restrikes.

The results in Table 6 were obtained by removing the fault at a current zero, that is, without forcing current zero. If the fault is in a confined space, such as under oil or in apparatus or cable insulation, the deionizing agents present may produce a rapid increase in arc drop, with the result that the fault is interrupted prior to a normal current zero. This forcing of a current zero increases the transient voltages as was discussed in connection with Figs. 43 and 44. It also increases the magnitude of the high-frequency current following a restrike, which decreases the X_0/X_1 ratio required to produce a high-frequency current zero following a restrike. This makes it difficult to select a suitable maximum X_0/X_1 ratio for application purposes because the ratio is influenced by the magnitude of the arc-extinction voltage assumed. As discussed above under arc characteristics, circuit breakers opening 12 000 and 13 200 volt circuits may infrequently have extinction voltages somewhat larger than normal line-to-ground crest voltage. Similar data are not available for fault arcs because this information is extremely difficult to obtain primarily because of the probability nature of the phenomenon.

To obtain some idea of the influence of arc-extinction voltage on the transient voltages produced by an arcing ground on a reactance grounded system, a special study was made on the computer using the same circuit and constants as above. A line-to-ground fault was applied at the

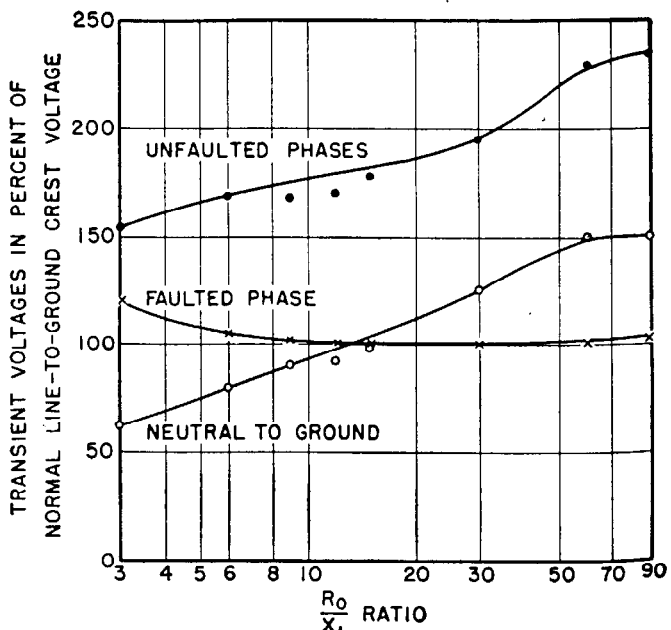


Fig. 46—Transient voltages with resistance grounding.

instant the 60-cycle voltage between phase *A* and ground was equal to its crest value, and removed approximately one-half cycle later. The circuit was opened slightly ahead of a normal 60-cycle current zero to give 100-percent extinction voltage. The fault was re-applied at crest recovery voltage across the fault. It was noted that no high-frequency current zero occurred following the restrike, with an X_0/X_1 ratio of four, but that such a zero was present with a ratio of six. The transient voltages did not exceed 260 percent with the ratio of four.

This analysis shows that the maximum transient voltages with reactance grounding are influenced by the X_0/X_1 ratio and by arc-extinction voltage. If the transient voltages are to be limited to 250 or 260 percent of normal line-to-ground crest voltage, the X_0/X_1 ratio should be limited to eight or four depending upon whether zero or 100-percent extinction voltage is assumed. In generator circuits, where faults can occur in confined spaces, it is suggested that the X_0/X_1 ratio be limited to three. This limit permits the application of 80-percent lightning arresters, and allows for arc-extinction voltages somewhat larger than normal line-to-ground crest voltage.

Studies were made for the case of a generator grounded through a resistor of 98 percent power factor. The circuit and constants were the same as used in the studies of reactance grounding. The results for two restrikes are summarized in Fig. 46, for R_0/X_1 ratios between 3 and 90. Although the data are based on two restrikes, there is no appreciable difference between the results with one and

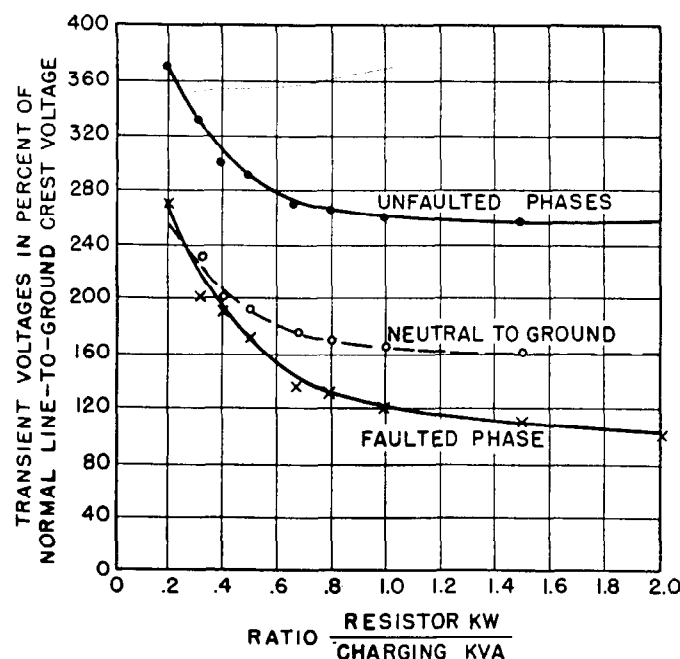


Fig. 47—Transient voltages with high-resistance grounding.

two restrikes. The fault to ground was always removed as the 60-cycle current went through zero because there were no high-frequency current zeros over the entire range of R_0/X_1 ratios considered. The transient voltages do not exceed 235 percent of normal line-to-ground crest voltage for any ratio considered.

Computer studies were also made with the same system grounded through the primary winding of a distribution transformer, having a resistor across the secondary winding as shown in Fig. 29 of Chap. 19. The transient voltages for this case are summarized in Fig. 47. The results are plotted as a function of the kilowatts loss in the resistor

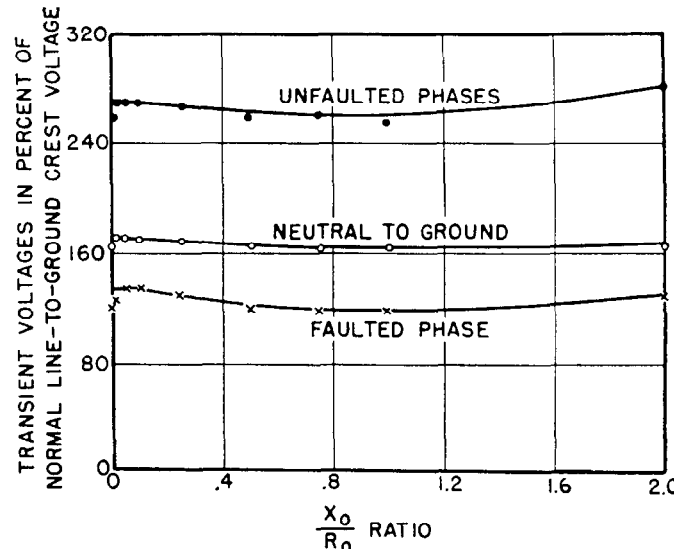


Fig. 48—Influence of reactance on transient voltages obtained with high-resistance grounding.

during a single-line-to-ground fault and the three-phase charging kva of the system during normal operation. Ratios of resistor loss to charging kva of one and larger will limit the transient voltages to approximately 260 percent of normal line-to-ground crest voltage.

The data in Fig. 47 are based on a resistor having unity power factor and a transformer having zero reactance. Practical resistors and transformers introduce reactance in the zero-sequence circuit. To show the effect of this reactance, studies were made for X_0/R_0 ratios of zero to two. The resistor loss-to-charging kva ratio was made equal to unity in this study. The results in Fig. 48 show that practical values of reactance have little influence on the transient voltages obtained.

REFERENCES

1. *Symmetrical Components* by C. F. Wagner and R. D. Evans (a book), McGraw-Hill Book Company, Inc., New York, 1933.
2. *Voltages Induced by Arcing Grounds*, by J. F. Peters and J. Slepian, A.I.E.E. *Transactions*, Vol. 42, April 1923, pages 478-493.
3. *The Klydonograph*, by J. F. Peters, *Electrical World*, April 19, 1924, pages 769-773.
4. *System Recovery Voltage Determination by Analytical and A-C Calculating Board Methods*, by R. D. Evans and A. C. Monteith, A.I.E.E. *Transactions*, Vol. 56, June 1937, pages 695-703.
5. *A Large-Scale General-Purpose Electric Analog Computer*, E. L. Harder and G. D. McCann, A.I.E.E. *Transactions*, Vol. 67, 1948, pages 664-673.
6. *Recovery Voltage Characteristics of Typical Transmission Sys-*

- tems and Relation to Protector-Tube Applications, by R. D. Evans and A. C. Monteith, *Electrical Engineering*, Vol. 57, August 1938, pages 432-443.
7. Voltage-Recovery Characteristics of Distribution Systems, R. L. Witzke, A.I.E.E. Technical Paper 49-53, 1949.
8. Power System Transients Caused by Switching and Faults, by R. D. Evans, A. C. Monteith and R. L. Witzke, *Electrical Engineering*, Vol. 58, August 1939, pages 386-394.
9. Klydonograph Surge Investigations, by J. H. Cox, P. H. McAuley and L. G. Huggins, A.I.E.E. *Transactions*, Vol. 46, February 1927, pages 315-329.
10. Lightning Investigation on the Appalachian Electric Power Company's Transmission System, by I. W. Gross and J. H. Cox, A.I.E.E. *Transactions*, Vol. 50, September 1931, page 1118.
11. Lightning Investigation on Transmission Lines—II, W. W. Lewis and C. M. Foust, A.I.E.E. *Transactions*, Vol. 50, September 1931, pages 1139-1146.
12. Overvoltages on Transmission Lines Due to Ground Faults as Affected by Neutral Impedances. Engineering Report No. 30, Joint Subcommittee on Development and Research, Edison Electric Institute and Bell Telephone System, November 15, 1934.
13. Reactance or Resistance Grounding? R. L. Witzke, *Electric Light and Power*, August 1939, pages 42-45.

CHAPTER 15

WAVE PROPAGATION ON TRANSMISSION LINES

Original Authors:

C. F. Wagner and G. D. McCann

Revised by:

C. F. Wagner

I. SIMPLE WAVES

A TRANSMISSION line can be regarded as made up of elements. If resistance is neglected, each element consists of a shunt capacitance and a series inductance as shown in Fig. 1. If a voltage is applied to one end of such a line, the first capacitor becomes charged immediately to the instantaneous applied voltage. However,

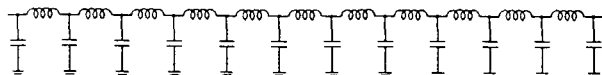


Fig. 1—Transmission line broken up into small elements.

because of the first series inductor, the second capacitor does not respond immediately but is delayed. Similarly, the third capacitor is delayed still more by the presence of the second inductor. Thus the farther removed from the end of the line the greater the delay. If the applied voltage is in the form of a surge, starting from zero and returning again to zero, it can be seen that the voltages on the intermediate condensers rise to some maximum value and return again to zero. The disturbance of the applied surge is thus propagated along the line in the form of a wave.

1. Mechanical Analogy

It can be shown with mathematical rigor that for a system of the kind just postulated (without series or shunt resistances and zero ground resistivity) the wave will be propagated along the line with undistorted or undimin-

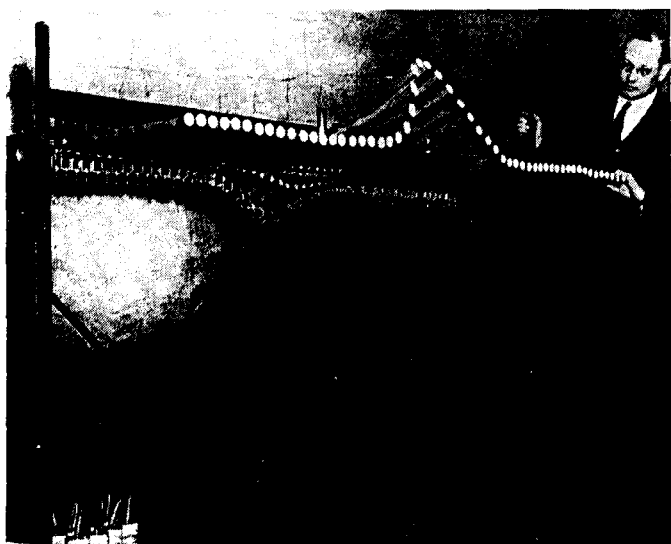


Fig. 2—Photograph of mechanical wave analogy.

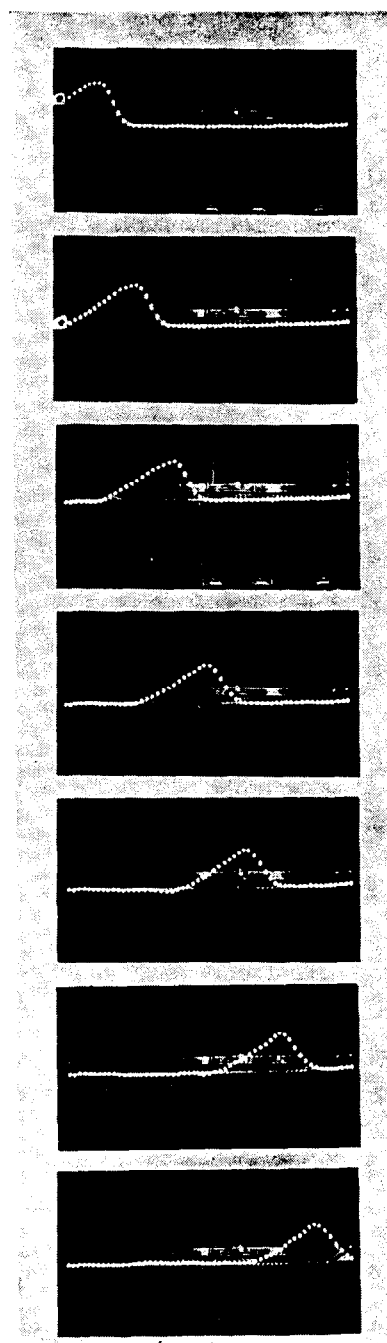


Fig. 3—Illustrating wave form of the traveling wave in a mechanical analogue for successive intervals of time.

ished amplitude. The same phenomenon can be demonstrated by means of a number of analogies. One which is particularly adapted to the present problem has been developed by Wagner¹ and is illustrated in Fig. 2. It consists of a number of aluminum arms mounted side by side. These arms are balanced about their center of rotation and their axes of rotation are in the same straight line. The only connection between adjacent arms is a flat spring, which offers a restraining torque when one arm is displaced with respect to the next. The mass of the arm corresponds to the inductance of the line and the spring to the capacitance. Fig. 3 illustrates what happens in this device when a disturbance is applied at one end. The wave moves along the line with essentially undiminished amplitude and unchanged wave form.

2. Current Wave, Surge Impedance and Surge Admittance

Knowing that the voltage surge moves along the line and imparts charge to the capacitors at any particular point only for the duration of the wave at that location, one can see that currents must flow in the connecting inductances, but only for the interval during which the surge exists at that point. That is, a wave of current should accompany the wave of voltage. It can be shown mathematically that the current wave will have exactly the same wave form as the voltage and at any instant will be proportional to the voltage. The constant of proportionality is known as the surge impedance and is usually designated by the symbol Z . It is equal to $\sqrt{\frac{L}{C}}$ where L is the inductance in henries per unit length of line and C is the capacity in farads per unit length of line. The dimensions of Z are those of a resistance and its value is expressible in ohms. Thus there exists the relation

$$e = iZ = i\sqrt{\frac{L}{C}} \quad (1)$$

where

e = instantaneous voltage
 i = instantaneous current.

The reciprocal of surge impedance is called the surge admittance and is usually designated by the symbol Y . Thus

$$i = Ye \quad (2)$$

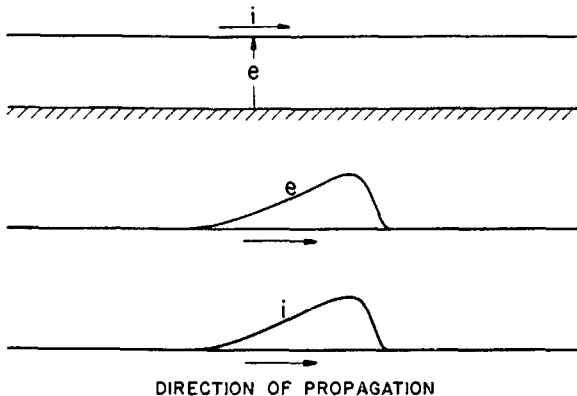


Fig. 4—Depicting a voltage wave and its associated current wave together with the positive sense assumed.

In Fig. 4 is depicted the general properties of traveling waves just enunciated. Note that the positive sense of potential is taken with respect to ground as zero and that the positive sense of current flow in the conductor is the same as the direction of propagation of the wave.

3. Line Constants

The inductance of a single conductor parallel to the earth, assuming an earth of zero resistivity, is

$$L = (2)(10^{-9}) \log_e \frac{2h}{r} \text{ in henries per cm.} \quad (3)$$

$$= (7.410)(10^{-4}) \log_{10} \frac{2h}{r} \text{ in henries per mile} \quad (4)$$

and its capacitance

$$C = \frac{10^{-11}}{18 \log_e \frac{2h}{r}} \text{ in farads per cm.} \quad (5)$$

$$= \frac{(3.882)(10^{-8})}{\log_{10} \frac{2h}{r}} \text{ in farads per mile.} \quad (6)$$

where h = height of conductor above ground

r = radius of conductor in same units.

The foregoing expression for inductance assumes that there is no flux within the conductor. This is the case for surges of short duration, because the current flows in a thin layer next to the surface—the phenomenon of "skin effect." For this reason ferrous conductors can be treated as non-ferrous conductors in considering traveling waves.

Making the same assumptions for cables (that all the current flows next to the return conductor) the inductance is

$$L = (7.410)(10^{-4}) \log_{10} \frac{r_2}{r_1} \text{ in henries per mile.} \quad (7)$$

and the capacitance is

$$C = \frac{(3.882)(10^{-8})k}{\log_{10} \frac{r_2}{r_1}} \text{ in farads per mile.} \quad (8)$$

where

r_1 = radius of conductor
 r_2 = inner radius of sheath
 k = permittivity

4. Evaluation of Surge Impedance

The surge impedance of a single aerial wire with ground return is

$$Z = \sqrt{\frac{L}{C}} = \sqrt{\frac{(7.410)(10^{-4}) \log_{10} \frac{2h}{r}}{(3.882)(10^{-8}) \log_{10} \frac{2h}{r}}} \\ = 138 \log_{10} \frac{2h}{r} \text{ ohms}$$
(9)

The curve of Fig. 5 will assist in the ready evaluation of this expression. In the absence of more definite information a surge impedance of 500 ohms is usually assumed.

For cables

$$Z = \frac{138}{\sqrt{k}} \log_{10} \frac{r_2}{r_1} \text{ ohms} \quad (10)$$

A good average value for this quantity is 50 ohms.

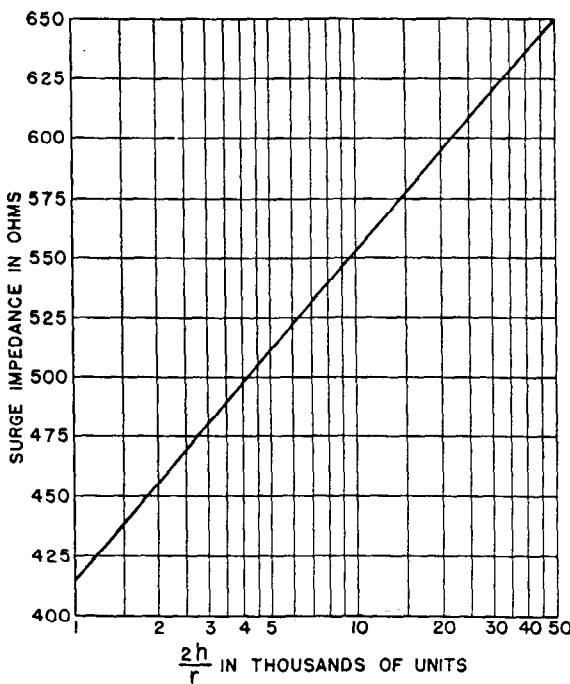


Fig. 5—Surge impedance of an aerial conductor.

5. Velocity of Propagation

The velocity of propagation of any electromagnetic disturbance in air is the same as that of light, namely 2.998×10^{10} cm. per sec. The only difference for transmission lines is that the conductor provides a guide. In terms of the constants of the line, this velocity is equal to $\frac{1}{\sqrt{CL}}$. To verify the velocity relation, substitute (3) and (5) into this expression giving

$$\text{velocity} = \frac{1}{\sqrt{CL}} = \frac{1}{\sqrt{(10^{-11})(2)(10^{-9}) \log \frac{2h}{r}}} = 3 \times 10^{10} \text{ cm per sec.} \quad (11)$$

A convenient though approximate figure of 1000 ft per microsecond (a more exact value being 984 ft per microsecond) is generally used in connection with line calculations.

Applying relation (11) to cables there results that

$$\text{velocity} = \frac{1}{\sqrt{CL}} = \frac{(3)(10^{10})}{\sqrt{k}} \text{ cm per sec.} \quad (12)$$

This likewise is a special case of a more general phenomenon, that the velocity of propagation of any disturbance in a medium of permittivity k varies inversely as the square root of the permittivity. Since the permittivity of materials used in cables varies from about 2.5 to 4.0, the velocity of propagation of surges in cables is about one-third to one-half that of light. Similarly a disturbance in a counterpoise buried in earth having a permittivity of say 6 propagates within the earth at a velocity of $\frac{1000}{\sqrt{6}}$ or 408 ft. per microsecond.

6. Mathematical Expression of Voltage and Current Wave

Mathematically a traveling wave can be designated as follows:

$$e = f(x - vt) \quad (13)$$

where x is the distance measured along the line and v is the velocity of propagation. With t fixed, plotting e as a function of x gives the voltage distribution along the line at that instant. With x fixed e gives the variation of the voltage with time at that point.

Similarly, the current wave is

$$i = \frac{e}{Z} = \frac{f(x - vt)}{Z} \quad (14)$$

7. Waves in Reverse Direction

The same relations as mentioned above apply to a wave traveling in the opposite direction when the positive sense of current is taken the same as the direction of propagation. This means that the positive sense of current would be the reverse of the wave moving in the opposite direction. For analytical work it is convenient that the positive sense of both currents be the same. By arbitrarily reversing the sign of one of the currents and making the corresponding

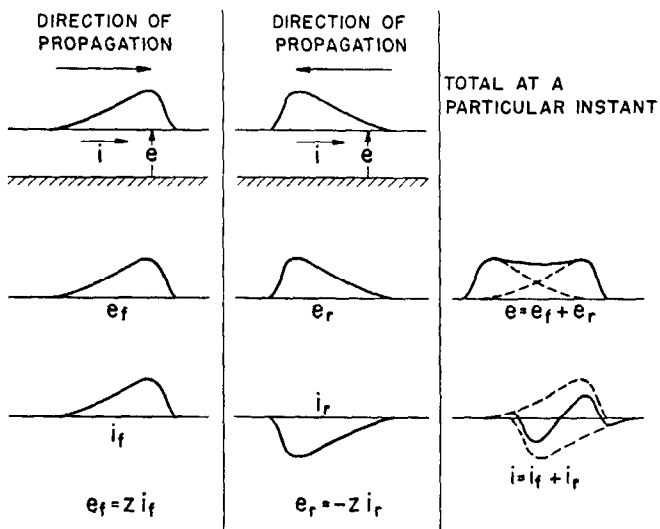


Fig. 6—Forward and backward voltage waves with their associated current waves and also the sum of the two.

changes in the equations, this difficulty may be avoided. Fig. 6 gives the conventions adopted for both types of waves together with the equations relating the voltages and currents. The waves moving from left to right are designated by the subscript f suggestive of forward moving and the wave from right to left by the subscript r suggestive of a wave moving in the reverse direction or a reflected wave.

8. Principle of Superposition

When two waves of this character meet, they do not influence each other but seem to pass through each other. An illustration of this phenomenon is shown in Fig. 7 in which two oppositely moving waves meet in the me-

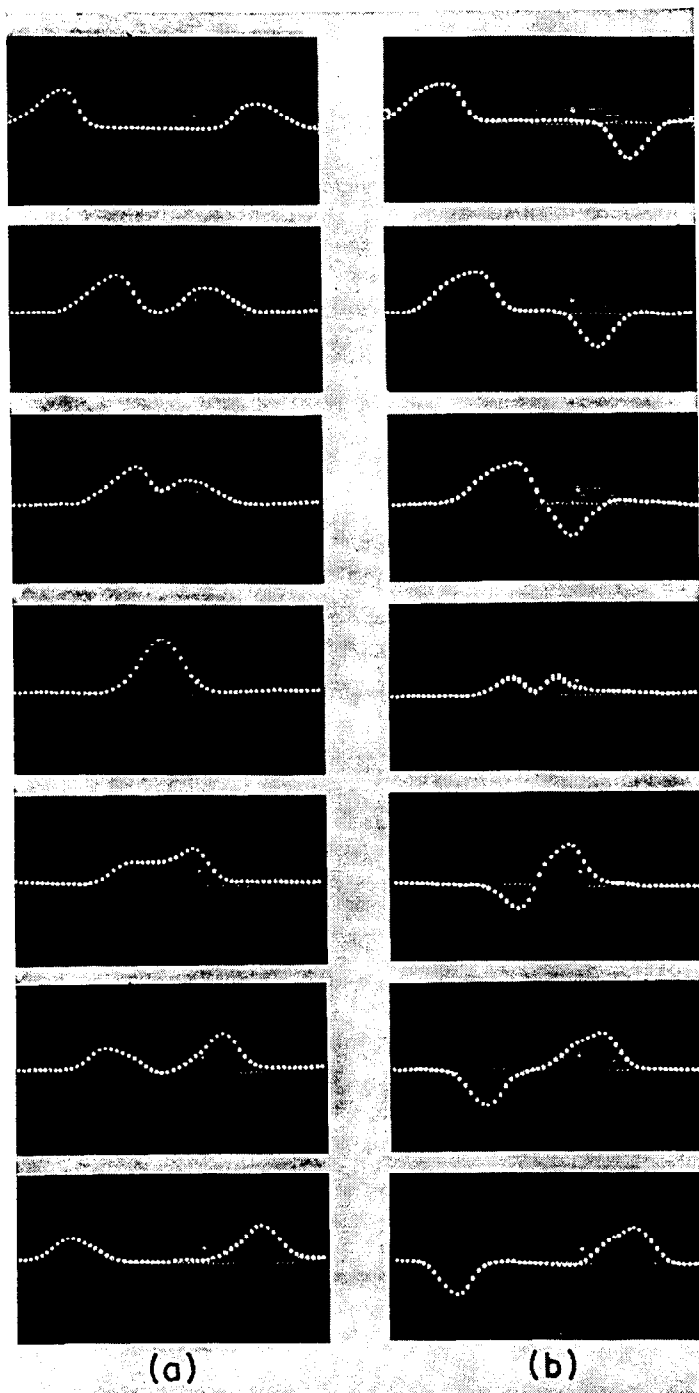


Fig. 7—Illustrating superposition of two waves upon each other.

(a) Two positive waves. (b) One positive and one negative wave.

chanical analogy described previously. Upon meeting, the instantaneous amplitudes of the two waves add together but, after passing through each other, remain undisturbed in magnitude and wave shape. Thus traveling waves may be said to follow the laws of superposition. Each component can be analyzed separately. The right hand column of Fig. 6 shows how the two voltage and current waves add at a particular instant.

II. POINTS OF DISCONTINUITY

When a simple voltage and current wave (e_f and i_f) moves along a line and meets a point of discontinuity reflections take place. If a resistor is connected across the end of a line, the reflections from this point are relatively simple to calculate but if the resistor is replaced by an inductor or capacitor the solution becomes more complicated. Some of the more usual cases will be analyzed in detail.

9. Relations for Simple Reflections from the End of the Line

In Fig. 8 let e_f and i_f be the instantaneous voltage and current of the forward wave at the point of discontinuity. These are usually the known quantities. Further, let e_r and i_r be the instantaneous voltage and current of the reflected wave at the point of discontinuity, and e and i the instantaneous voltage and current at the point of discontinuity. Thus

$$e = e_f + e_r \quad (15)$$

$$i = i_f + i_r \quad (16)$$

$$= \frac{e_f}{Z} - \frac{e_r}{Z} \quad (17)$$

From (17)

$$Zi = e_f - e_r \quad (18)$$

Adding (15) and (18)

$$e + Zi = 2e_f \quad (19)$$

This equation supplies a relation connecting e and i with the instantaneous value of the oncoming wave. The shunting network must supply another equation to provide the solution.

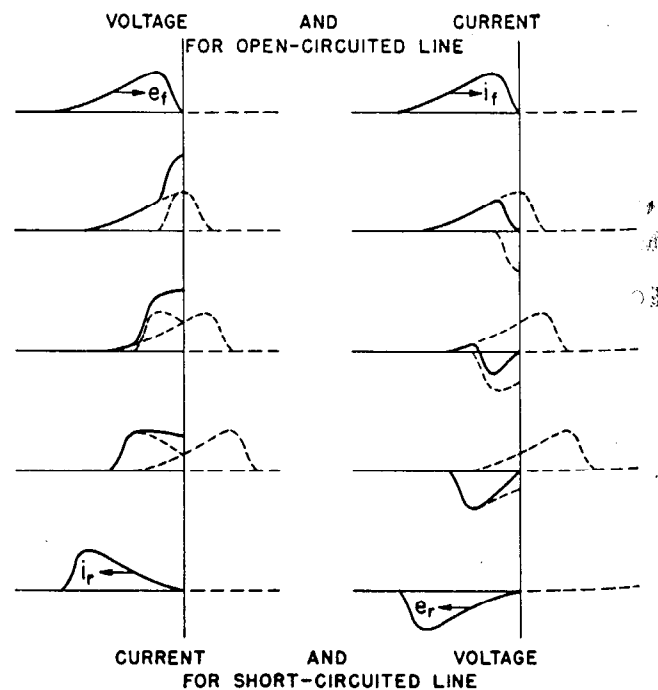


Fig. 8—Reflection of waves from open-circuited and from short-circuited end of line.

After e and i have been determined, e_r can be obtained by subtracting (18) from (15) giving

$$e_r = \frac{1}{2}(e - Z_i i) \quad (20)$$

An alternate form is obtained by inserting e from (19) into (20), giving

$$e_r = e_i - Z_i \quad (20a)$$

10. Line Terminated by a Resistance — Open and Short-Circuited Line

When the line is terminated by a resistance R , then

$$e = R i \quad (21)$$

Combining this with (19)

$$i = \frac{2}{R + Z} e_i \quad (22)$$

$$e = \frac{2R}{R + Z} e_i \quad (23)$$

And from (20)

$$e_r = \frac{R - Z}{R + Z} e_i \quad (24)$$

(a) **Open-Circuited Line.** If $R = \infty$, the condition which corresponds to an open-circuited line, then

$$e_r = e_i \quad (25)$$

Thus, the reflected wave is equal to the oncoming voltage wave. Also

$$e = 2e_i \quad (26)$$

a relation which proves the well-known doubling up of a voltage wave as it strikes the end of an open-circuited line. Equating e_r and e_i to their Zi equivalents from Fig. 6 there is obtained

$$i_r = -i_i \quad (27)$$

a relation that must be maintained since the currents at the end of an open line must be zero, that is, $i = i_i + i_r = 0$. The variations of the principle quantities at different instants are illustrated in Fig. 8.

(b) **Short-Circuited Line.** For the short-circuited condition R of Eq. (24) is zero, for which

$$e_r = -e_i \quad (28)$$

The reflected wave is the negative of the oncoming wave at any instant and the sum of the waves, e , is equal to zero. On the other hand, inserting the Zi equivalents of e_r and e_i in (28), there results that

$$i_r = i_i \quad (29)$$

which shows that the total current doubles at the end of the line. As shown in Fig. 8, the relations are the same as for the open-circuited line except that the voltages and currents are interchanged.

(c) **$R = Z$.** For this case as can be seen from (24), e_r is equal to zero and there is no reflected wave. Since the line has the same characteristic as that of a resistance it is evident that electrically there is no discontinuity. The wave merely disappears as the end of the line is reached.

(d) **Other Cases.** For other cases the reflected wave will be positive or negative depending upon the extent to which R is greater or less than Z .

11. Junction of Dissimilar Lines

Fig. 9 (a) illustrates the case in which the section to the left of a represents a line whose surge impedance is Z and the section to the right one whose surge impedance is Z' . Since the volt-ampere characteristics of a line are the same as those of a resistance, the reflections resulting when a wave approaches the junction point from the left are the same as though the line to the right of a were replaced by a resistance equal to Z' , as shown in Fig. 9 (b).

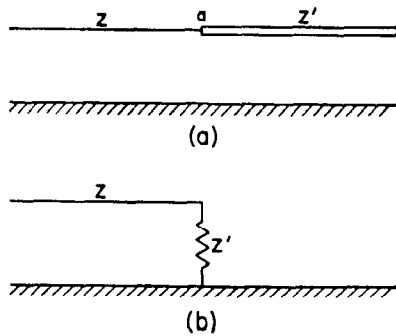


Fig. 9—Equivalent circuit of line terminating at (a) and continuing by a line of different surge impedance.

The instantaneous voltage, e , and the reflected wave at the junction point can be computed by Eqs. (23) and (24), respectively. The voltage, e , thus gives the wave shape of the wave propagated out along the line to the right of a .

12. Junction of Several Lines

When a surge travels along line A of Fig. 10 and strikes the junction point of two or more other lines that are separated a sufficient distance that mutual coupling between them is negligible, the reflections and transmitted voltages can be calculated by replacing the lines to the right of the junction points by a shunt resistance as in Fig. 9 in which the resistance is equal to the parallel surge impedance of all the lines to the right of a . Equal voltage waves are then propagated along lines B , C and D .

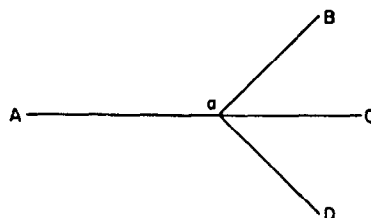


Fig. 10—Junction of several lines.

13. Single Line Terminated by an Inductance

The schematic diagram for this case is shown in Fig. 11. From the terminating network there results that

$$e = L \frac{di}{dt} \quad (30)$$

Combining this with Eq. (19)

$$2e_i = Zi + L \frac{di}{dt} \quad (31)$$

It will be observed that the solution of this equation is the same as the case for which the voltage $2e_f$ is applied to a resistance and inductance circuit in which the resistance

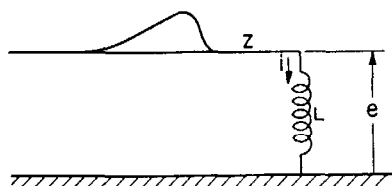


Fig. 11—Line terminated by an inductance.

is Z and the inductance is L . The current depends upon the character of the applied voltage.

If e_f is a square-topped wave of magnitude E , i approaches a magnitude of $\frac{2E}{Z}$ along an exponential curve

whose time constant is $\frac{L}{Z}$. The expression for this curve is

$$i = \frac{2E}{Z} \left[1 - e^{-\frac{Zt}{L}} \right] \quad (32)$$

From (30)

$$e = 2E e^{-\frac{Zt}{L}} \quad (33)$$

From (20), the reflected wave is

$$e_r = E \left[-1 + 2e^{-\frac{Zt}{L}} \right] \quad (34)$$

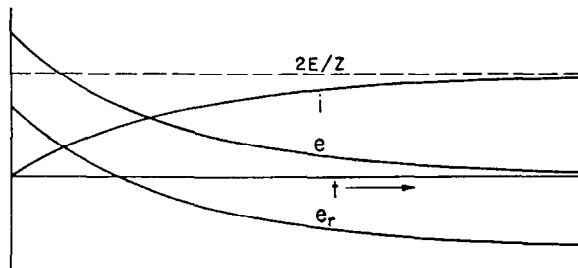


Fig. 12—Voltages and currents at the end of the line shown in Fig. 11 in response to a square-top wave having a maximum value of E .

Fig. 12 shows graphs of these curves and Fig. 13 successive positions of the oncoming and reflected wave. It will be observed that the circuit acts like an open-circuited line initially but finally takes on the characteristics of a short-circuited line. The voltage starts at a value twice that of the oncoming wave and finally reaches zero. The reflected wave starts at $+E$ and gradually approaches $-E$.

If instead of a square-topped wave the oncoming wave e_f of Eq. (31) is of a generalized form, such as shown in Fig. 14, the current response can be determined by the follow-up method described in Part VI, Sec. 20 of Chap. 6. Equation (31) characterizes the phenomenon as one in which the instantaneous value of i tends to approach, along an exponential curve whose time constant is $\frac{L}{Z}$, a value determined by the voltage at that instant divided by the surge impedance. Fig. 14 illustrates the graphical construction.

From (19)

$$e = 2e_f - Zi \quad (35)$$

which permits the determination of e since both e_f and i are now known. The reflected voltage wave can be de-

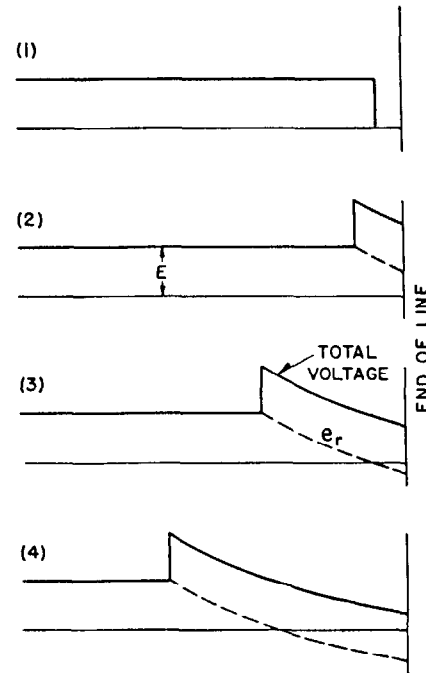


Fig. 13—Reflected wave and total voltage waves at successive instants upon a line terminated by an inductance in response to a square topped wave having a maximum value of E .

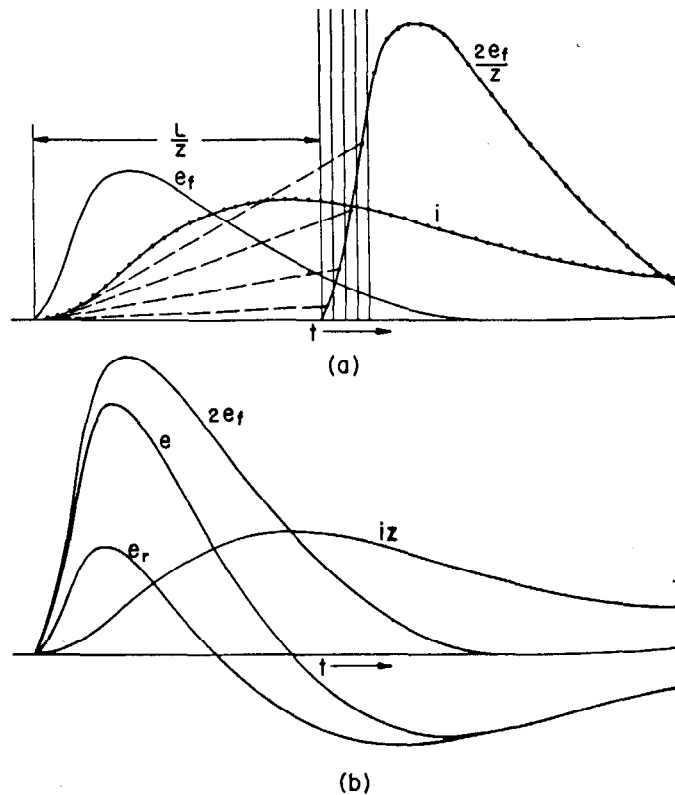


Fig. 14—Graphical method of analyzing line terminated by an inductance.

terminated through the use of Eq. (20a). All of these quantities are shown in Fig. 14. Fig. 15 illustrates the relative positions along the line of these waves at different instants.

14. Single Line Terminated by a Capacitor

Fig. 16 shows the schematic diagram for this case from which it may be seen that

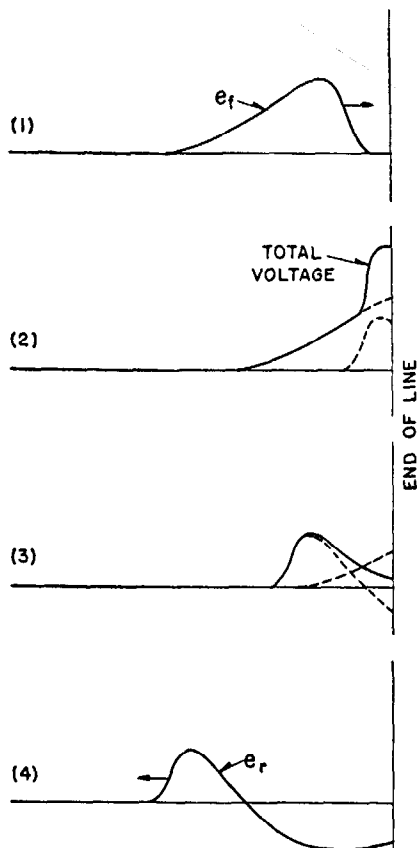


Fig. 15—Relative positions of waves of Fig. 14 along line at different instants.

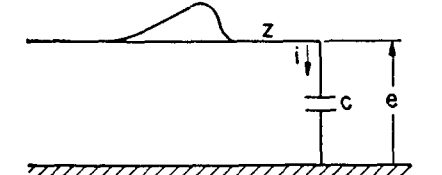


Fig. 16—Line terminated by a capacitor.

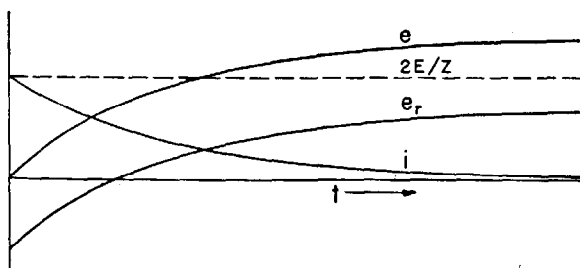


Fig. 17—Voltages and currents at the end of the line shown in Fig. 16 in response to a square-top wave having a maximum value of E .

$$e = \frac{1}{C} \int i dt$$

Substituting this expression for e into (19) there results that

$$2e_f = Zi + \frac{1}{C} \int i dt$$

This is the well known equation representing the charging of a capacitor through a resistance upon the application of a voltage $2e_f$.

If e_f is a square-topped wave of magnitude E , i is equal to

$$i = \frac{2E}{Z} e^{-\frac{t}{ZC}} \quad (36)$$

From (19)

$$e = 2e_f - Zi = 2E \left(1 - e^{-\frac{t}{ZC}} \right) \quad (37)$$

From (20a)

$$e_r = e_f - Zi = E \left[1 - 2e^{-\frac{t}{ZC}} \right] \quad (38)$$

These quantities are plotted as a function of time in

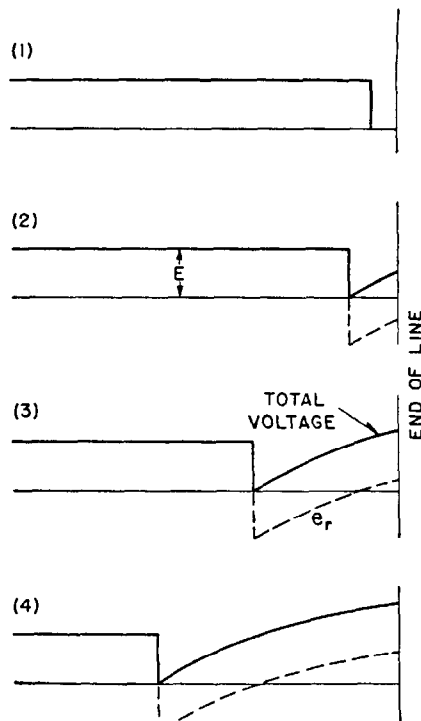


Fig. 18—Reflected and total voltage waves upon a line terminated by a capacitor in response to a square-topped wave having a maximum value (E).

Fig. 17. Fig. 18 shows the position of the reflected wave and the total voltage at different instants of time.

15. Special Case

A special case will be considered for which the voltage across the terminal equipment is a non-linear function of the current through it, such as for a lightning arrester. In Fig. 19 let the heavy full line represent the volt-ampere characteristic of the arrester and the dotted straight line

Z_i , the surge impedance of the line times the current through the arrester. From (19)

$$e_f = \frac{1}{2}(e + Z_i i) \quad (39)$$

This quantity is plotted also in Fig. 19. Since e_f is the magnitude of the oncoming wave at any instant, then i

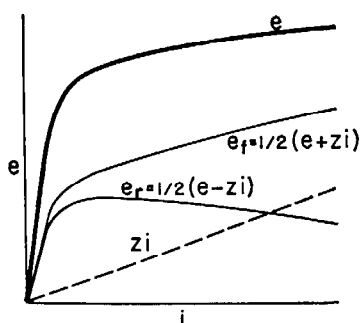


Fig. 19—Special case where voltage across terminal equipment is a known function of current through it.

and, consequently, e is known for any value of e_f and can be plotted as a function of time. Similarly, from (20), e_r can also be plotted against i and is known in terms of e and e_f .

16. Network Connected in Shunt Across a Continuous Line

The schematic diagram for this case is shown in Fig. 20. Let a wave travel from the left and approach the network. As the network is reached a reflection will occur

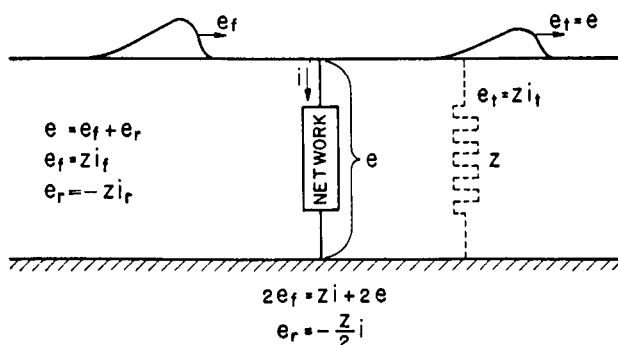


Fig. 20—Network connected in shunt across a continuous line.

and a voltage e is built up across the network. A wave, e_f is transmitted along the line to the right equal at any instant at the junction point to the voltage e . From the voltage conditions at the junction point

$$e_f + e_r = e \quad (40)$$

and from the current relations

$$i_f + i_r = i + i_t$$

$$\text{or } \frac{e_f - e_r}{Z} = i + \frac{e_t}{Z}$$

$$= i + \frac{e}{Z}$$

$$\text{or } e_f - e_r = Z_i + e$$
(41)

Adding (40) and (41)

$$2e_f = Z_i + 2e \quad (42)$$

The shunting network will provide another equation connecting e and i which in combination with Eq. (42) permits of the determination of e and i . Subtracting (40) and (41)

$$e_r = -\frac{Z}{2}i \quad (43)$$

Note that the line to the right can be replaced by a resistor Z in shunt across the network at the junction point as shown by the dotted line.

As an illustration of this case let the network be a resistor R . Then

$$e = R i$$

and substituting in (42)

$$2e_f = Z_i + 2R i$$

or

$$i = \frac{2}{Z + 2R} e_f \quad (44)$$

and

$$e = \frac{2R}{Z + 2R} e_f \quad (45)$$

The transmitted wave is also equal to (45) and the reflected wave is from (43)

$$e_r = -\frac{Z}{Z + 2R} e_f \quad (46)$$

III. LATTICE NETWORKS

When the circuit consists of a number of shunt impedances distributed along the line as in Fig. 21 (a), the solution is expedited and simplified by means of the lattice network by Bewley. While the system can be applied generally, it will be discussed principally with regard to shunt resistors.

17. Voltage Lattice Network

If in Fig. 21(a) a traveling wave e_f moves from the left to right toward a then upon reaching a , a transmitted wave and a reflected wave is produced. These waves can be expressed as follows

$$e_t = \text{transmitted wave} = \alpha_a e_f \quad (47)$$

$$e_r = \text{reflected wave} = \beta_a e_f \quad (48)$$

where α_a is the transmission coefficient which from (45) is equal to

$$\frac{2R_a}{Z + 2R_a} \quad (49)$$

and β_a is the reflection coefficient which from (46) is equal to

$$-\frac{Z}{Z + 2R_a} \quad (50)$$

So long as the line surge impedances are equal on both sides of the resistor then the transmitted and reflected waves are independent of the direction from which the wave propagates. If on the other hand the line is unsymmetrical with respect to the resistor this statement is untrue. Thus, if the line surge impedance to the left of the resistor is Z and to the right Z' , then for a wave mov-

ing from the left hand side at the point a the transmission coefficient is

$$\alpha_a = \frac{2RZ'}{RZ + RZ' + ZZ'} \quad (51a)$$

and the reflection coefficient is

$$\beta_a = \frac{RZ' - RZ - ZZ'}{RZ + RZ' + ZZ'} \quad (51b)$$

For a wave moving from the right to the left the transmission coefficient, γ_a , is

$$\gamma_a = \frac{2RZ}{RZ' + RZ + ZZ'} \quad (51c)$$

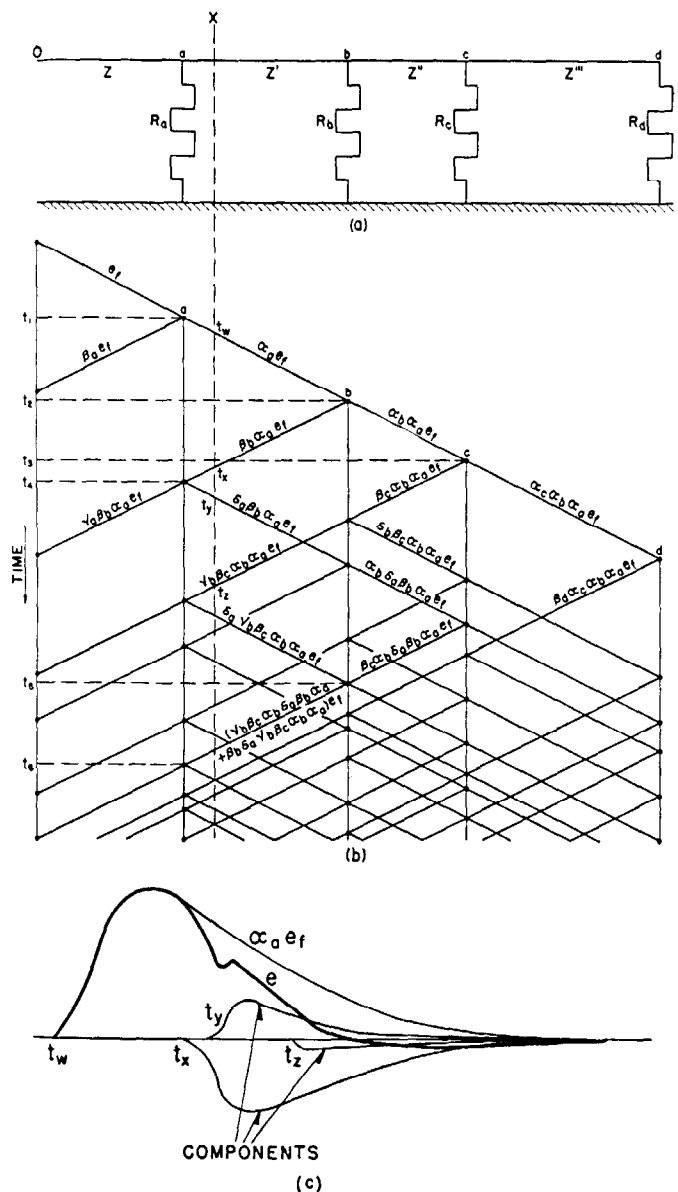


Fig. 21—Lattice network.

- (a) Equivalent circuit of line with several shunt impedances at distributed points.
- (b) Lattice network for voltages on above circuit.
- (c) Addition of components from lattice network to give actual voltage at a given point.

and the reflection coefficient, δ_a , is

$$\delta_a = \frac{RZ - RZ' - ZZ'}{RZ' + RZ + ZZ'} \quad (51d)$$

When the transmitted wave from a reaches b , another reflection and partial transmission occurs. The reflected wave from b is partially transmitted and reflected from a . This continues indefinitely throughout the network until the components have been reduced to zero. By means of the system² shown in Fig. 21 (b) account can be kept of each component not only in magnitude but in time. The horizontal distance represents length along the line and the vertical distance time. The inclined lines are so sloped that the vertical distance represents the time required for the original wave or a reflected component to reach the point designated. Let zero time be the instant at which the traveling wave e_f leaves 0. At time t_1 this wave has reached a . The reflected wave from this point is $\beta_a e_f$ which is sloped the opposite direction and is thus indicative of motion in the reverse direction. The transmitted wave from a , $\alpha_a e_f$ reaches b at time t_2 when a reflection $\beta_b \alpha_a e_f$ occurs and the wave $\alpha_b \alpha_a e_f$ is transmitted beyond this point. This latter wave reaches c at the time t_3 . Each wave whether it be transmitted or reflected has its own transmitted and reflected components. Where two waves coincide as at b for time t_5 where waves from a and c arrive at the same time, the reflected and transmitted waves from this point are added, as has been done for the wave between b and a between t_5 and t_6 .

To determine the actual voltage at any point such as X it is necessary to add the different components with their proper time relations as is shown in Fig. 21(c). The method is much simpler than this description might convey as numerical values simplify very greatly the appearance of the steps. In most cases the resistors are equal and equally spaced. If the voltage at any of the resistors is desired, the components of voltage on either one side or the other should be added *not* the components on both sides.

18. Current Lattice Network

So far consideration has been given only to the voltage waves in lattice networks. The currents can be obtained from the voltage components by merely dividing those that move from left to right by the proper line surge impedance Z and those that move from right to left by the corresponding $-Z$. The sign is determined simply by the direction of downward slope of the lines in Fig. 21(b). However, instead of using the voltage waves as a basis for the lattice network, the current waves can be used with equal facility. A similar set of equations employing transmission and reflection coefficients relates the transmitted and reflected waves to the oncoming wave approaching the discontinuity.

For waves, I_f , moving from left to right

$$i_t = \text{transmitted current wave} = \alpha_a i_f \quad (52)$$

$$i_r = \text{reflected current wave} = -\beta_a i_f \quad (53)$$

For waves, I_t , moving from right to left

$$i_t = \gamma_a i_f \quad (54)$$

$$i_r = -\delta_a i_f \quad (55)$$

For these equations the transmission and reflection coefficients are identical to those used for the voltages in the voltage lattice network for either the simple condition of uniform line surge impedance Z (see equations 49 and 50) or for the more general case of different surge impedances on each side of the point of discontinuity (see equations 51(a) to 51(d)). The negative signs in equations (53) and (55) for the reflected waves are due to difference in polarity relations between the current waves and their corresponding voltage waves for surges propagating in the two directions.

In accordance with Kirchoff's law, the current flowing in any of the shunt resistors is equal to the algebraic sum of the current waves moving into and out of the point. Where the line surge impedance Z is the same on both sides of the resistor, the resistor current can be given in terms only of the summation of the incoming waves from both left and right by the following equation

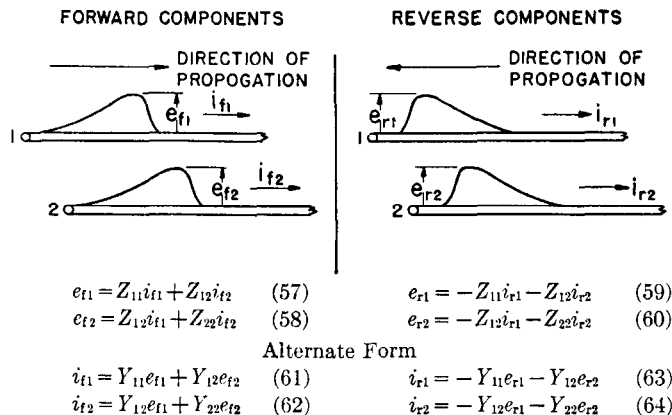
$$i_{(\text{resistor})} = \frac{2R}{Z+2R} \sum i_t \quad (56\text{a})$$

In summing the different components they must be added with the proper time displacement between them.

IV. MUTUALLY COUPLED CIRCUITS

19. Voltages and Currents for Two Parallel Conductors

Just as the steady-state voltage and current relations between two coupled electromagnetically or two electrostatically coupled circuits can be expressed in terms of two simple linear equations so also can the relations between voltages and currents associated with traveling waves in two parallel conductors be similarly expressed.



in which

$$Y_{11} = \frac{Z_{22}}{Z_{11}Z_{22} - Z_{12}^2} \quad (65)$$

$$Y_{22} = \frac{Z_{11}}{Z_{11}Z_{22} - Z_{12}^2} \quad (66)$$

$$Y_{12} = -\frac{Z_{12}}{Z_{11}Z_{22} - Z_{12}^2} \quad (67)$$

for total quantities

$$e_1 = e_{f1} + e_{r1} \quad (68)$$

$$e_2 = e_{f2} + e_{r2} \quad (69)$$

$$i_1 = i_{f1} + i_{r1} \quad (70)$$

$$i_2 = i_{f2} + i_{r2} \quad (80)$$

Fig. 22—Analytic representation of voltage and current waves on mutually-coupled circuits.

These relations for a pair of forward moving waves is given by Eqs. (57) and (58) of Fig. 22. The voltages are measured with respect to ground as zero potential and the positive sense of current flow is taken as from left to right. The corresponding relations for a reverse moving pair is given by Eqs. (59) and (60). The coefficients in these equations are called self and mutual surge impedances.

The converse relations for currents in terms of voltages are given by equations (61) to (64) in which the coefficients are called the self and mutual surge admittances. Equations (65) to (67) give the admittances in terms of the surge impedances.

For cases in which these components only are involved the total voltages and currents in the two conductors are given by Eqs. (68) to (80).

Where more than two conductors are involved these equations may be generalized quite readily by the addition of other terms. Thus, for three conductors Eqs. (57) and (58) would be extended by the addition of a third term involving the current in the third conductor with a coefficient equal to the mutual surge impedance. In addition a third equation would be introduced for e_{f3} . Similar additions would be incorporated throughout the system of equations.

20. Self and Mutual Surge Impedances

For most traveling waves the current flows near the surface of the conductor which permits neglecting the flux inside. In addition the earth can in nearly all cases be regarded as having perfect conductivity. For these assumptions the self and mutual impedances in terms of the nomenclature illustrated in Fig. 23 are

$$Z_{11} = 138 \log_{10} \frac{2h_1}{r_1} \text{ ohms} \quad (81)$$

$$Z_{12} = Z_{21} = 138 \log_{10} \frac{b}{a} \text{ ohms} \quad (82)$$

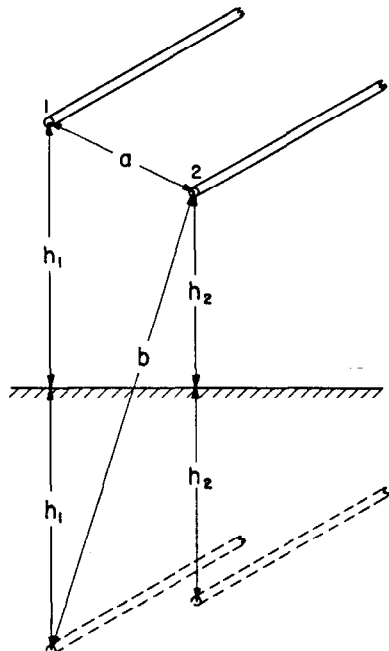


Fig. 23—Two parallel conductors with their images.

21. Several Conductors in Parallel

There are certain practical cases where surges are introduced simultaneously on several conductors in parallel and sufficient symmetry exists that it can be assumed that the voltage and currents are equal on each of them. For these assumptions an equivalent surge impedance can be determined which enables the treatment of the conductors as a single equivalent conductor.

For two conductors if the voltage, e , of the single equivalent conductor is taken as the mean of e_1 and e_2 and by assumption i_1 and i_2 are equal to $\frac{i}{2}$ where i is the total current, then from equations (57) and (58)

$$e = \frac{e_1 + e_2}{2} = \frac{1}{4}(Z_{11} + 2Z_{12} + Z_{22})i$$

Therefore, the equivalent surge impedance is

$$Z_{eq} = \frac{1}{4}(Z_{11} + 2Z_{12} + Z_{22}) \quad (83)$$

Upon substituting (81) and (82) this becomes

$$\begin{aligned} Z_{eq} &= 138 \log_{10} \sqrt{\frac{2h_1(b)}{r_1} \left(\frac{b}{a}\right)^2 \frac{2h_2}{r_2}} \\ &= 138 \log_{10} \frac{\sqrt{(2h_1)b^2(2h_2)}}{\sqrt{r_1 r_2 a^2}} \end{aligned} \quad (84)$$

from which it can be seen that the two conductors can be replaced by a single conductor whose radius is $\sqrt[4]{r_1 r_2 a^2}$ and height above ground is $\frac{1}{2}\sqrt[4]{4h_1 h_2 b^2}$. For most cases the height can be taken as the arithmetic mean of the two conductors and when they have equal radii

$$Z_{eq} = 138 \log_{10} \frac{(h_1 + h_2)}{\sqrt{ar}} \quad (85)$$

22. Wave on One Conductor with the Other Grounded

In order to clarify some of the physical concepts involved several specific cases will be considered. The first of these is shown in Fig. 24, in which a voltage wave is

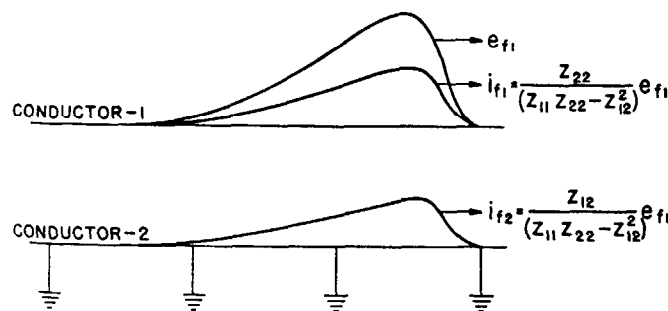


Fig. 24—Voltage and current relations for voltage applied to one conductor with other conductor grounded.

applied to conductor number 1 and conductor number 2 is grounded. Substituting the condition into Eq. (58) that e_{f2} is always zero, then

$$i_{f2} = -\frac{Z_{12}}{Z_{22}} i_{f1} \quad (86)$$

Substituting this value into (57)

$$e_{f1} = Z_{11} i_{f1} - \frac{Z_{12}^2}{Z_{22}} i_{f1} = \frac{Z_{11} Z_{22} - Z_{12}^2}{Z_{22}} i_{f1} \quad (87)$$

It can be seen that the only effect of the presence of the grounded conductor is to reduce the effective surge impedance of the ungrounded conductor.

23. Reflected and Transmitted Waves When One Conductor Is of Finite Length and Open Circuited

This case is illustrated in Fig. 25. Let it be assumed that the forward moving waves e_{f1} and e_{f2} are known and it is desired to determine their associated currents, the voltages

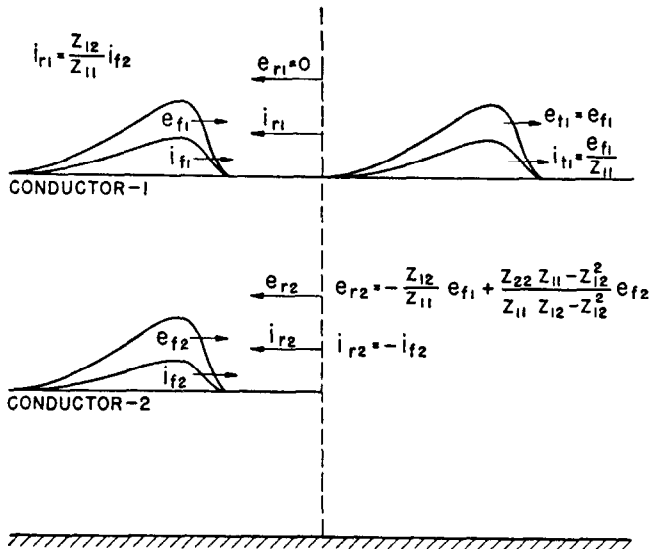


Fig. 25—Reflected and transmitted waves when one conductor is of finite length and open circuited.

and currents that will be reflected backward when the point corresponding to the end of the one line is reached, and the voltage and current transmitted beyond this point on conductor number 1. These quantities constitute the eight unknowns i_{f1} , i_{f2} , e_{r1} , e_{r2} , i_{r1} , i_{r2} , e_{t1} and i_{t1} . The eight equations required for their solutions are Eqs. (57) to (60) of Fig. 22 and the four following which apply at the point of discontinuity:

$$e_{f1} + e_{r1} = e_{t1} \quad (88)$$

$$e_{t1} = Z_{11} i_{t1} \quad (89)$$

$$i_{f1} + i_{r1} = i_{t1} \quad (90)$$

$$i_{f2} + i_{r2} = 0 \quad (91)$$

i_{f1} and i_{f2} can be determined from Eqs. (57) and (58) and then from Eq. (91) i_{r2} is known. By the combination of Eqs. (88), (89), and (90)

$$e_{f1} + e_{r1} = Z_{11}(i_{f1} + i_{r1})$$

Substituting in this equation the values of e_{f1} and e_{r1} as given by Eqs. (57) and (59) there results

$$Z_{12} i_{f2} - 2Z_{11} i_{r1} - Z_{12} i_{r2} = 0$$

which gives the equation for i_{r1} when the value of i_{r2} given by Eq. (91) is substituted

$$i_{r1} = \frac{Z_{12}}{Z_{11}} i_{f2} \quad (92)$$

Substituting the values of i_{r1} and i_{r2} given by Eqs. (91) and (92) into Eq. (59)

$$\begin{aligned} e_{r1} &= -Z_{11} \left(\frac{Z_{12}}{Z_{11}} \right) i_{f2} - Z_{12} (-i_{f2}) \\ e_{r1} &= 0 \end{aligned} \quad (93)$$

Thus there is no reflected voltage wave on conductor number 1 and the voltage e_{f1} is transmitted undistorted past the point of discontinuity.

Making similar substitutions in Eq. (60)

$$\begin{aligned} e_{r2} &= -Z_{12} \left(\frac{Z_{12}}{Z_{11}} i_{f1} \right) - Z_{22} (-i_{f1}) \\ e_{r2} &= \frac{Z_{22} Z_{11} - Z_{12}^2}{Z_{11}} i_{f1} \end{aligned} \quad (94)$$

From Eqs. (62), (66), and (67)

$$i_{f2} = -\frac{Z_{12}}{Z_{11} Z_{22} - Z_{12}^2} e_{f1} + \frac{Z_{11}}{Z_{11} Z_{22} - Z_{12}^2} e_{f2}$$

and substituting this value of i_{f2} into Eq. (94)

$$e_{r2} = -\frac{Z_{12}}{Z_{11}} e_{f1} + e_{f2} \quad (95)$$

The total voltage at the end of conductor number 2 is

$$e_2 = e_{f2} + e_{r2} = -\frac{Z_{12}}{Z_{11}} e_{f1} + 2e_{f2} \quad (96)$$

24. Reflected and Transmitted Waves When Conductor of Finite Length Is Grounded

For this case, which is illustrated in Fig. 26, the four additional equations to be used with Eqs. (57) to (60) are the following:

$$e_{f1} + e_{r1} = e_{t1} \quad (97)$$

$$e_{t1} = Z_{11} i_{t1} \quad (98)$$

$$i_{f1} + i_{r1} = i_{t1} \quad (99)$$

$$e_{f2} + e_{r2} = 0_t \quad e_{r2} = -e_{f2} \quad (100)$$

These eight equations can be solved for the eight unknowns with the results given in Fig. 26. The relations

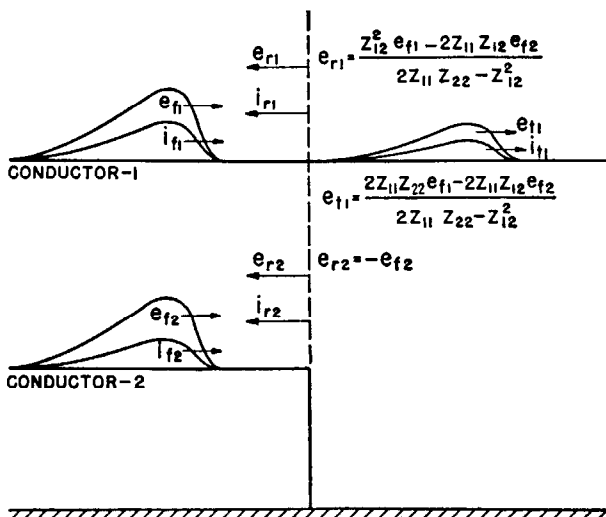


Fig. 26—Reflected and transmitted waves when conductor of finite length is grounded.

for the currents can be determined from the voltages by the equations given in Fig. 22.

25. Conditions at the Beginning of a Parallel

This case is illustrated in Fig. 27, and the point of discontinuity *A* will be discussed first. As in all the cases just considered, the original waves are regarded as ap-

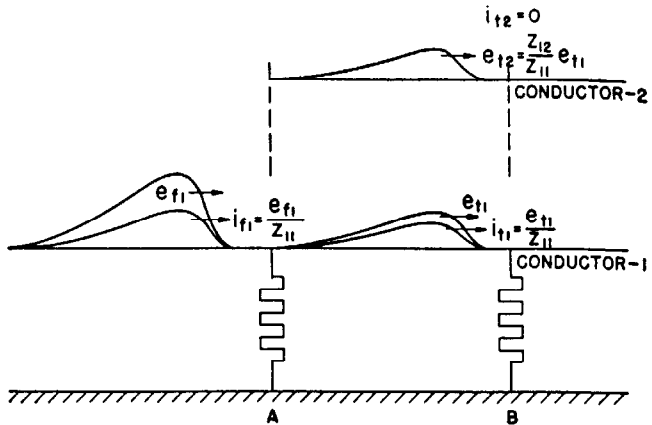


Fig. 27—Conditions at the beginning of a parallel.

proaching the point of discontinuity from the left-hand side. The reverse or backward moving waves of current and voltage to the right of *A* must therefore be equal to zero. Since no current can flow to the left of *A*, then the transmitted current wave in conductor number 2 must at all times be equal to zero. The only current present to the right of *A* is the transmitted current wave in conductor number 1. The presence of conductor number 2 cannot affect either the current or voltage in conductor number 1. Similarly, when considering the discontinuity at *B*, it follows that since the approaching current wave in conductor number 2 is zero then following the same reasoning as for *A*, the current in the conductor to the right of *B* must be zero and conductor number 2 can have no effect upon conductor number 1.

The transmitted and reflected waves in conductor number 1 can be calculated by neglecting the presence of conductor number 2.

26. Coupling Factor

In any case such as Fig. 27 in which the current in one conductor, such as number 2, is zero, the voltages are from Eqs. (57) and (58)

$$e_{t1} = Z_{11} i_{t1}$$

$$e_{t2} = Z_{12} i_{t1}$$

and

$$e_{t2} = \frac{Z_{12}}{Z_{11}} e_{t1} \quad (101)$$

Thus for this condition the voltage induced on conductor number 2 is related to that on conductor number 1 by the term $\frac{Z_{12}}{Z_{11}}$. This is commonly called the coupling factor and will be denoted by the symbol

$$K_{12} = \frac{Z_{12}}{Z_{11}} \quad (102)$$

The coupling factor can be written in terms of the physical constants of the conductors shown in Fig. 23, by the use of Eqs. (81) and (82)

$$K_{12} = \frac{\log \frac{b}{a}}{\log \frac{2h_1}{r_1}} \quad (103)$$

As will be shown subsequently, the coupling factor is of importance in calculating the voltages induced in conductors parallel to those struck directly by lightning. Values of the coupling factor between phase wire and ground wire for lines with one ground wire are given in the curves of Fig. 28 for a practical range of transmission line construction. For estimating purposes a value of 0.25 can be used. In Fig. 28 the coupling factor is plotted as a function of the spacing (a) between the ground wire and conductor for various ground wire heights (h). As shown by Eq. (103) it is also a function of the dimension (b) of Fig. 23 which is defined not only by (h) and (a) but by the angular position of the conductor relative to the ground wire and the vertical. However this angular position has little effect and the curves of Fig. 28 give the coupling factor to within about three percent for practical conductor positions. In addition the curves apply to a fixed ground wire diameter of $\frac{1}{2}$ inch. The practical range of ground wire sizes is from $\frac{3}{8}$ to $\frac{5}{8}$ inches and for this range the use of $\frac{1}{2}$ inch gives a maximum error of only five percent.

Coupling Factor Between Conductor and Two Ground Wires. If lightning strikes one conductor of a double ground wire system at midspan without flash-over, coupling factors between the ground wire system and phase conductors can be computed on the basis of involvement of one ground wire only as no current will flow in the other ground wire. This condition applies until the disturbance on the ground wire propagates to a point in the system such as a tower at which metallic connection is made between the two ground wires. If on the other hand the lightning strikes a tower top, then

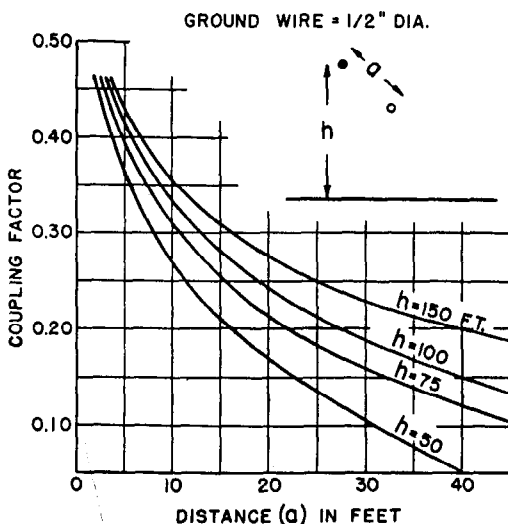


Fig. 28—Coupling factors between conductor and one ground wire $\frac{1}{2}$ inch in diameter.

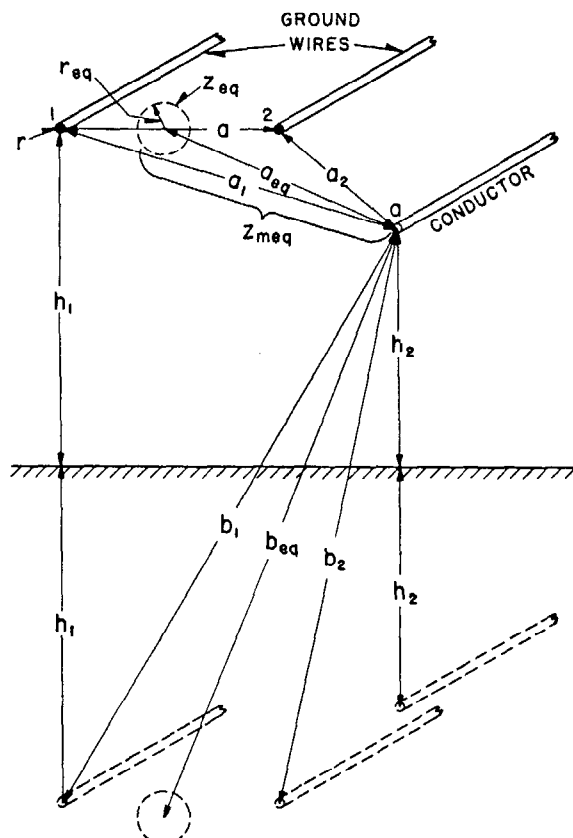


Fig. 29—Configuration for two ground wires and a conductor.

both ground wires are immediately involved. For cases in which both ground wires are involved the voltages and currents because of the usual symmetrical arrangement will be equal on the two ground wires. In Fig. 29 let the quantities referring to the ground wires be designated by the subscripts 1 and 2 and those on the conductor by the subscript a. The voltage induced on the conductor is given by

$$e_a = Z_{1a}i_1 + Z_{2a}i_2 = \frac{(Z_{1a} + Z_{2a})}{2}i_a$$

where

$$i_1 = i_2 = \frac{i}{2}$$

therefore, the equivalent mutual impedance is

$$Z_{m\text{eq}} = \frac{Z_{1a} + Z_{2a}}{2}$$

which from Eqs. (81) and (82) is

$$Z_{m\text{eq}} = 138 \log_{10} \frac{\sqrt{b_1 b_2}}{\sqrt{a_1 a_2}} \quad (104)$$

The two ground wires can be replaced by a single equivalent ground wire whose spacings are shown in Fig. 29. The coupling factor can then be written, by combining Eqs. (85) and (104), as

$$K = \frac{\log \frac{\sqrt{b_1 b_2}}{\sqrt{a_1 a_2}}}{\log \frac{2h_1}{\sqrt{ar}}} = \frac{\log \frac{b_{\text{eq}}}{a_{\text{eq}}}}{\log \frac{2h_1}{r_{\text{eq}}}} \quad (105)$$

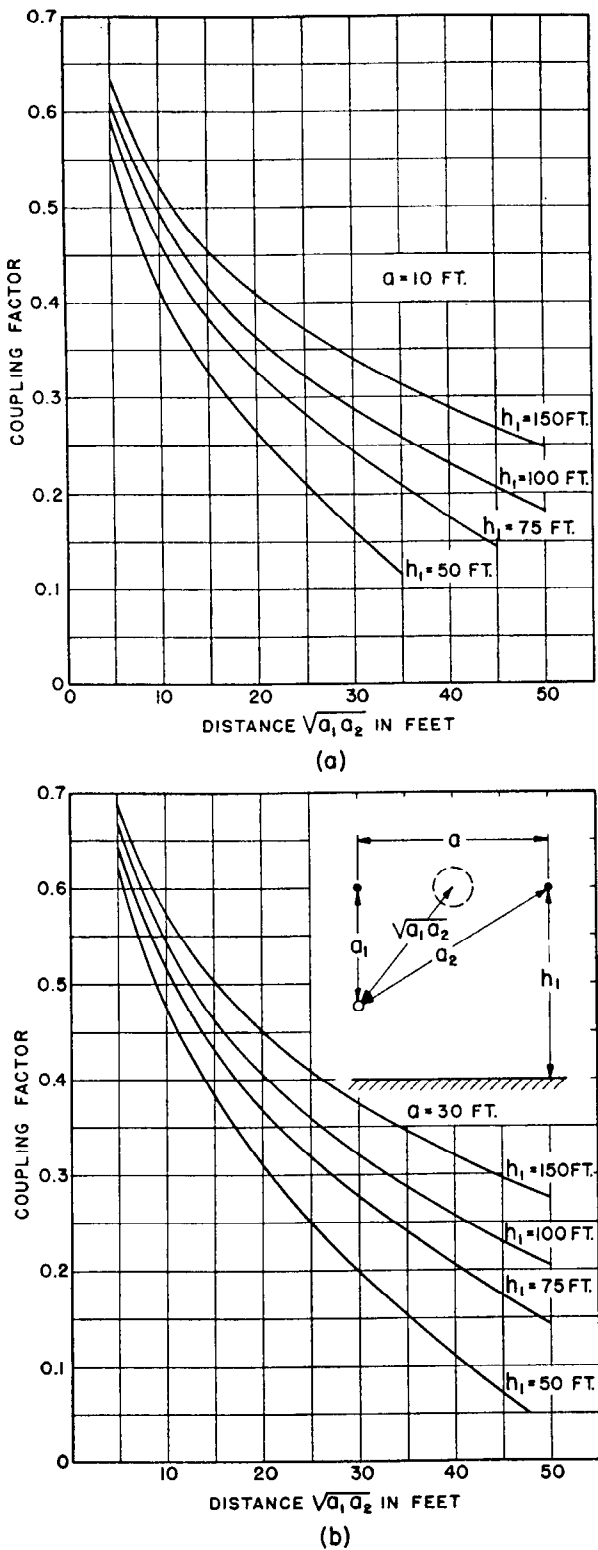


Fig. 30—Coupling factors for two ground wires of $\frac{1}{2}$ -inch diameter.

Fig. 30 gives values of this factor for practical ranges of ground wire and conductor configurations for ground wires of $\frac{1}{2}$ inch diameter. Calculations indicate that for practical configurations these curves are accurate to within about five percent regardless of the position of the con-

ductor with respect to the ground wires. Ground wire diameter has little effect upon coupling factor for values between $\frac{3}{8}$ and $\frac{5}{8}$ inches.

V. ATTENUATION AND DISTORTION

Aside from the effects of reflections at transition points, traveling waves are both attenuated and distorted as they propagate along a line. This is caused primarily by losses in the energy of the wave due to resistance, leakage, dielectric and corona loss. For sufficiently high voltages corona is the most important factor and due to it waves are attenuated within a few miles to a safe voltage.

The nature of the distortion produced is shown in the oscillograms of Fig. 31 which are typical of the results obtained by several studies made with artificial surges on transmission lines.³⁻¹⁰ Examination of these oscillograms shows that both the front and tail of the wave are sloped off by propagation.

Any of the possible types of losses will produce this effect. Above corona voltage, however, effects become much more pronounced.

27. Effect of Series Resistance

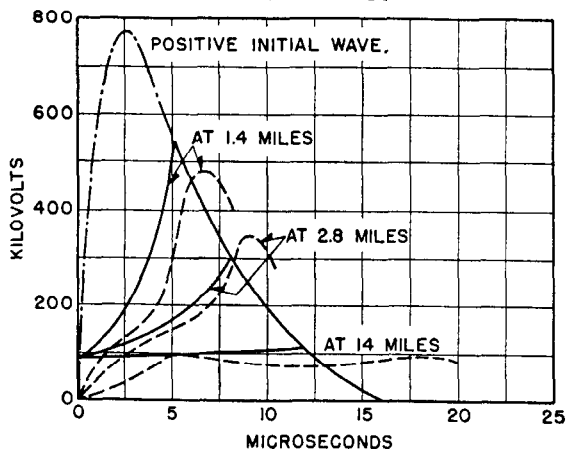
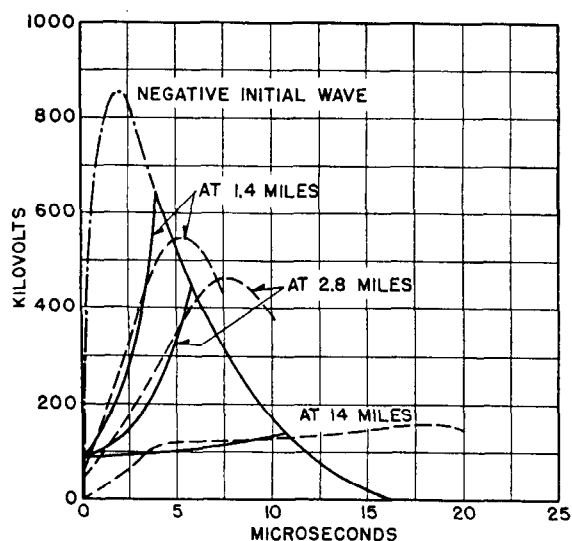
For the special case of the so-called "distortionless line"

$$\frac{R}{L} - \frac{G}{C} = 0 \quad (106)$$

where R is the series resistance and G the shunt conductance per unit length of line. For such a line, surges are attenuated without distortion. The attenuation in a distance x is equal to $e^{-\frac{R}{Z}x}$, which expresses the fraction to which the wave is reduced. The unit of x is dependent solely upon the unit used in expressing R .

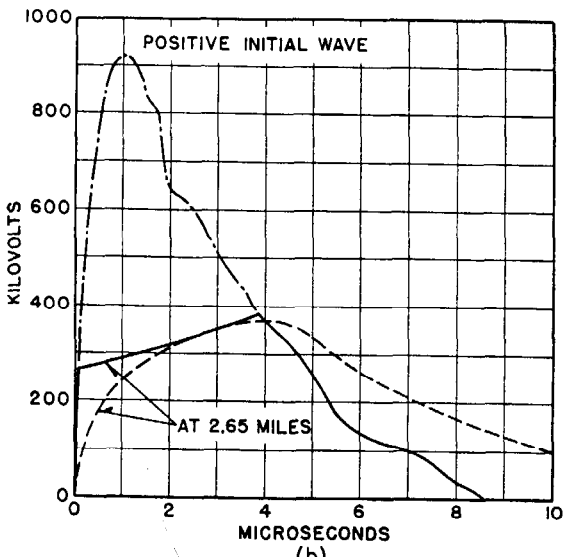
In actual transmission lines the shunt conductance is so low as to be negligible and the condition expressed by Eq. (106) is not satisfied. Thus in actual lines a surge is not only attenuated but also distorted. If, however, the distortion is neglected and the attenuation is derived on the basis of energy loss alone,¹² a factor equal to $e^{-\frac{R}{2Z}x}$ is obtained. Assuming a 0000 copper conductor of surge impedance 500 ohms and d-c resistance of 0.302 ohms per mile, the surge must travel 2300 miles to attenuate to one-half value. Of course, the resistance of the conductor under surge conditions, due to crowding of the current toward the surface, is much greater than that of the d-c value. To form some idea as to the order of magnitude of this effect, the resistance of the conductor at a frequency of 1 000 000 cycles can be calculated. At this frequency the resistance is 18 times the d-c value and assuming a resistance to surges of this magnitude it is found that the surge must travel 130 miles to attenuate to one-half value. In general it may be concluded that the attenuation due to resistance is negligible as compared to other factors, such as corona.

A more accurate indication of the resistance of a conductor under surge conditions is provided by Miller.¹³ If a square-front wave is applied to a conductor, all of the current initially crowds toward the periphery. The current density then "soaks" into the interior with a diffusion



(a)

DOTTED CURVES OSCILLOGRAMS BY BRUNE & EATON⁽⁹⁾
SOLID CURVES CALCULATED BY SKILLING & DYKES⁽²¹⁾



DOTTED CURVE OSCILLOGRAM BY CONWELL & FORTESCUE⁽⁸⁾
SOLID CURVE CALCULATED BY SKILLING & DYKES⁽²¹⁾

Fig. 31—Oscillograms of artificial surges showing attenuation and distortion.

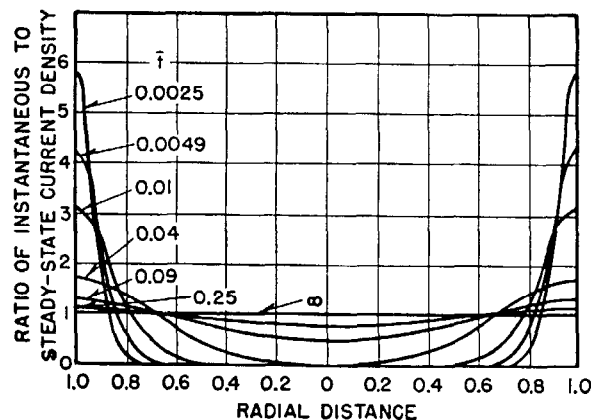


Fig. 32—Transient current distribution in solid rod.

"velocity," h , given by

$$h = \sqrt{\frac{\rho}{4\pi\mu}} \text{ in cm. per sec.}^{\frac{1}{2}} \quad (107)$$

where

ρ = Specific resistivity.

μ = Magnetic permeability.

For copper h is 11.6 cm per sec.^{1/2}; for aluminum 14.5; and for steel, if μ is assumed to be 1000, h is 1.9 cm per sec.^{1/2}.

For a solid round conductor, it is convenient to express the results in terms of a numeric given by the relation

$$\bar{t} = \left(\frac{h}{b}\right)^2 t \quad (108)$$

where t is time in seconds and b is the radius of the conductor in cm.

The current distribution within the conductor is shown in Fig. 32. With increasing time the current first crowds toward the periphery at zero time and then penetrates the

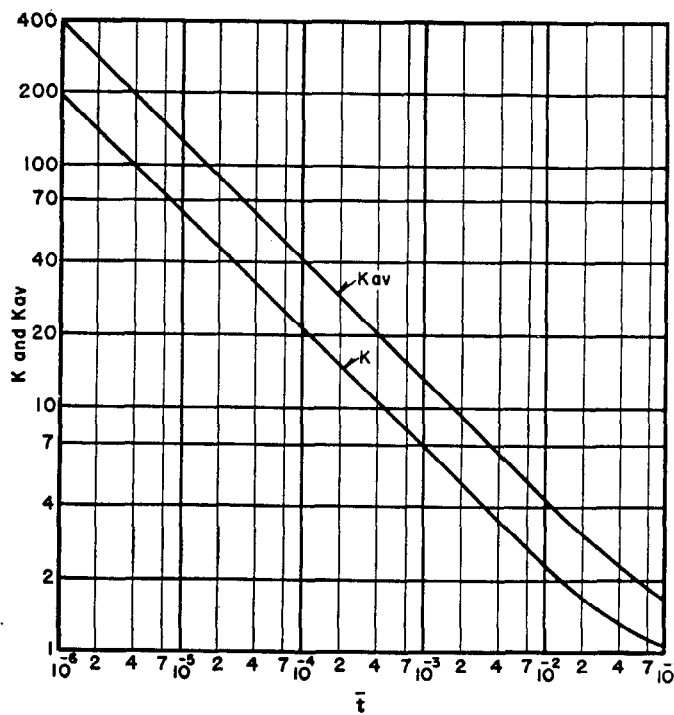


Fig. 33—Ratios of effective resistance to d-c resistance for a solid round conductor.

interior until at long times it is uniformly distributed over the cross section.

Let K define the ratio of the instantaneous resistance to the d-c resistance, and K_{av} the average of K up to the time t . Values of these quantities are given in Fig. 33. As a numerical example of the use of Fig. 33, suppose a constant current suddenly is applied to a solid copper rod $\frac{1}{2}$ inch in diameter, for which b is then $\frac{2.54}{2 \times 2} = 0.635$ cm. The values of t , K and K_{av} for various times is given by Table 1.

TABLE 1—VALUES OF t , K , AND K_{av} FOR DIFFERENT TIMES

t	10^{-7}	10^{-6}	10^{-5}	10^{-4}
t	3.35×10^{-5}	3.35×10^{-4}	3.35×10^{-3}	3.35×10^{-2}
K	36	12	3.6	1.4
K_{av}	70	22	7.0	2.5

These values give upper limits. For other than abrupt waves the effective resistance is smaller.

28. Empirical Data on Attenuation

Studies made by several investigators with klydonographs have yielded data on the attenuation of the crest magnitude of voltage waves due to lightning¹⁴⁻¹⁸. An empirical formula has been developed by Foust and Menger¹⁸ to fit such data. This formula, which assumes that the loss in the wave is proportional to the third power of the voltage, is shown in Fig. 34. Its absolute value depends upon the arbitrary constant K . In Fig. 34 are plotted curves from this formula which represent the envelope of all available field data and a curve which represents a common mean. Other empirical formulae have also been developed^{2, 20} which correspond (with the proper choice of the arbitrary constants) fairly closely to the

Foust and Menger formula in the high voltage range. Formulae of this type do not take into account the various important factors controlling attenuation and serve only to indicate its order of magnitude. Since the effect of distortion is not considered, the curves of Fig. 34 can be used for estimating purposes to determine the attenuation of the crest in a given distance for a surge of a given initial crest voltage by using the point on the curve corresponding to the initial voltage as a reference point. For example, examination of the mean curve of Fig. 34 indicates that a 2 000 kv surge will be attenuated to 750 kv in 6 miles and a 1 000 kv surge to 750 kv in 2.5 miles.

Since at the higher voltages corona is the most important factor, the effects of wave shape, polarity, and line construction on attenuation can be explained on the basis of their effect upon corona. Thus surges on large conductors should be attenuated more slowly than on small conductors. Likewise positive surges should be attenuated more rapidly than negative ones since corona loss is greater for positive waves.

The effect of some of the more important factors are shown by the curves of Fig. 35 obtained from studies with artificial surges. The curves give the effect of polarity and wave shape showing that short surges are attenuated more rapidly than long ones. Surges of the same voltage propagating on more than one conductor are shown to be attenuated less than a surge on only one conductor.

Ground wires appear to have slight effect on attenuation. Brune and Eaton⁹ found that at high voltages ground wires increased the attenuation slightly but at lower voltages decreased it. This appeared to be true for both polarities. McEachron, Hemstreet, and Rudge⁶, however, found that positive surges were not affected by the presence of a ground wire while negative surges were attenuated less.

In using the data of Fig. 34, the evidence indicates that the information from sharp chopped waves lay closer to the dotted curves and that information from slower waves lay closer to the dashed curve.

29. Corona

Attempts have been made to obtain analytical expressions for the effect of corona on distortion^{20, 22}. The best picture of the mechanism of corona power loss at the present time seems to be the following as given by Skilling and Dykes²²: "There is a critical electric gradient for air that cannot be exceeded. Any attempt to increase it results in profuse ionization of the air, and the charges liberated by ionization take up such positions in space that the gradient does not exceed this value."

"Shortly after its formation space charge becomes relatively immobile, probably due to the formation of relatively heavy ions whose mobility is almost negligible compared to electrons."

"The supply of space charge to the region about a conductor increases as long as the voltage increases and energy must be supplied for their formation from the conductor."

"After the crest of a voltage wave is reached and begins to decrease, the space charge remains practically constant in magnitude and position. During this time there is little

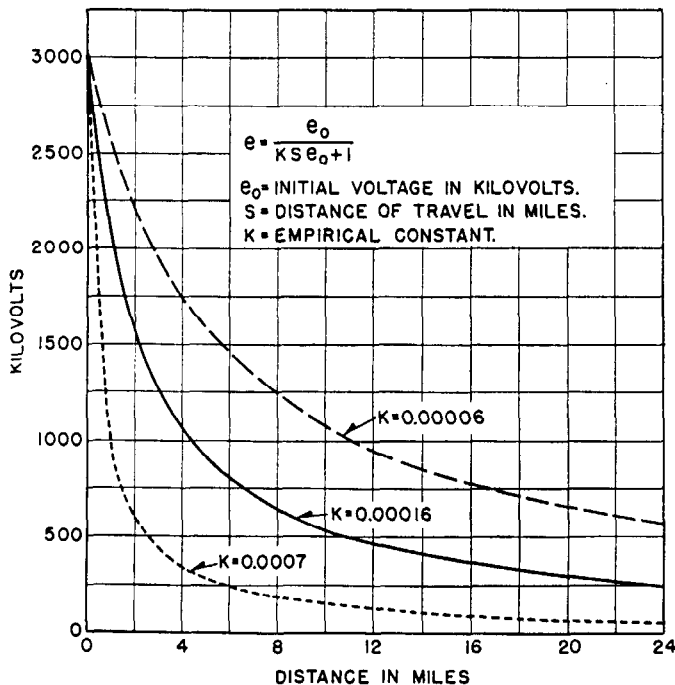


Fig. 34—Foust and Menger formula for determination of attenuation of crest magnitudes of voltage waves.

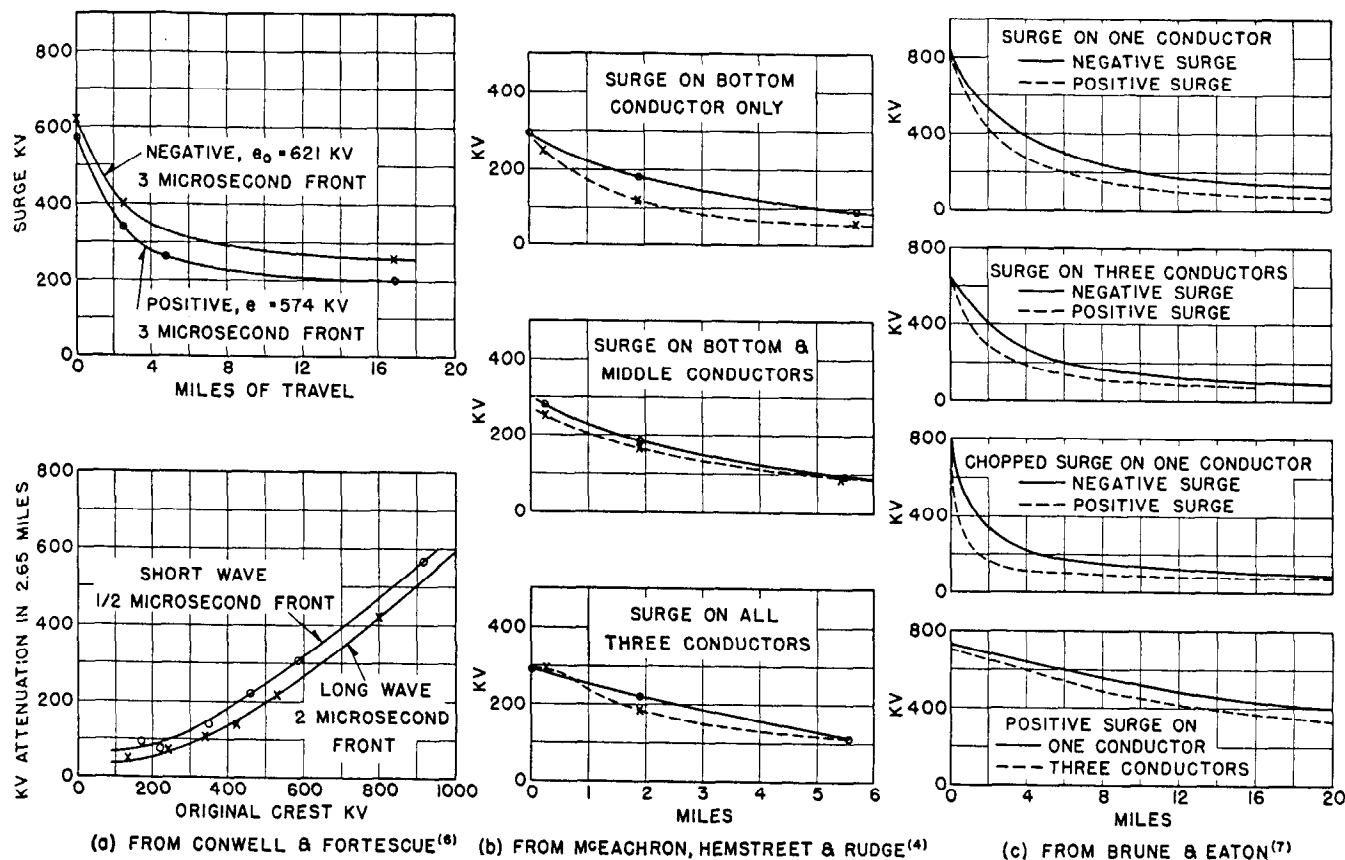


Fig. 35—Effect of the more important factors on attenuation.

(a) Effect of polarity and wave length. (b) Effect of propagation on more than one conductor. (c) Effect of polarity and propagation on more than one conductor.

loss in energy from the conductor, what there is being due to diffusion of ions in the electric field at a slow rate.”

Skilling and Dykes²² have developed an analytical method of determining the distortion which is produced by conversion of a portion of the energy of the wave into corona loss as the voltage rises to crest value. This decreases the net stored energy of the wave. Line loss is neglected after the voltage crest is reached. Distortion of the tail is not considered, and it is assumed that the crest of the wave is moved along the original tail. Examination of oscillograms showing corona distortion such as those of Fig. 31 indicate that this is a good assumption. The equation which they use for the energy per unit length of the wave is the following

$$\text{Energy} = \frac{1}{C} e^2 \quad (109)$$

which neglects distortion and the formation of space charge. The quadratic formula for corona loss per unit length is used in the form

$$\text{Loss} = \frac{K}{n} (e - e_0)^2 \quad (110)$$

where e_0 is the critical corona voltage and K and n are empirical constants which will be discussed later. This type of expression for power frequency corona loss was developed by Peek.

With analytical expressions for the initial surge voltage as given by the following

$$e = f_0(t) \quad (111)$$

$$t = F_0(e) \quad (112)$$

The equations which they developed for the corresponding quantities after the wave has propagated a distance x are

$$e = f_0 \left(t - \frac{K(e - e_0) + nCe}{nCv} x \right) \quad (113)$$

$$t = F_0(e) + \frac{K}{nCv} \left(\frac{e - e_0}{e} \right) x + \frac{x}{v} \quad (114)$$

where

t = time in seconds

e = voltage in volts

e_0 = corona starting voltage in volts (crest)

v = velocity of propagation of the wave in feet per second.

$= 9.84 \times 10^8$

C = capacitance of line in farads per foot

x = distance of travel in feet

K = the constant of Eq. (110) which relates crest voltage in volts to energy loss in joules per foot per half cycle, and which may be found from Peek's quadratic law or otherwise. It is equal to Peek's constant (which is expressed in kilowatts per kilovolt per mile) multiplied by

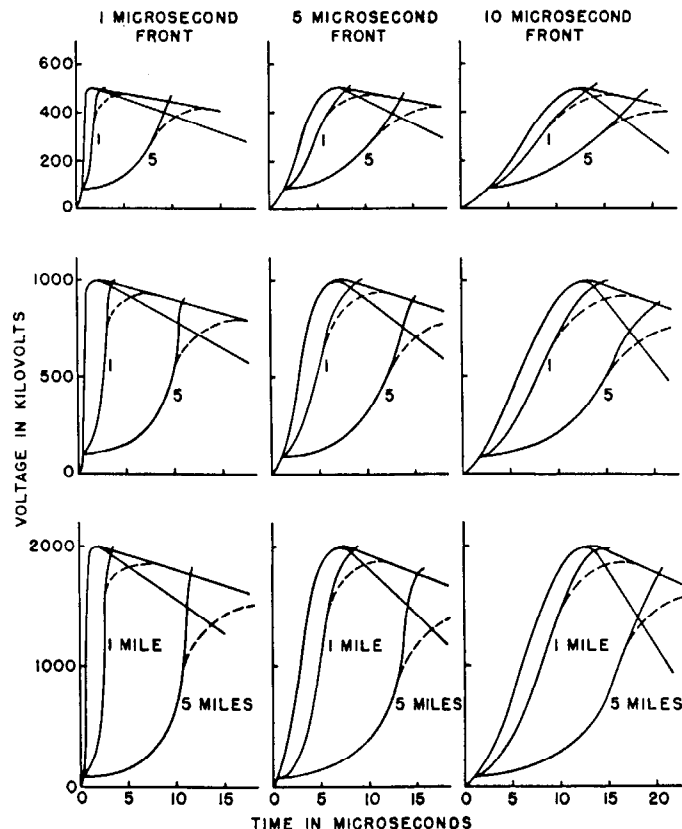


Fig. 36—Effect of corona in sloping the front of negative-voltage waves of different fronts and magnitudes.

$$\left(\frac{10^3}{5280 \times 10^6} = 1.895 \times 10^{-7} \right). \text{ For high voltage}$$

transmission lines K is of the order of 4×10^{-12} .

Skilling and Dykes describe the constant n as follows: "The factor n is a more or less constant factor which is needed to account for three differences between the corona of traveling waves and corona at power frequency. These are (1) the effect of mobility of charge (2) the fact that when voltage is alternating there is a space charge left over from one-half cycle to the next, and (3) the difference between positive and negative corona."

They found that good results could be obtained if $n=2\frac{1}{2}$ for positive waves and $n=4$ for negative waves.

Eq. (114) is more convenient for an actual calculation. This equation shows that at a distance x for every value of e on the front of the original wave there is a new value of t . If there were no distortion this would be the original value $F_0(e)$ from Eq. (112) plus $\frac{x}{v}$ the term which represents the time for the wave to travel the distance x . The term $\frac{K}{nCv} \left(\frac{e-e_0}{e} \right) x$ describes the distortion of the wave produced by corona. It is not necessary to know the analytical expression for the initial wave. The wave can be plotted graphically and successive values of voltage selected on the front of the wave with their corresponding times. To obtain the time it takes the voltage to rise from zero to this same value after the wave has traveled the distance x it is merely necessary to add to the initial time

the value $\frac{K}{nCv} \left(\frac{e-e_0}{e} \right) x$. In this manner the front of the distorted wave can be plotted. The crest of the wave is determined by plotting the distorted wave on the same figure with the initial wave, starting both at the same point. The crest is the point of intersection of the distorted front with the tail of the initial wave.

A comparison of calculations of distortion using this formula with oscilloscopes of actual cases is shown in Fig. 31 where the solid curve expresses waves calculated by Skilling and Dykes. As seen by these curves the calculated results conform closely to the oscilloscopes above the critical voltage except at the crest of the wave.

In order to obtain a better idea of the effect of corona in sloping off the front of voltages high enough to be of importance from an insulation standpoint calculations were made of the distortion of waves of different fronts and magnitudes after traveling different distances. These are shown in Fig. 36.

VI. 60-CYCLE STEADY-STATE PERFORMANCE

Misunderstanding sometimes occurs in the application of wave theory to the steady-state 60-cycle operation of transmission lines. This occurs particularly with regard to the no-load condition. The question is frequently asked, "Since it is known that the waves travel with the speed of light, should there not be a phase-angle displacement between the two ends of the line equivalent to the time required for the wave to travel the length of the line?" Actually, of course, at no load the phase displacement is very low and if the resistance is equal to zero the phase angle is also zero. This difficulty is resolved when the reflections are taken into consideration. To clarify this situation, consideration will be given to some simple 60-cycle conditions as applied to a resistanceless line.

As was shown in Section 10 of this chapter, if a resistance, equal to the surge impedance, is connected in shunt across the receiving end of a resistanceless line and a surge is impressed upon the line, no reflections occur at the receiving end. Under these same line conditions, if a 60-cycle voltage is impressed across the sending end, waves of voltage propagate along the line and no reflections occur. Since waves travel with the speed of light, 186 000 miles per second, then a full wave or 360 degrees phase displacement

occurs on a $\frac{186\,000}{60}$ or 3100-mile line. The phase displacement for a 300-mile line is $\frac{300}{3100} 360$ or 34.8 degrees and the voltages at the two ends are equal in magnitude.

The amount of power absorbed in the resistor $\left(\frac{E^2}{Z} \right)$, on a three-phase basis, where E is the line-to-line voltage) can be transmitted an indefinitely long distance with constant voltage all along the line. At this load the capacitive charging kva just equals the inductive reactive kva of the inductance. This particular load is called the "surge impedance load." If the resistance, which might be characterized as a "dead" load is replaced by synchronous equipment, other factors enter which limit the amount of

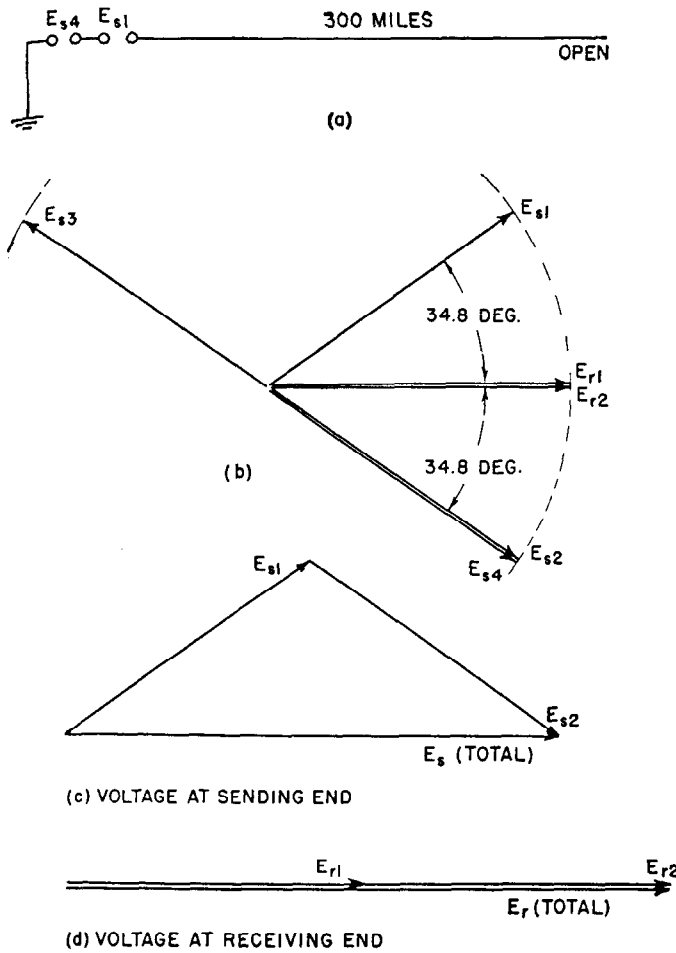


Fig. 37—Steady-state analysis by means of wave theory of an open-circuited resistanceless line 300 miles in length.

power that can be transmitted. For detailed consideration of these factors see the chapter on System Stability.

Now returning to the open circuit, let the voltage whose vector (or phasor) value is indicated by E_{s1} of Fig. 37 be impressed across the sending end of a 300-mile line. At a time later represented by the time required for the wave to traverse the line (34.8 deg.) the wave, E_{r1} , reaches the end of the line and is reflected with equal magnitude and phase position, E_{r2} . This wave reaches the sending end with a magnitude and phase position given by E_{s2} . This voltage is reflected with opposite polarity as given by E_{s3} . Now impress upon the line an additional voltage given by E_{s4} which is equal to E_{s2} . The purpose of this additional voltage is to annul the effect of E_{s3} in so far as the line is concerned. Both E_{s3} and E_{s4} propagate along the line but since they are equal and opposite they cancel each other. All reflections are now provided for adequately. At the sending end are the voltages E_{s1} , E_{s2} , E_{s3} and E_{s4} which add up to $E_{s(\text{total})}$ in (c). At the receiving end are the voltages E_{r1} and E_{r2} . Thus the voltage at the receiving end is in phase with that at the sending end and is greater by the reciprocal of the cosine of 34.8 degrees or 1.218.

REFERENCES

- Mechanical Demonstrator of Traveling Waves, by C. F. Wagner, *Electrical Engineering*, October, 1939, page 413.
- Traveling Waves on Transmission Systems, by L. V. Bewley (a book), John Wiley and Sons.
- Theoretical and Field Investigations of Lightning, by C. L. Fortescue, A. L. Atherton, and J. H. Cox, *A.I.E.E. Transactions*, Volume 48, 1929, page 449 (395).
- Cathode Ray Oscillograph Study of Artificial Surges on the Turner Falls Transmission Line, by K. B. McEachron and V. E. Goodwin, *A.I.E.E. Transactions*, 1929, Volume 48, page 475 (475).
- Study of the Effect of Short Lengths of Cable on Traveling Waves, by K. B. McEachron, J. G. Hemstreet, and H. P. Seelye, *A.I.E.E. Transactions*, Volume 49, 1930, page 1432 (527).
- Traveling Waves on Transmission Lines with Artificial Lightning, by K. B. McEachron, J. G. Hemstreet, and W. J. Rudge, *G. E. Review*, April, 1930, page 254 (722).
- Symposium on Lightning, by J. H. Cox and Edward Beck, *A.I.E.E. Transactions*, Volume 49, 1930, page 857 (732).
- Lightning Laboratory at Stillwater, New Jersey, by R. N. Conwell and C. L. Fortescue, *A.I.E.E. Transactions*, Volume 49, 1930, page 872 (746).
- Experimental Studies in the Propagation of Lightning Surges on Transmission Lines, by O. Brune and J. R. Eaton, *A.I.E.E. Transactions*, Volume 50, 1931, page 1132 (813).
- Attenuation and Successive Reflections of Traveling Waves, by J. C. Dowell, *A.I.E.E. Transactions*, Volume 50, 1931, page 551 (855).
- Electric Circuit Theory and Operational Calculus* (a book), John R. Carson, McGraw-Hill Book Company.
- Elektrische Schaltvorgänge*, by R. Rudenberg (a book), Julius Springer, Berlin.
- Diffusion of Electric Current Into Rods, Tubes and Flat Surfaces, by K. W. Miller, *A.I.E.E. Transactions*, Volume 66, 1947, page 1496.
- Lightning Investigation on the Ohio Power Co.'s 132-kv System — 1930, by Philip Sporn and W. L. Lloyd, Jr., *A.I.E.E. Transactions*, Volume 50, 1931, page 1111 (659).
- Lightning Investigation on the 220-kv System of the Penn. Power & Light Co. 1930, by Edgar Bell and A. L. Price, *A.I.E.E. Transactions*, Volume 50, 1931, page 1101 (691).
- Lightning Investigation on 220-kv System of the Penn. Power and Light Co. 1928-1929, by N. N. Smeloff and A. L. Price, *A.I.E.E. Transactions*, Volume 49, 1930, page 895 (712).
- Lightning Investigation on the Appalachian Electric Power Co.'s Transmission System, by I. W. Gross and J. H. Cox, *A.I.E.E. Transactions*, Volume 50, 1931, page 1118 (818).
- Surge Voltage Investigations on Transmission Lines, by W. W. Lewis, *A.I.E.E. Transactions*, Volume 47, 1928, page 1111 (281).
- Corona and Line Surges, by H. H. Skilling, *Electrical Engineering*, Oct. 1931.
- The Hysterisic Character of Corona Formation, by H. J. Ryan and H. H. Hemline, *A.I.E.E. Transactions*, Volume 50, 1931, page 798.
- Discussion, by E. W. Boehne, *A.I.E.E. Transactions*, Volume 50, 1931, page 558.
- Distortion of Traveling Waves by Corona, by H. H. Skilling and P. deK. Dykes, *A.I.E.E. Transactions*, Volume 56, 1937, page 850.

NOTE: Number in parentheses indicates page number in Lightning Reference Book.

CHAPTER 16

LIGHTNING PHENOMENA*

Original Authors:

C. F. Wagner and G. D. McCann

Revised by:

C. F. Wagner and J. M. Clayton

I. GENERAL CHARACTERISTICS

THE physical manifestations of lightning have been with us from the remotest times, but only comparatively recently have the phenomena become even partly understood. Franklin in his electrical experiments between 1740 and 1750 succeeded in identifying lightning as the static electricity of his time. Beyond this fact little was learned until within the past 35 years. The real incentive to obtain additional knowledge lay in the necessity of the electrical industry to protect against its effects. As longer transmission lines were built the need for reduction in outages due to lightning became more acute. This placed more stringent requirements upon lightning arresters and other protective devices. Largely through the co-operation of the utilities and manufacturers and through the use of special instruments such as the klydonograph, cathode-ray oscillograph, surge-crest ammeter, Boys camera, and fulchronograph, information of a very valuable character has been obtained regarding stroke mechanism and the voltages and currents associated with lightning.

1. Charge Formation

In spite of the great interest in the manner in which charges arise in thunderclouds, the question is still controversial. Some half-dozen theories have been advanced, but those of C. T. R. Wilson and of G. C. Simpson or modifications of them have received most consideration. Both theories postulate ascending currents of air and relative motion of rain drops of different sizes.

Wilson's theory¹ depends for its explanations upon the presence of large numbers of ions in the atmosphere. Many of these ions, both positive and negative, attach themselves to minute particles of dust and extremely small drops of water, called Aitken nuclei, to form large ions as contrasted with unattached or small ions. Over land the number of small ions of each sign ranges from about 300 to 1000 per cubic centimeter, and the large ions from 1000 to 80 000 per cubic centimeter. The small ions do not play an important part in Wilson's theory. The mobility of an ion is the steady velocity that can be attained under a voltage gradient of one volt per centimeter. The large ions have very low mobility ranging from 0.0003 to 0.0005 centimeter per second. Under a gradient of 10 000 volts per centimeter this would correspond to a velocity of only 3 centimeters per second.

Macky², in a study of the behavior of water drops when exposed to electric fields, found that a droplet of radius p

centimeters becomes elongated until at a critical field determined by the relation $F\sqrt{p} = 3875$ it becomes unstable. A luminous glow is formed at each end and the energy absorbed thereby results in evaporation of a portion of the water forming the droplet. This sets a limit to the size of drops in a thunderstorm. Thus, no drops greater than 0.15 centimeter in radius can persist in fields of 10 000 volts per centimeter. Air pressure has no influence upon the field at which this occurs. Macky suggests that in general the fields within thunderstorms will rise to a value of the order of 10 000 volts per centimeter before discharge occurs.

Wilson's theory premises the existence of the normal field which occurs during fair weather. This is generally directed downward, the direction which convention has adopted as positive. In magnitude it is of the order of one volt per centimeter at the surface of the earth and gradually decreases with altitude until at 30 000 feet it is only about 0.02 volt per centimeter. A relatively large drop of water (of say one millimeter radius) in such a field will become polarized by induction, the upper side acquiring a negative charge and the lower side a positive charge (see Fig. 1). The velocity of fall under the influence of gravity of such a charge will be 590 centimeters per second, which is large with respect to the velocity of the slowly moving ions even under the maximum field strength of 10 000 volts per centimeter. At the under surface of the drop a selective action with regard to the slowly moving ions occurs. The negative ions tend to be attracted and the positive ions repelled. No such selection occurs at the

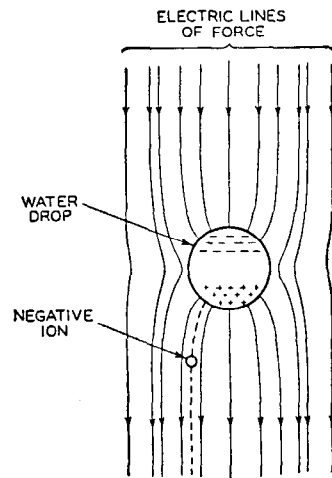


Fig. 1—Capture of negative ions by large falling drops.

*The material in sections I and II of this chapter is essentially the same as that presented in a series of articles by the original authors that appeared in August, September, and October, 1941 issues of *Electrical Engineering*. The material in section III is revised to include the results of field studies through 1949.

upper surface. As a result of this action, the drop accumulates negative charge. With the loss of the negatively charged ions the remaining large ions are predominantly positive. The smaller drops descend with a lower velocity and thus their velocity becomes more nearly equal to that of the velocity of the large ions under the influence of the electric field. It becomes possible then for the small drops of water to pick up positive charge by impact with the positive ions.

Thus, the original charges which were distributed at random and produce an essentially neutral space charge, become separated. The large drops carry the negative charges to the lower portions of the cloud and the small drops retain the positive charge in the upper portion. According to Wilson's theory the lower portion of the cloud is negatively charged and the upper portion, positively. This mechanism of discharge has been verified experimentally in the laboratory by Gott³ who actually obtained charge separation by this process.

The theory of G. C. Simpson⁴ also has been substantiated in part by laboratory experiments. It has been shown that a water drop of radius greater than 2.5 millimeters becomes flattened or unstable when it falls through still or ascending air. A large number of smaller drops are formed. The terminal or steady-state velocity of drops 0.25 centimeter in diameter is eight meters per second, which thus constitutes the limiting relative velocity of rain drops. No drops will fall to earth in an ascending current of air exceeding eight meters per second. It has also been shown that when water drops break up, the resulting droplets become positively charged and the air negatively.

The meteorological conditions within a cloud according to Simpson are shown in Fig. 2. The unbroken lines repre-

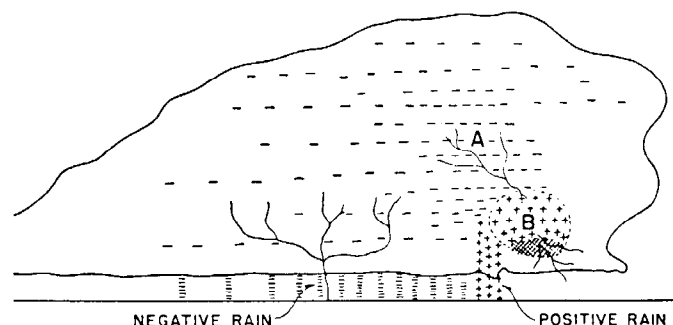


Fig. 3—Electrical conditions within thunderclouds⁴.

oval 8. The drops that do fall within this volume will be broken and the parts blown upward. The small drops that have been blown upward will recombine and fall back again, and so the process will be continued.

The distribution of electrical charge that will result from the conditions represented in Fig. 2 is shown diagrammatically in Fig. 3. The mechanism by which charge separation occurs is explained clearly by Simpson as follows:

"In the region where the vertical velocity exceeds eight meters a second there can be no accumulation of electricity. Above this region where the breaking and recombining of water drops take place (the region marked *B* in Fig. 3) here, every time a drop breaks, the water of which the drop is composed receives a positive charge. The corresponding negative charge is given to the air and is absorbed immediately by the cloud particles, which are carried away with the full velocity of the air current (neglecting the effect of the electrical field in resisting separation). The positively charged water, however, does not so easily pass out of the region *B*, for the small drops rapidly recombine and fall back again, only to be broken once more and to receive an additional positive charge. In this way the accumulated water in *B* becomes highly charged with positive electricity, and this is indicated by the plus signs in the diagram. The air with its negative charge passes out of *B* into the main cloud, so that the latter receives a negative charge. In what follows, the region *B* will be described as the region of separation, for here the negative electricity is separated from the positive electricity. The density of the negative charge obviously will be greatest just outside the region of separation, and this is indicated in Fig. 3 by the more numerous negative signs entered in the region around *A*."

In contrasting the two theories, it may be observed that Wilson's theory leads to the conclusion that the lower portion of a cloud is negatively charged and the upper portion positively. Simpson's theory as given above, on the other hand, leads to the converse—that an intense positive charge resides in the head of the cloud and that negative charge is distributed throughout the rest of the cloud. Wilson's experimental observations of field changes next to the ground indicated that a charge of positive electric moment, that is, a charge distribution equivalent to a positive charge above a negative charge, is destroyed in the process of most lightning discharges. In addition the results of magnetic-link investigations on electrical systems, as discussed hereinafter, indicate that approximately 90 percent of all strokes lower negative charge to the transmission system.

The direct contradiction between these two theories led Simpson and Scrase⁵ to investigate the charge distribution

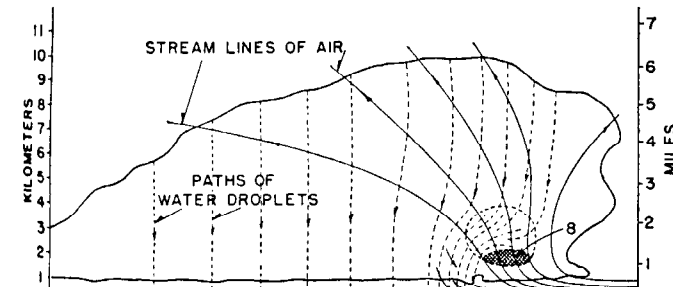


Fig. 2—Meteorological conditions within thunderclouds, according to Simpson.

resent lines of flow of the air, their distance apart being inversely proportional to the wind velocity. The air enters the storm from the right and passes under the forward end of the cloud where it takes an upward direction. Within the cross-hatched oval marked 8 the vertical component of the wind is more than eight meters per second; and outside less. For the reason just stated no water can fall through this area. The dotted lines show the general path of the larger drops as they fall to earth. The balloon-like surface of which the oval 8 forms the bottom represents a boundary within which the upward velocity is still very high. Only the larger drops are able to descend within the volume so formed and none are able to penetrate the

in a more direct manner. Free balloons equipped with clock-operated apparatus to measure electric gradient, atmospheric pressure, and relative humidity were released during storms. It was found that in general the main body of a thundercloud is negatively charged and the upper part positively charged. A concentration of positive charge appears to exist frequently in the base of the cloud. According to Simpson and Serase the cloud structure of the type shown in Fig. 4 offers a satisfactory explanation of

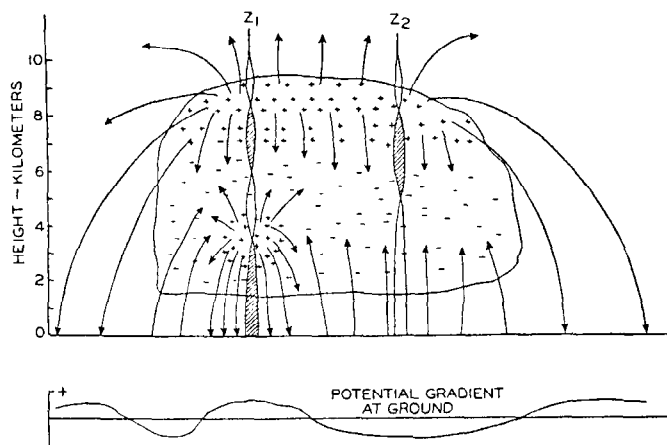


Fig. 4—Hypothetical case of a cloud with a positive charge in the upper part, a negative charge in the lower part and a small region of strong positive charge near the base.

practically all the soundings obtained in their investigations. The positive charge at the top of the cloud gives rise to the positive field encountered at the ground as the storm approaches and as it recedes. The negative charge contained in the lower half produces a negative field everywhere under the cloud except where the local concentrations of positive electricity produce positive fields. Further verification of this fact is offered by data obtained by Simpson and Serase by recording ground gradients during the passage of storm clouds. From the records of 20 storms it was found that the average length of time for which the potential gradient was appreciably disturbed from its fine-weather value was 75 minutes. By centering each record about the midpoint of the total period and dividing the record into five-minute intervals, the curve in Fig. 8 shows the percentage of frequency of positive potential gradient. The parts of the curve above the line corresponding to 50 percent represent a preponderance of positive gradient and those below a preponderance of negative gradient. It shows that the approach and recession of a storm usually are accompanied by positive gradients while the center of the cloud produces a negative gradient. This is what would occur if the lower portion of the cloud carried negative charge and the upper portion positive charge.

As between the Simpson and Wilson theories, the induction theory of Wilson seems to offer an adequate explanation of negative charge in the lower regions of the cloud and the concentration of positive electricity higher up in the cloud. It does not explain the positive charge found at the base of the clouds. However, quoting from Simpson and Serase:

"Our observations have shown quite conclusively that the boundary between the positive electricity in the upper part of the cloud and the negative electricity in the lower is in every case in a region of the cloud where the temperature is well below the freezing point and generally below -10 degrees centigrade. In this part of the cloud raindrops cannot exist. The cloud particles may be supercooled water, but on coalescing they would immediately freeze. The precipitation in the upper part of a cloud is in the form of crystals, either needles or plates, which tend to lie horizontally and to fall slowly in a series of nearly horizontal motions, first in one direction and then in another. These crystals cannot play the role of the raindrops in Wilson's theory, for in the first place they are nearly perfect nonconductors and so do not become electrically polarized, and, even if they do conduct, their shape and orientation is not favorable to the formation of induced charges, and finally their rate of fall relatively to the air is very slow. It is clear, therefore, that Wilson's influence theory cannot explain the separation of the charges found in the upper part of the thunder-clouds."

"It is well known that during blizzards in polar regions which are accompanied by large masses of blown snow, very strong electrical fields are set up near the earth's surface. These fields, with very few exceptions, are positive in direction; that is to say, in the same direction as the field in the upper part of a thundercloud. Simpson, in his discussion of the observations made in the Antarctic (Simpson 1919), suggested that the impact of ice crystals results in the ice becoming negatively charged and the air positively charged. The general settling of the negatively charged ice crystals relatively to the positively charged air would then result in a separation of electricity with the positive charge above the negative. This explanation, however, has not yet been confirmed by satisfactory laboratory experiments. Whatever the physical explanation may be, there seems little doubt that the upper separation of charge in a thunderstorm is in some way connected with the presence of ice crystals."

"There appear therefore to be two different physical processes taking place in a thunderstorm to produce the electrical effects: One is confined to the upper parts of the cloud where the temperature is below the freezing point, and the second occurs in the lower part of the cloud where the temperature is above the freezing point. There is reason to believe that the former is associated with the presence of ice crystals and the latter with raindrops, probably in the way described by Simpson in his breaking-drop theory."

Fig. 5 represents Simpson's revised diagram to illustrate the meteorological and electrical conditions in a thundercloud. This differs from his early conception illustrated in Fig. 3, in that a positive charge resides in the upper portion of the cloud above a region of separation from the negative charge, in which the temperature is between -10 and -20

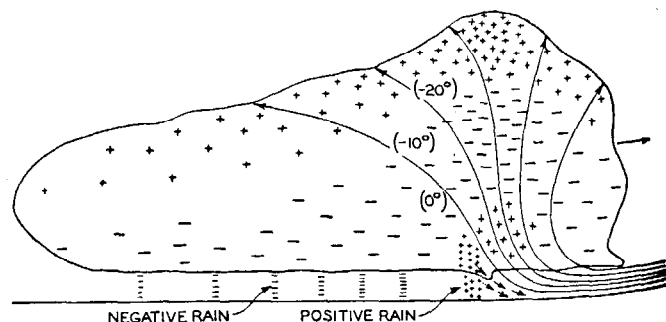


Fig. 5—Meteorological and electrical conditions within a thundercloud, according to Simpson's revised theory.